Impact of apical ABC transporters on pharmacokinetics of targeted anticancer drugs

Seng Chuan Tang

ISBN: 978-94-6182-296-3

Layout & printing: Off Page, www.offpage.nl

Cover: Chia Ling Tang

Impact of apical ABC transporters on pharmacokinetics of targeted anticancer drugs

De invloed van apicale ABC transporteiwitten op
de farmacokinetiek van doelgerichte kankergeneesmiddelen
(met een samenvatting in het Nederlands)

Proefschrift

ter verkrijging van de graad van doctor aan de Universiteit Utrecht
op gezag van de rector magnificus, prof. dr. G.J. van der Zwaan,
ingevolge het besluit van het college voor promoties
in het openbaar te verdedigen
op woensdag 3 juli 2013 des middags te 12.45 uur

door

Seng Chuan Tang

geboren op 16 april 1981 te Ipoh, Maleisië

Promotor: Prof. dr. J.H. Beijnen

Co-promotor: Dr. A.H. Schinkel

This thesis was accomplished with financial support from an academic staff training scheme fellowship sponsored by the Malaysian Ministry of Higher Education, Malaysia and partly from the Dutch Cancer Society grant 2007-3764.

Publication of this thesis was financially supported by the Netherlands Cancer Institute, Amsterdam, The Netherlands.

旭仔 (张国荣饰)：「我听人家說，世界上有一种鸟是沒有脚的。
它只可以一直的飞呀飞，飞得累了便在风中睡觉。
这种鸟儿一輩子只可以下地一次，那一次就是它死的時候……」
—《阿飞正传》王家卫

Yuddy (played by Leslie Cheung): I have heard there's a kind of bird with no legs.
All it can do is fly and fly, when it gets tired, it sleeps on the wind.
The bird can only land once in its whole life, that's the moment it dies.....
Quotes from the film "Days of Being Wild" directed by Wong Kar-Wai

Leescommissie:

Prof. dr. J.N.M. Schellens
Prof. dr. B. Olivier
Prof. dr. A. de Boer
Prof. dr. F.G.M. Russel
Dr. Sven Rottenberg

TABLE OF CONTENTS

CHAPTER 1

INTRODUCTION

1.1

MOUSE MODELS FOR ORAL DRUG ABSORPTION AND DISPOSITION

Seng Chuan Tang[1*], Jeroen J.M.A. Hendrikx[1,2*], Jos H. Beijnen[1,2] and Alfred H. Schinkel[1]

[1] Division of Molecular Oncology, the Netherlands Cancer Institute, Amsterdam, the Netherlands
[2] Department of Pharmacy & Pharmacology, Slotervaart Hospital, Amsterdam, the Netherlands

* These authors contributed equally to this paper

To be submitted in modified form to Curr Opin Pharmacol.

The problem of intestinal drug absorption

Intestinal absorption is an essential factor in the therapeutic use of virtually all orally administered drugs. Given its profound importance, it is surprising how little is clearly established about the transmembrane transport processes involved in the intestinal uptake of most drugs.

Almost every oral drug that needs to act systemically has to pass at least two membranes: the apical and basolateral membranes of the enterocytes (Figure 1). Only very small, hydrophilic drugs may be able to pass the tight junction barrier between the enterocytes. All others need to cross the enterocyte one way or another. Whereas some drugs may be lipophilic and small enough to pass the enterocyte membranes by passive diffusion at sufficient rates to be therapeutically relevant, this is unlikely to be the case for the great majority of drugs. Most will be too big, too polar or even charged, or have a combination of these properties. Only mediated transport, usually by various types of transmembrane transporters, will allow these molecules to pass the apical and the basolateral membranes of the enterocytes and thus to enter the bloodstream at sufficient rates. Surprisingly, for only very few drugs it is exactly clear what enterocyte transporters are involved.

This review aims to discuss a number of the enterocyte transmembrane transport systems that may play a role in the intestinal absorption of drugs, or in reducing their absorption. As we limit ourselves to transporters that have been studied in knockout mouse models, this review is by no means exhaustive. Also, in view of several other recent or parallel reviews, not much attention is given here to the roles of the Abcb1 and Abcg2 drug efflux transporters, or to the roles of the PepT1 peptide and Lat1, Lat2, and Tat1 amino acid transporters.

Equilibrative nucleoside transporter 1 (Ent1)

The equilibrative nucleoside transporter 1 (Ent1) is a member of the nucleoside transporter family and it can transport endogenous nucleosides bidirectionally across plasma membranes, probably by a facilitated diffusion mechanism, and thus dependent on the electrochemical gradient of the substrate across the membrane (Lu *et al.*, 2004). In the human intestinal tract, ENT1 is concentrated predominantly in the lateral membrane of the crypt cells, but it can also be found in the lateral and apical membranes of more superficial enterocytes (Govindarajan *et al.*, 2007). Ent1 mRNA is found broadly expressed in tissues of the mouse, including the intestine. This intestinal expression suggests a possible role of Ent1 in the intestinal absorption of drugs (Figure 1).

Endres *et al*. (2009b) used *Ent1*$^{-/-}$ mice to study *in vivo* drug disposition roles of Ent1, but data on the role of Ent1 in oral drug absorption are limited to the polar hepatitis C antiviral drug ribavirin (Endres *et al.*, 2009a). After oral administration of ^{3}H-labelled ribavirin, plasma concentrations of ribavirin and its primary metabolites were up to 3.7-fold decreased in *Ent*$^{-/-}$ mice compared to wild-type mice. Interestingly, plasma concentrations after intravenous administration in both strains were comparable, suggesting that the intestinal absorption of ribavirin (+ metabolites) is limited by Ent1, whereas its systemic clearance is not affected.

The most likely interpretation of these data is that Ent1, as a bidirectional equilibrative

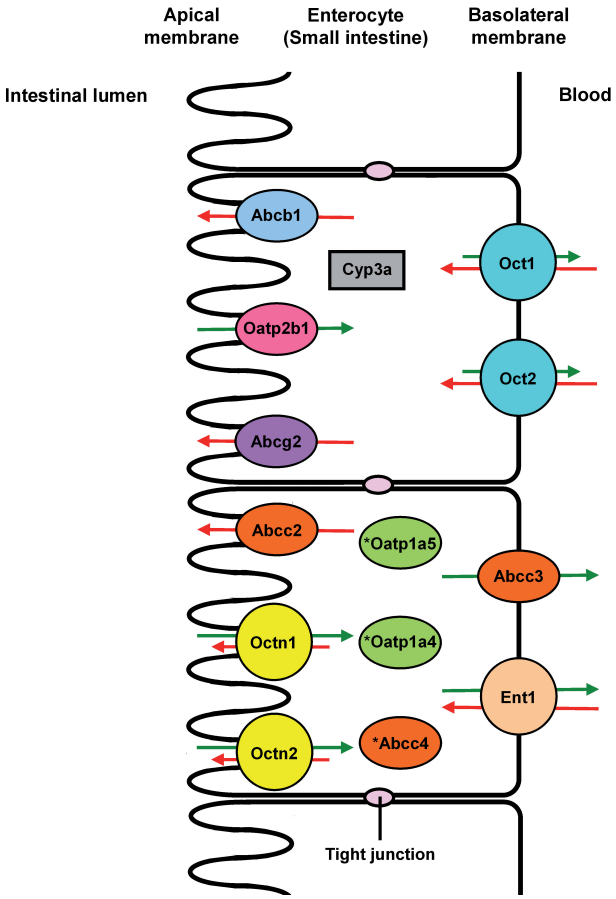

Figure 1. Schematic diagram illustrating the intestinal transporters and metabolizing enzyme discussed in this review. Efflux and/or influx transporters are localized at the apical or basolateral membrane of enterocytes in mouse small intestine. Transporters in the same color indicate that the transporters are from the same group. * indicates mRNA expression of mouse protein was detected in the small intestine, but its protein localization has not been established yet. Ovals indicate transporters with single directional transport, while circles indicate transporters with bidirectional transport. Green arrows indicate net absorptive direction of transport and red arrows indicate net excretory direction of transport. Long arrows indicate preferential transport and short arrows indicate less preferential transport directions by transporters that can mediate bidirectional transport.

transporter primarily present in basolateral membranes, is necessary for efficient egress of ribavirin (+ metabolites) from the enterocytes into blood. The preceding uptake of ribavirin from the intestinal lumen is likely mediated by the concentrative nucleoside transporters Cnt2 and/or Cnt3, which may also provide part of the driving force of the overall intestinal uptake. However, Ent1 can apparently be a rate-limiting step in this overall uptake process (Endres *et al*., 2009a). This interpretation was further supported

by recent intestinal perfusion studies with ribavirin in *Ent1*$^{-/-}$ mice (Moss *et al*., 2012). Extrapolating from these data, Ent1 may also be involved in the oral absorption of other nucleoside-like drugs.

Organic cation transporters (Oct) 1 and 2 (Slc22a1 and a2)

The organic cation transporters Oct1 and 2 are thought to be passive diffusion transporters for a diverse range of organic cations. Transport direction of substrates is thus dependent on their electrochemical gradient across the membrane. Oct1 and Oct2 are located at the basolateral membrane of polarized cells and mRNA is strongly expressed in various tissues among which the small intestine (Figure 1), especially for Oct1 (Koepsell *et al*., 2007). Using *Oct1*$^{-/-}$ mice, Jonker *et al*. (2001) demonstrated that small intestinal Oct1 can facilitate the direct intestinal excretion of the cation tetraethylammonium from blood to intestinal lumen after i.v. administration, but oral drug uptake studies (requiring transport in the other direction) have not been done with these mice.

The commonly prescribed antidiabetic drug metformin is a substrate of Oct1 and Oct2 and its pharmacokinetic behavior may be influenced by these transporters. Since both Oct1 and Oct2 mRNA are expressed in the small intestine (Figure 1), Higgins *et al*. (2012) measured plasma concentrations of metformin after oral administration in wild-type and *Oct1*;*Oct2*$^{-/-}$ mice. Plasma concentrations of metformin were substantially increased in *Oct1*;*Oct2*$^{-/-}$ mice, but the oral bioavailability ($AUC_{oral}/AUC_{i.v.}$) was not changed. In *Oct1*;*Oct2*$^{-/-}$ mice, $AUC_{0\text{-}inf}$ was increased 4.5-fold compared to wild-type, whereas the systemic clearance was decreased 4.5-fold, presumably by decreases in both renal and hepatic clearance. Thus, the increased metformin plasma concentrations were due to decreased systemic clearance in *Oct1*;*Oct2*$^{-/-}$ mice rather than to changes in intestinal absorption after oral administration. These results do not support a significant role of Oct1/2 in the intestinal absorption of metformin, although we cannot exclude that studies aimed more directly at measuring the intestinal absorption rate of metformin might reveal some contribution.

Organic cation transporters Octn1 and Octn2 (Slc22a4 and a5)

In contrast to Oct1 and Oct2, Octn1 and Octn2 are usually located at the apical membrane of epithelial cells (Figure 1) and mRNA is strongly expressed in the kidney. mRNA expression is also observed in various tissues such as liver, muscles and brain. In the small intestine of rodents, both Octn1 and Octn2 are substantially expressed in the apical membrane of enterocytes (Koepsell *et al*., 2007; Kato *et al*., 2006 Sugiura *et al*., 2010). Both transporters can transport the zwitterion L-carnitine and a variety of other organic cations and zwitterions including several drugs. Depending on the circumstances and substrate, they can translocate substrates in both directions. Transport can be Na^+-dependent, but doesn't have to be, and it may involve H^+/cation exchange. The data suggest a substantial flexibility in the modes of transport mediated by these transporters, and they have been implied both in uptake and secretory processes (Koepsell *et al*., 2007). Renal L-carnitine reabsorption is an important physiological function of Octn2 in both

humans and mice, preventing excessive loss of this essential cofactor in mitochondrial fatty acid beta-oxidation.

Sugiura *et al*. (2010) convincingly showed that the intestinal uptake of the dietary antioxidant and Octn1 substrate ergothioneine was strongly (~7-fold) decreased in *Octn1*$^{-/-}$ mice, using the everted intestinal sac method and analysis of remaining ergothioneine in the intestinal lumen after oral administration. Unexpectedly, however, plasma concentrations of oral ergothioneine were increased in *Octn1*$^{-/-}$ mice, instead of decreased. Intravenous administration showed that this could be attributed to a far lower hepatic extraction of ergothioneine in *Octn1*$^{-/-}$ compared to wild-type mice, which more than compensated for the lower oral absorption. In spite of this complication, interference with Octn1 activity in the intestine only, for instance by some drugs, might reduce the oral availability of Octn1 substrates.

Octn2 deficiency in Octn2-null mice limited the uptake of carnitine in small intestinal enterocytes *in vitro*, both assessed with Ussing chamber transepithelial transport, and with isolated enterocytes (Kato *et al*., 2006). The data suggested that Octn2 contributes to intestinal uptake of L-carnitine, but is not the only uptake process involved. Although the substrate preference of Octn2 for L-carnitine is more outspoken than that of Octn1, it still does transport several drugs. While not directly tested yet, it may therefore be that Octn2 can contribute to the intestinal absorption of some drugs.

In summary therefore, although the data with the compounds ergothioneine and L-carnitine so far do suggest that Octn1 and Octn2 may be analogously involved in the intestinal absorption of some drugs, direct experimental evidence for this is still lacking.

P-glycoprotein (Pgp; Abcb1a/b) and Cytochrome P450 3A (Cyp3a)

The role of the ATP-binding cassette (ABC) drug efflux transporter Abcb1a/1b in restricting intestinal drug uptake after oral administration of drugs, and its interplay with the drug-metabolizing enzyme Cytochrome P450 3A (Cyp3a) has been reviewed recently (van Waterschoot and Schinkel, 2011). Combination knockout mice lacking both Abcb1a/1b and Cyp3a were used to unravel the *in vivo* interplay between transporter and metabolizing enzyme. Data showed efficient collaboration between the two detoxifying systems in reducing the oral availability of shared substrate drugs (Figure 1), which however did not appear to be synergistic in nature.

Multidrug resistance-associated protein 2 (Mrp2; Abcc2)

The multidrug resistance-associated protein 2 (Mrp2; Abcc2) is also a member of the ABC drug efflux transporter family, and it can transport many drugs and drug conjugates. It is, amongst others, expressed in the apical membrane of enterocytes (Figure 1), where it could potentially reduce the intestinal absorption of drug substrates (Jedlitschky *et al*., 2006). As Abcc2 is also expressed in the bile canalicular membrane and in the apical membrane of renal proximal tubular cells it can contribute substantially to the systemic clearance of its substrates, which may affect the interpretation of oral pharmacokinetic studies in knockout mice.

Lagas *et al*. (2006) found that plasma concentrations after oral administration of the anticancer drug Abcb1 and Abcc2

substrate paclitaxel were unchanged in *Abcc2*$^{-/-}$ compared to wild-type mice, but 1.7-fold increased in *Abcb1a/b;Abcc2*$^{-/-}$ mice compared to *Abcb1a/b*$^{-/-}$ mice, which in their turn showed 8.5-fold higher plasma levels than wild-type mice. This suggests that the contribution of Abcc2 to reducing paclitaxel plasma concentrations only becomes evident in the absence of the highly efficient paclitaxel transporter Abcb1. Similar results were found for docetaxel and etoposide, with a dominant effect of Abcb1 over Abcc2 in restricting plasma AUC after oral drug administration (Lagas *et al.*, 2010a; van Waterschoot *et al.*, 2010). Further comparison with i.v. administration showed, however, that the oral bioavailability ($AUC_{oral}/AUC_{i.v.}$) of paclitaxel and etoposide was not increased, whereas that of docetaxel was. This suggests that most of the effect of Abcc2 deficiency on plasma AUC seen for paclitaxel and etoposide was due to reduced systemic clearance, but for docetaxel there may also be an increased intestinal absorption component.

Vlaming *et al.* (2011) reported that plasma concentrations of oral methotrexate were not significantly increased in *Abcc2*$^{-/-}$ compared to wild-type mice, but a 1.7-fold effect of Abcc2 deficiency was seen in the absence of Abcg2, which by itself also caused a 1.7-fold higher plasma AUC compared to wild-type mice. In this case therefore Abcg2 seemed to dominate Abcc2 effects. Interestingly, the effect of Abcc2 was lost in the absence of Abcc3 (see the section on Abcc3 below). Oral bioavailabilities were, however, not changed by the absence or presence of Abcc2, again suggesting that most effects on plasma AUC were mediated through altered systemic clearance.

Collectively, the data indicate that Abcc2 can limit oral plasma levels of drugs, but its effects can easily be obscured by other, dominant transporters. Moreover, plasma concentrations after oral administration of drugs are often increased in the absence of Abcc2 due to decreased systemic elimination rather than due to increased intestinal uptake, resulting in effectively unchanged oral bioavailability. Only for docetaxel there is a clear suggestion of altered intestinal absorption, which would merit further investigation.

Multidrug resistance-associated protein 3 (Mrp3, Abcc3)

Abcc3 also belongs to the ABC drug efflux transporter family, and it is able to transport bile acids (Belinsky *et al.*, 2005) and endogenous glucuronide conjugates (Zelcer *et al.*, 2006). In contrast to Abcc2, Abcc3 is expressed in the basolateral membrane of hepatocytes and enterocytes (Rost *et al.*, 2002; Shoji *et al.*, 2004; Zelcer *et al.*, 2006), where it mediates the basolateral efflux of substrates either from enterocytes or hepatocytes into the blood (Figure 1). With respect to xenobiotics, Abcc3 is active in the basolateral efflux of a broad range of glucuronides (Hirouchi *et al.*, 2009), sulfates (Zamek-Gliszczynski *et al.*, 2006), folates (Kitamura *et al.*, 2010), etoposide (Lagas *et al.*, 2010a) and methotrexate (Kitamura *et al.*, 2008).

Upon oral administration of methotrexate at 1 mg/kg, the plasma $AUC_{0\text{-}4hr}$ was 3.4-fold lower in *Abcc3*$^{-/-}$ mice than in wild-type mice (Kitamura *et al.*, 2008). Extensive pharmacokinetic analyses indicated that the bile canalicular clearance of methotrexate from plasma was increased, presumably because of reduced basolateral back-flux of methotrexate from the liver to blood in the absence of Abcc3. Oral bioavailability data,

however, in addition suggested reduced intestinal uptake of methotrexate. Everted intestinal sac experiments confirmed that the net intestinal uptake of methotrexate was considerably reduced in the duodenum of the *Abcc3*$^{-/-}$ mice, indicating that Abcc3 normally facilitates the absorptive efflux of methotrexate from the enterocyte to blood (Figure 1). Apparently, the decreased plasma levels of methotrexate in *Abcc3*$^{-/-}$ mice were due to both lower intestinal absorption and lower basolateral hepatic efflux.

In addition, upon oral administration of gemfibrozil, E3040, troglitazone, bisphenol A, and 4-methylumbelliferon, Abcc3 dysfunction caused a marked reduction in the plasma concentration of glucuronide conjugates of these compounds compared with wild-type mice (Hirouchi *et al.*, 2009). This finding suggests that Abcc3 plays a key role in the efflux of these glucuronide conjugates into the systemic circulation. However, it was not further investigated whether this resulted primarily from reduced efflux of these glucuronides from liver hepatocytes or from enterocytes, as glucuronidation can occur in both cell types.

Multidrug resistance-associated protein 4 (Mrp4, Abcc4)

The ABC drug efflux transporter Abcc4 can extrude a wide variety of endogenous organic anions and xenobiotics out of the cell, including steroid and bile acid conjugates (Zelcer et al., 2003), diuretics (Hasegawa *et al*., 2007), antibiotics (Ci *et al*., 2007) and antiviral drugs (Imaoka *et al*., 2007). The subcellular localization of Abcc4 is cell-type dependent. Abcc4 is localized apically in renal proximal tubular epithelial cells, but basolaterally in prostate tubuloacinar cells, hepatocytes, and choroid plexus epithelium (Russel *et al*., 2008). It is not exactly clear where Abcc4 resides in the intestine. In the human colonic cell line HT-29-CL19A, Li *et al*. (2007) found Abcc4 in both the apical and basolateral membrane, with a higher expression apically. Using Caco-2 cells, (Ming and Thakker, 2010) showed that Abcc4 is localized in the basolateral membrane of enterocytes (Figure 1). Based on the latter localization, Abcc4 might have a role in the intestinal absorption of drugs.

Upon intrajejunal administration of the polar cephalosporin antibiotic cefadroxil, portal and peripheral blood concentrations were similar in *Abcc4*$^{-/-}$ mice, but approximately 2-fold reduced in *Abcc3;Abcc4*$^{-/-}$ mice compared with wild-type mice. This suggested that the impact of Abcc4 on intestinal absorption of cefadroxil only became apparent in the absence of Abcc3 (de Waart *et al*., 2012). Ussing chamber experiments with isolated intestinal tissue indicated that Abcc4 deficiency, but not Abcc3 deficiency, resulted in reduced transepithelial absorption of cefadroxil. Collectively, the data strongly suggest that in mice, Abcc4 is mostly localized in the basolateral membrane of enterocytes, and can contribute to absorptive efflux of cefadroxil from enterocyte to blood. It should be noted, however, that the intrajejunal administration data do not exclude that increased biliary clearance of cefadroxil from blood, mainly due to the hepatic Abcc3/Abcc4 deficiency, may also have contributed to the lower cefadroxil blood levels in *Abcc3;Abcc4*$^{-/-}$ mice. This would be analogous to the situation described above for methotrexate in *Abcc3*$^{-/-}$ mice (Kitamura *et al*., 2008).

Organic anion-transporting polypeptides (OATP; SLCO) OATP1A and OATP1B

Organic anion-transporting polypeptides (Oatps, Slco) are Na^+-independent transmembrane transporters that can mediate the cellular uptake of a broad range of organic endogenous and exogenous compounds, including many drugs and their conjugates (Kalliokoski and Niemi, 2009). Human OATP1A2 and human and mouse OATP2B1 are thought to be located in the apical membrane of enterocytes, where they could potentially have an important role in intestinal uptake of drugs. In addition, mouse Oatp1a4 and Oatp1a5 mRNAs were detected in small intestine, but their protein localization has not been established yet (Figure 1). Although there are no straightforward orthologs between the human and mouse OATP1A and OATP1B family members, mouse intestinal Oatp1a4 and Oatp1a5 might have functions analogous to those of the single human OATP1A2 protein. In contrast, human OATP2B1 only has a single mouse ortholog, Oatp2b1.

To date, several knockout and transgenic mouse models have been generated to study the physiological and pharmacological functions of OATP1A and OATP1B transporters *in vivo* (Iusuf *et al*., 2012b). Mice lacking all Oatp1a/1b genes (*Oatp1a/1b*$^{-/-}$ mice) were generated to avoid any compensation by other Oatp1a or Oatp1b proteins (van de Steeg *et al*., 2010). A range of pharmacological functions of Oatp1a and Oatp1b proteins in the liver uptake and thus systemic clearance of several anticancer drugs, organic dyes, estrogen derivatives, antibiotics, statins and toxins could be established in the aforementioned mouse models as reviewed before (Iusuf *et al*., 2012b). However, directed studies to assess the impact on intestinal drug absorption of Oatp1a and Oatp1b proteins have so far only been performed in *Oatp1a/1b*$^{-/-}$ mice, with remarkably little success. Portal vein sampling tests of orally administered methotrexate, fexofenadine, pravastatin, and rosuvastatin have all failed to yield clear indications for reduced intestinal drug uptake due to the absence of Oatp1a and Oatp1b proteins, whereas the hepatic disposition of all these drugs was clearly affected (Iusuf *et al*., 2012a; Iusuf *et al*., 2013; van de Steeg *et al*., 2010). These results raise the question whether there may be extensive redundancy for uptake transporters of these drugs in the intestine, possibly including Oatp2b1 and drug uptake transporters of other families. Additional transporter gene knockout studies may potentially shed light on this question.

Intestinal efflux transporters ABCB1 and ABCG2 and their role in oral drug absorption

Oral administration of drugs is preferred over other routes of administration in patients because it is convenient, noninvasive, has lower costs, and avoids the need for frequent hospitalization or the discomfort of an injection which is also associated with the risk of infection. Additionally, chronic oral dosing of drugs, especially anticancer drugs, may have clinical benefits over intermittent therapy. However, oral administration of drugs can be confounded by limited oral availability and high interindividual variation. Especially for anticancer drugs where the therapeutic window is narrow, high variability of drug exposure may lead to treatment failure or serious toxicity in patients (Stuurman *et al*., 2013).

The intestine is an important barrier tissue that restricts the uptake of orally administered drugs. Upon oral administration, compounds may cross the intestinal epithelium either via the paracellular or transcellular route. A number of small hydrophilic, ionized drugs are absorbed via the paracellular pathway. However, absorption via this route is generally low since intercellular tight junctions restrict free transepithelial movement between the epithelial cells. Transcellular transport from the intestinal lumen to blood requires uptake across the apical membrane, followed by transport across the basolateral membrane towards the circulation. The transcellular absorption of hydrophilic drugs may be facilitated by carrier-mediated transporters, which are also used for the uptake of nutrients or micronutrients. Many orally administered drugs are lipophilic and, if they are not too big, they could cross the apical membrane at appreciable rates via passive diffusion (Murakami and Takano, 2008). Drugs that cross the apical membrane may be substrates for apical efflux transporters, which extrude compounds back into the intestinal lumen.

Two important players are the ATP-binding cassette (ABC) efflux transporters P-glycoprotein (MDR1, ABCB1) and breast cancer resistance protein (BCRP, ABCG2). These transporters can mediate the efflux of their substrates against a steep concentration gradient and in an ATP-dependent manner. We here focus on the roles of these two efflux transporters, since they are expressed in the apical membrane of intestinal epithelial cells (Maliepaard *et al.*, 2001), and have been shown to have a major impact on oral availability and tissue disposition of many anticancer drugs. ABCB1 shows extremely broad substrate specificity, with a tendency towards lipophilic and bulky amphipathic drugs such as taxanes, anthracyclines and vinca alkaloids (Sparreboom *et al*., 1997; van Asperen *et al*., 2000). ABCG2 can transport many drugs, including methotrexate, topotecan and SN-38 (de Vries *et al*., 2007; Nakatomi *et al*., 2001; Vlaming *et al*., 2009), as well as dietary toxins such as the carcinogen PhIP (2-amino-1-methyl-6-phenylimidazo[4,5-b]pyridine) (van Herwaarden *et al*., 2003) and a range of glucuronide and sulphate conjugates of exogenous and endogenous compounds (Borst and Oude Elferink, 2002; Leslie *et al*., 2005).

Using Abcb1 or Abcg2 knockout mice, Durmus *et al*. (2012) demonstrated for the TKI vemurafenib that the oral plasma $AUC_{0\text{-}24hr}$ in *Abcg2*$^{-/-}$ and *Abcb1a/b*$^{-/-}$ mice were 2.3-fold and 1.6-fold higher than in wild-type mice, respectively. The increase in plasma levels in *Abcg2*$^{-/-}$ mice was observed in the early phase after oral administration (30 min), whereas increased plasma levels were only observed after 4 hr in *Abcb1a/1b*$^{-/-}$ mice. This suggests that Abcg2 plays a more important role than Abcb1 in limiting the initial intestinal uptake of vemurafenib, whereas Abcb1 may be more important in the later clearance phase. Lagas *et al*. (2009) found for the oral TKI dasatinib that the plasma $AUC_{0\text{-}6hr}$ was about 1.7-fold and 2-fold increased in *Abcb1a/b*$^{-/-}$ and *Abcb1a/1b;Abcg2*$^{-/-}$ mice, respectively. Deficiency of Abcg2 had no impact on the oral plasma pharmacokinetics. A similar result was obtained for crizotinib, where the plasma $AUC_{0\text{-}24hr}$ in *Abcb1a/b*$^{-/-}$ and *Abcb1a/1b;Abcg2*$^{-/-}$ mice was 2.1- and 2.2-fold higher that that in wild-type mice after oral administration of crizotinib, respectively. Absence of Abcg2 only did not result in a significant change in plasma $AUC_{0\text{-}24hr}$

compared to wild-type mice (Tang *et al*., unpublished data). The latter two studies showed that Abcb1a/b, but not Abcg2, had an important role in restricting intestinal uptake of dasatinib and crizotinib. However, there is considerable overlap in substrate specificity between ABCB1 and ABCG2, and many other clinically used drugs including topotecan and the tyrosine kinase inhibitors (TKIs) dasatinib, lapatinib, imatinib, sorafenib, sunitinib and cediranib, are dual substrates of these transporters (Chen *et al*., 2009; de Vries *et al*., 2007; Lagas *et al*., 2010b; Polli *et al*., 2009; Tang *et al*., 2012; Wang *et al*., 2012; Zhou *et al*., 2009). Of note, we have often observed that plasma pharmacokinetics of many dual Abcb1 and Abcg2 substrate TKIs were not clearly affected by Abcb1 and Abcg2, whereas the impact of these proteins on brain accumulation of these drugs was usually very obvious (Lagas *et al*., 2010b; Tang *et al*., 2012). Factors such as differences in membrane permeability and drug uptake systems between these two barriers, as well as the usually far higher drug concentrations in the intestinal lumen, may be responsible for such apparent discrepancies.

Few studies have examined the regional distribution of these transporters in the mouse and human small intestinal tract. Mutch *et al*. (2004) found that the Abcb1a mRNA level increased along the small intestinal tract, with the highest expression found in the ileum of male CD-1 mice. In humans, ABCB1 mRNA expression varied substantially along the small intestinal tract. The highest ABCB1 mRNA expression was found in jejunum, followed by ileum and duodenum (Englund *et al*., 2006). Similar to mouse Abcb1a, the highest Abcg2 expression was observed in the ileum, while Abcg2 expression in duodenum and jejunum was about two-fold lower in wild-type mice with FVB background (Enokizono *et al*., 2007). Similar to human ABCB1, human jejunum has the highest ABCG2 mRNA expression, followed by ileum and duodenum (Englund *et al*., 2006). Taken together, in the mouse the highest Abcb1a and Abcg2 expressions were found in the mid- to distal small intestine, and the situation in the human small intestine is not too different. The nonhomogeneous distribution of these transporters in mouse small intestine may affect the oral absorption of orally administered drugs to some extent.

Conflict of interest: the authors indicated no potential conflict of interest

Acknowledgement of research support: An academic staff training scheme fellowship from the Malaysian Ministry of Higher Education to S.C.T.

REFERENCES

1. Belinsky MG, Dawson PA, Shchaveleva I, Bain LJ, Wang R, Ling V, Chen ZS, Grinberg A, Westphal H, Klein-Szanto A, Lerro A and Kruh GD (2005) Analysis of the in vivo functions of Mrp3. *Mol Pharmacol* **68**:160-168.
2. Borst P and Elferink RO (2002) Mammalian ABC transporters in health and disease. *Annu Rev Biochem* **71**:537-592.
3. Chen Y, Agarwal S, Shaik NM, Chen C, Yang Z and Elmquist WF (2009) P-glycoprotein and breast cancer resistance protein influence brain distribution of dasatinib. *J Pharmacol Exp Ther* **330**:956-963.
4. Ci L, Kusuhara H, Adachi M, Schuetz JD, Takeuchi K and Sugiyama Y (2007) Involvement of MRP4 (ABCC4) in the luminal efflux of

ceftizoxime and cefazolin in the kidney. *Mol Pharmacol* **71**:1591-1597.

5. de Vries NA, Zhao J, Kroon E, Buckle T, Beijnen JH and van Tellingen O (2007) P-glycoprotein and breast cancer resistance protein: two dominant transporters working together in limiting the brain penetration of topotecan. *Clin Cancer Res* **13**:6440-6449.
6. de Waart DR, van de Wetering K, Kunne C, Duijst S, Paulusma CC and Oude Elferink RP (2012) Oral availability of cefadroxil depends on ABCC3 and ABCC4. *Drug Metab Dispos* **40**:515-521.
7. Durmus S, Sparidans RW, Wagenaar E, Beijnen JH and Schinkel AH (2012) Oral availability and brain penetration of the B-RAFV600E inhibitor vemurafenib can be enhanced by the P-GLYCOprotein (ABCB1) and breast cancer resistance protein (ABCG2) inhibitor elacridar. *Mol Pharm* **9**:3236-3245.
8. Endres CJ, Moss AM, Govindarajan R, Choi DS and Unadkat JD (2009a) The role of nucleoside transporters in the erythrocyte disposition and oral absorption of ribavirin in the wild-type and equilibrative nucleoside transporter 1-/- mice. *J Pharmacol Exp Ther* **331**:287-296.
9. Endres CJ, Moss AM, Ke B, Govindarajan R, Choi DS, Messing RO and Unadkat JD (2009b) The role of the equilibrative nucleoside transporter 1 (ENT1) in transport and metabolism of ribavirin by human and wild-type or Ent1-/- mouse erythrocytes. *J Pharmacol Exp Ther* **329**:387-398.
10. Englund G, Rorsman F, Ronnblom A, Karlbom U, Lazorova L, Grasjo J, Kindmark A and Artursson P (2006) Regional levels of drug transporters along the human intestinal tract: co-expression of ABC and SLC transporters and comparison with Caco-2 cells. *Eur J Pharm Sci* **29**:269-277.
11. Enokizono J, Kusuhara H and Sugiyama Y (2007) Regional expression and activity of breast cancer resistance protein (Bcrp/Abcg2) in mouse intestine: overlapping distribution with sulfotransferases. *Drug Metab Dispos* **35**:922-928.
12. Govindarajan R, Bakken AH, Hudkins KL, Lai Y, Casado FJ, Pastor-Anglada M, Tse CM, Hayashi J and Unadkat JD (2007) In situ hybridization and immunolocalization of concentrative and equilibrative nucleoside transporters in the human intestine, liver, kidneys, and placenta. *Am J Physiol Regul Integr Comp Physiol* **293**:R1809-R1822.
13. Hasegawa M, Kusuhara H, Adachi M, Schuetz JD, Takeuchi K and Sugiyama Y (2007) Multidrug resistance-associated protein 4 is involved in the urinary excretion of hydrochlorothiazide and furosemide. *J Am Soc Nephrol* **18**:37-45.
14. Higgins JW, Bedwell DW and Zamek-Gliszczynski MJ (2012) Ablation of both organic cation transporter (OCT)1 and OCT2 alters metformin pharmacokinetics but has no effect on tissue drug exposure and pharmacodynamics. *Drug Metab Dispos* **40**:1170-1177.
15. Hirouchi M, Kusuhara H, Onuki R, Ogilvie BW, Parkinson A and Sugiyama Y (2009) Construction of triple-transfected cells [organic anion-transporting polypeptide (OATP) 1B1/multidrug resistance-associated protein (MRP) 2/MRP3 and OATP1B1/MRP2/MRP4] for analysis of the sinusoidal function of MRP3 and MRP4. *Drug Metab Dispos* **37**:2103-2111.
16. Imaoka T, Kusuhara H, Adachi M, Schuetz JD, Takeuchi K and Sugiyama Y (2007) Functional involvement of multidrug resistance-associated protein 4 (MRP4/ABCC4) in the renal elimination of the antiviral drugs adefovir and tenofovir. *Mol Pharmacol* **71**:619-627.
17. Iusuf D, Sparidans RW, van Esch A, Hobbs M, Kenworthy KE, van de Steeg E, Wagenaar E, Beijnen JH and Schinkel AH (2012a) Organic anion-transporting polypeptides 1a/1b control the hepatic uptake of pravastatin in mice. *Mol Pharm* **9**:2497-2504.
18. Iusuf D, van de Steeg E and Schinkel AH (2012b) Functions of OATP1A and 1B transporters in vivo: insights from mouse models. *Trends Pharmacol Sci* **33**:100-108.
19. Iusuf D, van Esch A, Hobbs MJ, Taylor MA, Kenworthy KE, van de Steeg E, Wagenaar E and Schinkel AH (2013) Murine Oatp1a/1b Uptake Transporters Control Rosuvastatin Systemic Exposure without Affecting Its Apparent Liver Exposure. *Mol Pharmacol*.
20. Jedlitschky G, Hoffmann U and Kroemer HK (2006) Structure and function of the MRP2 (ABCC2) protein and its role in drug disposition. *Expert Opin Drug Metab Toxicol* **2**:351-366.
21. Jonker JW, Wagenaar E, Mol CA, Buitelaar M, Koepsell H, Smit JW and Schinkel AH (2001) Reduced hepatic uptake and intestinal excretion of organic cations in mice with a

targeted disruption of the organic cation transporter 1 (Oct1 [Slc22a1]) gene. *Mol Cell Biol* **21**:5471-5477.

22. Kalliokoski A and Niemi M (2009) Impact of OATP transporters on pharmacokinetics. *Br J Pharmacol* **158**:693-705.
23. Kato Y, Sugiura M, Sugiura T, Wakayama T, Kubo Y, Kobayashi D, Sai Y, Tamai I, Iseki S and Tsuji A (2006) Organic cation/carnitine transporter OCTN2 (Slc22a5) is responsible for carnitine transport across apical membranes of small intestinal epithelial cells in mouse. *Mol Pharmacol* **70**:829-837.
24. Kitamura Y, Hirouchi M, Kusuhara H, Schuetz JD and Sugiyama Y (2008) Increasing systemic exposure of methotrexate by active efflux mediated by multidrug resistance-associated protein 3 (mrp3/abcc3). *J Pharmacol Exp Ther* **327**:465-473.
25. Kitamura Y, Kusuhara H and Sugiyama Y (2010) Basolateral efflux mediated by multidrug resistance-associated protein 3 (Mrp3/Abcc3) facilitates intestinal absorption of folates in mouse. *Pharm Res* **27**:665-672.
26. Koepsell H, Lips K and Volk C (2007) Polyspecific organic cation transporters: structure, function, physiological roles, and biopharmaceutical implications. *Pharm Res* **24**:1227-1251.
27. Lagas JS, Fan L, Wagenaar E, Vlaming ML, van Tellingen O, Beijnen JH and Schinkel AH (2010a) P-glycoprotein (P-gp/Abcb1), Abcc2, and Abcc3 determine the pharmacokinetics of etoposide. *Clin Cancer Res* **16**:130-140.
28. Lagas JS, van Waterschoot RA, Sparidans RW, Wagenaar E, Beijnen JH and Schinkel AH (2010b) Breast cancer resistance protein and P-glycoprotein limit sorafenib brain accumulation. *Mol Cancer Ther* **9**:319-326.
29. Lagas JS, van Waterschoot RA, van Tilburg VA, Hillebrand MJ, Lankheet N, Rosing H, Beijnen JH and Schinkel AH (2009) Brain accumulation of dasatinib is restricted by P-glycoprotein (ABCB1) and breast cancer resistance protein (ABCG2) and can be enhanced by elacridar treatment. *Clin Cancer Res* **15**:2344-2351.
30. Lagas JS, Vlaming ML, van Tellingen O, Wagenaar E, Jansen RS, Rosing H, Beijnen JH and Schinkel AH (2006) Multidrug resistance protein 2 is an important determinant of paclitaxel pharmacokinetics. *Clin Cancer Res* **12**:6125-6132.
31. Leslie EM, Deeley RG and Cole SP (2005) Multidrug resistance proteins: role of P-glycoprotein, MRP1, MRP2, and BCRP (ABCG2) in tissue defense. *Toxicol Appl Pharmacol* **204**:216-237.
32. Li C, Krishnamurthy PC, Penmatsa H, Marrs KL, Wang XQ, Zaccolo M, Jalink K, Li M, Nelson DJ, Schuetz JD and Naren AP (2007) Spatiotemporal coupling of cAMP transporter to CFTR chloride channel function in the gut epithelia. *Cell* **131**:940-951.
33. Lu H, Chen C and Klaassen C (2004) Tissue distribution of concentrative and equilibrative nucleoside transporters in male and female rats and mice. *Drug Metab Dispos* **32**:1455-1461.
34. Maliepaard M, Scheffer GL, Faneyte IF, van Gastelen MA, Pijnenborg AC, Schinkel AH, van de Vijver MJ, Scheper RJ and Schellens JH (2001) Subcellular localization and distribution of the breast cancer resistance protein transporter in normal human tissues. *Cancer Res* **61**:3458-3464.
35. Ming X and Thakker DR (2010) Role of basolateral efflux transporter MRP4 in the intestinal absorption of the antiviral drug adefovir dipivoxil. *Biochem Pharmacol* **79**:455-462.
36. Moss AM, Endres CJ, Ruiz-Garcia A, Choi DS and Unadkat JD (2012) Role of the equilibrative and concentrative nucleoside transporters in the intestinal absorption of the nucleoside drug, ribavirin, in wild-type and Ent1(-/-) mice. *Mol Pharm* **9**:2442-2449.
37. Murakami T and Takano M (2008) Intestinal efflux transporters and drug absorption. *Expert Opin Drug Metab Toxicol* **4**:923-939.
38. Mutch DM, Anderle P, Fiaux M, Mansourian R, Vidal K, Wahli W, Williamson G and Roberts MA (2004) Regional variations in ABC transporter expression along the mouse intestinal tract. *Physiol Genomics* **17**:11-20.
39. Nakatomi K, Yoshikawa M, Oka M, Ikegami Y, Hayasaka S, Sano K, Shiozawa K, Kawabata S, Soda H, Ishikawa T, Tanabe S and Kohno S (2001) Transport of 7-ethyl-10-hydroxycamptothecin (SN-38) by breast cancer resistance protein ABCG2 in human lung cancer cells. *Biochem Biophys Res Commun* **288**:827-832.
40. Polli JW, Olson KL, Chism JP, John-Williams LS, Yeager RL, Woodard SM, Otto V, Castellino S and Demby VE (2009) An unexpected synergist role of P-glycoprotein and breast cancer resistance protein on the central nervous system penetration of the tyrosine kinase inhibitor lapatinib (N-{3-chloro-4-[(3-fluorobenzyl)oxy]phenyl}-6-[5-({[2-

(methylsulfonyl)ethyl]amino }methyl)-2-furyl]-4-quinazolinamine; GW572016). *Drug Metab Dispos* **37**:439-442.

41. Rost D, Mahner S, Sugiyama Y and Stremmel W (2002) Expression and localization of the multidrug resistance-associated protein 3 in rat small and large intestine. *Am J Physiol Gastrointest Liver Physiol* **282**:G720-G726.
42. Russel FG, Koenderink JB and Masereeuw R (2008) Multidrug resistance protein 4 (MRP4/ABCC4): a versatile efflux transporter for drugs and signalling molecules. *Trends Pharmacol Sci* **29**:200-207.
43. Shoji T, Suzuki H, Kusuhara H, Watanabe Y, Sakamoto S and Sugiyama Y (2004) ATP-dependent transport of organic anions into isolated basolateral membrane vesicles from rat intestine. *Am J Physiol Gastrointest Liver Physiol* **287**:G749-G756.
44. Sparreboom A, van Asperen J, Mayer U, Schinkel AH, Smit JW, Meijer DK, Borst P, Nooijen WJ, Beijnen JH and van Tellingen O (1997) Limited oral bioavailability and active epithelial excretion of paclitaxel (Taxol) caused by P-glycoprotein in the intestine. *Proc Natl Acad Sci U S A* **94**:2031-2035.
45. Stuurman FE, Nuijen B, Beijnen JH and Schellens JH (2013) Oral Anticancer Drugs: Mechanisms of Low Bioavailability and Strategies for Improvement. *Clin Pharmacokinet*.
46. Sugiura T, Kato S, Shimizu T, Wakayama T, Nakamichi N, Kubo Y, Iwata D, Suzuki K, Soga T, Asano M, Iseki S, Tamai I, Tsuji A and Kato Y (2010) Functional expression of carnitine/organic cation transporter OCTN1/SLC22A4 in mouse small intestine and liver. *Drug Metab Dispos* **38**:1665-1672.
47. Tang SC, Lagas JS, Lankheet NA, Poller B, Hillebrand MJ, Rosing H, Beijnen JH and Schinkel AH (2012) Brain accumulation of sunitinib is restricted by P-glycoprotein (ABCB1) and breast cancer resistance protein (ABCG2) and can be enhanced by oral elacridar and sunitinib coadministration. *Int J Cancer* **130**:223-233.
48. van Asperen J, van Tellingen O and Beijnen JH (2000) The role of mdr1a P-glycoprotein in the biliary and intestinal secretion of doxorubicin and vinblastine in mice. *Drug Metab Dispos* **28**:264-267.
49. van de Steeg E, Wagenaar E, van der Kruijssen CM, Burggraaff JE, de Waart DR, Elferink RP, Kenworthy KE and Schinkel AH (2010) Organic anion transporting polypeptide 1a/1b-knockout mice provide insights into hepatic handling of bilirubin, bile acids, and drugs. *J Clin Invest* **120**:2942-2952.
50. van Herwaarden AE, Jonker JW, Wagenaar E, Brinkhuis RF, Schellens JH, Beijnen JH and Schinkel AH (2003) The breast cancer resistance protein (Bcrp1/Abcg2) restricts exposure to the dietary carcinogen 2-amino-1-methyl-6-phenylimidazo[4,5-b]pyridine. *Cancer Res* **63**:6447-6452.
51. van Waterschoot RA, Lagas JS, Wagenaar E, Rosing H, Beijnen JH and Schinkel AH (2010) Individual and combined roles of CYP3A, P-glycoprotein (MDR1/ABCB1) and MRP2 (ABCC2) in the pharmacokinetics of docetaxel. *Int J Cancer* **127**:2959-2964.
52. van Waterschoot RA and Schinkel AH (2011) A critical analysis of the interplay between cytochrome P450 3A and P-glycoprotein: recent insights from knockout and transgenic mice. *Pharmacol Rev* **63**:390-410.
53. Vlaming ML, Pala Z, van Esch A, Wagenaar E, de Waart DR, van de Wetering K, van der Kruijssen CM, Oude Elferink RP, van Tellingen O and Schinkel AH (2009) Functionally overlapping roles of Abcg2 (Bcrp1) and Abcc2 (Mrp2) in the elimination of methotrexate and its main toxic metabolite 7-hydroxymethotrexate in vivo. *Clin Cancer Res* **15**:3084-3093.
54. Vlaming ML, van Esch A, van de Steeg E, Pala Z, Wagenaar E, van Tellingen O and Schinkel AH (2011) Impact of abcc2 [multidrug resistance-associated protein (MRP) 2], abcc3 (MRP3), and abcg2 (breast cancer resistance protein) on the oral pharmacokinetics of methotrexate and its main metabolite 7-hydroxymethotrexate. *Drug Metab Dispos* **39**:1338-1344.
55. Wang T, Agarwal S and Elmquist WF (2012) Brain distribution of cediranib is limited by active efflux at the blood-brain barrier. *J Pharmacol Exp Ther* **341**:386-395.
56. Zamek-Gliszczynski MJ, Nezasa K, Tian X, Bridges AS, Lee K, Belinsky MG, Kruh GD and Brouwer KL (2006) Evaluation of the role of multidrug resistance-associated protein (Mrp) 3 and Mrp4 in hepatic basolateral excretion of sulfate and glucuronide metabolites of acetaminophen, 4-methylumbelliferone, and harmol in Abcc3-/- and Abcc4-/- mice. *J Pharmacol Exp Ther* **319**:1485-1491.
57. Zelcer N, Reid G, Wielinga P, Kuil A, van der Heijden I, Schuetz JD and Borst P (2003) Steroid and bile acid conjugates are substrates of human

multidrug-resistance protein (MRP) 4 (ATP-binding cassette C4). *Biochem J* **371**:361-367.

58. Zelcer N, van de Wetering K, de Waart R, Scheffer GL, Marschall HU, Wielinga PR, Kuil A, Kunne C, Smith A, van der Valk M, Wijnholds J, Elferink RO and Borst P (2006) Mice lacking Mrp3 (Abcc3) have normal bile salt transport, but altered hepatic transport of endogenous glucuronides. *J Hepatol* **44**:768-775.

59. Zhou L, Schmidt K, Nelson FR, Zelesky V, Troutman MD and Feng B (2009) The effect of breast cancer resistance protein and P-glycoprotein on the brain penetration of flavopiridol, imatinib mesylate (Gleevec), prazosin, and 2-methoxy-3-(4-(2-(5-methyl-2-phenyloxazol-4-yl)ethoxy)phenyl)propanoic acid (PF-407288) in mice. *Drug Metab Dispos* **37**:946-955.

1.2

DRUG EFFLUX TRANSPORTERS AT THE BLOOD-BRAIN BARRIER

Seng Chuan Tang and Alfred H. Schinkel

Division of Molecular Oncology, the Netherlands Cancer Institute, Amsterdam, the Netherlands

Blood-brain barrier and drug efflux transporters

Brain is separated from the systemic circulation by two physical barriers, namely the blood-brain barrier (BBB) and the blood-cerebrospinal fluid barrier. The blood-cerebrospinal fluid barrier is composed of a continuous layer of polarized epithelial cells lining the choroid plexus, whereas the BBB is formed by a monolayer of endothelial cells lining the brain blood capillaries. The capillary endothelium is characterized by the presence of tight junctions, absence of fenestrations, and sparse pinocytotic vesicular transport (Figure 1). The tight junctions between endothelial cells restrict paracellular movement of all but the smallest hydrophilic compounds, as well as macromolecules across the BBB. Besides paracellular transport, circulating molecules including hydrophobic drugs can gain access to the brain either by simple passive diffusion across the lipid bilayers of the BBB or by carrier-mediated transport. The carrier-mediated transport utilizes membrane-associated transporters that facilitate the influx or efflux of essential substrates (e.g., nutrients such as nucleosides, amino acids and glucose) and some hydrophobic drugs. These transporters are broadly divided into two categories: the solute carrier superfamily and the ATP-binding cassette (ABC) transporter superfamily. In this review, we will mainly focus on ABC transporters.

We limit ourselves here to the ABC transporters P-glycoprotein (P-gp; ABCB1) and breast cancer resistance protein (BCRP; ABCG2), which are expressed at the apical membrane of brain capillary endothelial cells that form the BBB (Figure 1). ABCB1 was first discovered by its ability to confer multidrug resistance in cancer cells (Juliano and Ling, 1976), where it functions as an efflux pump that can extrude a wide variety of anticancer drugs, including bulky amphipathic compounds such as taxanes, anthracyclines and vinca alkaloids. In rodents, two Abcb1 genes are present, encoding Abcb1a and Abcb1b, which have mostly overlapping substrate specificity but only partly overlapping tissue localization. Together they are thought to fulfill the same function(s) as the single human ABCB1. Both Abcb1a and Abcb1b are present in rodent brain, but only Abcb1a is localized in the blood capillaries of mice and rats, whereas Abcb1b is present only in brain parenchyma (Demeule *et al.*, 2002). Thus, ABCB1 substrate drugs entering the endothelial cells from the blood are immediately pumped back into the blood. Using a quantitative proteomic approach, the expression of Abcb1 is approximately 5-fold higher than that of Abcg2 in brain capillary endothelial cells isolated from male wild-type mice of FVB background (Agarwal *et al.*, 2012). These results were consistent with the findings that the expression level of Abcb1a was about 3-fold higher than that of Abcg2 at the BBB of the ddY mouse strain (Kamiie *et al.*, 2008).

Another member of the ABC superfamily, ABCG2, was first discovered in drug-resistant breast cancer cell lines *in vitro* (Doyle *et al.*, 1998) and has also been shown to confer resistance to many drugs, including mitoxantrone, prazosin, anthracyclines and some camptothecin derivatives. ABCG2 is expressed in the apical membrane of human and mouse brain capillary endothelial cells (Cisternino *et al.*, 2004; Cooray *et al.*, 2002). It was not that straightforward to establish the functional role of Abcg2 at the BBB

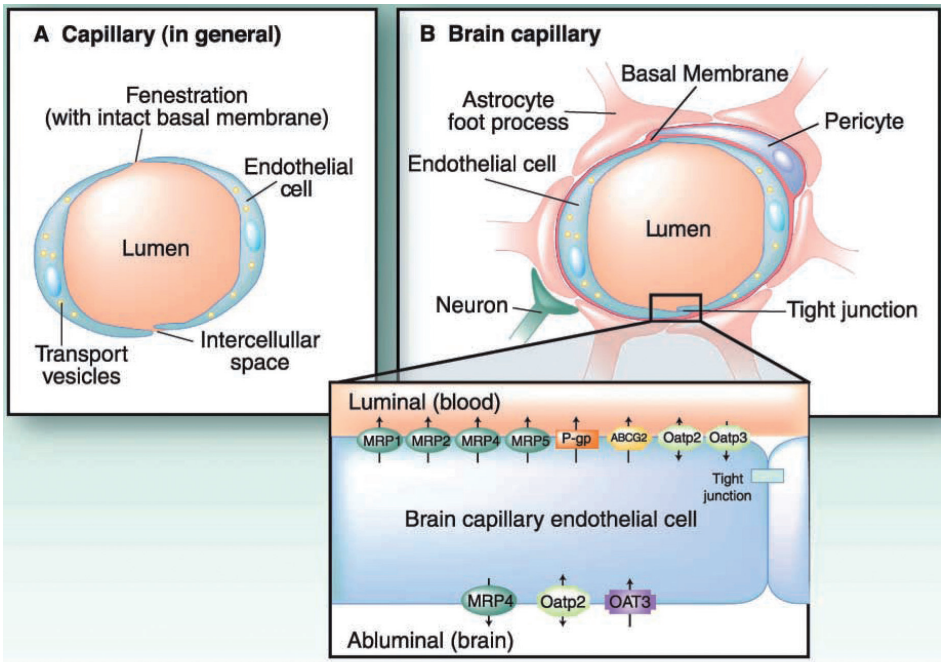

Figure 1. Tissue localization of influx and efflux drug transporters at the brain capillary endothelial cells forming the blood-brain barrier. Schematic comparison of a capillary in the periphery (A) with a brain capillary (B). Brain capillaries lack fenestration and have low pinocytosis and only a few pinocytotic vesicles. Tight junctions present between the cerebral endothelial cells form a diffusion barrier, which severely restricts penetration of water soluble-compounds, including polar drugs, into the brain. Consequently, drugs and other substances can enter the brain only by passive transcellular diffusion, which is restricted to lipophilic compounds, or by carrier-mediated transport. The enhanced illustration of a brain capillary endothelial cell in the lower part of figure illustrates the localization of drug efflux transporters at apical or basolateral membrane of brain capillary endothelial cell. Arrows show proposed direction of transport. Figure adapted from Deeken and Loscher, 2007.

using single Abcg2 knockout mice. Many studies have shown that when either Abcb1 or Abcg2 alone is absent, Abcg2 or Abcb1 can partly take over the function at the BBB for many shared substrate drugs such as topotecan, lapatinib and imatinib (de Vries *et al*., 2007; Polli *et al*., 2009; Zhou *et al*., 2009). Therefore, a combined Abcb1a/1b and Abcg2 knockout mouse model is an indispensable tool to study the overlapping functions of ABCB1 and ABCG2 in restricting brain penetration of dual substrate drugs.

Tyrosine kinase inhibitors and mammalian target of rapamycin inhibitors to treat brain metastases and glioblastoma

Brain metastases (BM) or secondary brain tumors are the most frequent intracranial tumors in adults and are 10-fold more common than primary brain neoplasms. Different brain tumor types exhibit remarkable differences in the tendency to spread to the brain, with lung cancer including both small cell and non-small cell

lung cancer having the highest BM incidence (16.3-19.9%), followed by kidney cancer (6.5-9.8%), melanoma (6.8-7.4%), breast cancer, especially the human epidermal growth factor receptor 2-positive and triple-negative forms (5.0-5.1%) and colorectal cancer (1.2-1.8%). The prognosis of patients with BM is poor, with median overall survival times of weeks to months in untreated patients. So far, chemotherapy has shown only limited or no activity in BM of most tumor types (Mehta *et al*., 2010). A possible explanation that could account only in part for the poor response of BM to targeted agents is that most of these agents are rapidly removed outside the central nervous system by efflux drug transporters like ABCB1 and ABCG2. Therefore, there is a critical need to improve brain penetration of targeted agents in patients with BM. There are several types of targeted agents being investigated in ongoing clinical trials, including TKIs and mTOR inhibitors (Preusser *et al*., 2012). These targeted agents are directed against specific growth factor receptors and/or other protein kinases that are frequently mutated or amplified in both the primary tumor and their secondary brain tumors, including HER2, polo-like kinase 1 (Plk1), EGFR, ALK, BRAF and the PI3K pathway. Since most of these targeted agents, including gefitinib, erlotinib, lapatinib, sorafenib, sunitinib, vemurafenib, and everolimus are transported substrates of ABCB1 and/or ABCG2, inhibition of ABCB1 and ABCG2 efflux transporters at the BBB might prove useful to increase brain penetration of these drugs. Many studies have shown that coadministration of the dual ABCB1 and ABCG2 inhibitor elacridar could markedly increase the brain penetration of these drugs in wild-type mice (Agarwal *et al*., 2010; Chen *et al*., 2009; Durmus *et al*., 2012; Lagas *et al*., 2009; Tang *et al*., 2012; Wang *et al*., 2012). However, the usefulness of elacridar in combination with targeted agents has yet to be demonstrated in humans.

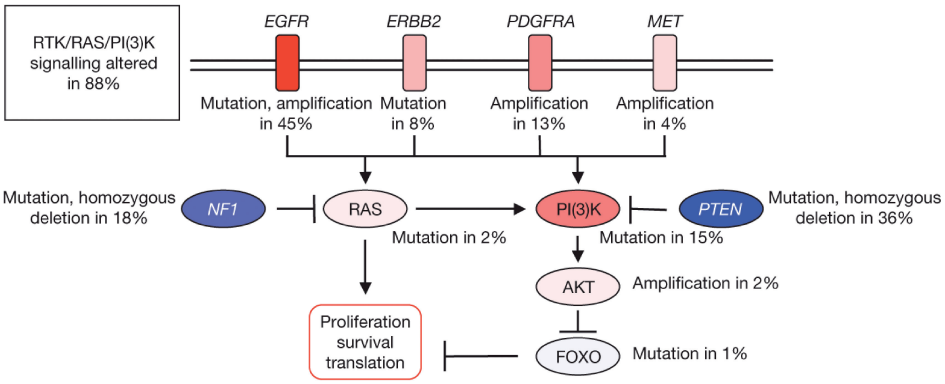

Figure 2: Frequent genetic alterations in the RTK/PI3K pathway in glioblastoma. Red indicates activating genetic alterations, with frequently altered genes showing deeper shades of red. Conversely, blue indicates inactivating alterations, with darker shades corresponding to a higher percentage of alteration. For each altered component in the pathway, the nature of the alteration and the percentage of tumours affected are indicated. Box contains the final percentage of glioblastomas with alterations in at least one known component gene of the pathway. Figure adapted from the TCGA publication TCGA Network, 2008.

Glioblastoma is the most common primary brain tumor in human adults (Furnari *et al.*, 2007). Patients with newly diagnosed glioblastoma have a median survival of approximately 1 year with generally poor responses to all therapeutic modalities (Mischel and Cloughesy, 2003). The Cancer Genome Atlas (TCGA) Research Network performed a comprehensive high-throughput genomic study to identify common somatic mutations and recurrent copy number alterations in human glioblastoma. This study reported that besides PTEN tumor suppressor gene alterations, 86% of the glioblastoma samples harboured at least one genetic event (either amplification or point mutation) in the core receptor tyrosine kinase (RTK)/ phosphatidylinositol 3-kinase (PI3K) pathway (Figure 2).

RTKs form a diverse group of transmembrane proteins that couple ligand binding to downstream signaling cascades and gene transcription. Activation of the RTK epidermal growth factor receptor either by amplification or mutation was observed in 45% of glioblastoma cases. Other RTKs, such as ERBB2, platelet derived growth factor receptor α (PDGFRA) and MET have been reported to be altered in glioblastoma, albeit at lower frequencies (Figure 2). PI3K is activated upon binding phosphorylated RTKs and/or adaptor proteins at the plasma membrane and then signals to multiple downstream effectors, such as protein kinase B (Akt) and the mammalian target of rapamycin (mTOR) (Figure 3) (Cantley, 2002). The PI3K/ Akt/mTOR pathway is known to promote cell growth, proliferation, survival and metabolism (Engelman *et al.*, 2006; Wullschleger *et al.*, 2006). In view of the frequent alterations in this pathway, tyrosine kinase inhibitors (TKIs) and mTOR inhibitors might prove useful either alone or in combination for the treatment of glioblastoma.

Brain accumulation of TKIs and mTOR inhibitors

The efficacy of chemotherapy treatment for primary or secondary brain tumors is often poor, possibly due to a low distribution or exposure of most drugs into the brain. An important factor for this low efficacy may be the presence of efflux transporters at the BBB that can effectively pump drugs out of the brain tissue. The use of transporter-expressing cell lines and transporter knockout mouse models has revealed that many clinically used drugs such as TKIs and mTOR inhibitors have limited brain distribution due to active efflux by ABCB1 and ABCG2. These *in vivo* data suggest that these agents may have limited utility for the treatment of brain tumors in humans. However, in preclinical and clinical studies, some of these agents have been shown to reduce growth of brain tumors.

In order to have a desirable therapeutic effect of these drugs against brain tumors, adequate amounts of drug must penetrate the BBB and reach the target tumor. Knowing that many of these TKIs and mTORs inhibitors are transported substrates of ABCB1 and/or ABCG2, an extensive effort has been made to test inhibitors that are able to modulate the function of ABCB1 and/or ABCG2. Originally aiming to improve the chemotherapy of multidrug-resistant tumors, a range of ABCB1 inhibitors has been developed, such as zosuquidar, elacridar, and tariquidar. Of these, elacridar (GF120918), a third generation ABCB1 modulator, was also found to inhibit ABCG2 transport (de Bruin *et al.*, 1999). It is therefore

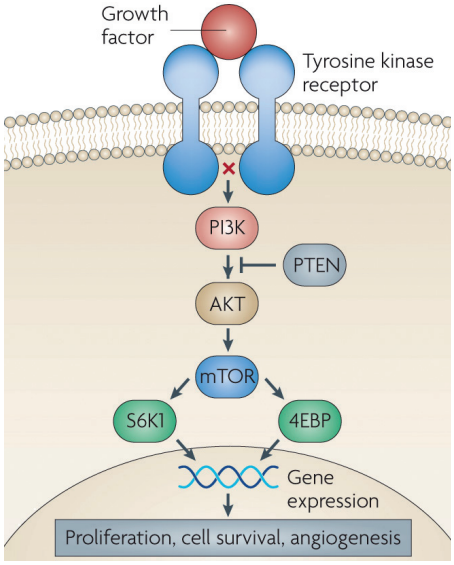

Figure 3. A simplified overview of the PI3K-AKT-mTOR pathway. Figure adapted from Holmes, 2011.

reasonable to use elacridar to inhibit ABCB1 and ABCG2 transporters at the BBB, aiming to obtain an increase in brain penetration of drugs that are substrates of both of these transporters. Many *in vivo* preclinical studies in mice have shown that coadministration of elacridar could profoundly increase brain accumulation of TKIs that are substrates of Abcb1 and/or Abcg2, to levels similar to those seen in genetic knockout mice (Agarwal *et al.*, 2010; Chen *et al.*, 2009; Durmus *et al.*, 2012; Lagas *et al.*, 2009; Tang *et al.*, 2012; Wang *et al.*, 2012). In addition, clinical data show that oral application of elacridar at 100 mg daily times five every 21 days was safe and able to increase the oral bioavailability of topotecan, although effects on brain accumulation were not assessed in this study (Kuppens *et al.*, 2007). Taken together, the use of elacridar might possibly represent a feasible strategy to improve the brain distribution of potentially effective TKIs and mTOR inhibitors in patients with glioblastoma or secondary brain tumors.

Disproportionate increase in brain accumulation of shared ABCB1 and ABCG2 substrates in mice lacking both ABCB1 and ABCG2

A striking finding from brain accumulation studies in knockout mice with shared ABCB1 and ABCG2 substrates is that the single disruption of *Abcb1a/1b* or *Abcg2* often has little or no detectable effect on brain accumulation, whereas simultaneous disruption of these two transporters results in a dramatic increase of brain accumulation of many TKIs. These findings have prompted researchers to envisage a synergistic or cooperative role of ABCB1 and ABCG2 in the efflux of dual substrates at the BBB. Recently, Kodaira *et al.* (2010) developed a straightforward pharmacokinetic model to explain this seemingly disproportionate effect of simultaneous removal of both transporters. It turns out that this simply results from the fact that the intrinsic efflux activities at the BBB of Abcb1 and Abcg2 are each considerably

larger than the remaining (most likely) passive, or lowly active efflux activity at the BBB. Thus, the disproportionate effect of simultaneous removal of both Abcb1 and Abcg2 on the accumulation of their shared substrates in the brain can be explained by their separate contributions to the net drug efflux at the BBB, without assuming any other direct or indirect interaction between ABCB1 and ABCG2.

Another tentative explanation to describe the relatively modest effect of the single Abcb1a/1b and Abcg2 knockouts on the brain accumulation of shared ABCB1 and ABCG2 substrates was that Abcb1a or Abcg2 might be upregulated in *Abcg2*(-/-) or *Abcb1a/1b*(-/-) mice, respectively. One study reported a 3-fold higher Abcg2 mRNA level in the brain microvessels of a spontaneously occurring Abcb1a-deficient variant in outbred CF-1 mice, when compared to Abcb1a-proficient mice in this population (Cisternino *et al.*, 2004). In contrast, extensive analyses of Abcb1a and Abcg2 expression in brain homogenates of, respectively, Abcb1a/1b and Abcg2 knockout mice of FVB background revealed no significant changes in RNA and/or protein levels in either strain (de Vries *et al.*, 2007; Jonker *et al.*, 2000; Lagas *et al.*, 2010; Agarwal *et al*., 2012). Moreover, in further accordance with the latter results, Kodaira *et al*. (2010) using specific substrates of either transporter, found negligible shifts in brain accumulation of the substrates in the single knockout strains of the complementary transporter. Taken together, these data indicate that there is no substantial change of Abcb1a and Abcg2 activity at the BBB of *Abcg2*(-/-) and *Abcb1a/1b*(-/-) mice in FVB strain background, respectively.

Conflict of interest: the authors indicated no potential conflict of interest

Acknowledgement of research support: An academic staff training scheme fellowship from the Malaysian Ministry of Higher Education to S.C.T.

REFERENCES

1. Agarwal S, Sane R, Gallardo JL, Ohlfest JR and Elmquist WF (2010) Distribution of gefitinib to the brain is limited by P-glycoprotein (ABCB1) and breast cancer resistance protein (ABCG2)-mediated active efflux. *J Pharmacol Exp Ther* **334**:147-155.
2. Agarwal S, Uchida Y, Mittapalli RK, Sane R, Terasaki T and Elmquist WF (2012) Quantitative proteomics of transporter expression in brain capillary endothelial cells isolated from P-glycoprotein (P-gp), breast cancer resistance protein (Bcrp), and P-gp/Bcrp knockout mice. *Drug Metab Dispos* **40**:1164-1169.
3. Chen Y, Agarwal S, Shaik NM, Chen C, Yang Z and Elmquist WF (2009) P-glycoprotein and breast cancer resistance protein influence brain distribution of dasatinib. *J Pharmacol Exp Ther* **330**:956-963.
4. Cisternino S, Mercier C, Bourasset F, Roux F and Scherrmann JM (2004) Expression, up-regulation, and transport activity of the multidrug-resistance protein Abcg2 at the mouse blood-brain barrier. *Cancer Res* **64**:3296-3301.
5. Cooray HC, Blackmore CG, Maskell L and Barrand MA (2002) Localisation of breast cancer resistance protein in microvessel endothelium of human brain. *Neuroreport* **13**:2059-2063.
6. de Bruin M, Miyake K, Litman T, Robey R and Bates SE (1999) Reversal of resistance by GF120918 in cell lines expressing the ABC half-transporter, MXR. *Cancer Lett* **146**:117-126.
7. de Vries NA, Zhao J, Kroon E, Buckle T, Beijnen JH and van Tellingen O (2007) P-glycoprotein and breast cancer resistance protein: two dominant transporters working together in limiting the brain penetration of topotecan. *Clin Cancer Res* **13**:6440-6449.
8. Deeken JF and Loscher W (2007) The blood-brain barrier and cancer: transporters, treatment, and Trojan horses. *Clin Cancer Res* **13**:1663-1674.

9. Demeule M, Regina A, Jodoin J, Laplante A, Dagenais C, Berthelet F, Moghrabi A and Beliveau R (2002) Drug transport to the brain: key roles for the efflux pump P-glycoprotein in the blood-brain barrier. *Vascul Pharmacol* **38**:339-348.
10. Doyle LA, Yang W, Abruzzo LV, Krogmann T, Gao Y, Rishi AK and Ross DD (1998) A multidrug resistance transporter from human MCF-7 breast cancer cells. *Proc Natl Acad Sci U S A* **95**:15665-15670.
11. Durmus S, Sparidans RW, Wagenaar E, Beijnen JH and Schinkel AH (2012) Oral availability and brain penetration of the B-RAFV600E inhibitor vemurafenib can be enhanced by the P-GLYCOprotein (ABCB1) and breast cancer resistance protein (ABCG2) inhibitor elacridar. *Mol Pharm* **9**:3236-3245.
12. Engelman JA, Luo J and Cantley LC (2006) The evolution of phosphatidylinositol 3-kinases as regulators of growth and metabolism. *Nat Rev Genet* **7**:606-619.
13. Furnari FB, Fenton T, Bachoo RM, Mukasa A, Stommel JM, Stegh A, Hahn WC, Ligon KL, Louis DN, Brennan C, Chin L, DePinho RA and Cavenee WK (2007) Malignant astrocytic glioma: genetics, biology, and paths to treatment. *Genes Dev* **21**:2683-2710.
14. Holmes D (2011) PI3K pathway inhibitors approach junction. *Nat Rev Drug Discov* **10**:563-564.
15. Jonker JW, Smit JW, Brinkhuis RF, Maliepaard M, Beijnen JH, Schellens JH and Schinkel AH (2000) Role of breast cancer resistance protein in the bioavailability and fetal penetration of topotecan. *J Natl Cancer Inst* **92**:1651-1656.
16. Juliano RL and Ling V (1976) A surface glycoprotein modulating drug permeability in Chinese hamster ovary cell mutants. *Biochim Biophys Acta* **455**:152-162.
17. Kamiie J, Ohtsuki S, Iwase R, Ohmine K, Katsukura Y, Yanai K, Sekine Y, Uchida Y, Ito S and Terasaki T (2008) Quantitative atlas of membrane transporter proteins: development and application of a highly sensitive simultaneous LC/MS/MS method combined with novel in-silico peptide selection criteria. *Pharm Res* **25**:1469-1483.
18. Kodaira H, Kusuhara H, Ushiki J, Fuse E and Sugiyama Y (2010) Kinetic analysis of the cooperation of P-glycoprotein (P-gp/Abcb1) and breast cancer resistance protein (Bcrp/Abcg2) in limiting the brain and testis penetration of erlotinib, flavopiridol, and mitoxantrone. *J Pharmacol Exp Ther* **333**:788-796.
19. Kuppens IE, Witteveen EO, Jewell RC, Radema SA, Paul EM, Mangum SG, Beijnen JH, Voest EE and Schellens JH (2007) A phase I, randomized, open-label, parallel-cohort, dose-finding study of elacridar (GF120918) and oral topotecan in cancer patients. *Clin Cancer Res* **13**:3276-3285.
20. Lagas JS, van Waterschoot RA, Sparidans RW, Wagenaar E, Beijnen JH and Schinkel AH (2010) Breast cancer resistance protein and P-glycoprotein limit sorafenib brain accumulation. *Mol Cancer Ther* **9**:319-326.
21. Lagas JS, van Waterschoot RA, van Tilburg VA, Hillebrand MJ, Lankheet N, Rosing H, Beijnen JH and Schinkel AH (2009) Brain accumulation of dasatinib is restricted by P-glycoprotein (ABCB1) and breast cancer resistance protein (ABCG2) and can be enhanced by elacridar treatment. *Clin Cancer Res* **15**:2344-2351.
22. Mehta MP, Paleologos NA, Mikkelsen T, Robinson PD, Ammirati M, Andrews DW, Asher AL, Burri SH, Cobbs CS, Gaspar LE, Kondziolka D, Linskey ME, Loeffler JS, McDermott M, Olson JJ, Patchell RA, Ryken TC and Kalkanis SN (2010) The role of chemotherapy in the management of newly diagnosed brain metastases: a systematic review and evidence-based clinical practice guideline. *J Neurooncol* **96**:71-83.
23. Mischel PS and Cloughesy TF (2003) Targeted molecular therapy of GBM. *Brain Pathol* **13**:52-61.
24. Polli JW, Olson KL, Chism JP, John-Williams LS, Yeager RL, Woodard SM, Otto V, Castellino S and Demby VE (2009) An unexpected synergist role of P-glycoprotein and breast cancer resistance protein on the central nervous system penetration of the tyrosine kinase inhibitor lapatinib (N-{3-chloro-4-[(3-fluorobenzyl)oxy]phenyl}-6-[5-({[2-(methylsulfonyl)ethyl]amino }methyl)-2-furyl]-4-quinazolinamine; GW572016). *Drug Metab Dispos* **37**:439-442.
25. Preusser M, Capper D, Ilhan-Mutlu A, Berghoff AS, Birner P, Bartsch R, Marosi C, Zielinski C, Mehta MP, Winkler F, Wick W and VON Deimling A (2012) Brain metastases: pathobiology and emerging targeted therapies. *Acta Neuropathol* **123**:205-222.
26. Tang SC, Lagas JS, Lankheet NA, Poller B, Hillebrand MJ, Rosing H, Beijnen JH and Schinkel AH (2012) Brain accumulation of sunitinib is restricted by P-glycoprotein (ABCB1) and breast

cancer resistance protein (ABCG2) and can be enhanced by oral elacridar and sunitinib coadministration. *Int J Cancer* **130**:223-233.

27. Wang T, Agarwal S and Elmquist WF (2012) Brain distribution of cediranib is limited by active efflux at the blood-brain barrier. *J Pharmacol Exp Ther* **341**:386-395.
28. Wullschleger S, Loewith R and Hall MN (2006) TOR signaling in growth and metabolism. *Cell* **124**:471-484.
29. Zhou L, Schmidt K, Nelson FR, Zelesky V, Troutman MD and Feng B (2009) The effect of breast cancer resistance protein and P-glycoprotein on the brain penetration of flavopiridol, imatinib mesylate (Gleevec), prazosin, and 2-methoxy-3-(4-(2-(5-methyl-2-phenyloxazol-4-yl)ethoxy) phenyl)propanoic acid (PF-407288) in mice. *Drug Metab Dispos* **37**:946-955.

1.3

THE ROLE OF CARBOXYLESTERASES IN DRUG METABOLISM AND PHARMACOKINETICS

Seng Chuan Tang and Alfred H. Schinkel

Division of Molecular Oncology, the Netherlands Cancer Institute, Amsterdam, the Netherlands

Function and regulation of carboxylesterases

Carboxylesterases (CESs) belong to the α/β serine hydrolase fold family that catalyzes the hydrolysis of a vast array of xenobiotics (Satoh and Hosokawa, 2006). Increasing evidence has shown that CESs contribute to certain aspects of cholesterol homeostasis and fatty acid metabolism through triglyceride, cholesteryl ester or retinyl ester hydrolysis (Parathath *et al*., 2011; Quiroga and Lehner, 2011; Schreiber *et al*., 2009). So far, five families of human CESs (CES1-CES5) have been classified based on sequence similarity, but the majority fall into the CES1 and CES2 families (Holmes *et al*., 2010). Although the amino acid sequence homology between human CES1 and CES2 is ~48% (Humerickhouse *et al*., 2000), there can be extensive differences between these two families in terms of substrate specificity, tissue distribution and gene regulation (Holmes *et al*., 2010; Jones *et al*., 2013; Satoh and Hosokawa, 2006; Staudinger *et al*., 2013). Human CES1 mainly hydrolyzes substrates with small alcohol groups and large acyl groups. In contrast, human CES2 enzyme efficiently hydrolyzes compounds with large alcohol groups and relatively smaller carboxylate groups (Satoh *et al*., 2002; Taketani *et al*., 2007). However, this distinction is not absolute. With respect to tissue distribution, mammalian CES1 is highly expressed in the liver (Hosokawa *et al*., 2001), whereas considerably lower expression is seen in the small intestine, kidney, lung, brain and macrophages (Munger *et al*., 1991). In contrast, mammalian CES2 is abundantly present in the small intestine (Schwer *et al*., 1997).

Mouse carboxylesterases also belong to five families, comprising 20 *Ces* genes including one pseudogene (*Ces2d*) and they are all located on chromosome 8. The mouse *Ces1* gene family has eight genes (*Ces1a*-*Ces1h*) and only a few of these genes have been analyzed in detail. Among these, *Ces1c* encodes a major mouse plasma esterase of 554 amino acid residues expressed in liver and lung and exhibiting lung surfactant convertase activity (Krishnasamy *et al*., 1998; Schwer *et al*., 1997); *Ces1d* encodes a mouse liver enzyme of 565 residues with triacylglycerol hydrolase activity (Dolinsky *et al*., 2001); and *Ces1e* encodes a liver CES of 562 residues and exhibiting β–glucuronidase-binding properties (Ovnic *et al*., 1991). *Ces1g* encodes a liver carboxylesterase of 565 amino acid residues exhibiting lipid metabolizing activity (Ellinghaus *et al*., 1998). It is interesting to note that there are significant species differences between human and mouse CES1 and CES2 proteins. Li *et al*. (2005) demonstrated that human plasma contains no significant CES enzyme activity, whereas most analyzed mouse strains usually have high levels of plasma Ces enzyme(s), which appears to be mainly Ces1c (Morton *et al*., 2005).

The role of human carboxylesterases in drug metabolism and clearance

Human carboxylesterases are responsible for the phase I drug metabolism and clearance of various drugs (Satoh and Hosokawa, 2006), as they catalyze the hydrolysis of a wide range of ester- and amide-containing drugs (Redinbo and Potter, 2005). However, the focus of this review is on cancer chemotherapy drugs such as irinotecan, capecitabine and LY2334737. Human CES1 and CES2 have different roles in prodrug activation, as shown for irinotecan, capecitabine and LY2334737. Irinotecan is an ester-containing prodrug that is hydrolysed by both CES1 and CES2 into its active metabolite, SN-38, but CES2 catalysis

is roughly 70 times more efficient than that of CES1 (Figure 1A) (Takai *et al*., 1997). Capecitabine requires a three-step activation process to form 5-fluorouracil, where the first step is the cleavage of an ester-bond by either CES1 or CES2 in the liver with similar kinetics (Figure 1B) (Miwa *et al*., 1998; Quinney *et al*., 2005). Although CES 1 and CES 2 are quite related at the amino acid and structural level, Pratt *et al*. (2013) demonstrated that the oral prodrug of gemcitabine, LY2334737 is cleaved by CES2, but not by CES1 (Figure 1C). Gemcitabine then undergoes sequential phosphorylation reactions to form the active di- and triphosphates, whose incorporation into DNA results in chain termination by interfering with DNA polymerase activity (Heinemann *et al*., 1988).

Selective inhibition of carboxylesterases

Given that mammalian carboxylesterases metabolize a wide range of drugs, the

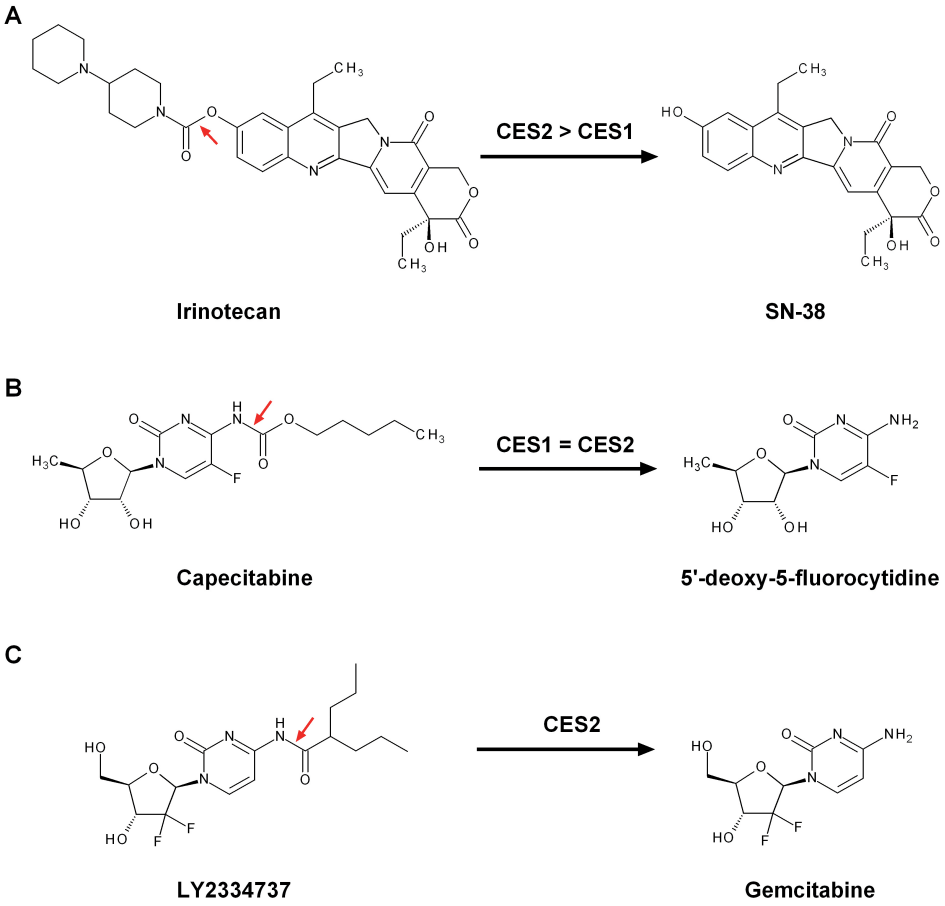

Figure 1. Carboxylesterase substrates. The chemical structure and hydrolysis of irinotecan (A), capecitabine (B) and LY2334737 (C) resulting in the formation of SN-38 (A), 5'-deoxy-5-fluorocytidine (B) and gemcitabine (C), respectively. The site of enzymatic cleavage is indicated by the red arrow.

application of selective inhibitors of this class of protein may have utility in modulating the metabolism, distribution and toxicity of drugs that are subjected to enzyme hydrolysis. For instance, for a drug that is deactivated after CES-mediated hydrolysis, co-administration of a specific CES inhibitor might delay the metabolism of this drug and thereby increase its half-life. In contrast, the morphine prodrug heroin is metabolized to morphine by CESs (Kamendulis *et al*., 1996; Pindel *et al*., 1997), and the use of selective inhibitors may delay the production of active metabolite, thus extending treatment window in patients with heroin overdose. Another example is the prodrug irinotecan, which is used for the treatment of colorectal cancer in adults (Armand *et al*., 1995), but can also cause acute diarrhea (immediately after drug administration) or delayed diarrhea. The delayed diarrhea is thought to arise, in part, from hydrolysis of irinotecan in the intestine by human intestinal CES2 to yield an active metabolite, SN-38 (Humerickhouse *et al*., 2000; Khanna *et al*., 2000; Morton *et al*., 2005). Therefore, selective inhibition of intestinal CES2 might prove useful in ameliorating the intestinal toxicity associated with this drug and further improve the efficacy of therapy.

Regulation of carboxylesterase mRNA levels

As CES enzymes play important roles in both drug activating and inactivating metabolism, the mechanisms that control their expression in liver and small intestine are of particular interest. Two members of the nuclear receptor superfamily of ligand–activated transcription factors, pregnane X receptor (PXR, NR1I2) and constitutive androstane receptor (CAR, NR1I3) have been shown to regulate hepatic and duodenal Ces2a expression in mice treated once daily for 4 days intraperitoneally with the PXR agonist pregnenolone 16α-carbonitrile (PCN), or the CAR agonist 1,4-bis[2-(3,5-dichloropyridyloxy)] benzene (TCPOBOP) (Xu *et al*., 2009). Analogous to previous work on *Ces2a*, Zhang *et al*. (2012) showed that CAR was involved in the induction of hepatic *Ces2a*, *Ces2c* and *Ces3a* in mice of C57BL/6 background treated once daily for four days with TCPOBOP intraperitoneally. In the same study, the authors demonstrated that PXR was required for the induction of hepatic *Ces2a* and *Ces2c* in mice receiving intraperitoneal doses of PCN daily for four days (Zhang *et al*., 2012). These findings were further supported by Jones *et al*. (2012), who showed that oral administration of PCN and TCPOBOP in A129/SvJ mice resulted in increased hepatic and duodenal mRNA levels of *Ces2a*. Treatment with the "sterol-sensing" LXR agonist T1317 resulted in increased mRNA expression of *Ces2a* in mouse liver and duodenum. The duodenal *Ces2a* mRNA levels were also increased by 4.3-fold upon oral administration of an FXR agonist, GW4064 (Jones *et al*., 2013). *Ces2c* mRNA levels were also increased in mice treated with an RXR agonist (LG268), a PPAR-α agonist (GW7647) and an LXR agonist (T1317) (Jones *et al*., 2013). Activation of PPAR-α by its agonist GW7647 resulted in increased expression of *Ces1d*, *Ces1e*, *Ces1f*, *Ces2c* and *Ces2e* in mouse liver. Mice treated with the PPAR-β agonist GW0742 demonstrated increased mRNA levels of hepatic *Ces1e* and *Ces2e* (Jones *et al*., 2013).

Complications in interpreting data generated from various knockout strains

We have previously shown that a range of Ces enzymes is highly upregulated in some of our

knockout strains such as *Abcb1a/1b*(-/-), *Cyp3a*(-/-) and *Abcb1a/1b;Cyp3a*(-/-) mice (Lagas *et al*., 2012). In addition, several knockout strains including *Abcg2*(-/-), *Abcb1a/1b;Abcg2*(-/-) and *Oatp1a/1b*(-/-) mice also show upregulation of several carboxylesterase mRNAs in the liver (Tang *et al*.,unpublished data; Iusuf *et al*. unpublished data). Some members of these carboxylesterases synthesized in the liver of knockout mice lack a C-terminal endoplasmic reticulum retention signal, and can therefore be secreted into the plasma (Holmes *et al*., 2010). This could obviously be a potential source of complications if a drug can be bound or hydrolyzed by these plasma enzymes. It is thus important to determine whether a drug is affected one way or another by mouse Ces enzymes when carrying out pharmacokinetic experiments.

CONCLUSION

Given the increasing number of clinically used drugs and prodrugs that are subject to CES hydrolysis or binding, it is important to understand the pattern of expression and substrate specificity of CESs that are involved in drug metabolism. This information is useful for designing successful ester-containing prodrugs and may help to further improve their oral availability. In addition, by understanding the role of CES in drug metabolism, selective CES inhibitors can be applied to modulate drug metabolism and pharmacokinetics, with the ultimate goal of improving drug therapy.

Conflict of interest: the authors indicated no potential conflict of interest

Acknowledgement of research support: An academic staff training scheme fellowship from the Malaysian Ministry of Higher Education to S.C.T.

REFERENCES

1. Armand JP, Ducreux M, Mahjoubi M, Abigerges D, Bugat R, Chabot G, Herait P, de Forni M and Rougier P (1995) CPT-11 (irinotecan) in the treatment of colorectal cancer. *Eur J Cancer* **31A**:1283-1287.
2. Dolinsky VW, Sipione S, Lehner R and Vance DE (2001) The cloning and expression of a murine triacylglycerol hydrolase cDNA and the structure of its corresponding gene. *Biochim Biophys Acta* **1532**:162-172.
3. Ellinghaus P, Seedorf U and Assmann G (1998) Cloning and sequencing of a novel murine liver carboxylesterase cDNA. *Biochim Biophys Acta* **1397**:175-179.
4. Heinemann V, Hertel LW, Grindey GB and Plunkett W (1988) Comparison of the cellular pharmacokinetics and toxicity of 2',2'-difluorodeoxycytidine and 1-beta-D-arabinofuranosylcytosine. *Cancer Res* **48**:4024-4031.
5. Holmes RS, Wright MW, Laulederkind SJ, Cox LA, Hosokawa M, Imai T, Ishibashi S, Lehner R, Miyazaki M, Perkins EJ, Potter PM, Redinbo MR, Robert J, Satoh T, Yamashita T, Yan B, Yokoi T, Zechner R and Maltais LJ (2010) Recommended nomenclature for five mammalian carboxylesterase gene families: human, mouse, and rat genes and proteins. *Mamm Genome* **21**:427-441.
6. Hosokawa M, Suzuki K, Takahashi D, Mori M, Satoh T and Chiba K (2001) Purification, molecular cloning, and functional expression of dog liver microsomal acyl-CoA hydrolase: a member of the carboxylesterase multigene family. *Arch Biochem Biophys* **389**:245-253.
7. Humerickhouse R, Lohrbach K, Li L, Bosron WF and Dolan ME (2000) Characterization of CPT-11 hydrolysis by human liver carboxylesterase isoforms hCE-1 and hCE-2. *Cancer Res* **60**:1189-1192.

8. Jones RD, Taylor AM, Tong EY and Repa JJ (2013) Carboxylesterases are uniquely expressed among tissues and regulated by nuclear hormone receptors in the mouse. *Drug Metab Dispos* **41**:40-49.
9. Kamendulis LM, Brzezinski MR, Pindel EV, Bosron WF and Dean RA (1996) Metabolism of cocaine and heroin is catalyzed by the same human liver carboxylesterases. *J Pharmacol Exp Ther* **279**:713-717.
10. Khanna R, Morton CL, Danks MK and Potter PM (2000) Proficient metabolism of irinotecan by a human intestinal carboxylesterase. *Cancer Res* **60**:4725-4728.
11. Krishnasamy S, Teng AL, Dhand R, Schultz RM and Gross NJ (1998) Molecular cloning, characterization, and differential expression pattern of mouse lung surfactant convertase. *Am J Physiol* **275**:L969-L975.
12. Lagas JS, Damen CW, van Waterschoot RA, Iusuf D, Beijnen JH and Schinkel AH (2012) P-glycoprotein, multidrug-resistance associated protein 2, Cyp3a, and carboxylesterase affect the oral availability and metabolism of vinorelbine. *Mol Pharmacol* **82**:636-644.
13. Li B, Sedlacek M, Manoharan I, Boopathy R, Duysen EG, Masson P and Lockridge O (2005) Butyrylcholinesterase, paraoxonase, and albumin esterase, but not carboxylesterase, are present in human plasma. *Biochem Pharmacol* **70**:1673-1684.
14. Miwa M, Ura M, Nishida M, Sawada N, Ishikawa T, Mori K, Shimma N, Umeda I and Ishitsuka H (1998) Design of a novel oral fluoropyrimidine carbamate, capecitabine, which generates 5-fluorouracil selectively in tumours by enzymes concentrated in human liver and cancer tissue. *Eur J Cancer* **34**:1274-1281.
15. Morton CL, Iacono L, Hyatt JL, Taylor KR, Cheshire PJ, Houghton PJ, Danks MK, Stewart CF and Potter PM (2005) Activation and antitumor activity of CPT-11 in plasma esterase-deficient mice. *Cancer Chemother Pharmacol* **56**:629-636.
16. Munger JS, Shi GP, Mark EA, Chin DT, Gerard C and Chapman HA (1991) A serine esterase released by human alveolar macrophages is closely related to liver microsomal carboxylesterases. *J Biol Chem* **266**:18832-18838.
17. Ovnic M, Swank RT, Fletcher C, Zhen L, Novak EK, Baumann H, Heintz N and Ganschow RE (1991) Characterization and functional expression of a cDNA encoding egasyn (esterase-22): the endoplasmic reticulum-targeting protein of beta-glucuronidase. *Genomics* **11**:956-967.
18. Parathath S, Dogan S, Joaquin VA, Ghosh S, Guo L, Weibel GL, Rothblat GH, Harrison EH and Fisher EA (2011) Rat carboxylesterase ES-4 enzyme functions as a major hepatic neutral cholesteryl ester hydrolase. *J Biol Chem* **286**:39683-39692.
19. Pindel EV, Kedishvili NY, Abraham TL, Brzezinski MR, Zhang J, Dean RA and Bosron WF (1997) Purification and cloning of a broad substrate specificity human liver carboxylesterase that catalyzes the hydrolysis of cocaine and heroin. *J Biol Chem* **272**:14769-14775.
20. Pratt SE, Durland-Busbice S, Shepard RL, Heinz-Taheny K, Iversen PW and Dantzig AH (2013) Human Carboxylesterase-2 Hydrolyzes the Prodrug of Gemcitabine (LY2334737) and Confers Prodrug Sensitivity to Cancer Cells. *Clin Cancer Res* **19**:1159-1168.
21. Quinney SK, Sanghani SP, Davis WI, Hurley TD, Sun Z, Murry DJ and Bosron WF (2005) Hydrolysis of capecitabine to 5'-deoxy-5-fluorocytidine by human carboxylesterases and inhibition by loperamide. *J Pharmacol Exp Ther* **313**:1011-1016.
22. Quiroga AD and Lehner R (2011) Role of endoplasmic reticulum neutral lipid hydrolases. *Trends Endocrinol Metab* **22**:218-225.
23. Redinbo MR and Potter PM (2005) Mammalian carboxylesterases: from drug targets to protein therapeutics. *Drug Discov Today* **10**:313-325.
24. Satoh T and Hosokawa M (2006) Structure, function and regulation of carboxylesterases. *Chem Biol Interact* **162**:195-211.
25. Satoh T, Taylor P, Bosron WF, Sanghani SP, Hosokawa M and La Du BN (2002) Current progress on esterases: from molecular structure to function. *Drug Metab Dispos* **30**:488-493.
26. Schreiber R, Taschler U, Wolinski H, Seper A, Tamegger SN, Graf M, Kohlwein SD, Haemmerle G, Zimmermann R, Zechner R and Lass A (2009) Esterase 22 and beta-glucuronidase hydrolyze retinoids in mouse liver. *J Lipid Res* **50**:2514-2523.
27. Schwer H, Langmann T, Daig R, Becker A, Aslanidis C and Schmitz G (1997) Molecular cloning and characterization of a novel putative carboxylesterase, present in human intestine and liver. *Biochem Biophys Res Commun* **233**:117-120.

28. Staudinger JL, Woody S, Sun M and Cui W (2013) Nuclear-receptor-mediated regulation of drug- and bile-acid-transporter proteins in gut and liver. *Drug Metab Rev* **45**:48-59.
29. Takai S, Matsuda A, Usami Y, Adachi T, Sugiyama T, Katagiri Y, Tatematsu M and Hirano K (1997) Hydrolytic profile for ester- or amide-linkage by carboxylesterases pI 5.3 and 4.5 from human liver. *Biol Pharm Bull* **20**:869-873.
30. Taketani M, Shii M, Ohura K, Ninomiya S and Imai T (2007) Carboxylesterase in the liver and small intestine of experimental animals and human. *Life Sci* **81**:924-932.
31. Xu C, Wang X and Staudinger JL (2009) Regulation of tissue-specific carboxylesterase expression by pregnane x receptor and constitutive androstane receptor. *Drug Metab Dispos* **37**:1539-1547.
32. Zhang Y, Cheng X, Aleksunes L and Klaassen CD (2012) Transcription factor-mediated regulation of carboxylesterase enzymes in livers of mice. *Drug Metab Dispos* **40**:1191-1197.

CHAPTER 2

PHARMACOKINETIC STUDIES ON TYROSINE KINASE INHIBITORS

2.1

BRAIN ACCUMULATION OF SUNITINIB IS RESTRICTED BY P-GLYCOPROTEIN (ABCB1) AND BREAST CANCER RESISTANCE PROTEIN (ABCG2) AND CAN BE ENHANCED BY ORAL ELACRIDAR AND SUNITINIB COADMINISTRATION

Seng Chuan Tang[1], Jurjen S. Lagas[1,2], Nienke A.G. Lankheet[2], Birk Poller[1], Michel J. Hillebrand[2], Hilde Rosing[2], Jos H. Beijnen[2], and Alfred H. Schinkel[1]

[1]Division of Molecular Biology, The Netherlands Cancer Institute, Amsterdam, The Netherlands
[2]Department of Pharmacy and Pharmacology, Slotervaart Hospital, Amsterdam, The Netherlands

Int J Cancer. 2012; 130(1): 223-33.

ABSTRACT

Sunitinib is an orally active, multi-targeted tyrosine kinase inhibitor which has been used for the treatment of metastatic renal cell carcinoma and imatinib-resistant gastrointestinal stromal tumors. We aimed to investigate the *in vivo* roles of the ATP-binding cassette drug efflux transporters ABCB1 and ABCG2 in plasma pharmacokinetics and brain accumulation of oral sunitinib, and the feasibility of improving sunitinib kinetics using oral coadministration of the dual ABCB1/ABCG2 inhibitor elacridar. We used *in vitro* transport assays and *Abcb1a/1b*$^{-/-}$, *Abcg2*$^{-/-}$ and *Abcb1a/1b/Abcg2*$^{-/-}$ mice to study the roles of ABCB1 and ABCG2 in sunitinib disposition. *In vitro*, sunitinib was a good substrate of murine (mu)ABCG2 and a moderate substrate of human (hu)ABCB1 and huABCG2. *In vivo*, the systemic exposure of sunitinib after oral dosing (10 mg kg^{-1}) was unchanged when muABCB1 and/or muABCG2 were absent. Brain accumulation of sunitinib was markedly (23-fold) increased in *Abcb1a/b/Abcg2*$^{-/-}$ mice, but only slightly (2.3-fold) in *Abcb1a/b*$^{-/-}$ mice, and not in *Abcg2*$^{-/-}$ mice. Importantly, a clinically realistic coadministration of oral elacridar and oral sunitinib to wild-type mice resulted in dramatically increased sunitinib brain accumulation, equaling levels in *Abcb1a/1b/Abcg2*$^{-/-}$ mice. This indicates complete inhibition of the blood-brain barrier transporters. High-dose intravenous sunitinib could saturate blood-brain barrier muABCG2, but not muABCB1A, illustrating a dose-dependent relative impact of the blood-brain barrier transporters. Brain accumulation of sunitinib is effectively restricted by both muABCB1 and muABCG2 activity. Complete inhibition of both transporters, leading to dramatically increased brain accumulation of sunitinib, is feasible and safe with a clinically realistic oral elacridar/sunitinib coadministration.

INTRODUCTION

ATP-binding cassette (ABC) drug efflux transporters, such as P-glycoprotein (P-gp; ABCB1), breast cancer resistance protein (BCRP; ABCG2) and multidrug resistance protein 2 (MRP2; ABCC2) play important roles in the absorption, distribution, excretion, and toxicity of xenobiotics.[1] Several groups have shown that many tyrosine kinase inhibitors (TKIs) used in cancer therapy are substrates of both ABCB1 and ABCG2,[2-4] suggesting that the interaction with these ABC transporters may also affect pharmacokinetics and toxicity of TKIs in patients. Especially the brain accumulation of a number of TKIs, including dasatinib, lapatinib, imatinib, sorafenib, gefitinib, tandutinib and erlotinib, appears to be importantly affected by both transporters.[5-11] Enhanced penetration of drugs across the blood-brain barrier (BBB) may improve the drug exposure (and hence therapeutic efficacy) of proliferating brain tumor margins or tumor micrometastases that are behind a functionally intact BBB. Therefore, there is currently great interest in strategies to improve the BBB permeation of anticancer drugs, especially (but not only) TKIs.[4,6-8,10]

The TKI sunitinib malate (SU11248; SUTENT) is an orally active, small-molecule

ATP-competitive multi-targeted inhibitor of vascular endothelial growth factor receptors type 1 and 2, the platelet-derived growth factor receptors α and β, the stem cell factor receptor c-KIT, FMS-like TK-3 receptor, and the glial cell-line derived neurotrophic factor receptor.[12] Sunitinib is approved by the Food and Drug Administration for the treatment of advanced or metastatic renal cell carcinoma (RCC) and imatinib-resistant gastrointestinal stromal tumors.[13,14] Patients diagnosed with RCC often show a high prevalence of metastases..[15] One of the metastatic sites of particular interest in these patients is brain and brain metastasis significantly contributes to mortality.[16] However, little is known about the effectiveness of sunitinib in RCC patients with brain metastases, since patients with cerebral lesions were excluded in those studies.[17-19] Currently, sunitinib is being tested in a phase II trial of recurrent glioblastoma multiforme (http://clinicaltrials.gov/ct2/show/NCT00535379).

Clinically, sunitinib is administered orally.[20] Oral application of TKIs is particularly important in view of patient comfort, health care costs and the need for a relatively continuous treatment schedule. ABC transporters may affect both oral availability and brain accumulation of TKIs, and their interaction with sunitinib is therefore of great interest. To date, several studies have demonstrated interactions of sunitinib with ABC efflux transporters.[21-24] First, Dai *et al*. showed that sunitinib completely reverses ABCG2-mediated multidrug resistance through inhibition of the drug efflux function of ABCG2.[21] Shukla *et al*. demonstrated that sunitinib is able to interact at the substrate binding pocket of ABCB1 and ABCG2, with higher affinity for ABCG2 compared with ABCB1.[22] Furthermore, Hu *et al*. showed *in vitro* transport of sunitinib by ABCB1, but not by ABCG2, and that the absence of *Abcb1a/1b* in mice had no effect on plasma pharmacokinetics, whereas brain accumulation was moderately increased by 2.9-fold in *Abcb1a/1b* knockout animals versus controls.[23] The recent demonstration that ABCB1-mediated efflux was specifically abrogated by siRNA knockdown of *ABCB1* expression in a K562/Dox cell line further supported that sunitinib is transported by human ABCB1.[24]

ABC efflux transporters can have a profound effect on oral availability, tissue distribution, elimination, and tumor cell penetration of substrate anticancer drugs, and hence on their optimal pharmacological application, therapeutic efficacy, and toxicity.[1,25] The aim of this study was to establish to what extent sunitinib is transported by huABCB1, huABCG2, huABCC2, muABCG2 and muABCC2 *in vitro*, and what the consequences are for oral availability and brain accumulation of sunitinib as judged in knockout mouse models. Furthermore, we tested whether, in a clinically realistic coadministration schedule of oral sunitinib and oral elacridar (a dual ABCB1 and ABCG2 inhibitor), either of these parameters could be improved, with the ultimate aim of improving therapeutic efficacy. We also aimed to obtain better insight into the factors that determine the relative impact of ABCB1 and ABCG2 on the brain accumulation of sunitinib, as such insights may help efforts to overcome the BBB for therapeutic purposes.

MATERIALS AND METHODS

Chemicals and Reagents

Sunitinib malate was purchased from Sequoia Research Products (Pangbourne, UK). Elacridar hydrochloride was kindly provided by GlaxoSmithKline (Stevenage, UK). [^{14}C] Inulin was obtained from Amersham (Little Chalfont, UK). Methoxyflurane (Metofane®) was supplied by Medical Developments Australia (Melbourne, Australia). Heparin (5000 IU ml^{-1}) was obtained from Leo Pharma BV (Breda, the Netherlands). Bovine serum albumin (BSA), fraction V, was purchased from Roche (Mannheim, Germany). High-performance liquid chromatography grade acetonitrile and methanol were purchased from Biosolve (Valkenswaard, The Netherlands). Ammonia 25% was purchased from Merck (Darmstadt, Germany). The stable isotope labeled sunitinib was purchased from AlsaChim (Illkirch, France). All other chemicals and reagents were obtained from Sigma-Aldrich (Steinheim, Germany).

Cell lines and transport assays

Polarized Madin-Darby Canine Kidney-II (MDCK-II) cells and MDCK-II subclones transduced with hu*ABCB1*, hu*ABCC2*, hu*ABCG2*, mu*Abcc2* or mu*Abcg2* cDNA were used and cultured as described previously.[26-30] Transepithelial transport assays were performed on microporous polycarbonate membrane filters (3.0 µm pore size, 24 mm diameter, Transwell 3414, Costar, Cambridge, MA) as described.[6,31] Active transport was expressed by the relative transport ratio (*r*), defined as *r* = percentage apically directed transport divided by basolaterally directed translocation after 4 hr.

Animals

Mice were housed and handled according to institutional guidelines complying with Dutch legislation. Male wild-type, *Abcb1a/1b*$^{-/-}$,[32] *Abcg2*$^{-/-}$,[27] and *Abcb1a/1b/Abcg2*$^{-/-}$ mice,[33] all of a >99% FVB genetic background, were used between 10 and 14 weeks of age. Animals were kept in a temperature-controlled environment with a 12-hr light/12-hr dark cycle and they received a standard diet (AM-II, Hope Farms B.V., Woerden, The Netherlands) and acidified water *ad libitum*.

Drug solutions

For oral administration, sunitinib malate was dissolved in dimethyl sulfoxide (DMSO) at a concentration of 25 mg ml^{-1} and further diluted with 50 mM sodium acetate buffer (pH 4.6) to yield a concentration of 1.5 mg ml^{-1}. For intravenous administration, sunitinib malate was dissolved in DMSO at a concentration of 75 mg ml^{-1} and further diluted with 50 mM sodium acetate buffer (pH 4.6) to yield a concentration of 4, 6, 8 and 10 mg ml^{-1}. Elacridar hydrochloride was dissolved in DMSO at a concentration of 150 mg ml^{-1} and further diluted with 50 mM sodium acetate buffer (pH 4.6) to yield a concentration of 15 mg ml^{-1}.

Sunitinib plasma and brain pharmacokinetics

To minimize variation in absorption on oral administration, mice were fasted for 4 hr before sunitinib malate was administered by gavage into the stomach, using a blunt-ended needle. Multiple blood samples (~50 µl) were collected from the tail vein at 15 and 30 min, and 1, 2, and 4 hr, using lithium-heparinized capillary tubes (Sarstedt, Numbrecht, Germany). At 6 hr, mice were

anesthetized with isoflurane and blood was collected by cardiac puncture. Immediately thereafter mice were sacrificed by cervical dislocation and brains were rapidly removed. Brains were homogenized with 1 ml of 4% BSA and stored at -20°C until analysis. Blood samples were centrifuged at 2,100 *g* for 6 min at 4°C, and the plasma fraction was collected and stored at -20°C until analysis. Brain accumulation was corrected for the amounts of drug in the brain vasculature (*i.e.*, 1.4% of the plasma concentration right before the brains were isolated).[3] Brain accumulation after oral administration was calculated by determining the sunitinib brain concentration at 6 hr relative to the plasma $AUC_{0\text{-}6,}$ as the AUC better reflects the overall sunitinib exposure of the brain over time than the plasma concentration at 6 hr after administration.

Brain accumulation of oral sunitinib in combination with oral elacridar treatment

Mice were fasted for 4 hr before oral administration of either elacridar or elacridar vehicle. Two hours later, sunitinib malate was administered orally. One hour after sunitinib malate administration, mice were anesthetized with methoxyflurane and blood was collected by cardiac puncture. Immediately thereafter mice were sacrificed and blood and brains were processed as described above.

Plasma pharmacokinetics of intravenous sunitinib in mice

FVB wild-type mice received 20 mg kg^{-1} of sunitinib malate by intravenous administration in the tail vein. At 3, 10, 30 and 60 min after administration animals were anesthetized with isoflurane and blood was collected by cardiac puncture. Immediately thereafter mice were sacrificed and blood and brains were processed as described above.

Saturation of BBB efflux transport by sunitinib

To determine the maximum tolerated dose of sunitinib, mice received a single intravenous bolus of sunitinib malate at doses of 20, 30, 40 and 50 mg kg^{-1} body weight. Sunitinib malate at 20 mg kg^{-1} was selected for the following experiment. At 10 min or 1 hr after sunitinib malate intravenous administration mice were anesthetized with isoflurane and blood was collected by cardiac puncture. Immediately thereafter mice were sacrificed and blood and brains were processed as described above.

Drug Analysis

Sunitinib concentrations in plasma and brain homogenates were determined using a sensitive and specific liquid chromatography coupled with tandem mass spectrometry (LC-MS/MS) assay. Chromatography was carried out using a solvent delivery system LC-20AD Prominence (Shimadzu, Kyoto, Japan), consisting of an autosampler, binary pump, degasser and column oven. Chromatographic separations of the analytes were carried out on a Gemini C18 column, 50 × 2.0 mm internal diameter (Phenomenex, Torrance, CA). A mobile phase consisting of eluent A (10 mM ammonium hydroxide in water) and eluent B (1 mM ammonium hydroxide in methanol) was pumped through the column with a flow of 0.25 ml min^{-1}. Gradient elution was used starting with 55% eluent B for 0.5 min. A linear gradient was applied from 0.5 to 3.0 min (from 55% to 80% eluent B) and from 6.0 to 6.1 min (from 80%

to 100% eluent B). The percentage of eluent B was reduced to 55% from 8.0 to 8.1 min and the column was reconditioned for 4 min before the next injection. The retention time for sunitinib was 5.2 min. The mass spectrometric analyses were performed using a Finnigan TSQ Quantum Ultra Triple Quadrupole Spectrometer equipped with an electrospray ion source (Thermo Fisher, Waltham, MA). The mass spectrometer was operating in positive mode, and, using selective multiple reaction monitoring at unit resolution, sunitinib was detected at the transition from m/z 399 to 283, and the stable labeled isotope $^{2}H_{10}$-sunitinib from m/z 409 to 283 (used as internal standard). Samples were pretreated with acetonitrile to precipitate the proteins, and the supernatants were diluted 1:1, v/v (sample extract: eluent A) before injection (10 µl).

Pharmacokinetic calculations and statistical analysis

Pharmacokinetic parameters were calculated by noncompartmental methods using the software package PK Solutions 2.0.2 (Summit Research Services, Ashland, OH). The area under the plasma concentration-time curve was calculated using the trapezoidal rule, without extrapolating to infinity. The maximum drug concentration in plasma (C_{max}) and the time to reach maximum drug concentration in plasma (T_{max}) were determined directly from individual concentration-time data. Data are presented as means ± SD. One-way analysis of variance (ANOVA) was used to determine significance between groups, after which post-hoc tests with Bonferroni correction were performed for comparison between individual groups. For relative brain accumulation, Student's *t*-test (unpaired, two-tailed) was used to determine the significance between *Abcb1a/1b*$^{-/-}$ and wild-type mice. Differences were considered statistically significant when $P < 0.05$.

RESULTS

In vitro transport of sunitinib

In the parental MDCK-II cells there was no significant polarized transport of sunitinib (Fig. 1*a*). In cells overexpressing huABCB1 and huABCG2, there was clear apically directed transport of sunitinib (Figs. 1*b* and 1c), whereas in cells expressing muABCG2 (Fig. 1*d*) transport was very high. Addition of 5 µM elacridar, a potent dual inhibitor of ABCB1 and ABCG2, resulted in complete inhibition of polarized sunitinib transport in all these cell lines (Figs. 1e-1*h*). Sunitinib was not significantly transported by human or murine ABCC2 (Figs. 1*i* and 1*j*). Elacridar, which is not a significant huABCC2 and muABCC2 inhibitor at 5 µM,[6] was added in the latter assays to suppress any transport of sunitinib by low-level endogenous canine ABCB1.

Effect of muABCB1 and muABCG2 on plasma pharmacokinetics of sunitinib in mice

Since sunitinib is given orally to cancer patients, we first studied the plasma concentration of sunitinib over time after oral administration at 10 mg kg^{-1} to wild-type, *Abcb1a/1b*$^{-/-}$, *Abcg2*$^{-/-}$ and *Abcb1a/1b/Abcg2*$^{-/-}$ mice (Fig. 2*a*). As shown in Figure 2*a* and Table 1, there were no statistically significant differences in oral $AUC_{(0\text{-}6)}$ among all strains. Other systemic parameters (C_{max} and T_{max}) of all knockout strains were also not statistically significantly changed compared to wild-type values (Table 1). These results indicate that muABCB1 and muABCG2 do not

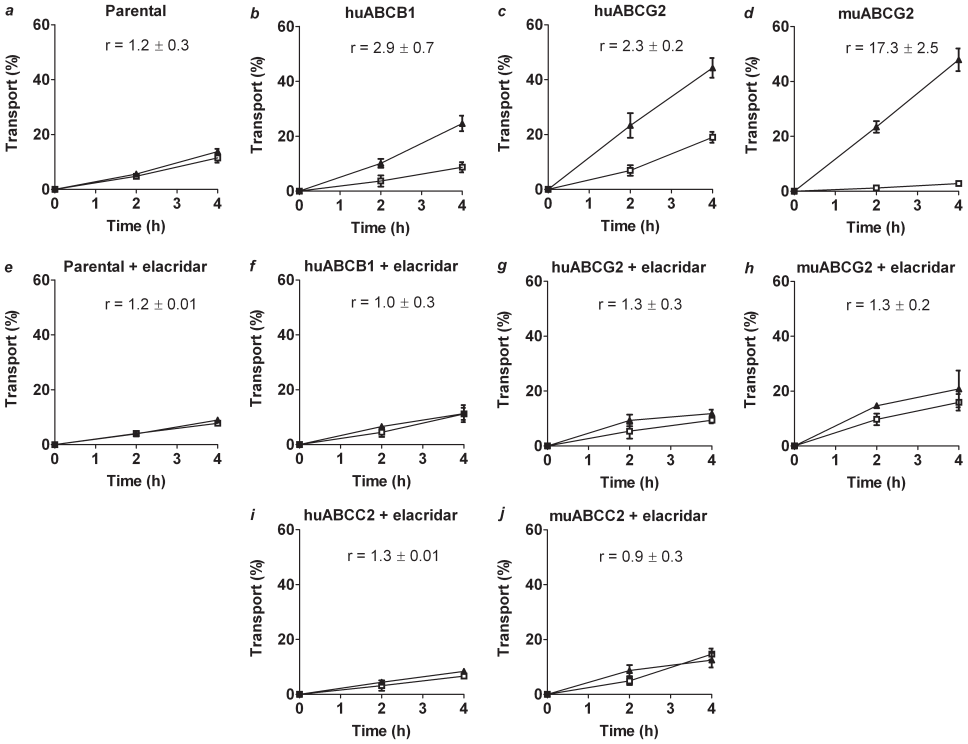

Figure 1. Transepithelial transport of sunitinib (5 μM) was assessed using either MDCK-II parental cells (*a* and *e*) or MDCK-II cells transduced with hu*ABCB1* (*b* and *f*), hu*ABCG2* (*c* and *g*), mu*Abcg2* (*d* and *h*), hu*ABCC2* (*i*) or mu*Abcc2* (*j*) cDNA. At *t* = 0 hr, sunitinib was applied in one compartment (apical or basolateral), and the amount of drug appearing in the opposite compartment at *t* = 2 and 4 hr was measured by LC-MS/MS and plotted as the percentage of the amount of initially applied drug. Elacridar (5 μM) was applied to inhibit huABCB1, huABCG2, or muABCG2 (*e*–*h*) or endogenous canine ABCB1 (*i* and *j*). ▲, translocation from basolateral to apical compartment; □, translocation from apical to basolateral compartment. Points, mean (n = 3); bars, SD. At *t* = 4 hr, 1% of transport is approximately equal to an apparent permeability coefficient (P_{app}) of 0.30×10^{-6} cm s^{-1}.

have a substantial role in the oral availability of sunitinib.

Effect of muABCB1 and muABCG2 on brain accumulation of sunitinib in mice

As shown in Figure 2*b*, the relative brain accumulation, determined 6 hr after oral administration and corrected for the plasma $AUC_{0\text{-}6}$, was not significantly different in *Abcb1a/1b*$^{-/-}$ and *Abcg2*$^{-/-}$ mice as compared with wild-type mice using the ANOVA test. Hu *et al*. previously found that the sunitinib brain concentration was significantly increased by 2.9-fold in *Abcb1a/1b*$^{-/-}$ mice as compared with wild-type mice.[23] Indeed, we found a 2.3-fold increase in brain concentration of sunitinib in *Abcb1a/1b*$^{-/-}$ mice, which was statistically significant when compared to wild-type values using the Student's *t*-test (*P* = 0.038; Table 1). Thus,

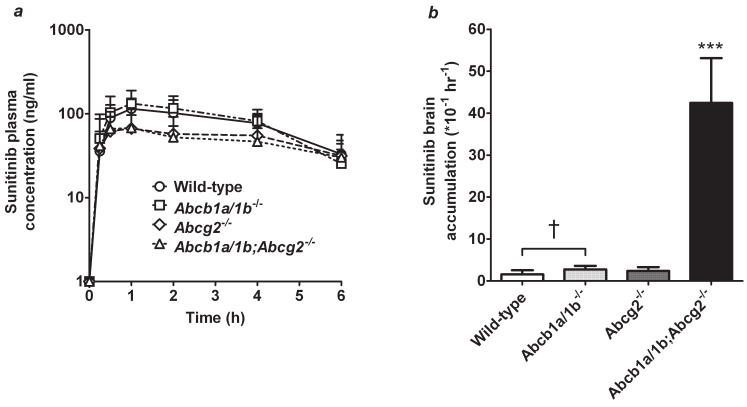

Figure 2. Plasma concentration-time curves (*a*) and relative brain accumulation at t = 6 hr (*b*) of sunitinib in male wild-type, *Abcb1a/1b*$^{-/-}$, *Abcg2*$^{-/-}$ and *Abcb1a/1b/Abcg2*$^{-/-}$ mice after oral administration of 10 mg kg^{-1} sunitinib malate. Relative brain accumulation was calculated by dividing brain concentration by the $AUC_{0\text{-}6}$ and analyzed using Student's t-test. Points, mean (n = 6-8); bars, SD. Columns, mean (n = 6-8); bars, SD. ***, $P < 0.001$, compared with wild-type mice (one-way ANOVA); †, $P < 0.05$, compared with wild-type mice (Student's t-test).

although muABCB1 and muABCG2 appear to be largely redundant, muABCG2 is unable to fully take over muABCB1 function at the BBB. In contrast to the small shifts observed in the single knockout mice, *Abcb1a/b/Abcg2*$^{-/-}$ mice had a 27–fold increase in brain accumulation relative to wild-type mice ($P < 0.001$; Table 1). These results indicate that brain accumulation of sunitinib was primarily restricted by both muABCB1 and muABCG2, with muABCB1 being slightly more important (see also below). Apparently, each of these transporters can to a large extent take over the function of the other transporter at the BBB. Only when both transporters are absent simultaneously, a very large increase in brain accumulation of sunitinib can occur.

Effect of the dual ABCB1 and ABCG2 inhibitor elacridar on sunitinib brain accumulation

We wanted to assess to what extent the dual ABCB1 and ABCG2 inhibitor elacridar could modulate the oral availability and brain accumulation of sunitinib. In view of the potential clinical importance of oral application for both sunitinib and elacridar, we administered elacridar (100 mg kg^{-1}) orally 2 hr prior to oral sunitinib malate (10 mg kg^{-1}) to the wild-type and *Abcb1a/1b/Abcg2*$^{-/-}$ strains, and assessed plasma and brain sunitinib levels 1 hr later, *i.e.*, around the sunitinib T_{max}. As shown in Figure 3*a*, sunitinib plasma concentrations were not significantly different among the strains, regardless of administration with or without elacridar. In vehicle-treated mice, brain concentrations of sunitinib in *Abcb1a/1b/Abcg2*$^{-/-}$ mice were 9.8-fold increased compared with wild-type values, but brain concentrations of sunitinib were not significantly increased in *Abcb1a/1b*$^{-/-}$ and *Abcg2*$^{-/-}$ mice as tested by ANOVA (Fig. 3*b*). However, elacridar treatment drastically increased brain concentrations in wild-type mice (12-fold), to levels equal to those in

Table 1. Pharmacokinetic parameters, brain concentrations, and relative brain accumulation of sunitinib after oral administration of 10 mg kg^{-1} sunitinib malate to various mouse strains

	Genotype			
	Wild-type	***Abcb1a/1b*$^{-/-}$**	***Abcg2*$^{-/-}$**	***Abcb1a/1b;Abcg2*$^{-/-}$**
$AUC_{(0-6)}$, ng ml^{-1} hr^{-1}	445.4 ± 202.8	513.9 ± 144.9	310.9 ± 171.6	287.8 ± 87.7
Fold increase $AUC_{(0-6)}$	1.00	1.15	0.70	0.65
C_{max}, ng ml^{-1}	114.8 ± 38.1	132.2 ± 56.8	66.9 ± 46.1	67.7 ± 29.2
T_{max}, hr	1.0	1.0	1.0	1.0
C_{brain}, ng g^{-1}	57.8 ± 10.9	133.2 ± 32.1†††	75.1 ± 44.8	1353.7 ± 557.6***
Fold increase C_{brain}	1.0	2.3	1.3	23.4
P_{brain} (*10^{-1} hr^{-1})	1.6 ± 1.0	2.8 ± 0.8†	2.4 ± 0.9	42.4 ± 10.7***
Fold increase P_{brain}	1.0	1.7	1.5	26.9

Data are means ± SD (n = 6-8). All parameters obtained for knockout strains were compared with those for wild-type mice.
***, $P < 0.001$, compared with wild-type mice (one-way ANOVA); †, $P < 0.05$, †††, $P < 0.001$ compared with wild-type mice (Student's *t*-test).
Abbreviations: AUC, area under plasma concentration-time curve; C_{max}, maximum plasma concentration; T_{max}, time to reach maximum drug concentration in plasma; C_{brain}, brain concentration at 6 hr after oral administration; P_{brain}, relative brain accumulation at 6 hr after oral administration, calculated by determining the sunitinib brain concentration relative to the $AUC_{(0-6)}$.

Abcb1a/1b/Abcg2$^{-/-}$ mice (Fig. 3*b*). The sunitinib brain concentrations in *Abcb1a/1b/Abcg2*$^{-/-}$ mice were not significantly affected by elacridar treatment. Very similar results were obtained when the brain-to-plasma ratios at $t = 1$ hr were plotted (Supporting Information Fig. 1). These data indicate that oral elacridar treatment could completely and specifically inhibit the activity of muABCB1 and muABCG2 in the BBB, leading to highly increased sunitinib concentrations in the brain. Moreover, we did not observe any significant acute toxicity effects of the coadministration of oral elacridar and sunitinib malate, either behavioral, or upon dissection of the animals (see below for acute sunitinib toxicity effects). This suggests that this coadministration regimen may be relatively safe, at least in mice.

Plasma pharmacokinetics and brain accumulation of intravenous sunitinib in mice

In efforts to saturate the ABC transporter activity in the BBB of mice by giving high intravenous dosages of sunitinib (see below), we observed a surprisingly low plasma clearance rate. A very low clearance rate of sunitinib from plasma has previously been reported in rats and monkeys.[34] We therefore analyzed plasma and brain pharmacokinetics of sunitinib in FVB wild-type mice after an intravenous administration of sunitinib malate (20 mg kg^{-1}). Sunitinib was fairly rapidly distributing from plasma until about 10 min, but then the plasma clearance rate became very low up to at least 1 hr (Supporting Information Fig. 2A). Interestingly, the brain accumulation of sunitinib was already high at 3 min in wild-type mice, and subsequently

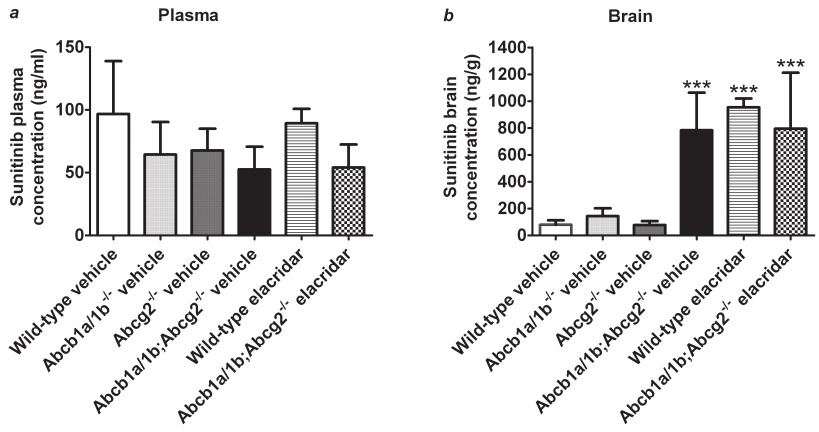

Figure 3. Plasma (*a*) and brain (*b*) concentrations of sunitinib for male wild-type, *Abcb1a/1b*$^{-/-}$, *Abcg2*$^{-/-}$ and *Abcb1a/1b/Abcg2*$^{-/-}$ mice 1 hr after oral administration of 10 mg kg^{-1} sunitinib malate. Sunitinib malate was administered 2 hr after the oral administration of either elacridar (100 mg kg^{-1}) or elacridar vehicle. Columns, means (n = 5); bars, SD. ***, $P < 0.001$, compared with wild-type mice (one-way ANOVA). None of the plasma concentrations in Fig. 3*a* differed significantly from the wild-type vehicle values.

decreased slowly (Supporting Information Fig. 2B). This indicates that, upon intravenous administration, there is a very rapid initial accumulation of sunitinib in the brain, followed by a relatively low clearance rate.

Saturation of muABCG2-mediated sunitinib transport in the BBB of mice

The observation that shared muABCB1 and muABCG2 substrates show only a very small, or even undetectable increase in brain accumulation in single knockout mice, but a very marked increase in combination knockout mice is quite common.[5,6,8,35] We reasoned that a possible difference in *in vivo* efficacy of muABCB1 and muABCG2 at the BBB might become more obvious if we could saturate one (or both) of the transporters with high plasma levels of the drug. Pilot experiments indicated that 20 mg kg^{-1} was the highest intravenous sunitinib dose tolerated by all mouse strains. At doses above 20 mg kg^{-1}, we observed dilated blood vessels throughout the body and brain hemorrhage, often resulting in rapid lethal effects (data not shown). The knockout strains were not more susceptible than the wild-type mice, suggesting that muABCB1 and muABCG2 are not limiting for this high-dose acute toxicity. We therefore applied sunitinib intravenously at 20 mg kg^{-1} and determined plasma and brain sunitinib levels at 10 min and 1 hr in wild-type, *Abcb1a/1b*$^{-/-}$, *Abcg2*$^{-/-}$, and *Abcb1a/1b/Abcg2*$^{-/-}$ mice. In line with the very low sunitinib plasma clearance rate after 10 min (Supporting Information Fig. 2A), plasma concentrations hardly decreased between 10 min and 1 hr (Figs. 4*a* and 4*b*). They also did not differ between the strains, suggesting that muABCB1 and muABCG2 have also little impact on the intravenous clearance of sunitinib. Interestingly, however, comparison of Figures 4c and 2*b* shows that the pattern of sunitinib brain concentrations between the strains at t = 10 min was now qualitatively different from

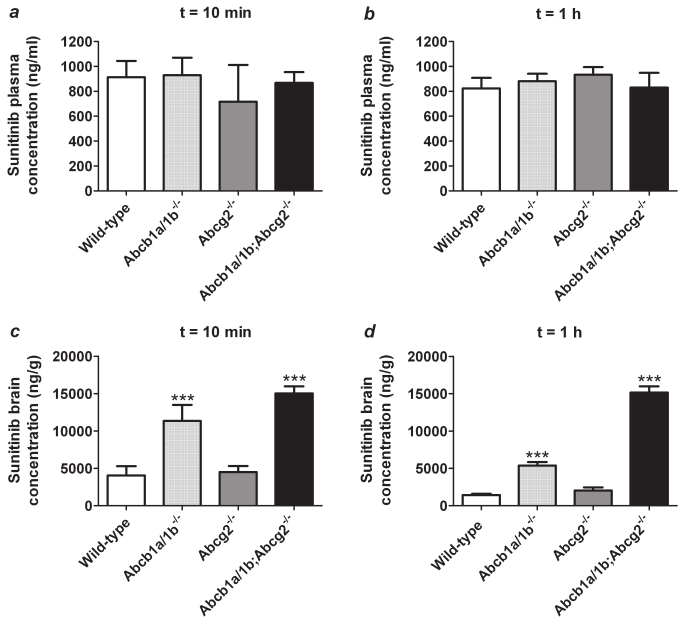

Figure. **4.** Upper panels, plasma concentrations of sunitinib in male wild-type, *Abcb1a/1b*$^{-/-}$, *Abcg2*$^{-/-}$ and Abcb1a/1b/Abcg2$^{-/-}$ mice 10 min (*a*) or 1 hr (*b*) after intravenous injection of 20 mg kg^{-1} sunitinib malate. Lower panels, brain concentrations of sunitinib in male wild-type, *Abcb1a/1b*$^{-/-}$, *Abcg2*$^{-/-}$ and *Abcb1a/1b/Abcg2*$^{-/-}$ mice 10 min (*c*) or 1 hr (*d*) after intravenous injection of 20 mg kg^{-1} sunitinib malate. Columns, means (n = 5); bars, SD. ***, $P < 0.001$, compared with wild-type mice (one-way ANOVA).

that observed after oral dosing (and thus much lower plasma exposure). Brain levels in the *Abcb1a/1b*$^{-/-}$ mice were now markedly higher than in wild-type, and nearly equal to those in *Abcb1a/1b/Abcg2*$^{-/-}$ mice, whereas brain levels in *Abcg2*$^{-/-}$ mice were still equal to those in wild-type mice (Fig. 4*c*). At 1 hr, brain levels in wild-type, *Abcb1a/1b*$^{-/-}$ and *Abcg2*$^{-/-}$ mice had all clearly decreased relative to 10 min, but in *Abcb1a/1b/Abcg2*$^{-/-}$ mice they were still virtually unchanged (Fig. 4*d*). Moreover, the brain concentration in *Abcb1a/1b*$^{-/-}$ mice, while still markedly higher than that in wild-type mice, was now clearly reduced compared to that in *Abcb1a/1b/Abcg2*$^{-/-}$ mice (Fig. 4*d*). These data suggest that at very high initial sunitinib plasma concentrations (*i.e.*, before 10 min, see also Supporting Information Fig. 2), BBB muABCG2 (in the *Abcb1a/1b*$^{-/-}$ mice) was virtually completely saturated, resulting in brain accumulation levels similar to those in *Abcb1a/1b/Abcg2*$^{-/-}$ mice. In contrast, BBB muABCB1 (in the *Abcg2*$^{-/-}$ mice) was not completely saturated, and still able to reduce effective brain accumulation to levels similar to those in wild-type brain. Only well after 10 min, with lower plasma levels, the efflux capacity of muABCG2 became apparent by the gradual decrease in brain sunitinib levels in *Abcb1a/1b*$^{-/-}$ mice, whereas brain efflux in *Abcb1a/1b/Abcg2*$^{-/-}$ mice was still virtually absent. As expected, also muABCB1 (in the *Abcg2*$^{-/-}$ mice) was able to further reduce brain levels of sunitinib after 10 min.

DISCUSSION

In our study, we show that the TKI sunitinib was transported *in vitro* by huABCB1 and huABCG2 and by muABCG2, but not by huABCC2 or muABCC2. Although the absence of *Abcb1a/1b* and *Abcg2* in knockout mice did not significantly affect the oral availability of sunitinib, we observed a profound effect (23-fold increase) on sunitinib brain accumulation when both transport systems were absent from the BBB. In contrast, single absence of *Abcb1a/1b* had only a small effect (2.3-fold increase), and single absence of *Abcg2* had no significant effect on brain accumulation of sunitinib. We could demonstrate in mice that, using an oral coadministration schedule of sunitinib and elacridar, BBB muABCB1 and muABCG2 were fully and specifically inhibited, resulting in highly increased brain sunitinib levels. Finally, we have shown that very high plasma concentrations of sunitinib can lead to partial or complete saturation of muABCB1 and muABCG2 transport activities in the BBB, resulting in qualitative changes in the relative impact of these transporters on sunitinib brain accumulation.

Our *in vitro* results are generally consistent with previous reports on the interaction of sunitinib with huABCB1 and huABCG2, including the demonstration that huABCB1 transports sunitinib *in vitro*,[23,24] and that sunitinib can inhibit huABCG2, and stimulate its ATPase activity.[21,22] Our finding that sunitinib is transported by huABCG2 (and muABCG2) is in line with the latter. It does seem to conflict with an earlier report that huABCG2 does not transport sunitinib noticeably.[23] However, there may have been relatively low activity of huABCG2 in the cell line used by Hu *et al*.[23] and transepithelial transport assays are in our experience often more sensitive than cellular accumulation assays in detecting ABCB1 and ABCG2 substrates. We have repeatedly noticed that, for unknown reasons, it is more difficult to obtain transduced cell lines with good and stable expression of huABCG2, than of muABCG2. Perhaps the human protein is better at extruding some essential cellular nutrient (*e.g.*, folate or vitamin B2) than the mouse variant, giving growth problems for colonies with high expression, or it may be less stable or less efficiently routed in the canine MDCK-II cells than the mouse protein. However this may be, the modest transport of sunitinib by huABCG2 compared to muABCG2 that we found in our cell lines (Fig. 1) may thus underestimate the *in vivo* transport capacity of huABCG2. At the same time, our *in vivo* mouse brain accumulation results confirm that sunitinib is a good muABCG2 substrate. The modest effect of single *Abcb1a/1b* deficiency on sunitinib brain accumulation, and the absence of an effect on oral AUC of sunitinib are in line with the *in vivo* results of Hu *et al*.[23]

Even though sunitinib is a good muABCB1 and muABCG2 substrate *in vivo*, with a marked effect on brain accumulation, we observed no significant effect of *Abcb1a/1b* and Abcg2 deficiency on sunitinib oral availability (Fig. 2*a*). Similar findings have been obtained with several other shared ABCB1 and ABCG2 substrate drugs, including imatinib[8] and sorafenib[7], but not with dasatinib,[6] illustrating the diversity in behavior of the individual TKIs. It could be that this lack of effect on oral bioavailability is due to saturation of efflux transporters by the high intestinal concentration of sunitinib.

Other factors such as profound differences in tightness and drug uptake systems between the enterocyte apical membrane and the BBB endothelial luminal membrane may also be responsible for such differences.

Our data show that we can drastically increase the brain accumulation of sunitinib, using an oral coadministration schedule of elacridar and sunitinib that might also be feasible in a clinical setting (Fig. 3*b*). Importantly, the plasma exposure level of elacridar used in our study is achievable in humans, as demonstrated by Kemper *et al.*, who showed that a patient receiving 1000 mg of elacridar orally had almost the same elacridar plasma concentration as mice treated with 100 mg kg^{-1} of elacridar orally.[36] In our study, plasma levels of sunitinib were not substantially changed by the elacridar treatment (Fig. 3*a*), and we did not observe significant toxicity in the coadministration regimen. This could imply that it may be possible to further improve the efficacy of sunitinib against brain metastases and possibly also primary brain tumors by coadministration with an ABCB1/ABCG2 inhibitor. It has been noted before that sunitinib has an intrinsically high brain accumulation among TKIs, even in wild-type mice,[23] and it appears to have some activity against cerebral metastases in patients with RCC.[37] A further boosting of passage of sunitinib across the BBB by inhibiting huABCB1 and huABCG2 is likely to enhance such activity.

It is sometimes considered that the BBB in larger brain tumors is often disrupted, and that the therapeutic gain of enhancing BBB penetration of anticancer drugs will therefore be limited. However, this view disregards the substantial heterogeneity inside tumors and their vasculature,[38] where for instance glioma blood vessels can locally display even higher huABCG2 expression (and other BBB markers) than vessels in surrounding normal brain tissue, or the fact that the invasive rims of the tumor are likely to be partially protected by the normal BBB in the surrounding brain tissue. The latter will also apply to small micrometastases in the brain that have not yet recruited their own blood vessel formation. In addition, if individual tumor cells themselves substantially express huABCB1 and/or huABCG2, even in parts of the tumor where the BBB is disrupted, inhibition of these transporters will likely also improve the response to chemotherapy with sunitinib.[39] In view of these potential gains, it might be interesting to set up a clinical trial of oral coadministration of sunitinib (or other TKIs) and elacridar. Since several other TKIs are similarly affected by ABCB1 and ABCG2 in the BBB (*e.g.*, dasatinib, lapatinib, imatinib, erlotinib, sorafenib, gefitinib and tandutanib), this strategy may well be worth investigating in patients for those drugs as well. However, as always, great caution must be exercised in translating the results obtained in mice to the human clinical situation, as there may be species-specific differences in transporter efficacy and susceptibility to toxicity of the various treatments.

We found that the brain accumulation of sunitinib, like that of several other TKIs and other drugs, is critically dependent on the activity of both Abcb1a/1b and Abcg2. Like with many of the other TKIs, the single disruption of *Abcb1a/1b* or *Abcg2* in mice has only little or even no detectable effect on brain accumulation, whereas simultaneous disruption of the two transporters results in a dramatic increase. This disproportionate

effect has led some researchers to envisage a synergistic role of ABCB1 and ABCG2 in the BBB.[9] However, Kodaira *et al*. have performed a careful kinetic analysis of the data using a straightforward pharmacokinetic model of the blood-brain (and blood-testis) barrier. This revealed that the seemingly disproportionate effect of simultaneous removal of both transporters simply resulted from the fact that the intrinsic efflux transport activities at the BBB of muABCB1 and muABCG2 are both considerably larger than the remaining (most likely passive) efflux activity.[5] Using the model, virtually all synergistic brain accumulation data could be readily explained by the single or combined activity of both transporters. Importantly, there was no need to invoke any change in the intrinsic efflux transport activity of either ABCB1 or ABCG2. Our results for the separate and combined impact of *Abcb1* and *Abcg2* knockout on brain penetration of sunitinib are qualitatively identical to those described for erlotinib, dasatinib, imatinib and lapatinib, and they can therefore most likely be explained by the same mechanism.[5] Also for sunitinib there is thus no reason to invoke a mechanistic synergistic interaction between muABCB1 and muABCG2 at the BBB.

Some groups have reported modest upregulation of muABCG2 in the BBB of *Abcb1a*-deficient CF-1 mice,[40] and it has been speculated that muABCB1A might be upregulated in the BBB of *Abcg2* knockout mice. Such shifts, if present, might also explain the relatively modest effect of the single *Abcb1a/1b* and *Abcg2* knockouts on the brain accumulation of shared ABCB1 and ABCG2 substrates. However, extensive analyses of muABCG2 and muABCB1A expression in brain homogenates of, respectively, *Abcb1a/1b* and *Abcg2* knockout mice of FVB background revealed no significant changes in RNA and/or protein levels in either strain.[7,41,42] Moreover, Kodaira *et al*., using specific transport substrates for either transporter, found negligible shifts in brain accumulation of these substrates in the single knockout strains of the complementary transporter.[5] This suggests that there is no substantial change of muABCG2 or muABCB1A activity in the BBB of the FVB background *Abcb1a/1b* or *Abcg2* knockout mice, respectively.

To deepen our insight into the interaction between muABCB1, muABCG2 and sunitinib in the BBB, but also to consider a potentially clinically relevant approach to overcome the BBB for sunitinib, we have tried to saturate the transporters with high intravenous dosing of sunitinib. Using 20 mg kg^{-1}, the highest intravenous sunitinib malate dose tolerated by all mouse strains, we could indeed nearly completely saturate muABCG2, but not muABCB1 (Fig. 4*c*), and this resulted in a qualitative change in the brain accumulation pattern between the different strains compared to the non-saturated situation (Fig. 3*b*). The results indicate that for sunitinib transport at the BBB, muABCG2 is more readily saturated than muABCB1. They also indicate a generally lower impact of the BBB efflux transporters at high plasma sunitinib concentrations. Nevertheless, this saturation approach probably has little clinical potential, as it required near-lethal doses of sunitinib. The oral coadministration of ABCB1/ABCG2 inhibitors like elacridar with sunitinib (and other TKIs) therefore seems a much more attractive approach to improve brain accumulation of TKIs, and thus, hopefully, their therapeutic potential.

ACKNOWLEDGEMENTS

An academic staff training scheme fellowship from the Malaysian Ministry of Science, Technology and Innovation to S.C.T. and a Swiss National Science Foundation fellowship to B.P. We thank Dilek Iusuf, Selvi Durmus and Kazuya Maeda for critical reading of the manuscript.

REFERENCES

1. Glavinas H, Krajcsi P, Cserepes J, Sarkadi B. The role of ABC transporters in drug resistance, metabolism and toxicity. *Curr Drug Deliv* 2004;1:27-42.
2. Burger H, van Tol H, Boersma AW, Brok M, Wiemer EA, Stoter G, Nooter K. Imatinib mesylate (STI571) is a substrate for the breast cancer resistance protein (BCRP)/ABCG2 drug pump. *Blood* 2004;104:2940-2.
3. Dai H, Marbach P, Lemaire M, Hayes M, Elmquist WF. Distribution of STI-571 to the brain is limited by P-glycoprotein-mediated efflux. *J Pharmacol Exp Ther* 2003;304:1085-92.
4. Chen Y, Agarwal S, Shaik NM, Chen C, Yang Z, Elmquist WF. P-glycoprotein and breast cancer resistance protein influence brain distribution of dasatinib. *J Pharmacol Exp Ther* 2009;330:956-63.
5. Kodaira H, Kusuhara H, Ushiki J, Fuse E, Sugiyama Y. Kinetic analysis of the cooperation of P-glycoprotein (P-gp/Abcb1) and breast cancer resistance protein (Bcrp/Abcg2) in limiting the brain and testis penetration of erlotinib, flavopiridol, and mitoxantrone. *J Pharmacol Exp Ther* 2010;333:788-96.
6. Lagas JS, van Waterschoot RA, van Tilburg VA, Hillebrand MJ, Lankheet N, Rosing H, Beijnen JH, Schinkel AH. Brain accumulation of dasatinib is restricted by P-glycoprotein (ABCB1) and breast cancer resistance protein (ABCG2) and can be enhanced by elacridar treatment. *Clin Cancer Res* 2009;15:2344-51.
7. Lagas JS, van Waterschoot RA, Sparidans RW, Wagenaar E, Beijnen JH, Schinkel AH. Breast cancer resistance protein and P-glycoprotein limit sorafenib brain accumulation. *Mol Cancer Ther* 2010;9:319-26.
8. Oostendorp RL, Buckle T, Beijnen JH, van Tellingen O, Schellens JH. The effect of P-gp (Mdr1a/1b), BCRP (Bcrp1) and P-gp/BCRP inhibitors on the in vivo absorption, distribution, metabolism and excretion of imatinib. *Invest New Drugs* 2009;27:31-40.
9. Polli JW, Olson KL, Chism JP, John-Williams LS, Yeager RL, Woodard SM, Otto V, Castellino S, Demby VE. An unexpected synergist role of P-glycoprotein and breast cancer resistance protein on the central nervous system penetration of the tyrosine kinase inhibitor lapatinib (N-{3-chloro-4-[(3-fluorobenzyl)oxy]phenyl}-6-[5-({[2-(methylsulfonyl)ethy l]amino}methyl)-2-furyl]-4-quinazolinamine; GW572016). *Drug Metab Dispos* 2009;37:439-42.
10. Agarwal S, Sane R, Gallardo JL, Ohlfest JR, Elmquist WF. Distribution of gefitinib to the brain is limited by P-glycoprotein (ABCB1) and breast cancer resistance protein (ABCG2)-mediated active efflux. *J Pharmacol Exp Ther* 2010;334:147-55.
11. Yang JJ, Milton MN, Yu S, Liao M, Liu N, Wu JT, Gan L, Balani SK, Lee FW, Prakash S, Xia CQ. P-glycoprotein and Breast Cancer Resistance Protein affect disposition of tandutinib, a tyrosine kinase inhibitor. *Drug Metab Lett* 2010.
12. Chow LQ, Eckhardt SG. Sunitinib: from rational design to clinical efficacy. *J Clin Oncol* 2007;25:884-96.
13. Goodman VL, Rock EP, Dagher R, Ramchandani RP, Abraham S, Gobburu JV, Booth BP, Verbois SL, Morse DE, Liang CY, Chidambaram N, Jiang JX, *et al*. Approval summary: sunitinib for the treatment of imatinib refractory or intolerant gastrointestinal stromal tumors and advanced renal cell carcinoma. *Clin Cancer Res* 2007;13:1367-73.
14. Rock EP, Goodman V, Jiang JX, Mahjoob K, Verbois SL, Morse D, Dagher R, Justice R, Pazdur R. Food and Drug Administration drug approval summary: Sunitinib malate for the treatment of gastrointestinal stromal tumor and advanced renal cell carcinoma. *Oncologist* 2007;12:107-13.
15. Flanigan RC, Campbell SC, Clark JI, Picken MM. Metastatic renal cell carcinoma. *Curr Treat Options Oncol* 2003;4:385-90.
16. Hall WA, Djalilian HR, Nussbaum ES, Cho KH. Long-term survival with metastatic cancer to the brain. *Med Oncol* 2000;17:279-86.

17. Motzer RJ, Rini BI, Bukowski RM, Curti BD, George DJ, Hudes GR, Redman BG, Margolin KA, Merchan JR, Wilding G, Ginsberg MS, Bacik J, *et al*. Sunitinib in patients with metastatic renal cell carcinoma. *JAMA* 2006;295:2516-24.
18. Motzer RJ, Hutson TE, Tomczak P, Michaelson MD, Bukowski RM, Rixe O, Oudard S, Negrier S, Szczylik C, Kim ST, Chen I, Bycott PW, *et al*. Sunitinib versus interferon alfa in metastatic renal-cell carcinoma. *N Engl J Med* 2007;356:115-24.
19. Motzer RJ, Michaelson MD, Redman BG, Hudes GR, Wilding G, Figlin RA, Ginsberg MS, Kim ST, Baum CM, Deprimo SE, Li JZ, Bello CL, *et al*. Activity of SU11248, a multitargeted inhibitor of vascular endothelial growth factor receptor and platelet-derived growth factor receptor, in patients with metastatic renal cell carcinoma. *J Clin Oncol* 2006;24:16-24.
20. Socinski MA, Novello S, Brahmer JR, Rosell R, Sanchez JM, Belani CP, Govindan R, Atkins JN, Gillenwater HH, Pallares C, Tye L, Selaru P, *et al*. Multicenter, phase II trial of sunitinib in previously treated, advanced non-small-cell lung cancer. *J Clin Oncol* 2008;26:650-6.
21. Dai CL, Liang YJ, Wang YS, Tiwari AK, Yan YY, Wang F, Chen ZS, Tong XZ, Fu LW. Sensitization of ABCG2-overexpressing cells to conventional chemotherapeutic agent by sunitinib was associated with inhibiting the function of ABCG2. *Cancer Lett* 2009;279:74-83.
22. Shukla S, Robey RW, Bates SE, Ambudkar SV. Sunitinib (Sutent, SU11248), a small-molecule receptor tyrosine kinase inhibitor, blocks function of the ATP-binding cassette (ABC) transporters P-glycoprotein (ABCB1) and ABCG2. *Drug Metab Dispos* 2009;37:359-65.
23. Hu S, Chen Z, Franke R, Orwick S, Zhao M, Rudek MA, Sparreboom A, Baker SD. Interaction of the multikinase inhibitors sorafenib and sunitinib with solute carriers and ATP-binding cassette transporters. *Clin Cancer Res* 2009;15:6062-9.
24. Haouala A, Rumpold H, Untergasser G, Buclin T, Ris HB, Widmer N, Decosterd LA. siRNA-mediated knock-down of P-glycoprotein expression reveals distinct cellular disposition of anticancer tyrosine kinases inhibitors. *Drug Metab Lett* 2010;4:114-9.
25. Gottesman MM, Fojo T, Bates SE. Multidrug resistance in cancer: role of ATP-dependent transporters. *Nat Rev Cancer* 2002;2:48-58.
26. Evers R, Kool M, van Deemter L, Janssen H, Calafat J, Oomen LC, Paulusma CC, Oude Elferink RP, Baas F, Schinkel AH, Borst P. Drug export activity of the human canalicular multispecific organic anion transporter in polarized kidney MDCK cells expressing cMOAT (MRP2) cDNA. *J Clin Invest* 1998;101:1310-9.
27. Jonker JW, Buitelaar M, Wagenaar E, van der Valk MA, Scheffer GL, Scheper RJ, Plosch T, Kuipers F, Elferink RP, Rosing H, Beijnen JH, Schinkel AH. The breast cancer resistance protein protects against a major chlorophyll-derived dietary phototoxin and protoporphyria. *Proc Natl Acad Sci U S A* 2002;99:15649-54.
28. Bakos E, Evers R, Calenda G, Tusnady GE, Szakacs G, Varadi A, Sarkadi B. Characterization of the amino-terminal regions in the human multidrug resistance protein (MRP1). *J Cell Sci* 2000;113 Pt 24:4451-61.
29. Pavek P, Merino G, Wagenaar E, Bolscher E, Novotna M, Jonker JW, Schinkel AH. Human breast cancer resistance protein: interactions with steroid drugs, hormones, the dietary carcinogen 2-amino-1-methyl-6-phenylimidazo(4,5-b) pyridine, and transport of cimetidine. *J Pharmacol Exp Ther* 2005;312:144-52.
30. Zimmermann C, van de Wetering K, van de Steeg E, Wagenaar E, Vens C, Schinkel AH. Species-dependent transport and modulation properties of human and mouse multidrug resistance protein 2 (MRP2/Mrp2, ABCC2/Abcc2). *Drug Metab Dispos* 2008;36:631-40.
31. Schinkel AH, Wagenaar E, van Deemter L, Mol CA, Borst P. Absence of the mdr1a P-Glycoprotein in mice affects tissue distribution and pharmacokinetics of dexamethasone, digoxin, and cyclosporin A. *J Clin Invest* 1995;96:1698-705.
32. Schinkel AH, Mayer U, Wagenaar E, Mol CA, van Deemter L, Smit JJ, van der Valk MA, Voordouw AC, Spits H, van Tellingen O, Zijlmans JM, Fibbe WE, *et al*. Normal viability and altered pharmacokinetics in mice lacking mdr1-type (drug-transporting) P-glycoproteins. *Proc Natl Acad Sci U S A* 1997;94:4028-33.
33. Jonker JW, Freeman J, Bolscher E, Musters S, Alvi AJ, Titley I, Schinkel AH, Dale TC. Contribution of the ABC transporters Bcrp1 and Mdr1a/1b to the side population phenotype in mammary gland and bone marrow of mice. *Stem Cells* 2005;23:1059-65.
34. Haznedar JO, Patyna S, Bello CL, Peng GW, Speed W, Yu X, Zhang Q, Sukbuntherng J, Sweeny DJ, Antonian L, Wu EY. Single- and

multiple-dose disposition kinetics of sunitinib malate, a multitargeted receptor tyrosine kinase inhibitor: comparative plasma kinetics in non-clinical species. *Cancer Chemother Pharmacol* 2009;64:691-706.

35. Polli JW, Humphreys JE, Harmon KA, Castellino S, O'Mara MJ, Olson KL, John-Williams LS, Koch KM, Serabjit-Singh CJ. The role of efflux and uptake transporters in [N-{3-chloro-4-[(3-fluorobenzyl)oxy]phenyl}-6-[5-({[2-(methylsulfonyl)ethy l]amino}methyl)-2-furyl]-4-quinazolinamine (GW572016, lapatinib) disposition and drug interactions. *Drug Metab Dispos* 2008;36:695-701.
36. Kemper EM, Jansen B, Brouwer KR, Schellens JH, Beijnen JH, van Tellingen O. Bioanalysis and preliminary pharmacokinetics of the acridonecarboxamide derivative GF120918 in plasma of mice and humans by ion-pairing reversed-phase high-performance liquid chromatography with fluorescence detection. *J Chromatogr B Biomed Sci Appl* 2001;759:135-43.
37. Medioni J, Cojocarasu O, Belcaceres JL, Halimi P, Oudard S. Complete cerebral response with sunitinib for metastatic renal cell carcinoma. *Ann Oncol* 2007;18:1282-3.
38. de Vries NA, Bruggeman SW, Hulsman D, de Vries HI, Zevenhoven J, Buckle T, Hamans BC, Leenders WP, Beijnen JH, van Lohuizen M, Berns AJ, van Tellingen O. Rapid and robust transgenic high-grade glioma mouse models for therapy intervention studies. *Clin Cancer Res* 2010;16:3431-41.
39. Carcaboso AM, Elmeliegy MA, Shen J, Juel SJ, Zhang ZM, Calabrese C, Tracey L, Waters CM, Stewart CF. Tyrosine kinase inhibitor gefitinib enhances topotecan penetration of gliomas. *Cancer Res* 2010;70:4499-508.
40. Cisternino S, Mercier C, Bourasset F, Roux F, Scherrmann JM. Expression, up-regulation, and transport activity of the multidrug-resistance protein Abcg2 at the mouse blood-brain barrier. *Cancer Res* 2004;64:3296-301.
41. de Vries NA, Zhao J, Kroon E, Buckle T, Beijnen JH, van Tellingen O. P-glycoprotein and breast cancer resistance protein: two dominant transporters working together in limiting the brain penetration of topotecan. *Clin Cancer Res* 2007;13:6440-9.
42. Jonker JW, Smit JW, Brinkhuis RF, Maliepaard M, Beijnen JH, Schellens JH, Schinkel AH. Role of breast cancer resistance protein in the bioavailability and fetal penetration of topotecan. *J Natl Cancer Inst* 2000;92:1651-6.

SUPPORTING INFORMATION

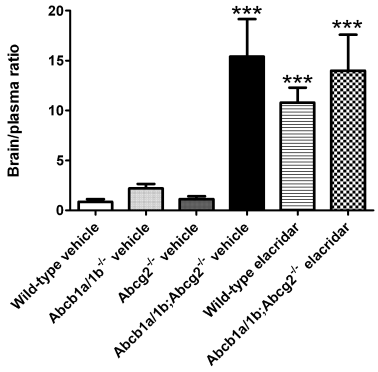

Supporting Information Figure 1. Brain-to-plasma ratios of sunitinib for male wild-type, *Abcb1a/1b*$^{-/-}$, *Abcg2*$^{-/-}$ and *Abcb1a/1b;Abcg2*$^{-/-}$ mice 1 hr after oral administration of 10 mg kg^{-1} sunitinib malate. Sunitinib malate was administered 2 hr after the oral administration of either vehicle or elacridar vehicle (100 mg kg^{-1}). Columns, means (n = 5); bars, SD. ***, $P < 0.001$, compared with vehicle-treated wild-type mice (one-way ANOVA).

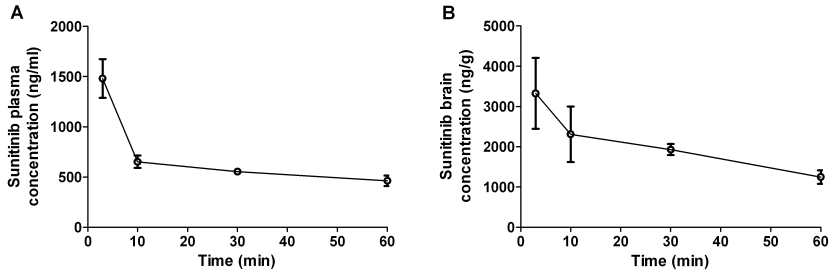

Supporting Information Figure 2. Plasma concentration-time curve (A) and brain concentration-time curve (B) of sunitinib in male wild-type mice after an intravenous dose of 20 mg kg^{-1} sunitinib malate. Points, means (n = 4); bars, SD.

2.2

P-GLYCOPROTEIN (ABCB1) AND BREAST CANCER RESISTANCE PROTEIN (ABCG2) RESTRICT BRAIN ACCUMULATION OF THE ACTIVE SUNITINIB METABOLITE *N*-DESETHYL SUNITINIB

Seng Chuan Tang, Nienke A.G. Lankheet, Birk Poller, Els Wagenaar, Jos H. Beijnen, and Alfred H. Schinkel

S.C.T., B.P., E.W., A.H.S.: Division of Molecular Biology, The Netherlands Cancer Institute, Amsterdam, The Netherlands
N.A.G.L., J.H.B.: Department of Pharmacy and Pharmacology, Slotervaart Hospital, Amsterdam, The Netherlands

J Pharmacol Exp Ther. 2012; 341(1): 164-73.

ABSTRACT

N-desethyl sunitinib is a major and pharmacologically active metabolite of the tyrosine kinase inhibitor and anticancer drug sunitinib. Because the combination of *N*-desethyl sunitinib and sunitinib represents total active drug exposure, we investigated the impact of several multidrug efflux transporters on plasma pharmacokinetics and brain accumulation of *N*-desethyl sunitinib, after sunitinib administration to wild-type and transporter knockout mice. In vitro, *N*-desethyl sunitinib was a good transport substrate of human ABCB1 and ABCG2 and murine Abcg2, but not of ABCC2 or Abcc2. At 5 μM, ABCB1 and ABCG2 contributed almost equally to *N*-desethyl sunitinib transport. In vivo, the systemic exposure of *N*-desethyl sunitinib after oral dosing of sunitinib malate (10 mg/kg) was unchanged when Abcb1 and/or Abcg2 were absent. However, brain accumulation of *N*-desethyl sunitinib was markedly (13.7-fold) increased in *Abcb1a/1b*(-/-)/*Abcg2*(-/-) mice, but not in *Abcb1a/1b*(-/-) or *Abcg2*(-/-) mice. In the absence of the ABCB1 and ABCG2 inhibitor elacridar, brain concentrations of *N*-desethyl sunitinib were detectable only in *Abcb1a/1b*(-/-)/*Abcg2*(-/-) mice after sunitinib administration. Combined elacridar plus *N*-desethyl sunitinib treatment increased *N*-desethyl sunitinib plasma and brain exposures, but not brain-to-plasma ratios in wild-type mice. In conclusion, brain accumulation of *N*-desethyl sunitinib is effectively restricted by both Abcb1 and Abcg2. The effect of elacridar treatment in improving brain accumulation of *N*-desethyl sunitinib in wild-type mice was limited as compared with its effect on sunitinib brain accumulation.

INTRODUCTION

ATP-binding cassette (ABC) efflux transporters, such as P-glycoprotein (P-gp; ABCB1), breast cancer resistance protein (BCRP; ABCG2), and multidrug resistance protein 2 (MRP2; ABCC2), can have a significant impact on the absorption, distribution, excretion, and toxicity of xenobiotics (Glavinas et al., 2004). Several groups have shown that many tyrosine kinase inhibitors (TKIs) used in cancer therapy are substrates of both ABCB1 and ABCG2 (Burger et al., 2004; Dai et al., 2003; Bihorel et al., 2007; Chen et al., 2009; Lagas et al., 2009; Oostendorp et al., 2009; Lagas et al., 2010), and found that the interaction with these ABC transporters may affect oral availability and brain accumulation of TKIs.

The TKI sunitinib malate (SU11248; Sutent, Pfizer, New York) is an orally active, small-molecule ATP-competitive multi-targeted inhibitor of vascular endothelial growth factor receptors type 1 and 2, the platelet-derived growth factor receptors α and β, the stem cell factor receptor c-KIT, FMS-like TK-3 receptor, and the glial cell-line derived neurotrophic factor receptor (Chow and Eckhardt, 2007). Sunitinib is approved by the US Food and Drug Administration for the treatment of advanced or metastatic renal cell carcinoma (RCC) and imatinib-resistant gastrointestinal stromal tumors. Sunitinib displays an intrinsically high brain penetration among TKIs, and it is currently

being tested in a phase II clinical trial of recurrent glioblastoma multiforme (http://clinicaltrials.gov/ct2/show/NCT00535379).

After administration, sunitinib is metabolized primarily by cytochrome P450 3A4 to a major and pharmacologically active metabolite, *N*-desethyl sunitinib (supplemental Fig.1) (Houk et al., 2009). This is further metabolized by cytochrome P450 3A4 to an inactive compound (Adams and Leggas, 2007). In patients, plasma sunitinib and *N*-desethyl sunitinib accounted for 42% and 24%, respectively, of the total plasma radioactivity area under the plasma concentration-time curve $(AUC)_{0-\infty}$ (Adams and Leggas, 2007). Given that *N*-desethyl sunitinib has a similar kinase inhibitory effect as sunitinib in vitro and similar plasma protein binding characteristics, the combination of sunitinib plus *N*-desethyl sunitinib represents the total pharmacodynamically active drug in plasma. *N*-desethyl sunitinib may thus well account for one third of the therapeutic effect of oral sunitinib. Previously, we have shown that sunitinib is transported in vitro by human ABCB1, ABCG2, and by murine Abcg2, but not by human ABCC2 or murine Abcc2 (Tang et al., 2012). Simultaneous deficiency of Abcb1a/1b and Abcg2, but not single Abcb1a/1b or Abcg2 deficiency, resulted in highly increased brain levels of sunitinib in knockout mouse strains. We also demonstrated in wild-type mice that a clinically realistic oral coadministration of sunitinib and the dual ABCB1 and ABCG2 inhibitor elacridar could result in highly increased brain sunitinib levels (Tang et al., 2012). However, little is known so far about the interactions of *N*-desethyl sunitinib with ABC transporters in vitro, or in vivo after sunitinib treatment.

In view of their expression in pharmacokinetically important organs and broad substrate specificity, we wanted to establish to what extent *N*-desethyl sunitinib is transported by human ABCB1, ABCG2 and ABCC2 and by murine Abcg2 and Abcc2 in vitro, and what the consequences are for systemic availability and brain accumulation of *N*-desethyl sunitinib after oral administration of sunitinib as judged in knockout mouse models. We further tested whether these pharmacokinetic parameters of *N*-desethyl sunitinib could be improved by a clinically realistic coadministration of oral elacridar and oral sunitinib, with the ultimate aim of improving overall therapeutic efficacy of sunitinib and its metabolite. We also aimed to obtain better insight into the factors that determine the relative impact of Abcb1 and Abcg2 on the brain accumulation of *N*-desethyl sunitinib after sunitinib intravenous administration. This may help efforts to overcome the blood-brain barrier (BBB) for therapeutic purposes.

MATERIALS AND METHODS

Chemicals and reagents

Sunitinib malate was purchased from Sequoia Research Products (Pangbourne, UK). *N*-desethyl sunitinib was purchased from Toronto Research Chemicals Inc. (North York, ON, Canada). Elacridar [GF120918; *N*-[4-[2-(1,2,3,4-tetrahydro-6,7-dimethoxy-2-isoquinolinyl)ethyl]-phenyl)-9,10-dihydro-5-methoxy-9-oxo-4-acridine carboxamide hydrochloride] (Evers et al., 2000) was kindly provided by GlaxoSmithKline (Stevenage, UK). Zosuquidar [LY-335979; (*R*)-4-((1*aR*,6*R*,10*bS*)-1,2-difluoro-1,1*a*,6,10*b*-tetrahydrodibenzo-(*a*,e)cyclopropa(c)cycloheptan-6-yl)-

α-((5-quinoloyloxy)methyl)-1-piperazine ethanol, trihydrochloride] (Eli Lilly & Co., Indianapolis, IN) was a kind gift of Dr. O. van Tellingen (The Netherlands Cancer Institute, Amsterdam, The Netherlands). Ko143 [(3*S*,6*S*,12a*S*)-1,2,3,4,6,7,12,12*a*-octahydro-9-methoxy-6-(2-methylpropyl)-1,4-dioxopyrazino[1',2':1,6]pyrido[3,4-*b*]indole-3-propanoic acid 1,1-dimethylethyl ester] was previously described (Allen et al., 2002). [^{14}C]Inulin was obtained from GE Healthcare (Little Chalfont, Buckinghamshire, UK). Methoxyflurane (metofane) was supplied by Medical Developments Australia (Melbourne, Australia). Isoflurane (forane) was obtained from Abbott Laboratories Ltd (Queenborough, UK). Heparin (5000 IU/ml) was obtained from Leo Pharmaceuticals BV (Breda, The Netherlands). Bovine serum albumin (fraction V) was obtained from Roche Diagnostics (Mannheim, Germany). High-performance liquid chromatography grade acetonitrile and methanol were purchased from Biosolve (Valkenswaard, The Netherlands). Ammonia 25% was purchased from Merck (Darmstadt, Germany). The stable isotope-labeled sunitinib was purchased from AlsaChim (Illkirch, France). All other chemicals and reagents were obtained from Sigma-Aldrich (Steinheim, Germany).

Cell lines and transport assays

Polarized Madin-Darby canine kidney II (MDCKII) cells and their subclones transduced with human *ABCB1*, *ABCC2*, *ABCG2*, murine *Abcc2* or *Abcg2* cDNA were used and cultured as described previously (Bakos et al., 2000; Evers et al., 1998; Pavek et al., 2005; Zimmermann et al., 2008; Jonker et al., 2000). Recently, Poller et al. (2011) generated a MDCKII cell line simultaneously overexpressing both ABCB1 and ABCG2 to better study the interplay of both transporters in vitro. Transepithelial transport assays were performed as described previously with minor modifications (Pavek et al., 2005). Two hours before starting the experiment, cells were washed with prewarmed phosphate-buffered saline and preincubated with 2 ml of Opti-MEM either alone or containing the dual ABCB1 and ABCG2 inhibitor elacridar (5 μM), the ABCB1 inhibitor zosuquidar (5 μM), the ABCG2 inhibitor Ko143 (1 μM) or a combination of zosuquidar and Ko143, which were present in both compartments during a 2-h preincubation period and during the transport experiment. Experiments were started (t = 0 h) by replacing the medium in one compartment (either basolateral or apical) with fresh Opti-MEM medium, either with or without inhibitor and containing 5 μM *N*-desethyl sunitinib. Cells were incubated at 37°C in 5% CO_2, and 50 μl aliquots were taken at t = 2 h and 4 h for determination of drug concentration. Transport was calculated as the fraction of drug found in the acceptor compartment relative to the total amount added to the donor compartment at the beginning of the experiment. Transport is given as mean percentage ± S.D. (n = 3). Membrane tightness was assessed in parallel using the same cells seeded on the same day and at the same density, by analyzing transepithelial [^{14}C] inulin (3.3 kBq/well) leakage. Leakage had to remain <1% of the total added radioactivity per hour. Active transport was expressed by the relative transport ratio (r), defined as r = percentage apically directed transport divided by basolaterally directed translocation after 4 h. Because of some interday variation in transport ratios, we directly compared only transport ratios determined on the same day.

Animals

Mice were housed and handled according to institutional guidelines complying with Dutch legislation. Male wild-type, *Abcb1a/1b*(-/-) (Schinkel et al., 1997), *Abcg2*(-/-) (Jonker et al., 2002), and *Abcb1a/1b*(-/-)/*Abcg2*(-/-) (Jonker et al., 2005) mice, all of a >99% FVB genetic background, were used between 10 and 14 weeks of age. Animals were kept in a temperature-controlled environment with a 12-h light/12-h dark cycle and they received a standard diet (AM-II, Hope Farms, Woerden, The Netherlands) and acidified water ad libitum.

Drug solutions

Drug solutions for sunitinib and oral elacridar were prepared as previously described (Tang et al., 2012). For intravenous administration, elacridar hydrochloride was first dissolved in dimethyl sulfoxide (DMSO) at 150 mg/ml and further diluted with a mixture of ethanol, polyethylene glycol 200, and 5% glucose (2:6:2, v/v) to obtain a concentration of 4 mg/ml. *N*-desethyl sunitinib was dissolved in DMSO at a concentration of 50 mg/ml and further diluted with 50 mM sodium acetate buffer, pH 4.6 to yield a concentration of 1 mg/ml. In all drug formulations, drugs and/or modulators were completely dissolved, also during administration to the mice.

Animal experiments

All the animal experiments in which sunitinib was given either orally or intravenously were carried out as described previously (Tang et al., 2012). After oral sunitinib administration, multiple blood samples (~50 µl) were collected from the tail vein at 15 and 30 min, and 1, 2, and 4 hr. At 6 hr, blood was collected by cardiac puncture under isoflurane anesthesia. This allowed determination of plasma concentration-time curves for each individual mouse.

Brain accumulation of *N*-desethyl sunitinib in combination with intravenous elacridar treatment

Values of lower limit of quantification (LLQ) for *N*-desethyl sunitinib were 7.5 ng/g for the oral sunitinib in combination with oral elacridar brain accumulation experiment and 13.5 ng/g for the BBB efflux transport saturation experiment. This difference was caused by an improvement in the detection method to enhance sensitivity during the course of our studies. To circumvent detection problems of *N*-desethyl sunitinib in brain homogenates, we injected *N*-desethyl sunitinib (5 mg/kg) directly into the tail vein of wild-type and knockout mice 15 min after an intravenous injection of either elacridar or vehicle in solution form. Blood and brain were isolated 60 min after *N*-desethyl sunitinib administration and processed as described previously (Tang et al., 2012).

Drug analysis

Determination of *N*-desethyl sunitinib and the internal standard sunitinib-$^{2}H_{10}$ was performed on a sensitive and specific liquid chromatography coupled with tandem mass spectrometry assay. The analytical method that was described previously (Lankheet et al., 2011; Tang et al., 2012) was used for the detection of sunitinib and *N*-desethyl sunitinib in plasma and brain homogenates. *N*-desethyl sunitinib was detected at the transition from m/z 371 to 283 with a retention time of 3.8 min. In case the (usually minor) E-isomer of *N*-desethyl sunitinib was detected in addition to the main Z-isomer, we report the combined concentration of both isomers.

Pharmacokinetic calculations and statistical analysis

Pharmacokinetic parameters were calculated by noncompartmental methods using the software package PK Solutions 2.0.2 (Summit, Research Services, Ashland, OH). The AUC was calculated by using the trapezoidal rule, without extrapolating to infinity. The AUC and maximum drug concentration in plasma (C_{max}) were determined directly from individual concentration-time data. Data are presented as means ± S.D. For parametric statistical analysis, the individual values of Figs. 6, C to F and 7, A and D were log-transformed to obtain equality in variances. One-way analysis of variance (ANOVA) was used to determine significance between groups, after which post-hoc tests with Bonferroni correction were performed for comparison between individual groups. Between-group comparisons of genotype or elacridar effect were made by using the two-tailed unpaired Student's *t*-test. Differences were considered statistically significant when $p < 0.05$.

RESULTS

In vitro transport of *N*-desethyl sunitinib

Transepithelial drug transport was tested by using polarized monolayers of MDCKII parental cells and various ABC transporter-overexpressing derivative cell lines. *N*-desethyl sunitinib was modestly transported in the apical direction in the parental MDCKII cell line (transport ratio *r* of 2.1; Fig. 1A), presumably by the low-level endogenous canine ABCB1. In cells overexpressing human ABCB1, there was clear apically directed transport of *N*-desethyl sunitinib, with an *r* of 15.1 (Fig. 1B). *N*-desethyl sunitinib was also actively transported by human ABCG2 or murine Abcg2, with transport ratios of 6.0 and 6.6, respectively (Fig. 1, C and D). Addition of elacridar, a dual inhibitor of ABCB1 and ABCG2, completely inhibited polarized transport in MDCKII parental and MDCKII-ABCB1 cells (Fig. 1, E and F). However, elacridar at 5 μM did not completely inhibit the apical transport of *N*-desethyl sunitinib in MDCKII-ABCG2 cells (*r* reduced from 6.0 to 1.8) (Fig. 1G), and had only a minimal effect on MDCKII cells overexpressing mouse Abcg2 (Fig. 1H). Elacridar at 5 μM does not modulate ABCC2/Abcc2 activity (Evers et al., 2000), and was therefore used to suppress any transport by endogenous canine ABCB1 in cells overexpressing human ABCC2 or murine Abcc2. Under these conditions, we did not observe polarized transport of *N*-desethyl sunitinib by either ABCC2 or Abcc2 (Fig 1, I and J).

Because we did not observe complete inhibition of ABCG2- and Abcg2-mediated *N*-desethyl sunitinib transport by elacridar, we investigated whether transport of *N*-desethyl sunitinib in these cell lines could be completely inhibited with the specific and high-affinity ABCG2 inhibitor Ko143. The specific ABCB1 inhibitor zosuquidar was added to suppress any contribution of endogenous canine ABCB1 (Fig. 2A). *N*-desethyl sunitinib was actively transported in cells overexpressing human ABCG2 and murine Abcg2, with transport ratios of 13.5 and 20.3 versus 1.0 in parental cells (Fig. 2, B and C). The addition of Ko143 resulted in extensive inhibition of polarized transport in all these cell lines (Fig. 2, D and E). Collectively, *N*-desethyl sunitinib was a good transport substrate of human ABCB1, ABCG2, and murine Abcg2, but not of human ABCC2 and murine Abcc2. Elacridar at 5 μM could only partially inhibit *N*-desethyl sunitinib transport by human ABCG2 and especially

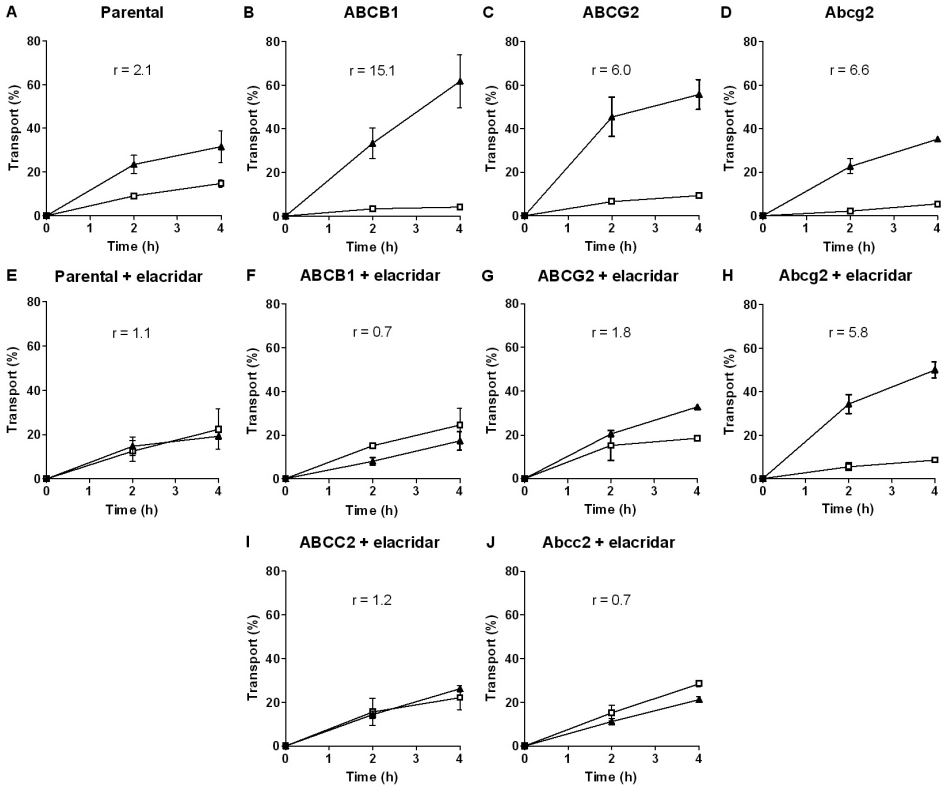

Fig. 1. Transepithelial transport of *N*-desethyl sunitinib (5 μM) assessed by using MDCKII parental cells (A and E) or MDCKII cells transduced with human *ABCB1* (B and F), human *ABCG2* (C and G), murine *Abcg2* (D and H), human *ABCC2* (I), or murine *Abcc2* (J) cDNA. At t = 0 h, *N*-desethyl sunitinib was applied in one compartment (apical or basolateral), and the amount of drug appearing in the opposite compartment at t = 2 and 4 h was measured by liquid chromatography coupled with tandem mass spectrometry and plotted as the percentage of the amount of initially applied drug (n = 3). Elacridar (5 μM) was applied to inhibit human and/or endogenous canine ABCB1 (E-J). ▲, translocation from basolateral to apical compartment; □, translocation from apical to basolateral compartment. Points, means (n = 3); bars, S.D. At t = 4 h, 1% of transport is approximately equal to an apparent permeability coefficient (P_{app}) of 0.30×10^{-6} cm/s.

mouse Abcg2, a rather unusual observation, as in our experience in vitro transport of most Abcg2 substrates can be completely inhibited by 5 μM elacridar.

N-desethyl sunitinib transport in MDCKII-ABCB1/ABCG2 cells

We tested the relative contributions of human ABCB1 and ABCG2 to *N*-desethyl sunitinib transport at 5 and 20 μM in the absence or presence of Ko143 and zosuquidar in MDCKII cells simultaneously overexpressing ABCB1 and ABCG2 (Poller et al., 2011). Without inhibitor, we measured transport ratios of 13.3 and 16.5 at 5 and 20 μM, respectively (supplemental Fig. 2, A and B). The ABCG2-mediated *N*-desethyl sunitinib transport in the presence of zosuquidar was reduced from an r of 9.7 at 5 μM to 5.8 at 20 μM (supplemental Fig. 2, C and D).

Upon blocking ABCG2 with Ko143, we observed ABCB1-mediated *N*-desethyl sunitinib transport ratios of 6.7 and 6.0 at 5 and 20 μM, respectively (supplemental Fig. 2, E and F). Active transport of *N*-desethyl sunitinib at both 5 and 20 μM was completely abolished when both Ko143 and zosuquidar were present (supplemental Fig. 3, G and H). Taken together, the contribution of ABCG2 to *N*-desethyl sunitinib transport is almost equal to that of ABCB1 at 5 and 20 μM, although some initial ABCG2 saturation may occur at 20 μM.

Impact of Abcb1 and Abcg2 on plasma pharmacokinetics of *N*-desethyl sunitinib after oral sunitinib treatment

Because the parent compound sunitinib is given orally to cancer patients, we first studied the plasma concentration of *N*-desethyl sunitinib over time after oral sunitinib malate administration at 10 mg/kg to wild-type, *Abcb1a/1b*(-/-), *Abcg2*(-/-), and *Abcb1a/1b*(-/-)/*Abcg2*(-/-) mice. As shown in Fig. 3A and Table 1, there were no statistically significant differences in oral AUC or C_{max} of

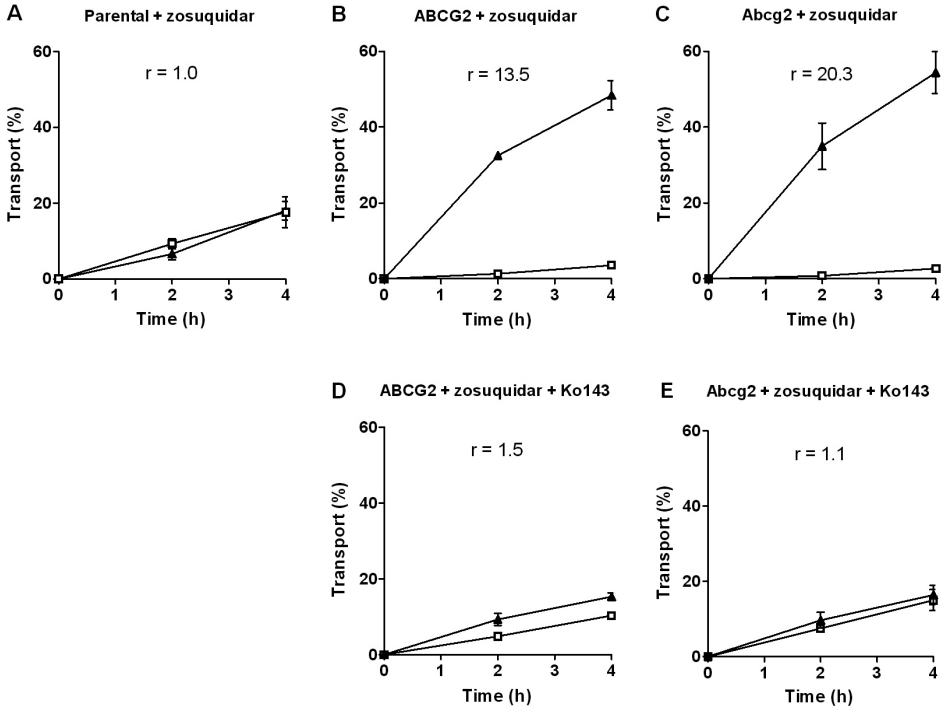

Fig. 2. Transepithelial transport of *N*-desethyl sunitinib (5 μM) assessed by using MDCKII parental cells (A) or MDCKII cells transduced with human ABCG2 (B and D) or murine Abcg2 (C and E) cDNA. *N*-desethyl sunitinib application and measurement was as described in the legend of Fig. 1. B and C, the ABCB1 inhibitor zosuquidar (5 μM) was applied to specifically measure ABCG2/Abcg2-mediated transport. D and E, the ABCG2 inhibitor Ko143 (1 μM) was additionally applied to verify ABCG2/Abcg2-mediated transport. ▲, translocation from basolateral to apical compartment; □, translocation from apical to basolateral compartment. Points, means (n = 3); bars, S.D. At t = 4 h, 1% of transport is approximately equal to an apparent permeability coefficient (P_{app}) of 0.30×10^{-6} cm/s.

N-desethyl sunitinib between the strains. The metabolite/parent drug AUC ratios ranged between 33% and 40% (Table 1) and also did not differ significantly between the strains. These ratios are similar to those observed in humans (Shirao et al., 2010). These results indicate that Abcb1 and Abcg2 do not have a substantial role in, or effect on, the availability, metabolism or elimination of *N*-desethyl sunitinib after oral sunitinib administration.

Impact of Abcb1 and Abcg2 on brain accumulation of *N*-desethyl sunitinib after oral sunitinib administration

As shown in Fig. 3B, the relative brain accumulation of *N*-desethyl sunitinib, determined 6 h after oral administration of sunitinib and corrected for the plasma $AUC_{0\text{-}6h}$, was not significantly different in *Abcb1a/1b*(-/-) and *Abcg2*(-/-) mice as compared with wild-type mice. In contrast, *Abcb1a/1b*(-/-)/*Abcg2*(-/-) mice had a 13.7–fold increased brain accumulation ($p < 0.05$; see also Table 1). This indicates that brain accumulation of *N*-desethyl sunitinib was primarily restricted by both Abcb1 and Abcg2. Apparently, each of these transporters can largely take over the function of the other transporter at the BBB when knocked out. Only when both transporters are simultaneously absent can a large increase in brain accumulation of *N*-desethyl sunitinib occur.

Influence of elacridar on *N*-desethyl sunitinib brain accumulation after oral sunitinib administration

We wanted to assess the effect of elacridar on plasma pharmacokinetics and brain accumulation of *N*-desethyl sunitinib after oral sunitinib administration, given that elacridar markedly increased the brain accumulation of sunitinib, although not its oral bioavailability (Tang et al., 2012). In view of the potential clinical importance of oral application for

Table 1. Pharmacokinetic parameters, brain concentrations (t = 6 h), and relative brain accumulation of *N*-desethyl sunitinib after oral administration of 10 mg/kg sunitinib malate to various mouse strains

	Genotype			
	Wild-type	*Abcb1a/1b*(-/-)	*Abcg2*(-/-)	*Abcb1a/1b*(-/-)/Abcg2(-/-)
Plasma $AUC_{(0\text{-}6)}$, ng.h/ml	152 ± 12.9	170 ± 49.6	125 ± 66.4	95.8 ± 41.1
Fold change $AUC_{(0\text{-}6)}$	1.00	1.12	0.82	0.63
Sunitinib $AUC_{(0\text{-}6)}$ [a], ng.h /ml	445 ± 203	514 ± 145	311 ± 172	288 ± 88
N-desethyl sunitinib-to-sunitinib AUC ratio	0.34	0.33	0.40	0.33
C_{max}, ng/ml	36.3 ± 4.00	33.6 ± 7.00	24.9 ± 12.4	24.8 ± 15.2
C_{brain}, ng/g	10.1 ± 0.94	11.8 ± 5.20	13.2 ± 2.20	80.7 ± 40.0**
Fold change C_{brain}	1.00	1.20	1.30	8.00
P_{brain} ($x10^{-1}$ h^{-1})	0.67 ± 0.12	0.73 ± 0.34	1.27 ± 0.60	9.20 ± 5.90*
Fold change P_{brain}	1.00	1.10	1.90	13.7

C_{brain}, brain concentration; P_{brain}, relative brain accumulation at 6 h after oral administration, calculated by determining the *N*-desethyl sunitinib brain concentration relative to the $AUC_{(0\text{-}6)}$.
[a] Sunitinib AUC data for comparison were taken from Tang et al. (2012).
*, $P < 0.05$; **, $P < 0.01$, compared with wild-type mice (one-way ANOVA). Data are means (n = 3-7) ± S.D.

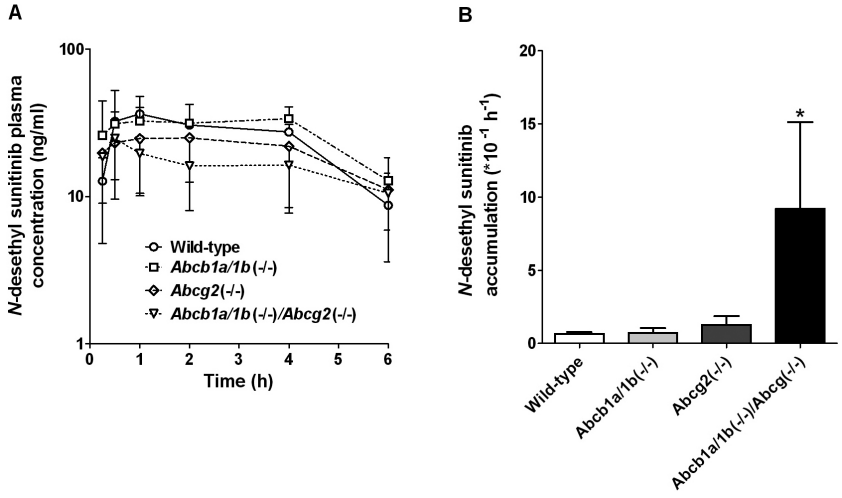

Fig. 3. Plasma concentration-time curves (A) and relative brain accumulation at t = 6 h (B) of *N*-desethyl sunitinib in male wild-type, *Abcb1a/1b*(-/-), *Abcg2*(-/-), and *Abcb1a/1b*(-/-)/*Abcg2*(-/-) mice following oral administration of 10 mg/kg sunitinib malate. Multiple blood samples (~50 µl) were collected from the tail vein at 15 and 30 min, and 1, 2, and 4 h by using lithium-heparinized capillary tubes. Relative brain accumulation was calculated by dividing brain concentration at t = 6 h by the $AUC_{0\text{-}6}$. Columns, means (n = 3-7); bars, S.D. *, $p < 0.05$, compared with wild-type mice (one-way ANOVA).

both sunitinib and elacridar, we administered elacridar (100 mg/kg) orally 2 h before oral sunitinib malate (10 mg/kg) to the wild-type and *Abcb1a/1b*(-/-)/*Abcg2*(-/-) strains, and assessed plasma and brain *N*-desethyl sunitinib levels 1 h later, i.e., around the sunitinib time to reach maximum drug concentration in plasma (supplemental Table 1). As shown in Fig. 4A, *N*-desethyl sunitinib plasma concentrations were not significantly different among the strains, regardless of administration with or without elacridar. The plasma metabolite-to-sunitinib ratios were not significantly different either (supplemental Fig. 3). In vehicle-treated mice, brain concentrations of *N*-desethyl sunitinib in wild-type, *Abcb1a/1b*(-/-) and *Abcg2*(-/-) mice were below the LLQ (~7.5 ng/g). However, brain concentrations of *N*-desethyl sunitinib in *Abcb1a/1b*(-/-)/*Abcg2*(-/-) mice were just above this limit. Elacridar treatment increased brain concentrations in wild-type mice to levels equal to those in *Abcb1a/1b*(-/-)/*Abcg2*(-/-) mice (Fig. 4B). The *N*-desethyl sunitinib brain concentrations in *Abcb1a/1b*(-/-)/*Abcg2*(-/-) mice were not significantly affected by elacridar treatment. These data suggest that oral elacridar treatment could inhibit the activity of Abcb1 and Abcg2 in the BBB, leading to increased *N*-desethyl sunitinib concentrations in the brain. However, the size of this effect could not be assessed in the absence of quantifiable brain values for vehicle-treated wild-type mice.

Influence of elacridar on plasma and brain exposure of intravenous *N*-desethyl sunitinib

To circumvent these quantification problems, we injected *N*-desethyl sunitinib directly at an intravenous dose of 5 mg/kg to wild-type

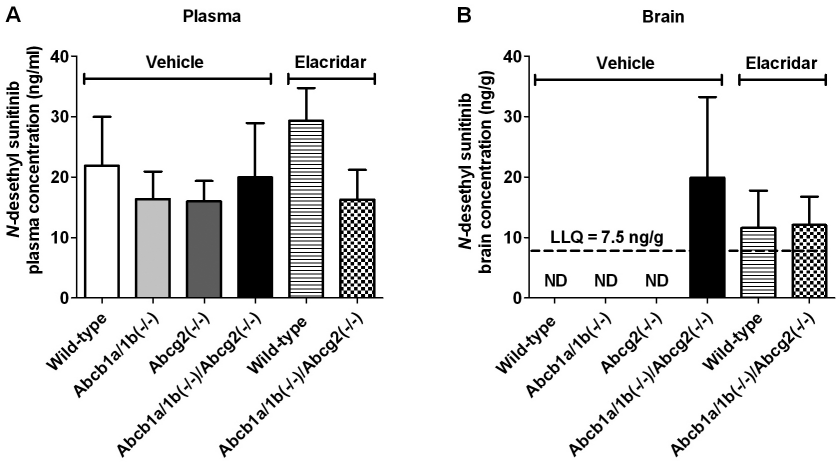

Fig. 4. Plasma (A) and brain (B) concentrations of *N*-desethyl sunitinib in male wild-type, *Abcb1a/1b*(-/-), *Abcg2*(-/-), and *Abcb1a/1b*(-/-)/*Abcg2*(-/-) mice 1 h after oral administration of 10 mg/kg sunitinib malate with or without elacridar administration. Sunitinib malate was administered 2 h after the oral administration of either elacridar (100 mg/kg) or vehicle. Columns, means (n = 5); bars, S.D. ND, not detectable.

and *Abcb1a/1b*(-/-)/*Abcg2*(-/-) mice 15 min after intravenous vehicle or elacridar administration, and we measured plasma and brain concentrations 1 h later. In the absence of elacridar, the plasma concentrations of *N*-desethyl sunitinib in *Abcg2*(-/-) and *Abcb1a/1b*(-/-)/*Abcg2*(-/-) mice, but not in *Abcb1a/1b*(-/-) mice, were 1.9-fold higher than in wild-type mice (Fig. 5A). Elacridar treatment increased the *N*-desethyl sunitinib plasma levels in wild-type mice to levels equal to those in *Abcb1a/1b*(-/-)/*Abcg2*(-/-) mice, and significantly higher than in vehicle-treated wild-type mice (Fig. 5B). Collectively, these data suggest that Abcg2, but not Abcb1a/1b, may contribute to plasma elimination of intravenous *N*-desethyl sunitinib. In the absence of elacridar, brain concentrations of *N*-desethyl sunitinib were not significantly different in wild-type, *Abcb1a/1b*(-/-), and *Abcg2*(-/-) mice, but they were increased 13.2–fold in *Abcb1a/1b*(-/-)/*Abcg2*(-/-) mice compared with wild-type mice (Fig. 5C). Intravenous elacridar increased *N*-desethyl sunitinib brain concentrations (3.3-fold) in wild-type mice compared with wild-type mice without elacridar, but this level was still 4-fold lower than seen in *Abcb1a/1b*(-/-)/*Abcg2*(-/-) mice without elacridar (Fig. 5D). We were surprised to find that the *N*-desethyl sunitinib brain levels found in *Abcb1a/1b*(-/-)/*Abcg2*(-/-) mice pretreated with elacridar were 35% lower than in these mice given *N*-desethyl sunitinib alone (Fig. 5D). This suggests some inhibition by elacridar of *N*-desethyl sunitinib brain uptake. In the absence of elacridar, brain-to-plasma ratios in *Abcb1a/1b*(-/-)/*Abcg2*(-/-) mice, but not *Abcb1a/1b*(-/-) and *Abcg2*(-/-) mice, were markedly increased compared with wild-type mice (Fig. 5E). When looking at brain-to-plasma ratios, the difference between wild-type mice treated with elacridar or vehicle even lost

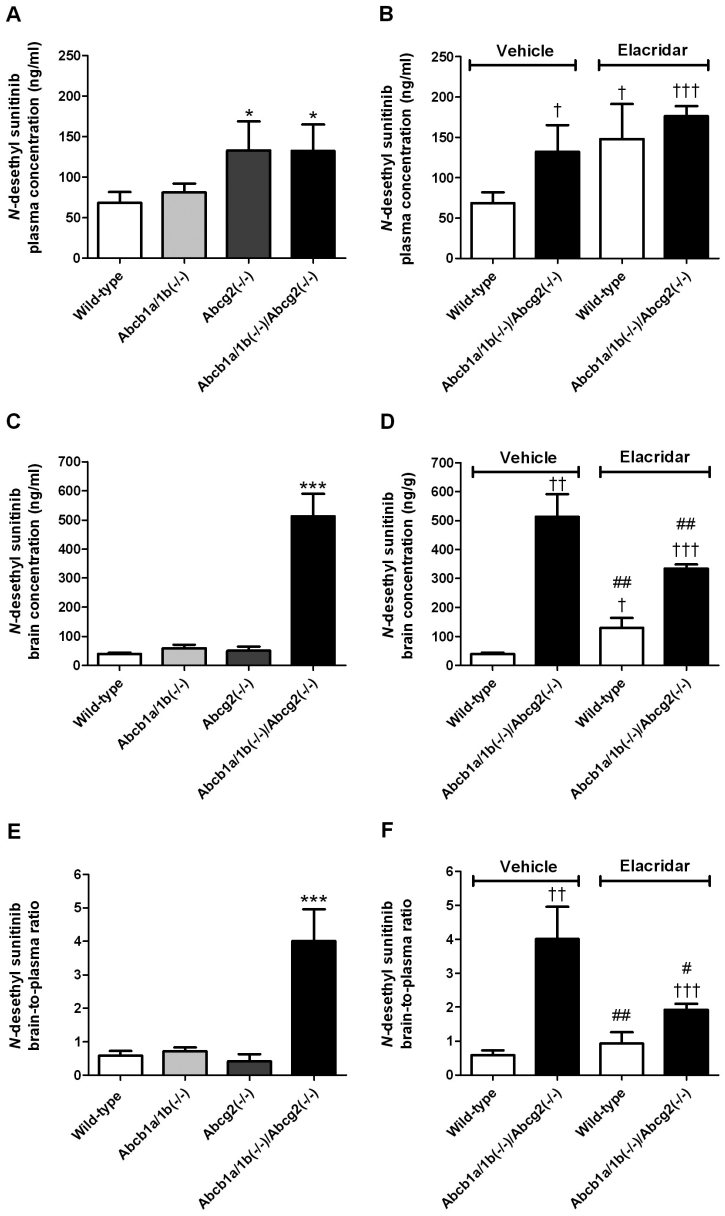

Fig. 5. Effect of genetic deletion on plasma (A) and brain (C) concentrations and brain-to-plasma ratios (E) of *N*-desethyl sunitinib in male wild-type, *Abcb1a/1b*(-/-), *Abcg2*(-/-), and *Abcb1a/1b*(-/-)/*Abcg2*(-/-) mice 1 h after intravenous injection of 5 mg/kg of *N*-desethyl sunitinib. Effect of elacridar on plasma (B) and brain (D) concentrations and brain-to-plasma ratios (F) in wild-type and *Abcb1a/1b*(-/-)/*Abcg2*(-/-) mice. *N*-desethyl sunitinib was administered 15 min after intravenous administration of either elacridar (10 mg/kg) or vehicle. Columns, means (n = 3-4); bars, S.D. *, $p < 0.05$, ***, $p < 0.001$, compared with wild-type mice receiving vehicle (one-way ANOVA). †, $p < 0.05$, ††, $p < 0.01$, †††, $p < 0.001$ compared with wild-type mice receiving vehicle (Student's *t*-test). #, $p < 0.05$, ##, $p < 0.01$ compared with *Abcb1a/1b*(-/-)/*Abcg2*(-/-) receiving vehicle (Student's *t*-test).

statistical significance (Fig. 5F, compare white bars). However, the brain-to-plasma ratios of *Abcb1a/1b*(-/-)/*Abcg2*(-/-) mice treated either with elacridar or vehicle were still significantly increased compared with wild-type mice without elacridar (Fig. 5F). The results indicate that the effect of intravenous elacridar in enhancing brain accumulation of *N*-desethyl sunitinib is quite limited, and that there may even be some inhibition of *N*-desethyl sunitinib uptake into the brain. This results in somewhat higher brain concentrations as compared with wild-type mice given *N*-desethyl sunitinib alone, but far less than the concentrations seen in mice genetically lacking both transporters.

Partial saturation of Abcg2-mediated *N*-desethyl sunitinib transport in the BBB of mice following high-dose sunitinib

We wanted to study the impact of Abcb1 and Abcg2 on brain accumulation of *N*-desethyl sunitinib following a high intravenous sunitinib administration (20 mg/kg) in knockout models. Plasma concentrations of *N*-desethyl sunitinib in *Abcg2*(-/-) and *Abcb1a/1b*(-/-)/*Abcg2*(-/-) mice, but not in *Abcb1a/1b*(-/-) mice, were modestly but significantly higher compared with wild-type mice at t = 10 min (Fig. 6A). At 1 h, plasma levels of this metabolite had increased relative to 10 min in all strains and the plasma levels in *Abcg2*(-/-) mice were still significantly higher than those in wild-type mice (Fig. 6B). Ten minutes after intravenous sunitinib administration, brain levels of *N*-desethyl sunitinib were not detectable in wild-type, *Abcg2*(-/-) and *Abcb1a/1b*(-/-) mice, but marginally detectable in *Abcb1a/1b*(-/-)/*Abcg2*(-/-) mice (Fig 6C). At 1 h, *N*-desethyl sunitinib brain concentrations were detectable in all strains, and brain concentrations in *Abcb1a/1b*(-/-) and *Abcb1a/1b*(-/-)/*Abcg2*(-/-) mice, but not *Abcg2*(-/-) mice, were significantly higher than those in wild-type mice (Fig. 6D). Brain-to-plasma ratios were also significantly increased in *Abcb1a/1b*(-/-)/*Abcg2*(-/-) mice, but not in *Abcb1a/1b*(-/-) mice (supplemental Fig. 4A). Upon high-dose intravenous sunitinib administration, the plasma *N*-desethyl sunitinib-to-sunitinib ratios were lower than after oral administration of sunitinib (10 mg/kg), but not significantly different among all strains except in *Abcg2*(-/-) mice, which displayed a 1.4-fold increase relative to wild-type mice (supplemental Fig. 4B).

DISCUSSION

In this study, we show that *N*-desethyl sunitinib is actively transported in vitro by human ABCB1 and ABCG2 and murine Abcg2, but not by human ABCC2 or murine Abcc2. We also demonstrate in MDCKII cells stably coexpressing human ABCB1 and ABCG2 that the contribution of ABCG2 to *N*-desethyl sunitinib transport at 5 μM is nearly equal to that of ABCB1. Upon oral sunitinib administration, the plasma $AUC_{0\text{-}6h}$ of *N*-desethyl sunitinib did not differ among wild-type, *Abcb1a/1b*(-/-), *Abcg2*(-/-), and *Abcb1a/1b*(-/-)/*Abcg2*(-/-) strains. However, we found a profound effect (13.7-fold) on *N*-desethyl sunitinib brain accumulation when both transport systems were absent from the BBB. In addition, brain concentrations of *N*-desethyl sunitinib were increased to just above the LLQ by concomitant oral elacridar treatment in wild-type mice. After intravenous administration of *N*-desethyl sunitinib,

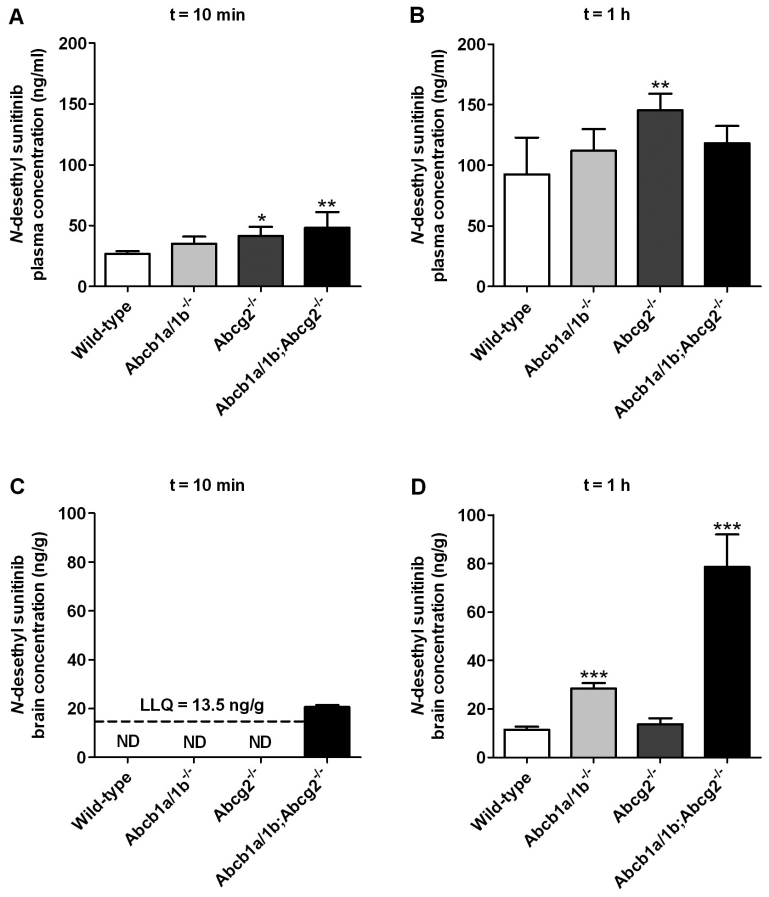

Fig. 6. Plasma concentrations (A and B) and brain concentrations (C and D) of *N*-desethyl sunitinib in male wild-type, *Abcb1a/1b*(-/-), *Abcg2*(-/-), and *Abcb1a/1b*(-/-)/*Abcg2*(-/-) mice 10 min (A and C) or 1 h (B and D) after intravenous injection of 20 mg/kg sunitinib malate. Columns, means (n = 5); bars, S.D. *, $p < 0.05$, **, $p < 0.01$, ***, $p < 0.001$, compared with wild-type mice (one-way ANOVA). ND, not detectable.

Abcg2 deficiency was found to modestly enhance its systemic plasma levels, which may suggest a role in *N*-desethyl sunitinib elimination. In *Abcb1a/1b*(-/-)/*Abcg2*(-/-) mice, but not in *Abcb1a/1b*(-/-) and *Abcg2*(-/-) mice, the brain levels of intravenously administered *N*-desethyl sunitinib were highly increased compared with wild-type mice. Thus, the brain accumulation of *N*-desethyl sunitinib, similar to that of its parent compound sunitinib, critically depends on the efflux activity of both Abcb1 and Abcg2. Intravenous elacridar increased *N*-desethyl sunitinib plasma and brain levels, but had no significant impact on the brain-to-plasma ratios of *N*-desethyl sunitinib in wild-type mice.

Our data suggest that there was no substantial role of Abcb1a/1b and Abcg2 in plasma pharmacokinetics of *N*-desethyl

sunitinib after oral sunitinib administration. Accordingly, plasma levels of *N*-desethyl sunitinib were not substantially changed upon oral coadministration of elacridar and sunitinib (Fig. 4A). Upon direct intravenous administration, however, plasma levels of *N*-desethyl sunitinib were 1.9-fold increased in *Abcg2*(-/-) and *Abcb1a/1b*(-/-)/*Abcg2*(-/-) mice compared with vehicle-treated wild-type mice, but not in *Abcb1a/1b*(-/-) mice (Fig. 6A). These results suggest that Abcg2 might play a role in the systemic elimination of *N*-desethyl sunitinib after intravenous administration. In the presence of elacridar, plasma concentrations of *N*-desethyl sunitinib in wild-type and *Abcb1a/1b*(-/-)/*Abcg2*(-/-) mice were not different, suggesting that intravenous elacridar reduces the plasma elimination of *N*-desethyl sunitinib in wild-type mice, presumably via Abcg2. Similarly, Lagas et al. (2009) demonstrated previously that elacridar can inhibit the systemic elimination of the TKI dasatinib via Abcb1 and/or Abcg2. Our data suggest that a possible systemic elimination contribution of Abcg2 only became apparent at higher plasma levels (which would occur especially shortly after intravenous *N*-desethyl sunitinib administration), but not at lower plasma levels (after oral sunitinib administration). One could speculate that at low plasma levels, alternative (non-Abcg2) *N*-desethyl sunitinib elimination processes predominate, but that these become saturated at higher plasma levels. If Abcg2 is not yet saturated at these levels, it will have a much more marked impact on *N*-desethyl sunitinib plasma concentrations than at lower plasma levels.

Like for many other shared Abcb1a/1b and Abcg2 substrates, the single disruption of Abcb1a/1b or Abcg2 in mice has only little effect on the brain accumulation of *N*-desethyl sunitinib, whereas simultaneous disruption of the two transporters results in a dramatic increase in *N*-desethyl sunitinib brain accumulation. This disproportionate effect has led some researchers to envisage a compensatory change with upregulation of one transporter in the BBB of single knockout strains for the other transporter. However, extensive analyses of Abcg2 or Abcb1a expression in brain homogenates of, respectively, Abcb1a/1b or Abcg2 knockout mice as used by us revealed no significant change in the RNA and/or protein levels in either strain (Lagas et al., 2010; de Vries et al., 2007; Jonker et al., 2000). Moreover, Kodaira et al. (2010), using specific transport substrates for either transporter, found negligible shifts in brain accumulation of these substrates in the single knockout strains of the complementary transporter. This suggests that there is no substantial change in Abcb1a or Abcg2 activity in the BBB of the FVB background Abcg2 or Abcb1a/1b knockout mice, respectively. Kodaira et al. (2010) further showed that a (physiologically based) pharmacokinetic model of Abcb1a and Abcg2 activity in the BBB could readily describe the seemingly disproportionate effect of the combined disruption of these transporters compared with the single disruptions, without invoking changes in activity of the remaining transporter.

Our data show that the brain accumulation of *N*-desethyl sunitinib was highly increased in *Abcb1a/1b*(-/-)/*Abcg2*(-/-) mice 6 h after oral sunitinib administration. Therefore, we studied the brain accumulation of *N*-desethyl sunitinib after an oral coadministration schedule of elacridar and sunitinib that

might also be feasible in a clinical setting. In this context it is important to note that the plasma exposure level of elacridar used in our study is also achievable in humans, as demonstrated by Kemper et al. (2001), who showed that a patient receiving 1000 mg of elacridar orally had almost the same elacridar plasma concentrations as mice treated with 100 mg/kg of elacridar orally. Somewhat disappointingly, brain levels of *N*-desethyl sunitinib were only just above the LLQ under this coadministration scheme (Fig. 4B). Direct intravenous administration of *N*-desethyl sunitinib at a dose of 5 mg/kg to wild-type mice resulted in higher brain levels of *N*-desethyl sunitinib, but still far lower than those in *Abcb1a/1b*(-/-)/*Abcg2*(-/-) mice (Fig. 5, A, C, and E). The results of Fig. 5, D and F suggest that elacridar could not fully inhibit the BBB efflux transporters with respect to *N*-desethyl sunitinib, resulting in lower brain accumulation compared with genetic deletion of Abcb1a/1b and Abcg2. Unexpectedly, elacridar treatment in *Abcb1a/1b*(-/-)/*Abcg2*(-/-) mice also lowered brain *N*-desethyl sunitinib levels compared with vehicle-treated mice, whereas plasma levels were not significantly affected (Fig. 5, B, D, and F). One speculative explanation is that this reduction effect might be caused by the inhibition of putative uptake transporters for *N*-desethyl sunitinib into the brain. Note that such a reduction was not observed for the parent drug sunitinib (Tang et al., 2012).

Even though elacridar is generally an effective inhibitor for ABCB1 and ABCG2 in vitro and in vivo, elacridar has been shown to be a better inhibitor of Abcb1 than Abcg2 in vitro (Allen et al., 2002; Matsson et al., 2009). We observed complete inhibition of ABCB1-mediated *N*-desethyl sunitinib transport, but only partial inhibition of human ABCG2- and especially murine Abcg2-mediated *N*-desethyl sunitinib transport (Fig. 1, C, D, G, and H). Note that, given the apparent difference in sensitivity to elacridar between mouse Abcg2 and human ABCG2, it could be that the effects of elacridar would be more pronounced in humans than in mice. In vivo, we were still able to observe a significant increase in brain concentration in wild-type mice treated with elacridar in combination with *N*-desethyl sunitinib, but the change in brain-to-plasma ratio was not statistically significant. The increase in the brain concentrations of *N*-desethyl sunitinib in wild-type mice could therefore be partly caused by the increased plasma concentrations in wild-type mice treated with elacridar (Fig. 5B). Our in vitro finding of poor Abcg2 inhibition by elacridar thus seems to be in agreement with our in vivo findings. Apparently, elacridar is overall not an efficient enough inhibitor of Abcg2-mediated transport of *N*-desethyl sunitinib. One could speculate that its affinity for Abcg2 is not high enough, because the high-affinity ABCG2/Abcg2 inhibitor Ko143 did completely inhibit transport in vitro. Thus, higher concentrations of elacridar may be needed to fully inhibit Abcg2 than to inhibit Abcb1 in the BBB. For *N*-desethyl sunitinib, however, increasing elacridar dosage might be counterproductive as we cannot exclude that it might also inhibit brain uptake more strongly.

Our *in vitro* data with ABCB1- and ABCG2-overexpressing MDCKII cells suggest that the transport contribution of ABCG2 in these cells is almost equal to that of ABCB1 at 5 μM *N*-desethyl sunitinib. Possibly beginning saturation of ABCG2-mediated, but not of ABCB1-mediated, *N*-desethyl

sunitinib transport occurs at 20 μM. We have previously observed that plotting inverse transport ratios (AB/BA, or 1/*r*) obtained with this cell line yields good qualitative correlations with brain penetration data, especially for topotecan and sorafenib, but somewhat less for sunitinib (Poller et al., 2011). For its metabolite *N*-desethyl sunitinib, however, we again found a very good in vitro-in vivo correlation between brain concentration in the various wild-type and knockout strains and transcellular transport data obtained at 5 and 20 μM (Supplemental Fig. 5, compare C-F).

To obtain a better understanding of the relative ability of sunitinib and *N*-desethyl sunitinib to penetrate the brain, we compared the data obtained in this study with our previous findings for sunitinib (compare Table 1 and Supplemental Table 1). In wild-type mice, sunitinib has a 2.4-fold higher brain penetration than *N*-desethyl sunitinib, with a P_{brain} of 1.6 and 0.67 observed for sunitinib and *N*-desethyl sunitinib, respectively. Six hours after oral sunitinib administration (10 mg/kg), sunitinib brain concentrations were 5.7-fold higher than *N*-desethyl sunitinib brain concentrations seen in wild-type mice. In addition, elacridar did not completely inhibit transport activity of human ABCG2 and murine Abcg2-mediated *N*-desethyl sunitinib transport in vitro, suggesting that *N*-desethyl sunitinib is a more avid human ABCG2 and murine Abcg2 substrate than sunitinib. Elacridar increased the brain-to-plasma ratio of sunitinib 12-fold (Tang et al., 2012), but that of its metabolite only 1.6-fold in wild-type mice (Fig. 5F). Therefore, elacridar had a much greater effect on the brain concentration of sunitinib than on that of *N*-desethyl sunitinib.

To the best of our knowledge, this is the first study demonstrating that Abcb1 and Abcg2 together restrict *N*-desethyl sunitinib brain accumulation, but not plasma pharmacokinetics of *N*-desethyl sunitinib upon oral sunitinib administration. Abcg2 may modestly enhance systemic elimination of *N*-desethyl sunitinib administered intravenously. Despite its effect on plasma and brain concentrations, intravenous elacridar had no significant impact on brain-to-plasma ratios of *N*-desethyl sunitinib in wild-type mice. Together with our previous findings on sunitinib, the effect of elacridar is more pronounced for the brain accumulation of sunitinib than for that of *N*-desethyl sunitinib. Therefore, coadministration of elacridar seems a more attractive strategy for sunitinib than for *N*-desethyl sunitinib in improving the clinical efficacy against brain metastases and brain tumors positioned behind a functionally intact BBB.

Acknowledgements. This work was supported by the Dutch Cancer Society [Grant 2007-3764]; an academic staff training scheme fellowship from the Malaysian Ministry of Science, Technology, and Innovation (to S.C.T.); and a postdoctoral fellowship from the Swiss National Science Foundation [Grant PBBSP3-128567] (to B.P.). We thank Dilek Iusuf and Selvi Durmus for critical reading of the manuscript.

REFERENCES

1. Adams VR and Leggas M (2007) Sunitinib malate for the treatment of metastatic renal cell carcinoma and gastrointestinal stromal tumors. *Clin Ther* **29**:1338-1353.
2. Allen JD, van Loevezijn A, Lakhai JM, van der Valk M, van Tellingen O, Reid G, Schellens JH, Koomen GJ, and Schinkel AH (2002) Potent and specific inhibition of the breast cancer resistance protein multidrug transporter in vitro and in mouse intestine by a novel analogue of fumitremorgin C. *Mol Cancer Ther* **1**:417-425.
3. Bakos E, Evers R, Calenda G, Tusnady GE, Szakacs G, Varadi A, and Sarkadi B (2000) Characterization of the amino-terminal regions in the human multidrug resistance protein (MRP1). *J Cell Sci* **113**:4451-4461.
4. Bihorel S, Camenisch G, Lemaire M, and Scherrmann JM (2007) Influence of breast cancer resistance protein (Abcg2) and p-glycoprotein (Abcb1a) on the transport of imatinib mesylate (Gleevec) across the mouse blood-brain barrier. *J Neurochem* **102**:1749-1757.
5. Burger H, van Tol H, Boersma AW, Brok M, Wiemer EA, Stoter G, and Nooter K (2004) Imatinib mesylate (STI571) is a substrate for the breast cancer resistance protein (BCRP)/ABCG2 drug pump. *Blood* **104**:2940-2942.
6. Chen Y, Agarwal S, Shaik NM, Chen C, Yang Z, and Elmquist WF (2009) P-glycoprotein and breast cancer resistance protein influence brain distribution of dasatinib. *J Pharmacol Exp Ther* **330**:956-963.
7. Chow LQ and Eckhardt SG (2007) Sunitinib: from rational design to clinical efficacy. *J Clin Oncol* **25**:884-896.
8. Dai H, Marbach P, Lemaire M, Hayes M, and Elmquist WF (2003) Distribution of STI-571 to the brain is limited by P-glycoprotein-mediated efflux. *J Pharmacol Exp Ther* **304**:1085-1092.
9. de Vries NA, Zhao J, Kroon E, Buckle T, Beijnen JH, and van Tellingen O (2007). P-glycoprotein and breast cancer resistance protein: two dominant transporters working together in limiting the brain penetration of topotecan. *Clin Cancer Res* **13**:6440-6449.
10. Evers R, Kool M, Smith AJ, van Deemter L, de Haas M, and Borst P (2000) Inhibitory effect of the reversal agents V-104, GF120918 and Pluronic L61 on MDR1 Pgp-, MRP1- and MRP2-mediated transport. *Br J Cancer* **83**:366-374.
11. Evers R, Kool M, van Deemter L, Janssen H, Calafat J, Oomen LC, Paulusma CC, Oude Elferink RP, Baas F, Schinkel AH, and Borst P (1998) Drug export activity of the human canalicular multispecific organic anion transporter in polarized kidney MDCK cells expressing cMOAT (MRP2) cDNA. *J Clin Invest* **101**:1310-1319.
12. Glavinas H, Krajcsi P, Cserepes J, and Sarkadi B (2004) The role of ABC transporters in drug resistance, metabolism and toxicity. *Curr Drug Deliv* **1**:27-42.
13. Houk BE, Bello CL, Kang D, and Amantea M (2009) A population pharmacokinetic meta-analysis of sunitinib malate (SU11248) and its primary metabolite (SU12662) in healthy volunteers and oncology patients. *Clin Cancer Res* **15**:2497-2506.
14. Jonker JW, Smit JW, Brinkhuis RF, Maliepaard M, Beijnen JH, Schellens JH, and Schinkel AH (2000) Role of breast cancer resistance protein in the bioavailability and fetal penetration of topotecan. *J Natl Cancer Inst* **92**:1651-1656.
15. Jonker JW, Buitelaar M, Wagenaar E, van der Valk MA, Scheffer GL, Scheper RJ, Plosch T, Kuipers F, Elferink RP, Rosing H, Beijnen JH, and Schinkel AH (2002) The breast cancer resistance protein protects against a major chlorophyll-derived dietary phototoxin and protoporphyria. *Proc Natl Acad Sci U S A* **99**:15649-15654.
16. Jonker JW, Freeman J, Bolscher E, Musters S, Alvi AJ, Titley I, Schinkel AH, and Dale TC (2005) Contribution of the ABC transporters Bcrp1 and Mdr1a/1b to the side population phenotype in mammary gland and bone marrow of mice. *Stem Cells* **23**:1059-1065.
17. Kemper EM, Jansen B, Brouwer KR, Schellens JH, Beijnen JH, and van Tellingen O (2001) Bioanalysis and preliminary pharmacokinetics of the acridonecarboxamide derivative GF120918 in plasma of mice and humans by ion-pairing reversed-phase high-performance liquid chromatography with fluorescence detection. *J Chromatogr B Biomed Sci Appl* 759:135-143.
18. Kodaira H, Kusuhara H, Ushiki J, Fuse E, and Sugiyama Y (2010) Kinetic analysis of the cooperation of P-glycoprotein (P-gp/Abcb1) and breast cancer resistance protein (Bcrp/Abcg2) in limiting the brain and testis penetration of erlotinib, flavopiridol, and mitoxantrone. *J Pharmacol Exp Ther* **333**:788-796.

19. Lagas JS, van Waterschoot RA, Sparidans RW, Wagenaar E, Beijnen JH, and Schinkel AH (2010) Breast cancer resistance protein and P-glycoprotein limit sorafenib brain accumulation. *Mol Cancer Ther* **9**:319-326.
20. Lagas JS, van Waterschoot RA, van Tilburg VA, Hillebrand MJ, Lankheet N, Rosing H, Beijnen JH, and Schinkel AH (2009) Brain accumulation of dasatinib is restricted by P-glycoprotein (ABCB1) and breast cancer resistance protein (ABCG2) and can be enhanced by elacridar treatment. *Clin Cancer Res* **15**:2344-2351.
21. Lankheet NA, Blank CU, Mallo H, Adriaansz S, Rosing H, Schellens JH, Huitema AD, and Beijnen JH (2011) Determination of sunitinib and its active metabolite N-desethylsunitinib in sweat of a patient. *J Anal Toxicol* **35**:558-565.
22. Matsson P, Pedersen JM, Norinder U, Bergstrom CA, and Artursson P (2009) Identification of novel specific and general inhibitors of the three major human ATP-binding cassette transporters P-gp, BCRP and MRP2 among registered drugs. *Pharm Res* **26**:1816-1831.
23. Oostendorp RL, Buckle T, Beijnen JH, van Tellingen O, and Schellens JH (2009) The effect of P-gp (Mdr1a/1b), BCRP (Bcrp1) and P-gp/BCRP inhibitors on the in vivo absorption, distribution, metabolism and excretion of imatinib. *Invest New Drugs* **27**:31-40.
24. Pavek P, Merino G, Wagenaar E, Bolscher E, Novotna M, Jonker JW, and Schinkel AH (2005) Human breast cancer resistance protein: interactions with steroid drugs, hormones, the dietary carcinogen 2-amino-1-methyl-6-phenylimidazo(4,5-b)pyridine, and transport of cimetidine. *J Pharmacol Exp Ther* **312**:144-152.
25. Poller B, Wagenaar E, Tang SC, and Schinkel AH (2011) Double-Transduced MDCKII Cells to Study Human P-Glycoprotein (ABCB1) and Breast Cancer Resistance Protein (ABCG2) Interplay in Drug Transport across the Blood-Brain Barrier. *Mol Pharm* **8**:571-82.
26. Schinkel AH, Mayer U, Wagenaar E, Mol CA, van Deemter L, Smit JJ, van der Valk MA, Voordouw AC, Spits H, van Tellingen O, Zijlmans JM, Fibbe WE, and Borst P (1997) Normal viability and altered pharmacokinetics in mice lacking mdr1-type (drug-transporting) P-glycoproteins. *Proc Natl Acad Sci U S A* **94**:4028-4033.
27. Shirao K, Nishida T, Doi T, Komatsu Y, Muro K, Li Y, Ueda E, and Ohtsu A (2010) Phase I/II study of sunitinib malate in Japanese patients with gastrointestinal stromal tumor after failure of prior treatment with imatinib mesylate. *Invest New Drugs* **28**:866-875.
28. Tang SC, Lagas JS, Lankheet NA, Poller B, Hillebrand MJ, Rosing H, Beijnen JH, and Schinkel AH (2012) Brain accumulation of sunitinib is restricted by P-glycoprotein (ABCB1) and breast cancer resistance protein (ABCG2) and can be enhanced by oral elacridar and sunitinib coadministration. *Int J Cancer* **130**:223-233.
29. Zimmermann C, van de Wetering K, van de Steeg E, Wagenaar E, Vens C, and Schinkel AH (2008) Species-dependent transport and modulation properties of human and mouse multidrug resistance protein 2 (MRP2/Mrp2, ABCC2/Abcc2). *Drug Metab Dispos* **36**:631-640.

SUPPORTING INFORMATION

Supplemental Table 1. Pharmacokinetic parameters, brain concentrations (t = 6 h), and relative brain accumulation of sunitinib after oral administration of 10 mg/kg sunitinib malate to various mouse strains

	Genotype			
	Wild-type	*Abcb1a/1b*(-/-)	*Abcg2*(-/-)	*Abcb1a/1b*(-/-)/*Abcg2*(-/-)
Plasma $AUC_{(0-6)}$[a], ng.h/ml	445.4 ± 202.8	513.9 ± 144.9	310.9 ± 171.6	287.8 ± 87.7
Fold change $AUC_{(0-6)}$	1.00	1.15	0.70	0.65
C_{max}[a], ng/ml	114.8 ± 38.1	132.2 ± 56.8	66.9 ± 46.1	67.7 ± 29.2
T_{max}[a], h	1.0	1.0	1.0	1.0
C_{brain}[a], ng/g	57.8 ± 10.9	133.2 ± 32.1	75.1 ± 44.8	1353.7 ± 557.6***
Fold change C_{brain}	1.0	2.3	1.3	23.4
P_{brain}[a], ($x10^{-1}$ h^{-1})	1.6 ± 1.0	2.8 ± 0.8	2.4 ± 0.9	42.4 ± 10.7***
Fold change P_{brain}	1.0	1.7	1.5	26.9

Data are means (n = 6-8) ± S.D. All parameters obtained for knockout strains were compared with those for wild-type mice.
[a] Data for comparison were taken from Tang et al. (2012). ***, $p < 0.001$, compared with wild-type mice (one-way ANOVA).

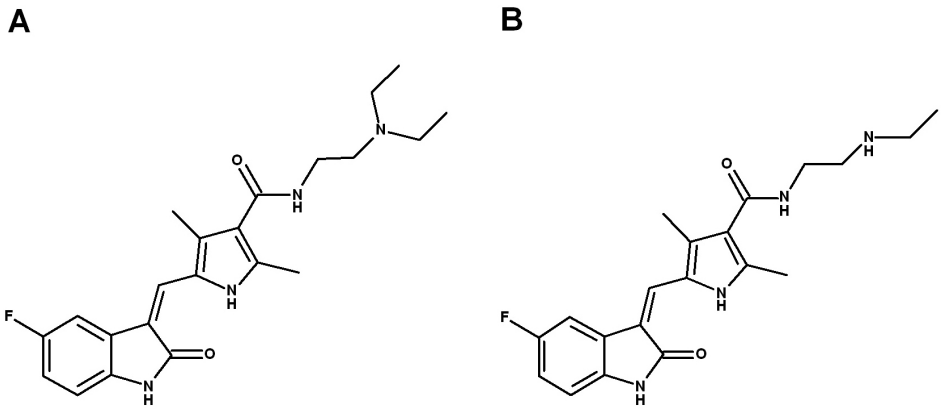

Supplemental Figure 1. Molecular structures of sunitinib (A) and *N*-desethyl sunitinib (B).

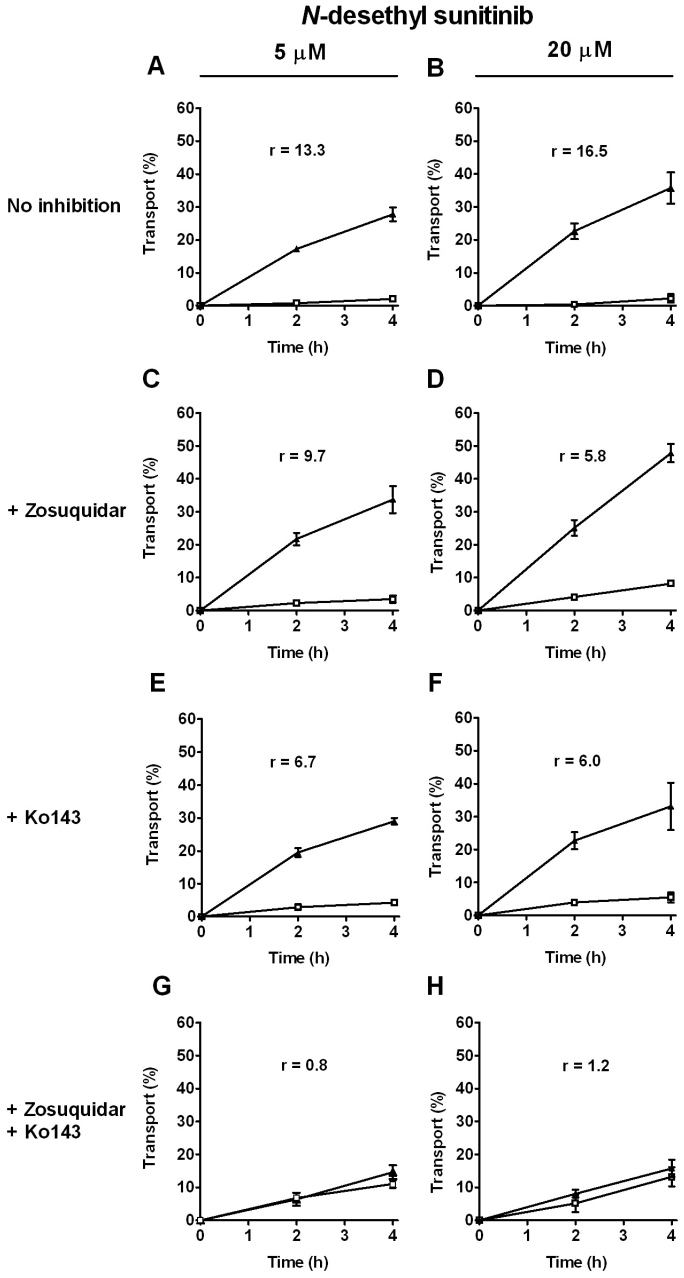

Supplemental Figure 2. Concentration-dependent transepithelial transport of *N*-desethyl sunitinib assessed using MDCKII-ABCB1/ABCG2 cells. Transport was measured in the absence of inhibitor (A and B), in the presence of 5 μM of zosuquidar to block ABCB1 (C and D), in the presence of 1 μM of Ko143 to inhibit ABCG2 (E, F), or in the presence of both inhibitors (G, H). ▲, translocation from basolateral to apical compartment; □, translocation from apical to basolateral compartment. Points, means (n = 3); bars, S.D. At t = 4 h, 1% of transport is approximately equal to an apparent permeability coefficient (P_{app}) of 0.30 × 10^{-6} cm/s.

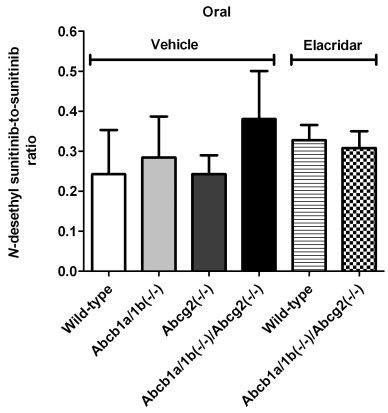

Supplemental Figure 3. Plasma *N*-desethyl sunitinib-to-sunitinib concentration ratios in male wild-type, *Abcb1a/1b*(-/-), *Abcg2*(-/-), and *Abcb1a/1b*(-/-)/*Abcg2*(-/-) mice 1 h after a single oral dose of 10 mg/kg sunitinib malate with or without oral elacridar administration (100 mg/kg). Columns, means (n = 4-5); bars, S.D.

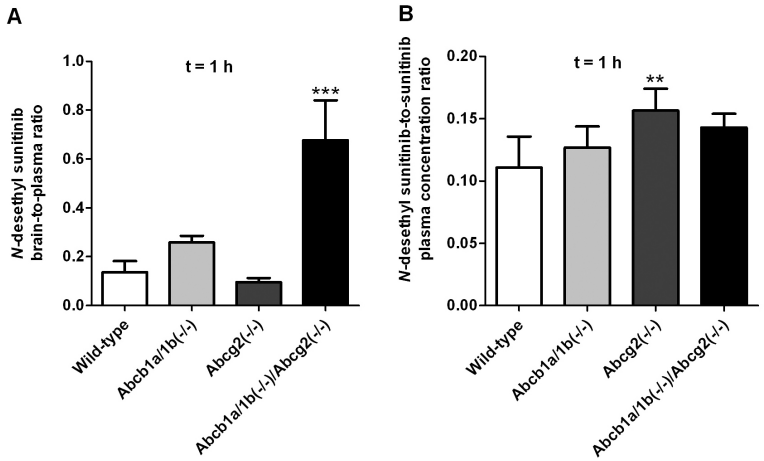

Supplemental Figure 4. Brain-to-plasma concentration ratios of *N*-desethyl sunitinib (A) and plasma *N*-desethyl sunitinib-to-sunitinib concentration ratios (B) for male wild-type, *Abcb1a/1b*(-/-), *Abcg2*(-/-), and *Abcb1a/1b*(-/-)/*Abcg2*(-/-) mice 1 h after intravenous administration of 20 mg/kg sunitinib malate. Columns, means (n = 4-5); bars, S.D. **, $p < 0.01$, ***, $p < 0.001$, compared with wild-type mice (one-way ANOVA).

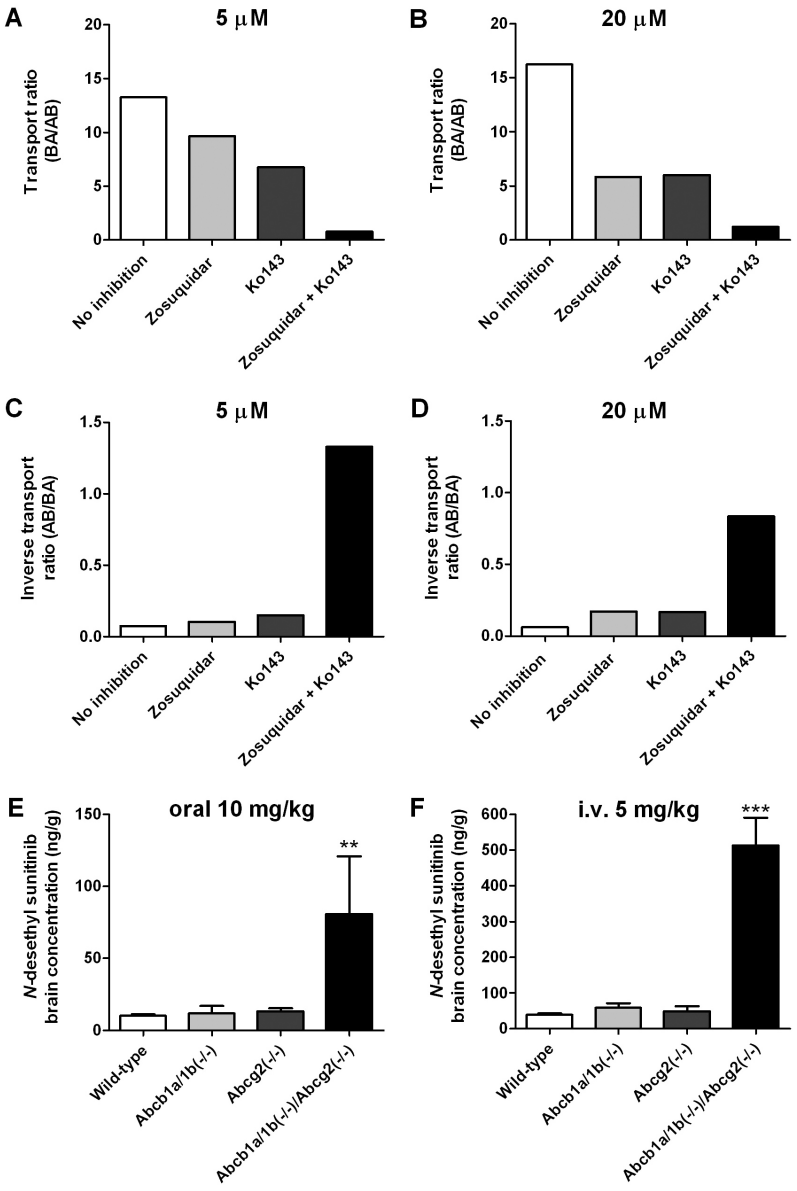

Supplemental Figure 5. Comparison of in vitro transport ratios (A, B) and inverse transport ratios (C, D) of *N*-desethyl sunitinib in MDCKII-ABCB1/ABCG2 cells with in vivo brain concentrations of *N*-desethyl sunitinib (E and F) in wild-type, *Abcb1a/1b*(-/-), *Abcg2*(-/-) and *Abcb1a/1b*(-/-)/*Abcg2*(-/-) mice. In vitro, *N*-desethyl sunitinib was applied at 5 μM (A and C) or 20 μM (B and D). Basolaterally directed (AB) and apically directed (BA) translocation data of *N*-desethyl sunitinib were used to calculate transport ratios (BA/AB) and inverse transport ratios (AB/BA). Results are expressed as mean values (n = 3). *N*-desethyl sunitinib brain concentrations (means ± SD; n = 4) were measured 6 h after oral administration of 10 mg/kg of sunitinib malate (E) or 1 h after intravenous administration of 5 mg/kg *N*-desethyl sunitinib (F), respectively. **, $p < 0.01$, ***, $p < 0.001$, compared with wild-type mice (one-way ANOVA).

2.3

INCREASED ORAL AVAILABILITY AND BRAIN ACCUMULATION OF THE ALK INHIBITOR CRIZOTINIB BY COADMINISTRATION OF THE P-GLYCOPROTEIN (ABCB1) AND BREAST CANCER RESISTANCE PROTEIN (ABCG2) INHIBITOR ELACRIDAR

Seng Chuan Tang[1], Luan N. Nguyen[1], Rolf W. Sparidans[2], Els Wagenaar[1], Jos H. Beijnen[2,3] and Alfred H. Schinkel[1]

[1] Division of Molecular Oncology, The Netherlands Cancer Institute, Amsterdam, The Netherlands
[2] Division of Pharmacoepidemiology and Clinical Pharmacology, Department of Pharmaceutical Sciences, Faculty of Science, Utrecht University, Utrecht, The Netherlands
[3] Department of Pharmacy and Pharmacology, Slotervaart Hospital, Amsterdam, The Netherlands

Submitted for publication

ABSTRACT

Crizotinib is an oral tyrosine kinase inhibitor approved for treating patients with non-small cell lung cancer (NSCLC) containing an anaplastic lymphoma kinase (ALK) rearrangement. We used knockout mice to study the roles of P-glycoprotein (ABCB1) and breast cancer resistance protein (ABCG2) in plasma pharmacokinetics and brain accumulation of oral crizotinib, and the feasibility of improving crizotinib kinetics using coadministration of the dual ABCB1/ABCG2 inhibitor elacridar. *In vitro*, crizotinib was a good transport substrate of human ABCB1, but not of human ABCG2 or murine Abcg2. With low-dose oral crizotinib (5 mg/kg), *Abcb1a/1b*$^{-/-}$ and *Abcb1a/1b;Abcg2*$^{-/-}$ mice had an ~2-fold higher plasma AUC than wild-type mice, and a markedly (~40-fold) higher brain accumulation at 24 hr. Also at 4 hr, crizotinib brain concentrations were ~25-fold, and brain-to-plasma ratios ~14-fold higher in *Abcb1a/1b*$^{-/-}$ and *Abcb1a/1b;Abcg2*$^{-/-}$ mice than in wild-type mice. High-dose oral crizotinib (50 mg/kg) resulted in comparable plasma pharmacokinetics between wild-type and *Abcb1a/1b*$^{-/-}$ mice, suggesting saturation of intestinal Abcb1. Nonetheless, brain accumulation at 24 hr was still ~70-fold higher in *Abcb1a/1b*$^{-/-}$ than in wild-type mice. Importantly, oral elacridar coadministration increased the plasma and brain concentrations and brain-to-plasma ratios of crizotinib in wild-type mice, equaling the levels in *Abcb1a/1b;Abcg2*$^{-/-}$ mice. Our results indicate that crizotinib oral availability and brain accumulation were primarily restricted by Abcb1 at a non-saturating dose, and that coadministration of elacridar with crizotinib could substantially increase crizotinib oral availability and delivery to the brain. This principle might be used to enhance therapeutic efficacy of crizotinib against brain metastases in NSCLC patients.

INTRODUCTION

Lung cancer remains the leading cause of cancer deaths in western countries.[1] Patients with non-small cell lung cancer (NSCLC), accounting for approximately 80% of all lung cancer cases,[2] are often diagnosed at advanced stages of the disease. A subset of NSCLC was shown to have a small inversion within chromosome 2p, which results in the formation of a fusion gene comprising portions of the echinoderm microtubule associated protein-like 4 (EML4) gene and the anaplastic lymphoma kinase (ALK) gene.[3] The EML4-ALK fusion results in constitutive activation of ALK kinase activity, which promotes cell proliferation, survival and cell cycling.[4]

Since the identification of ALK rearrangements in ~7% of NSCLC as a new and promising molecular target for treatment,[3] considerable effort has focused on developing drugs with the potential to inhibit ALK activity.[3,5,6] In August 2011, the US Food and Drug Administration granted accelerated approval for crizotinib (PF-02341066, structure shown in Figure 1A), the first orally administered tyrosine kinase inhibitor (TKI) to treat NSCLC patients harboring EML4-ALK translocations.[7] Crizotinib inhibits ALK phosphorylation, and signal

transduction leading to G1/S phase cell cycle arrest and induction of apoptosis in various cell lines harboring an ALK translocation.[8,9]

It has been shown that ATP-binding cassette (ABC) drug efflux transporters, such as P-glycoprotein (P-gp; ABCB1) and breast cancer resistance protein (BCRP; ABCG2) can affect plasma pharmacokinetics and particularly brain distribution of many TKIs used in cancer therapy.[10-13] In this context, it is also worth noting that many TKIs that are currently being evaluated in glioma, a primary brain tumor, have poor brain penetration due to ABCB1- and ABCG2-mediated efflux.[10,14,15] 10 of 31 NSCLC patients with an ALK gene rearrangement (32%) were diagnosed with metastatic disease to the brain.[16] Recently, a case report in a NSCLC patient showed a low penetration of crizotinib within cerebrospinal fluid, a surrogate (albeit not ideal) marker for brain penetration of a drug.[17] Therefore, it is important to understand the mechanism that limits brain accumulation of crizotinib in NSCLC patients, who are likely to develop brain metastases. We and others have previously shown that coadministration of the dual ABCB1 and ABCG2 inhibitor elacridar could significantly increase brain distribution of several TKIs including dasatinib,[12] gefitinib,[18] sunitinib[19] and vemurafenib.[11]

In vitro, crizotinib has been found to be a transported substrate and an inhibitor of ABCB1 (http://www.accessdata.fda.gov/drugsatfda_docs/nda/2011/202570Orig1s000ClinPharmR.pdf).[20] However, little is known about the *in vivo* role of ABCB1 and possibly ABCG2 in plasma pharmacokinetics and brain accumulation of crizotinib. The aim of this study was to establish to what extent crizotinib is transported by human ABCB1 and ABCG2, and mouse Abcg2 *in vitro*, and what the consequences are for oral availability and brain accumulation of crizotinib as judged in knockout mouse models. Furthermore, we tested whether, in an oral coadministration of the dual ABCB1/ABCG2 inhibitor elacridar with crizotinib, either of these parameters could be improved, with the ultimate aim of potentially improving therapeutic efficacy of crizotinib, especially against brain metastases of ALK-positive NSCLC patients.

MATERIALS AND METHODS

Chemicals and reagents

Crizotinib and elacridar hydrochloride were purchased from Sequoia Research Products (Pangbourne, UK). Zosuquidar (Eli Lilly, Indianapolis, USA) was a kind gift of Dr. O. van Tellingen (The Netherlands Cancer Institute, Amsterdam, The Netherlands) and Ko143 was obtained from Tocris Bioscience (Bristol, UK). Dipotassium-EDTA microvettes were obtained from Sarstedt (Numbrecht, Germany). EDTA disodium salt pH 8.0 was from Cambrex BioScience Inc. (Rockland, ME). Bovine serum albumin, fraction V, was purchased from Roche (Mannheim, Germany). Isoflurane (Forane) was from Abbott Laboratories (Queenborough, Kent, UK). All other chemicals and reagents were obtained from Sigma-Aldrich (Steinheim, Germany).

Cell lines and transport assays

Polarized Madin-Darby canine kidney-II (MDCK-II) cells and MDCK-II subclones transduced with *huABCB1*, *huABCG2* or *muAbcg2* cDNA were used and cultured as previously described.[21-24] Transepithelial transport assays were performed using 12-well Transwell® plates (Corning Inc., USA). The parental and variant subclones were seeded at a density of 2.5×10^5 cells per well and cultured for

3 days to form an intact monolayer. Membrane tightness was assessed by measurement of transepithelial electrical resistance.

Two hours prior to starting the transport experiment, cells were washed twice with pre-warmed PBS and pre-incubated with Opti-MEM medium (Invitrogen, USA), either alone or containing relevant inhibitors for 2 hr. The transepithelial transport experiment was started (t = 0) by replacing the incubation medium with Opti-MEM medium containing 5 μM crizotinib either alone or in combination with relevant inhibitors in the donor compartment. In the acceptor compartments, the corresponding inhibition solutions were added with the exclusion of crizotinib. The final concentrations of zosuquidar and Ko143 in the solutions were 5 μM and 1 μM, respectively. Plates were kept at 37°C in 5% CO_2 during the experiment, and 50 μl aliquots were taken from the acceptor compartment at 2, 4 and 8 hr. Samples were stored at -30°C until LC-MS/MS analysis. Total amount of drug transported to the acceptor compartment was calculated after correction for volume loss for each time point. Experiments were performed in triplicate and the mean amount of transport (±SD) was shown. Active transport was expressed by the relative transport ratio (*r*), defined as *r* = apically directed amount of transport divided by basolaterally directed amount of translocation, at a defined time point.

Animals

Mice were housed and handled according to institutional guidelines complying with Dutch legislation. Male wild-type, *Abcb1a/1b*$^{-/-}$,[25] *Abcg2*$^{-/-}$[23] and *Abcb1a/1b;Abcg2*$^{-/-}$[26] mice, all of a >99% FVB genetic background, were used between 8 and 14 weeks of age. Animals were kept in a temperature-controlled environment with a 12-hr light/12-hr dark cycle and received a standard diet (AM-II, Hope Farms B.V., Woerden, The Netherlands) and acidified water *ad libitum*.

Drug solutions

Crizotinib was dissolved in dimethyl sulfoxide (25 mg/ml) and further diluted with 50 mM sodium acetate buffer (pH 4.6) to obtain a concentration of 5 or 0.5 mg/ml. Crizotinib was administered orally at 50 or 5 mg/kg body weight (10 ml/kg). Elacridar hydrochloride was dissolved in dimethyl sulfoxide (106 mg/ml) in order to get 100 mg pure elacridar per 1 ml of dimethyl sulfoxide. The stock solution was further diluted with a mixture of Polysorbate 80, ethanol and water [20:13:67 (v/v/v)] to yield a concentration of 10 mg/ml pure elacridar, and orally administered at a dose of 100 mg/kg body weight (10 ml/kg).

Plasma pharmacokinetics and relative brain accumulation of crizotinib in mice

To minimize variation in absorption on oral administration, mice were fasted for 3 hr before crizotinib was administered by gavage into the stomach, using a blunt-ended needle. Tail vein blood sampling was performed at 0.25, 0.5, 1, 2, 4, and 8 hr time points after oral administration, using microvettes containing dipotassium-EDTA. Twenty-four hours after oral administration, mice were anesthetized with isoflurane and blood was collected by cardiac puncture. Blood samples were collected in eppendorf tubes containing 0.5 M disodium-EDTA as an anticoagulant. Immediately thereafter, mice were sacrificed by cervical dislocation and brains were rapidly removed. Plasma was isolated from the blood by centrifugation at 2,100 *g* for 6 min at 4°C, and the plasma fraction was collected and stored at

-30°C until analysis. Brains were homogenized with 1 ml of 4% bovine serum albumin and stored at -30°C until analysis. Relative brain accumulation after oral administration was calculated by determining the crizotinib brain concentration at 24 hr relative to the plasma $AUC_{0\text{-}24hr}$, as the AUC better reflects the overall crizotinib exposure of the brain over time than the plasma concentration at 24 hr after oral administration.

Plasma and brain exposure of crizotinib in mice

Crizotinib was administered orally as described above. Blood and brains were isolated 4 hr after oral crizotinib administration, and processed as described above. The brain concentrations were corrected for the amount of drug present in the brain vasculature, i.e. 1.4% of the plasma concentration right before the brains were isolated.[27]

Brain accumulation of crizotinib in combination with oral elacridar

Mice were fasted for 3 hr before oral administration of either elacridar (100 mg/kg) or elacridar vehicle. Two hours later, crizotinib (5 mg/kg) was administered to mice orally. Blood and brains were isolated 4 hr after crizotinib oral administration, and processed as described above. The brain concentrations were corrected for the amount of drug in the brain vasculature.

Crizotinib analysis

Crizotinib concentrations in Opti-MEM medium, plasma and brain homogenates were analyzed by liquid chromatography coupled to tandem mass spectrometry as described previously.[28] Values of lower limit of quantification (LLQ) for crizotinib were initially 10 ng/ml and 31.2 ng/g, later improved to 2.5 ng/ml and 7.8 ng/g for the plasma and brain homogenates, respectively.

Statistical analysis

Pharmacokinetic parameters were calculated by non-compartmental methods using the software package PK Solutions 2.0.2 (Summit Research Services, Ashland, OH). The area under the plasma concentration-time curve was calculated using the trapezoidal rule, without extrapolating to infinity. The maximum drug concentration in plasma (C_{max}) and the time to reach maximum drug concentration in plasma (T_{max}) were determined directly from mean concentration-time data. Data are presented as means ± SD. For parametric statistical analysis, the individual values of Figure 3A and Figure 4 were log-transformed to obtain equality of variances. One-way analysis of variance (ANOVA) was used to determine significance between groups, after which post-hoc tests with Bonferroni correction were performed for comparison between individual groups. Differences were considered statistically significant when $P < 0.05$.

RESULTS

In vitro transport of crizotinib

Transepithelial drug transport was tested using polarized monolayers of MDCKII parental cells and its subclones overexpressing human ABCB1, human ABCG2 and mouse Abcg2. In the parental cells, there was a weak but significant apically directed transport of crizotinib (r = 1.4, Figure 1B), which was not substantially inhibited with the ABCB1 inhibitor zosuquidar (r = 1.3, Figure 1C), suggesting that it was mediated by a lowly active endogenous transporter of unknown identity. In cells overexpressing human ABCB1, there was pronounced apically directed

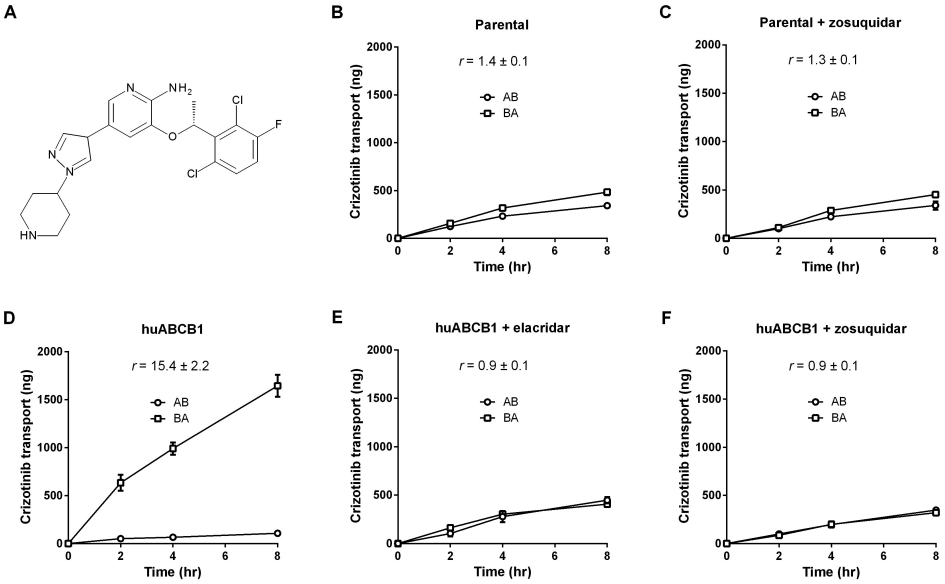

Figure 1. Molecular structure of crizotinib (A). Transepithelial transport of crizotinib (5 µM) assessed in MDCK-II cells either nontransduced (B, C) or transduced with hu*ABCB1* cDNA (D, E and F). At t = 0 hr, crizotinib was applied in the donor compartment and the concentrations in the acceptor compartment at t = 2, 4 and 8 hr were measured and plotted as crizotinib transport (ng) in the graphs (n = 3). Elacridar (5 µM) or zosuquidar (5 µM) were applied to inhibit ABCB1 transport activity. *r*, relative transport ratio. Points, mean; bars, SD. ▲, translocation from apical to basolateral compartment; □, translocation from basolateral to apical compartment. Data represent mean ± SD (n = 3). 1000 ng transport at t = 8 hr corresponds to an apparent permeability coefficient (P_{app}) of 1.4 x 10^{-5} cm/s.

transport of crizotinib, with an *r* ratio of 15.4 (Figure 1D), which was completely inhibited by elacridar at 5 µM (Figure 1E) and zosuquidar at 5 µM (*r* reduced from 15.4 to 0.9 in both cases) (Figure 1F), indicating that elacridar and zosuquidar are good inhibitors for human ABCB1-mediated crizotinib transport.

The specific ABCB1 inhibitor zosuquidar was added to inhibit any contribution of endogenous canine ABCB1 in subsequent experiments with MDCKII cells overexpressing human ABCG2 and mouse Abcg2. Ko143, a specific ABCG2 inhibitor was used to inhibit the transport activity of human ABCG2 or murine Abcg2. We did not observe polarized transport of crizotinib by human ABCG2 and murine Abcg2 either with zosuquidar alone or in combination with Ko143 (Figure 2A, B, C and D). Crizotinib thus was a good transport substrate of human ABCB1, but not of human ABCG2 or murine Abcg2.

Effect of Abcb1a/1b and Abcg2 on plasma pharmacokinetics and relative brain accumulation of oral crizotinib (5 mg/kg)

Based on pilot experiments, in order to obtain plasma levels of crizotinib in mice similar to steady-state therapeutic plasma concentrations in patients, we dosed crizotinib orally at 5 mg/kg. We then investigated the separate and combined effect of Abcb1a/1b and Abcg2 on the plasma concentration of crizotinib over time in wild-type, *Abcb1a/1b*$^{-/-}$,

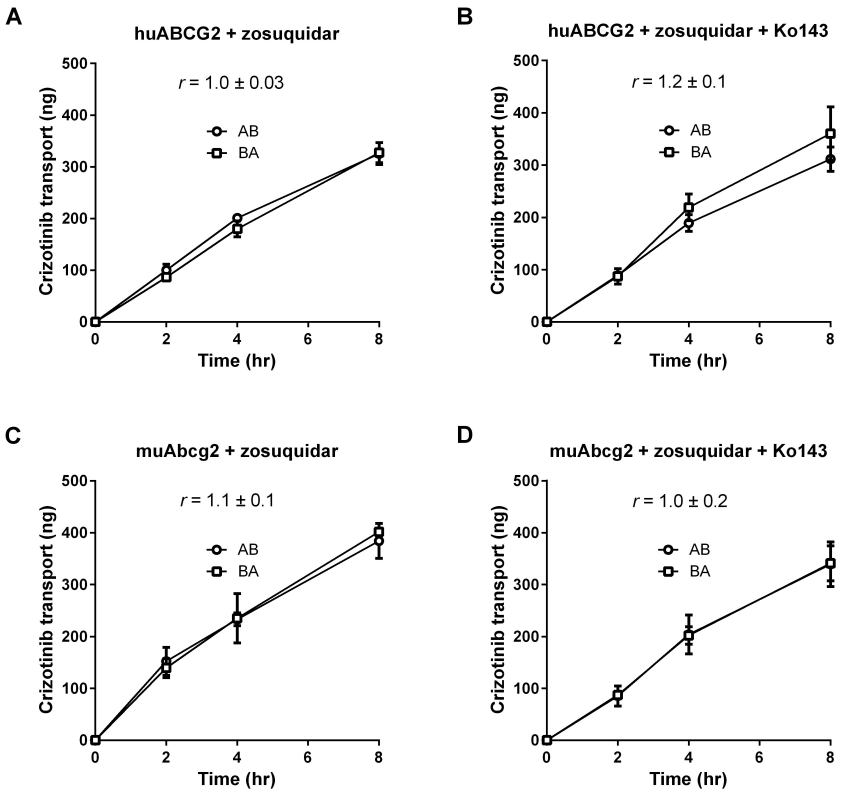

Figure 2. Transepithelial transport of crizotinib (5 μM) assessed in MDCK-II cells either transduced with hu*ABCG2* (A, B) or mu*Abcg2* cDNA (C, D). At t = 0 hr, crizotinib was applied in the donor compartment and the concentrations in the acceptor compartment at t = 2, 4 and 8 hr were measured and plotted as crizotinib transport (ng) in the graphs (n = 3). Zosuquidar (5 μM) and/or Ko143 were applied to inhibit ABCB1, ABCG2 or Abcg2, respectively. *r*, relative transport ratio. Points, mean; bars, SD. ▲, translocation from apical to basolateral compartment; □, translocation from basolateral to apical compartment. Data represent mean ± SD (n = 3). 1000 ng transport at t = 8 hr corresponds to an apparent permeability coefficient (P_{app}) of 1.4 x 10^{-5} cm/s.

Abcg2$^{-/-}$ and *Abcb1a/1b;Abcg2*$^{-/-}$ mice. The latter two strains were included to reveal any additional, possibly indirect, effects of the Abcg2 knockout on plasma and brain pharmacokinetics of crizotinib. The plasma $AUC_{0\text{-}24hr}$ in *Abcb1a/1b*$^{-/-}$ and *Abcb1a/1b;Abcg2*$^{-/-}$ mice was 2.1- and 2.2-fold higher than that in wild-type mice, respectively (Figure 3A and Table 1, $P < 0.001$). Absence of Abcg2 resulted in a 1.3-fold higher plasma $AUC_{0\text{-}24hr}$ compared to wild-type mice, which was not statistically significant (Table 1). Any increase in plasma levels in *Abcg2*$^{-/-}$ mice was only apparent at 0.5 and 2 hr (Figure 3A). The increase in plasma levels in *Abcb1a/1b*$^{-/-}$ and *Abcb1a/1b;Abcg2*$^{-/-}$ mice was apparent from very early on (30 min), and lasted up till at least 2 hr (Figure 3A). Thereafter, from a similar C_{max} at 4 hrs, a clearly slower decrease in crizotinib plasma concentrations was seen

Table 1: Plasma and brain pharmacokinetic parameters of crizotinib in wild-type, *Abcb1a/1b*$^{-/-}$, *Abcg2*$^{-/-}$ and *Abcb1a/1b;Abcg2*$^{-/-}$ mice after oral administration of 5 mg/kg crizotinib

	Genotype			
	Wild-type	*Abcb1a/1b*$^{-/-}$	*Abcg2*$^{-/-}$	*Abcb1a/1b;Abcg2*$^{-/-}$
Plasma pharmacokinetics and brain exposure at 24 hr				
$AUC_{(0\text{-}24hr)}$, ng/ml.hr	1086 ± 185	2237 ± 131***	1408 ± 294	2392 ± 266***
Fold increase $AUC_{(0\text{-}24hr)}$	1.0	2.1	1.3	2.2
C_{max}, ng/ml	203.7 ± 39.1	244.0 ± 22.8	225.8 ± 54.4	245.4 ± 45.6
T_{max}, hr	4.0	4.0	2.0	4.0
C_{brain}, ng/g	≤7.8 ± 0.2	617.7 ± 139.1***	≤8.2 ± 0.9	792.5 ± 102.3***
Fold increase C_{brain}	1.0	79.5	1.1	102.0
P_{brain} ($*10^{-2}$ hr^{-1})	≤0.73 ± 0.13	27.6 ± 5.9***	≤0.60 ± 0.09	33.2 ± 2.8***
Fold increase P_{brain}	1.0	37.7	0.8	45.2
Plasma and brain exposure at 4 hr				
C_{4hr}, ng/ml	146.5 ± 40.4	269.7 ± 53.9**	208.2 ± 43.7	259.7 ± 19.3**
Fold increase C_{4hr}	1.0	1.8	1.4	1.8
C_{brain}, ng/g	32.9 ± 7.1	760.3 ± 61.5***	29.1 ± 11.1	886.2 ± 255.4***
Fold increase C_{brain}	1.0	23.1	0.9	26.9
Brain-to-plasma ratio	0.23 ± 0.03	3.17 ± 0.98***	0.18 ± 0.03	3.44 ± 0.77***
Fold increase brain-to-plasma ratio	1.0	13.9	0.78	15.1

Data represent mean ± SD (n = 5). The plasma concentrations of crizotinib at 24 hr in all wild-type and 3/5 *Abcg2*$^{-/-}$ mice were below the LLQ and therefore for calculation purposes replaced with the LLQ value of 2.5 ng/ml. The brain concentrations of crizotinib at 24 hr in 4/5 wild-type and all *Abcg2*$^{-/-}$ mice were below the LLQ and therefore for calculation purposes replaced with the LLQ value of 7.8 ng/g. All parameters obtained for knockout strains were compared with those for wild-type mice. ** and *** indicate $P < 0.01$ and $P < 0.001$ compared with wild-type mice, respectively.
Abbreviations: $AUC_{0\text{-}24hr}$: area under plasma concentration-time curve; C_{max}, maximum plasma concentration; T_{max}, time to reach maximum drug concentration in plasma; C_{brain}: brain concentration of crizotinib; P_{brain}: relative brain accumulation of crizotinib at 24 hr after oral administration, calculated by determining the crizotinib brain concentration relative to the $AUC_{0\text{-}24hr}$; C_{4hr}: plasma concentration of crizotinib at 4 hr after oral administration.

in *Abcb1a/1b*$^{-/-}$ and *Abcb1a/1b;Abcg2*$^{-/-}$ mice as compared to wild-type and *Abcg2*$^{-/-}$ mice (Figure 3A).

At 24 hr after crizotinib administration, the relative brain accumulations in *Abcb1a/1b*$^{-/-}$ and *Abcb1a/1b;Abcg2*$^{-/-}$ mice were 37.7- and 45.2-fold higher than that in wild-type mice, respectively (Figure 3D and Table 1). In contrast, the relative brain accumulation in *Abcg2*$^{-/-}$ mice was similar to that found in wild-type mice (Figure 3B and Table 1). These results indicate that Abcb1 has a large contribution in restricting brain accumulation, and a modest contribution in restricting the oral availability of crizotinib, whereas Abcg2 has little or no contribution in either in line with the *in vitro* results.

Effect of Abcb1a/1b and Abcg2 on plasma and brain exposure of oral crizotinib around the T_{max}

We subsequently assessed the effect of Abcb1 and Abcg2 on crizotinib plasma exposure and brain accumulation around the

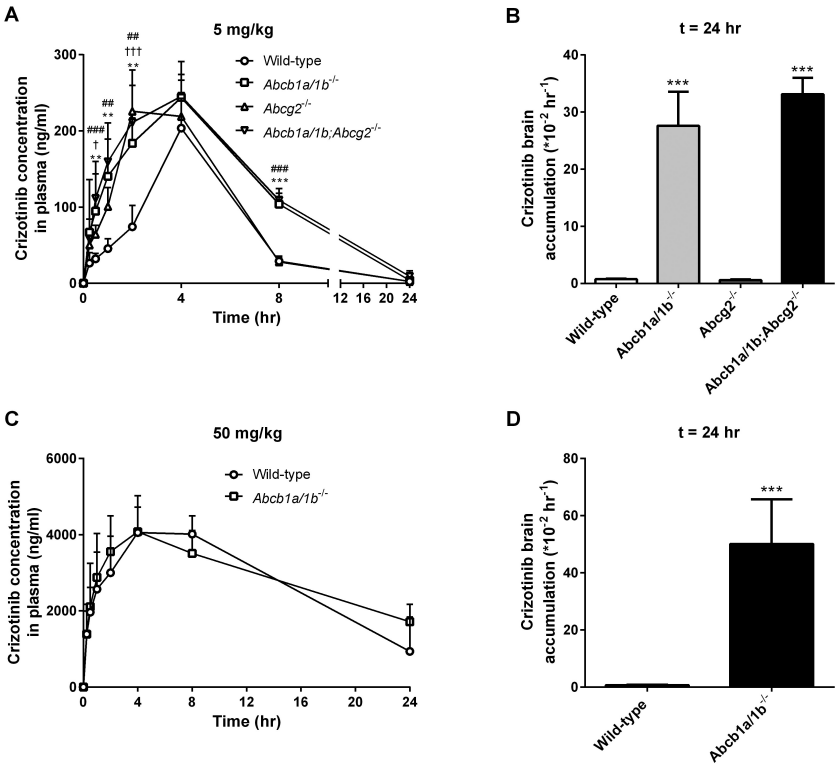

Figure 3. Plasma concentration-time curves (A) and relative brain accumulation at 24 hr (B) of crizotinib in wild-type, *Abcb1a/1b*$^{-/-}$, *Abcg2*$^{-/-}$ and *Abcb1a/1b;Abcg2*$^{-/-}$ mice receiving 5 mg/kg (upper panels) crizotinib orally. Plasma concentration-time curves (C) and relative brain accumulation at 24 hr (D) of crizotinib in wild-type and *Abcb1a/1b*$^{-/-}$ mice receiving 50 mg/kg (lower panels) crizotinib orally. Data represent mean ± SD (n = 5). Statistical significance compared to wild-type mice at each time point is indicated by * for *Abcb1a/1b*$^{-/-}$, † for *Abcg2*$^{-/-}$, and # for *Abcb1a/1b;Abcg2*$^{-/-}$ mice, respectively. Symbols indicate $P < 0.05$, $P < 0.01$ and $P < 0.001$ for one, two, and three symbols, respectively. For the 5 mg/kg crizotinib experiment, the plasma concentrations of crizotinib at 24 hr in all wild-type and 3/5 *Abcg2*$^{-/-}$ mice were below the LLQ (or undetectable) and therefore for calculation purposes replaced with the LLQ value of 2.5 ng/ml. The brain concentrations of crizotinib at 24 hr in 4/5 wild-type and all *Abcg2*$^{-/-}$ mice were below the LLQ (or undetectable) and therefore for calculation purposes replaced with the LLQ value of 7.8 ng/g.

T_{max} (4 hr). Crizotinib (5 mg/kg) was orally administered to wild-type, *Abcb1a/1b*$^{-/-}$, *Abcg2*$^{-/-}$ and *Abcb1a/1b;Abcg2*$^{-/-}$ mice. As shown in Figure 4A, plasma levels of crizotinib at 4 hr were similar between wild-type and *Abcg2*$^{-/-}$ mice. However, *Abcb1a/1b*$^{-/-}$ and *Abcb1a/1b;Abcg2*$^{-/-}$ mice both had 1.8-fold increased crizotinib plasma concentrations as compared with wild-type mice, while no significant difference was seen between the two (Figure 4A). Brain-to-plasma ratios were calculated to correct for the differences in plasma concentrations. The brain concentration and brain-to-plasma ratio were not increased in *Abcg2*$^{-/-}$ mice in comparison to wild-type mice

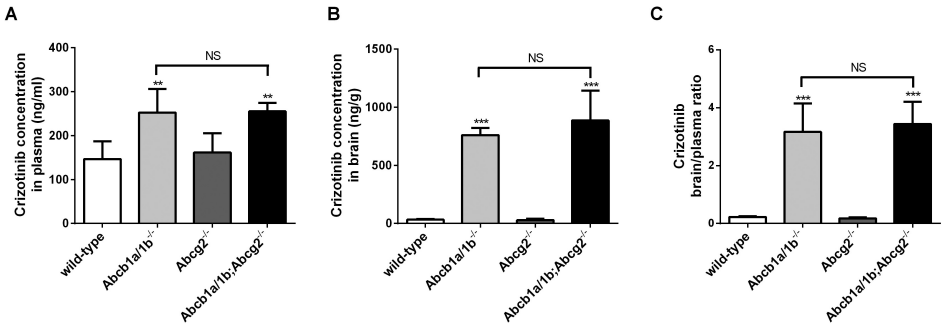

Figure 4. Plasma concentration (A), brain concentration (B) and brain-to-plasma ratio (C) of crizotinib at 4 hr in wild-type, *Abcb1a/1b*$^{-/-}$, *Abcg2*$^{-/-}$ and *Abcb1a/1b;Abcg2*$^{-/-}$ mice receiving 5 mg/kg crizotinib orally. Data represent mean ± SD (n = 5). ** and *** indicate $P < 0.01$ and $P < 0.001$ respectively compared to wild-type mice. NS indicates no significant difference between the indicated pairs.

2.3

(Figure 4B and C). In contrast, *Abcb1a/1b*$^{-/-}$ and *Abcb1a/1b;Abcg2*$^{-/-}$ mice had 23.1- and 26.9-fold higher brain concentrations relative to wild-type mice, respectively (Figure 4B and Table 1), resulting in 13.9- and 15.1-fold higher brain-to-plasma ratios (Figure 4C and Table 1). Collectively, these results indicate that Abcb1 restricts brain accumulation to a larger extent than oral availability upon oral crizotinib administration.

Effect of Abcb1a/1b on plasma pharmacokinetics and relative brain accumulation of oral crizotinib (50 mg/kg)

Patients usually receive an oral dose of 250 mg of crizotinib. Purely based on theoretical considerations, a physiologically equivalent oral single dose in mice should be 50 mg/kg, i.e., 10 times higher than the 5 mg/kg we used previously. As we were also interested in possible saturation effects that might occur at higher intestinal and plasma levels of crizotinib, we studied the plasma concentration of crizotinib over time in wild-type and *Abcb1a/1b*$^{-/-}$ mice receiving crizotinib orally at 50 mg/kg. At this dosage, the plasma $AUC_{0\text{-}24hr}$ in *Abcb1a/1b*$^{-/-}$ mice was comparable to that in wild-type mice (Figure 3C and Supplementary Table 1), and the AUCs were 62- and 31-fold higher, respectively, than in the same strains receiving 5 mg/kg (cf. Table 1). This suggests that Abcb1 no longer had a detectable impact on the plasma pharmacokinetics of crizotinib at a dose of 50 mg/kg, and that the increase in AUC in both strains between 5 and 50 mg/kg was well more than linear.

Brain distribution of crizotinib was also analyzed 24 hr after oral administration of 50 mg/kg crizotinib. The relative brain accumulation at 24 hr in *Abcb1a/1b*$^{-/-}$ mice was 70-fold higher than in wild-type mice (Figure 3D and Supplementary Table 1). Collectively, these data indicate that brain accumulation, but not plasma exposure of crizotinib was restricted by Abcb1 upon oral administration of a high dose of crizotinib.

Effect of the dual ABCB1 and ABCG2 inhibitor elacridar on crizotinib plasma and brain exposure

We next tested to what extent the dual ABCB1 and ABCG2 inhibitor elacridar could modulate the oral bioavailability and brain accumulation

of crizotinib. In view of the potential clinical importance of oral application for both crizotinib and elacridar, we administered elacridar (100 mg/kg) orally 2 hr prior to oral crizotinib (5 mg/kg) to the wild-type and *Abcb1a/1b;Abcg2*$^{-/-}$ strains and assessed plasma and brain crizotinib levels 4 hr later, *i.e.*, around the crizotinib T_{max}. In vehicle-treated mice, plasma concentrations of crizotinib were 1.5-fold higher in *Abcb1a/1b;Abcg2*$^{-/-}$ mice compared to wild-type mice (Figure 5A), although this was not statistically significant. Pretreatment with elacridar resulted in a 2.2-fold increase in plasma concentrations in wild-type mice as compared with wild-type mice without elacridar (Figure 5A). In the presence of elacridar, plasma concentrations were not different between wild-type and *Abcb1a/1b;Abcg2*$^{-/-}$ mice (Figure 5A), suggesting that elacridar could significantly increase crizotinib plasma exposure in wild-type mice to levels equal to those in *Abcb1a/1b;Abcg2*$^{-/-}$ mice.

In the absence of elacridar, brain concentrations of crizotinib were 21-fold higher in *Abcb1a/1b;Abcg2*$^{-/-}$ mice than in wild-type mice (Figure 5B). In contrast to the modest effect on plasma concentrations, elacridar drastically increased the brain concentrations of crizotinib in wild-type mice by 25.7-fold, resulting in similar brain levels as observed for *Abcb1a/1b;Abcg2*$^{-/-}$ mice with or without elacridar (Figure 5B). Correcting for plasma levels, in the absence of elacridar, brain-to-plasma ratios in *Abcb1a/1b;Abcg2*$^{-/-}$ mice were 14.5-fold higher than in wild-type mice (Figure 5C). Oral elacridar increased the brain-to-plasma ratios in wild-type mice by 11.9-fold, to levels similar to those in *Abcb1a/1b;Abcg2*$^{-/-}$ mice either with elacridar or vehicle (Figure 5C). The crizotinib brain concentrations and brain-to-plasma ratios in *Abcb1a/1b;Abcg2*$^{-/-}$ mice were not significantly affected by oral elacridar treatment (Figure 5B and C). These data indicate that oral elacridar treatment could completely and specifically inhibit the activity of mouse Abcb1 in the BBB and small intestine, leading to highly increased crizotinib concentrations in the brain, and modestly increased plasma concentrations.

DISCUSSION

We found that crizotinib is transported by human ABCB1, but not by human ABCG2 or murine Abcg2 *in vitro*. Upon oral administration of a medium dose

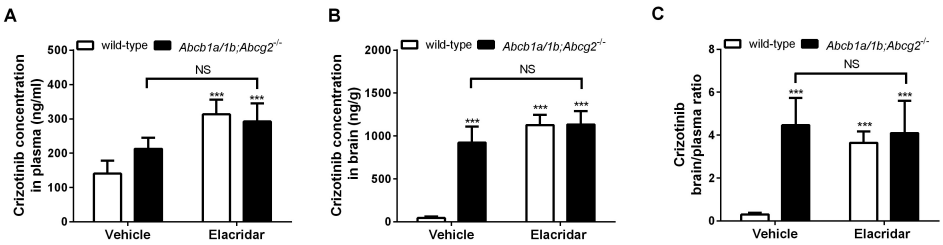

Figure 5. Plasma concentration (A), brain concentration (B) and brain-to-plasma ratio (C) of crizotinib at 4 hr in wild-type and *Abcb1a/1b;Abcg2*$^{-/-}$ mice receiving 5 mg/kg crizotinib orally. Data represent mean ± SD (n = 5). *** indicates $P < 0.001$ compared to wild-type mice. NS indicates no significant difference between the indicated pairs.

of crizotinib (5 mg/kg), plasma AUCs in *Abcb1a/1b*$^{-/-}$ and *Abcb1a/1b;Abcg2*$^{-/-}$ mice, but not in *Abcg2*$^{-/-}$ mice, were ~2-fold higher than in wild-type mice, suggesting that oral absorption and/or systemic clearance of crizotinib was controlled by Abcb1 but not by Abcg2. Importantly, the brain accumulation of crizotinib was highly increased in *Abcb1a/1b*$^{-/-}$ and *Abcb1a/1b;Abcg2*$^{-/-}$ mice, but not in *Abcg2*$^{-/-}$ mice. At a high oral dose of 50 mg/kg, the absence of Abcb1a/1b in knockout mice no longer affected the oral availability of crizotinib, but crizotinib brain accumulation was still profoundly increased. We could further demonstrate in mice that, using oral coadministration of crizotinib (5 mg/kg) and elacridar, BBB Abcb1 was fully and specifically inhibited, resulting in highly increased brain crizotinib levels in wild-type mice, whereas crizotinib oral availability was about 2-fold increased.

Our *in vitro* results are generally consistent with previous reports on the interaction of crizotinib with human ABCB1 and human ABCG2, including the demonstration that human ABCB1, but not human ABCG2 transports crizotinib *in vitro*, and that crizotinib can inhibit human ABCB1-mediated transport and stimulate its ATPase activity in a dose-dependent manner (http://www.accessdata.fda.gov/drugsatfda_docs/nda/2011/202570Orig1s000ClinPharmR.pdf).[20] Collectively, all data indicate that crizotinib is a good transport substrate of ABCB1/Abcb1 and thus potentially a competitive inhibitor for other ABCB1 substrates.

In human pharmacokinetic studies, the highest crizotinib concentration achieved in plasma after repeated dosing at 250 mg b.i.d. was 327 ng/ml (http://www.accessdata.fda.gov/drugsatfda_docs/nda/2011/202570Orig1s000ClinPharmR.pdf). However, we found that the plasma concentration obtained in wild-type mice receiving a single oral dose of 50 mg/kg of crizotinib, a dose which is theoretically equivalent to a human single oral dose of 250 mg, was 12.4-fold higher than that in human plasma. This discrepancy is likely explained by species-specific drug metabolism and transport. Regardless, we lowered the dose in mice to 5 mg/kg, aiming to achieve similar plasma concentrations as observed in patients routinely treated with crizotinib, and performed most of our further analyses with this dose.

When comparing our mouse data of crizotinib doses of 5 mg/kg and 50 mg/kg (a 10-fold dosage increase), it was striking that the increase in plasma AUCs was more than linear, ~60-fold in wild-type mice and ~30-fold in Abcb1a/1b knockout mice. Moreover, the ~2-fold difference in plasma AUC seen between wild-type and Abcb1a/1b knockout mice at 5 mg/kg was gone at 50 mg/kg. These results strongly suggest that the contribution of most likely intestinal Abcb1a/1b in restricting the oral availability of crizotinib became saturated between the two dosages. Such saturation by high intestinal drug concentrations could well explain a more than linear increase in plasma AUC. However, since also the Abcb1a/1b knockout mice displayed a more than linear increase in AUC, it is likely that also one or more other crizotinib availability-restricting system(s) became saturated. Since this cannot have been Abcb1a/1b or Abcg2, it may have been another crizotinib efflux transporter of unknown identity, or possibly a crizotinib-metabolizing enzyme. These data once again illustrate that the relative impact of drug transporters on pharmacokinetics can be

quite dose-dependent, as seen before with, for instance vemurafenib.[11] However, it is also clear that Abcb1b in the BBB was not saturated at all by the highly increased plasma levels of crizotinib upon 50 mg/kg crizotinib dosing.

Our *in vitro* and *in vivo* data suggest that any role of Abcg2 in limiting crizotinib oral absorption or brain accumulation is minimal or absent. In contrast, the role of Abcb1 in plasma pharmacokinetics and brain accumulation is very clear at a non-saturating dose. Prior to the T_{max}, *Abcb1a/1b*$^{-/-}$ and *Abcb1a/1b;Abcg2*$^{-/-}$ mice showed steeper increases in crizotinib concentrations, suggesting that Abcb1 plays a role in restricting the oral absorption of crizotinib. It is worth noting that the mean C_{max} of crizotinib in wild-type mice at low dose (5 mg/kg) was quite similar to a range of C_{max} (100 to 135 ng/ml) observed in healthy subjects and in patients with advanced solid tumors following a single 250 mg oral dose of crizotinib (http://www.accessdata.fda.gov/drugsatfda_docs/nda/2011/202570Orig1s000ClinPharmR.pdf). Therefore our results in mice may adequately reflect the situation in humans. After the T_{max}, plasma crizotinib levels in *Abcb1a/1b*$^{-/-}$ and *Abcb1a/1b;Abcg2*$^{-/-}$ mice decreased more slowly than in wild-type and *Abcg2*$^{-/-}$ mice (Figure 3A), suggesting a role of Abcb1a/1b in plasma clearance of crizotinib. Taken together, Abcb1 had a modest effect on the oral availability of crizotinib during both the intestinal absorption and systemic clearance phases in mice.

Interestingly, in spite of the large decrease in plasma crizotinib levels between 4 hr and 24 hr (Table 1, Figure 3A), the brain concentrations were very similar at these two time points in *Abcb1a/1b*$^{-/-}$ and *Abcb1a/1b;Abcg2*$^{-/-}$ mice (Table 1, Figure 4B). This suggests that crizotinib is hardly cleared from the brain in single Abcb1a/1b and combination knockout mice. One could speculate that there is possibly a relatively tight binding of crizotinib to brain components once it enters the brain tissue. However, when Abcb1 is present at the BBB, the brain concentrations decreased markedly in the wild-type and *Abcg2*$^{-/-}$ mice between 4 and 24 hr (Table 1), indicating good clearance of crizotinib from the brain by this transporter. It is interesting to note that in a NSCLC patient, a very low drug level (0.616 ng/ml) was found in the cerebrospinal fluid 5 hr after a dose of crizotinib 250 mg,[17] suggesting poor brain penetration of crizotinib in patients. A low brain drug level may hinder the antitumor effect of this drug in metastatic brain tumors,[29] which commonly occur in NSCLC patients.

Our studies in mice showed that inhibition of ABCB1 by elacridar may be an effective way to improve brain distribution of crizotinib. We and others have previously shown that elacridar can be used to improve the brain accumulation of various drugs that are substrates of Abcb1 and Abcg2.[11,12,14,15,19] Since the clinical use of crizotinib utilizes chronic oral dosing, to effectively improve crizotinib delivery with elacridar, it must also be administered chronically. Hence, elacridar oral dosing was preferred over intravenous dosing. Another reason is that the elimination $t_{1/2}$ of elacridar in mice after an oral dose of 100 mg/kg was close to 20 hr, approximately 5-fold greater than the $t_{1/2}$ after intraperitoneal or intravenous dosing.[30] Our data show that we can drastically increase the brain accumulation of crizotinib (25.4-fold) to levels similar to those in mice with a genetic deletion of Abcb1, and modestly increase the systemic exposure of crizotinib

(2.2-fold). It is noteworthy that, at the dose used, we did not observe any sign of acute toxicity in wild-type or knockout mice, either with or without elacridar treatment. These results suggest that oral coadministration of elacridar and crizotinib may be used to further improve the therapeutic efficacy against brain metastases and also primary brain tumors, without inducing systemic toxicity as a result of increased plasma drug exposure. Further experiments will be needed to determine whether increased therapeutic concentrations of crizotinib in the brain (and hence possibly in the tumor) will ultimately lead to a more favorable therapeutic efficacy in NSCLC patients with brain metastases.

Acknowledgements

This work was supported by an academic staff training scheme fellowship from the Malaysian Ministry of Higher Education to S.C.T. and in part by the Dutch Cancer Society [grant 2007-3764]. We thank Dilek Iusuf and Selvi Durmus for critical reading of the manuscript.

REFERENCES

1. Jemal A, Center MM, Desantis C, Ward EM. Global patterns of cancer incidence and mortality rates and trends. *Cancer Epidemiol Biomarkers Prev* 2010;19:1893-907.
2. Herbst RS, Heymach JV, Lippman SM. Lung cancer. *N Engl J Med* 2008;359:1367-80.
3. Soda M, Choi YL, Enomoto M, Takada S, Yamashita Y, Ishikawa S, Fujiwara S, Watanabe H, Kurashina K, Hatanaka H, Bando M, Ohno S, *et al*. Identification of the transforming EML4-ALK fusion gene in non-small-cell lung cancer. *Nature* 2007;448:561-6.
4. Chen Y, Takita J, Choi YL, Kato M, Ohira M, Sanada M, Wang L, Soda M, Kikuchi A, Igarashi T, Nakagawara A, Hayashi Y, *et al*. Oncogenic mutations of ALK kinase in neuroblastoma. *Nature* 2008;455:971-4.
5. Koivunen JP, Mermel C, Zejnullahu K, Murphy C, Lifshits E, Holmes AJ, Choi HG, Kim J, Chiang D, Thomas R, Lee J, Richards WG, *et al*. EML4-ALK fusion gene and efficacy of an ALK kinase inhibitor in lung cancer. *Clin Cancer Res* 2008;14:4275-83.
6. Soda M, Takada S, Takeuchi K, Choi YL, Enomoto M, Ueno T, Haruta H, Hamada T, Yamashita Y, Ishikawa Y, Sugiyama Y, Mano H. A mouse model for EML4-ALK-positive lung cancer. *Proc Natl Acad Sci U S A* 2008;105:19893-7.
7. Kwak EL, Bang YJ, Camidge DR, Shaw AT, Solomon B, Maki RG, Ou SH, Dezube BJ, Janne PA, Costa DB, Varella-Garcia M, Kim WH, *et al*. Anaplastic lymphoma kinase inhibition in non-small-cell lung cancer. *N Engl J Med* 2010;363:1693-703.
8. Christensen JG, Zou HY, Arango ME, Li Q, Lee JH, McDonnell SR, Yamazaki S, Alton GR, Mroczkowski B, Los G. Cytoreductive antitumor activity of PF-2341066, a novel inhibitor of anaplastic lymphoma kinase and c-Met, in experimental models of anaplastic large-cell lymphoma. *Mol Cancer Ther* 2007;6:3314-22.
9. McDermott U, Iafrate AJ, Gray NS, Shioda T, Classon M, Maheswaran S, Zhou W, Choi HG, Smith SL, Dowell L, Ulkus LE, Kuhlmann G, *et al*. Genomic alterations of anaplastic lymphoma kinase may sensitize tumors to anaplastic lymphoma kinase inhibitors. *Cancer Res* 2008;68:3389-95.
10. Chen Y, Agarwal S, Shaik NM, Chen C, Yang Z, Elmquist WF. P-glycoprotein and breast cancer resistance protein influence brain distribution of dasatinib. *J Pharmacol Exp Ther* 2009;330:956-63.
11. Durmus S, Sparidans RW, Wagenaar E, Beijnen JH, Schinkel AH. Oral availability and brain penetration of the B-RAFV600E inhibitor vemurafenib can be enhanced by the P-GLYCOprotein (ABCB1) and breast cancer resistance protein (ABCG2) inhibitor elacridar. *Mol Pharm* 2012;9:3236-45.
12. Lagas JS, van Waterschoot RA, van Tilburg VA, Hillebrand MJ, Lankheet N, Rosing H, Beijnen JH, Schinkel AH. Brain accumulation of dasatinib is restricted by P-glycoprotein (ABCB1) and breast cancer resistance protein

(ABCG2) and can be enhanced by elacridar treatment. *Clin Cancer Res* 2009;15:2344-51.

13. Mittapalli RK, Vaidhyanathan S, Sane R, Elmquist WF. Impact of P-glycoprotein (ABCB1) and breast cancer resistance protein (ABCG2) on the brain distribution of a novel BRAF inhibitor: vemurafenib (PLX4032). *J Pharmacol Exp Ther* 2012;342:33-40.
14. Bihorel S, Camenisch G, Lemaire M, Scherrmann JM. Influence of breast cancer resistance protein (Abcg2) and p-glycoprotein (Abcb1a) on the transport of imatinib mesylate (Gleevec) across the mouse blood-brain barrier. *J Neurochem* 2007;102:1749-57.
15. Breedveld P, Pluim D, Cipriani G, Wielinga P, van Tellingen O, Schinkel AH, Schellens JH. The effect of Bcrp1 (Abcg2) on the in vivo pharmacokinetics and brain penetration of imatinib mesylate (Gleevec): implications for the use of breast cancer resistance protein and P-glycoprotein inhibitors to enable the brain penetration of imatinib in patients. *Cancer Res* 2005;65:2577-82.
16. Doebele RC, Lu X, Sumey C, Maxson DA, Weickhardt AJ, Oton AB, Bunn PA, Jr., Baron AE, Franklin WA, Aisner DL, Varella-Garcia M, Camidge DR. Oncogene status predicts patterns of metastatic spread in treatment-naive nonsmall cell lung cancer. *Cancer* 2012;118:4502-11.
17. Costa DB, Kobayashi S, Pandya SS, Yeo WL, Shen Z, Tan W, Wilner KD. CSF concentration of the anaplastic lymphoma kinase inhibitor crizotinib. *J Clin Oncol* 2011;29:e443-e445.
18. Agarwal S, Sane R, Gallardo JL, Ohlfest JR, Elmquist WF. Distribution of gefitinib to the brain is limited by P-glycoprotein (ABCB1) and breast cancer resistance protein (ABCG2)-mediated active efflux. *J Pharmacol Exp Ther* 2010;334:147-55.
19. Tang SC, Lagas JS, Lankheet NA, Poller B, Hillebrand MJ, Rosing H, Beijnen JH, Schinkel AH. Brain accumulation of sunitinib is restricted by P-glycoprotein (ABCB1) and breast cancer resistance protein (ABCG2) and can be enhanced by oral elacridar and sunitinib coadministration. *Int J Cancer* 2012;130:223-33.
20. Zhou WJ, Zhang X, Cheng C, Wang F, Wang XK, Liang YJ, To KK, Zhou W, Huang HB, Fu LW. Crizotinib (PF-02341066) reverses multidrug resistance in cancer cells by inhibiting the function of P-glycoprotein. *Br J Pharmacol* 2012;166:1669-83.
21. Bakos E, Evers R, Calenda G, Tusnady GE, Szakacs G, Varadi A, Sarkadi B. Characterization of the amino-terminal regions in the human multidrug resistance protein (MRP1). *J Cell Sci* 2000;113 Pt 24:4451-61.
22. Evers R, Kool M, van Deemter L, Janssen H, Calafat J, Oomen LC, Paulusma CC, Oude Elferink RP, Baas F, Schinkel AH, Borst P. Drug export activity of the human canalicular multispecific organic anion transporter in polarized kidney MDCK cells expressing cMOAT (MRP2) cDNA. *J Clin Invest* 1998;101:1310-9.
23. Jonker JW, Buitelaar M, Wagenaar E, van der Valk MA, Scheffer GL, Scheper RJ, Plosch T, Kuipers F, Elferink RP, Rosing H, Beijnen JH, Schinkel AH. The breast cancer resistance protein protects against a major chlorophyll-derived dietary phototoxin and protoporphyria. *Proc Natl Acad Sci U S A* 2002;99:15649-54.
24. Pavek P, Merino G, Wagenaar E, Bolscher E, Novotna M, Jonker JW, Schinkel AH. Human breast cancer resistance protein: interactions with steroid drugs, hormones, the dietary carcinogen 2-amino-1-methyl-6-phenylimidazo(4,5-b) pyridine, and transport of cimetidine. *J Pharmacol Exp Ther* 2005;312:144-52.
25. Schinkel AH, Mayer U, Wagenaar E, Mol CA, van Deemter L, Smit JJ, van der Valk MA, Voordouw AC, Spits H, van Tellingen O, Zijlmans JM, Fibbe WE, *et al*. Normal viability and altered pharmacokinetics in mice lacking mdr1-type (drug-transporting) P-glycoproteins. *Proc Natl Acad Sci U S A* 1997;94:4028-33.
26. Jonker JW, Freeman J, Bolscher E, Musters S, Alvi AJ, Titley I, Schinkel AH, Dale TC. Contribution of the ABC transporters Bcrp1 and Mdr1a/1b to the side population phenotype in mammary gland and bone marrow of mice. *Stem Cells* 2005;23:1059-65.
27. Dai H, Marbach P, Lemaire M, Hayes M, Elmquist WF. Distribution of STI-571 to the brain is limited by P-glycoprotein-mediated efflux. *J Pharmacol Exp Ther* 2003;304:1085-92.
28. Sparidans RW, Tang SC, Nguyen LN, Schinkel AH, Schellens JH, Beijnen JH. Liquid chromatography-tandem mass spectrometric assay for the ALK inhibitor crizotinib in mouse plasma. *J Chromatogr B Analyt Technol Biomed Life Sci* 2012;905:150-4.
29. Lockman PR, Mittapalli RK, Taskar KS, Rudraraju V, Gril B, Bohn KA, Adkins CE, Roberts A, Thorsheim HR, Gaasch JA, Huang S, Palmieri D, *et al*. Heterogeneous blood-tumor barrier permeability determines drug efficacy in experimental brain metastases of breast cancer. *Clin Cancer Res* 2010;16:5664-78.

30. Sane R, Agarwal S, Elmquist WF. Brain distribution and bioavailability of elacridar after different routes of administration in the mouse. *Drug Metab Dispos* 2012;40:1612-9.

Supplementary Table 1. Pharmacokinetic parameters, brain concentrations and relative brain accumulation of crizotinib in wild-type and *Abcb1a/1b*$^{-/-}$ mice after oral administration of 50 mg/kg crizotinib

	Genotype	
	Wild-type	*Abcb1a/1b*$^{-/-}$
$AUC_{(0\text{-}24hr)}$, ng/ml.hr	67316 ± 11191	69665 ± 10449
Fold increase $AUC_{(0\text{-}24hr)}$	1.0	1.0
C_{max}, ng/ml	4055.2 ± 669.8	4076.2 ± 949.2
T_{max}, hr	4.0	4.0
C_{brain}, ng/g	487.9 ± 137.9	33632.1 ± 4343.5 ***
Fold increase C_{brain}	1.0	68.9
P_{brain} ($*10^{-2}$ hr^{-1})	0.72 ± 0.13	50.1 ± 15.7 ***
Fold increase P_{brain}	1.0	69.8

Data represent mean ± SD (n = 5). *** indicates $P < 0.001$ compared with wild-type mice.
Abbreviations: $AUC_{0\text{-}24hr}$: area under plasma concentration-time curve; C_{max}, maximum plasma concentration; T_{max}, time to reach maximum drug concentration in plasma; C_{brain}: brain concentration of crizotinib at 24 hr after oral administration; P_{brain}: relative brain accumulation of crizotinib at 24 hr after oral administration, calculated by determining the crizotinib brain concentration relative to the $AUC_{0\text{-}24hr}$.

2.4

IMPACT OF P-GLYCOPROTEIN (ABCB1) AND BREAST CANCER RESISTANCE PROTEIN (ABCG2) GENE DOSAGE ON PLASMA PHARMACOKINETICS AND BRAIN ACCUMULATION OF DASATINIB, SORAFENIB AND SUNITINIB

Seng Chuan Tang, Niels de Vries, Rolf W. Sparidans, Els Wagenaar, Jos H. Beijnen and Alfred H. Schinkel

S.C.T., E.W., A.H.S.: Division of Molecular Oncology, The Netherlands Cancer Institute, Amsterdam, The Netherlands
R.W.S., J.H.B.: Division of Pharmacoepidemiology & Clinical Pharmacology, Department of Pharmaceutical Sciences, Faculty of Science, Utrecht University, Utrecht, The Netherlands
N.d.V., J.H.B.: Department of Pharmacy & Pharmacology, Slotervaart Hospital, Amsterdam, The Netherlands

Submitted for publication

ABSTRACT

Low brain accumulation of anticancer drugs due to efflux transporters may limit chemotherapeutic efficacy, necessitating better understanding of the underlying mechanisms. P-glycoprotein (Abcb1a/1b) and breast cancer resistance protein (Abcg2) combination knockout mice often display disproportionately increased brain accumulation of shared drug substrates compared to single transporter knockout mice. A recent pharmacokinetic model could explain this phenomenon. To experimentally test this model and its wider relevance for tyrosine kinase inhibitors (TKIs) and other drugs, we selected dasatinib, sorafenib and sunitinib because of their divergent oral availability and brain accumulation profiles: brain accumulation of dasatinib is mainly restricted by Abcb1, that of sorafenib mainly by Abcg2, and that of sunitinib equally by Abcb1 and Abcg2. We analyzed the effect of halving the efflux activity of these transporters at the blood-brain barrier (BBB) by generating heterozygous *Abcb1a/1b;Abcg2* knockout mice, and testing plasma and brain levels of the drugs after oral administration at 10 mg/kg. RT-PCR analysis confirmed ~2-fold decreased expression of both transporters in brain. Interestingly, whereas complete knockout of the transporters caused 24- to 36-fold increases in brain accumulation of the drugs, the heterozygous mice only displayed 1.6- to 1.9-fold increases of brain accumulation relative to wild-type mice. These results are well in line with the pharmacokinetic model of Kodaira et al. (2010), and provide strong support for its validity for a wider range of drugs. Moreover, retrospective analysis of fetal accumulation of drugs across the placenta in Abcb1a/1b heterozygous knockout pups suggests that this model equally applies to the maternal-fetal barrier.

INTRODUCTION

Dasatinib, sorafenib and sunitinib are orally active, small-molecule multi-targeted tyrosine kinase inhibitors (TKIs) used for the treatment of cancer. Dasatinib (Sprycel; BMS-354825), a potent second generation BCR-ABL kinase inhibitor (Lombardo et al., 2004), used as first-line treatment for adult patients newly diagnosed with Philadelphia chromosome-positive chronic myelogenous leukemia in chronic phase (Kantarjian et al., 2010). Sorafenib (Nexavar, BAY43-9006), a Raf kinase and vascular endothelial growth factor receptor inhibitor, is currently used for the treatment of patients with unresectable hepatocellular carcinoma and advanced renal cell carcinoma (Escudier et al., 2007; Llovet et al., 2008). Sunitinib (Sutent, SU11248) is a receptor tyrosine kinase inhibitor that is used in the therapy of progressive, well-differentiated pancreatic neuroendocrine tumors, metastatic renal cell carcinoma and imatinib-resistant gastrointestinal stromal tumor (Goodman et al., 2007; Raymond et al., 2011; Rock et al., 2007).

ATP-binding cassette (ABC) transporters such as P-glycoprotein (P-gp; ABCB1) and

breast cancer resistance protein (BCRP; ABCG2) are highly expressed in small intestinal epithelium and at the blood-brain barrier (BBB), where they can limit the oral availability, but especially the brain accumulation of many clinically used TKIs (see also Supplemental Figure 1) (Agarwal et al., 2010; Chen et al., 2009; Durmus et al., 2012; Lagas et al., 2009; Lagas et al., 2010; Mittapalli et al., 2012; Polli et al., 2009; Tang et al., 2012). There is considerable overlap in the substrate specificity between Abcb1 and Abcg2, and many TKIs, including dasatinib, sorafenib, and sunitinib, are dual substrates of these transporters (Agarwal et al., 2010; Chen et al., 2009; Lagas et al., 2009; Lagas et al., 2010; Tang et al., 2012). Dasatinib, sorafenib, and sunitinib can be classified into three different groups based on their known *in vivo* characteristics with regard to brain accumulation profiles (Supplemental Figure 1). For instance, brain accumulation of dasatinib is mainly restricted by Abcb1, whereas Abcg2 plays a more important role in limiting brain accumulation of sorafenib. For sunitinib, Abcb1 and Abcg2 contribute equally to its restricted brain accumulation. With respect to oral availability, dasatinib is primarily restricted by Abcb1, whereas plasma pharmacokinetics of sorafenib and sunitinib are not affected by Abcb1 and/or Abcg2.

A striking finding from brain accumulation studies with shared Abcb1 and Abcg2 substrates is that the single disruption of *Abcb1a/1b* or *Abcg2* in mice often has little or no detectable effect on brain accumulation, whereas simultaneous disruption of these two transporters results in a dramatic increase of brain accumulation of many TKIs (see also Supplemental Figure 1) (Agarwal et al., 2010; Chen et al., 2009; Kodaira et al., 2010; Lagas et al., 2009; Lagas et al., 2010; Polli et al., 2009; Tang et al., 2012; Zhou et al., 2009). These findings have prompted researchers to envisage a synergistic or cooperative role of ABCB1 and ABCG2 in the efflux of dual substrates at the BBB. However, Kodaira et al. (2010) developed a straightforward pharmacokinetic model that describes that the seemingly disproportionate effect of simultaneous removal of both transporters can simply result from the fact that the intrinsic efflux transport activities at the BBB of Abcb1 and Abcg2 are each considerably larger than the remaining (passive, or lowly active) efflux activity at the BBB. Therefore, the seemingly synergistic effect of the removal of both Abcb1 and Abcg2 on the accumulation of their shared substrates in the brain can be explained by their separate contributions to the net efflux at the BBB, without postulating any direct or indirect interaction between Abcb1 and Abcg2.

The theoretical model of Kodaira et al. (2010) predicts that halving the amount of active transporter-mediated drug efflux activity at the BBB should also result in only a minor increase of drug accumulation into the brain (never more than 2-fold), even if complete removal of the active transporter-mediated efflux results in a very large increase in brain accumulation. In order to test this prediction, we aimed to analyze the effect of halving the active efflux transporter activity at the BBB by using wild-type, heterozygous *Abcb1a/1b*(+/-);*Abcg2*(+/-) and homozygous *Abcb1a/1b*(-/-);*Abcg2*(-/-) mice, with 2, 1, and 0 active gene copies of each of the active transporters, respectively, and study the effect on TKI brain accumulation. We chose dasatinib, sorafenib, and sunitinib as TKIs in view of their widely different behavior

with respect to impact of the individual transporters on brain accumulation, their different intrinsic capacity to accumulate into the brain, and their different plasma levels upon oral administration (Supplemental Figure 1). This functional diversity makes it more likely that consistent results obtained for these three drugs will also be valid for a much wider range of drugs affected by Abcb1 and Abcg2.

MATERIALS AND METHODS

Chemicals and reagents

Dasatinib, sorafenib and sunitinib were purchased from Sequoia Research Products (Pangbourne, UK). Heparin (5000 IU/ml) was obtained from Leo Pharma BV (Breda, The Netherlands). Lithium-heparinized microvettes and dipotassium-EDTA microvettes were obtained from Sarstedt (Numbrecht, Germany). EDTA disodium salt pH 8.0 was from Cambrex BioScience Inc. (Rockland, ME). Bovine serum albumin (BSA), fraction V, was purchased from Roche (Mannheim, Germany). Isoflurane (Forane) was from Abbott Laboratories (Queenborough, Kent, UK). All other chemicals and reagents were obtained from Sigma-Aldrich (Steinheim, Germany).

Animals

Mice were housed and handled according to institutional guidelines complying with Dutch legislation. Male wild-type, *Abcb1a/1b*(+/-);*Abcg2*(+/-) and *Abcb1a/1b*(-/-);*Abcg2*(-/-) (Jonker et al., 2005) mice, all of a >99% FVB genetic background, were used between 8 and 14 weeks of age. Animals were kept in a temperature-controlled environment with a 12-hr light/12-hr dark cycle and received a standard diet (AM-II, Hope Farms B.V., Woerden, The Netherlands) and acidified water *ad libitum*. *Abcb1a/1b*(+/-);*Abcg2*(+/-) mice were the F1 of a cross between FVB wild-type and *Abcb1a/1b*(-/-);*Abcg2*(-/-) mice.

Drug solutions

Dasatinib was dissolved in dimethyl sulfoxide (DMSO) at a concentration of 25 mg/ml and 25-fold diluted with 50 mM sodium acetate buffer (pH 4.6) to obtain a concentration of 1 mg/ml. Sorafenib tosylate was dissolved in DMSO (25 mg/ml) and 25-fold diluted with Cremophor EL/ethanol/water (1:1:6, v/v/v). Sunitinib malate was dissolved in DMSO at a concentration of 25 mg/ml and further diluted with 50 mM sodium acetate buffer (pH 4.6) to yield a concentration of 1 mg/ml. Dasatinib, sorafenib and sunitinib were administered orally at 10 mg/kg body weight (10 ml/kg).

Plasma pharmacokinetics and relative brain accumulation of TKIs in mice

To minimize variation in absorption upon oral administration, mice were fasted for 3 hr before dasatinib, sorafenib or sunitinib were administered by gavage into the stomach, using a blunt-ended needle. To prevent blood from coagulating, heparin was used for the dasatinib and sunitinib pharmacokinetic experiments, whereas EDTA was used for the sorafenib pharmacokinetic experiment. Tail vein blood sampling was performed at 0.25, 0.5, 1, 2 and 4 hr time-points after oral administration, using either microvettes containing dipotassium-EDTA or lithium heparin. Six hours after oral administration, mice were anesthetized with isoflurane and blood was collected by cardiac puncture, in which 0.5 M disodium-EDTA or 5000 IU/ml heparin were used as anticoagulants. Immediately thereafter, mice were sacrificed by cervical dislocation and brains were rapidly removed. Plasma was

isolated from the blood by centrifugation at 2,100 *g* for 6 min at 4°C, and the plasma fraction was collected and stored at -20°C until analysis. Brains were homogenized with 1 ml of 4% BSA and stored at -20°C until analysis. Relative brain accumulation after oral administration was calculated by determining the drug brain concentration at 6 hr relative to the plasma $AUC_{0\text{-}6hr}$, as the AUC better reflects the overall drug exposure of the brain over time than the plasma concentration at 6 hr after oral administration.

Drug analyses

Dasatinib, sorafenib and sunitinib concentrations in plasma and brain homogenates were analyzed by liquid chromatography coupled to tandem mass spectrometry as described previously (Lagas et al., 2009; Sparidans et al., 2009; Tang et al., 2012, respectively). Lower limit of quantification (LLQ) values for dasatinib and sunitinib were 5 ng/ml and 15.6 ng/g for the plasma and brain homogenates, respectively. LLQ values for sorafenib were 10 ng/ml and 31.2 ng/g for the plasma and brain homogenates, respectively.

RNA isolation, cDNA synthesis and real-time RT-PCR

RNA isolation from mouse brain and small intestine and subsequent cDNA synthesis and RT-PCR were performed as described (Lagas et al., 2012). To circumvent detection of non-functional RNA which is transcribed from the *Abcb1a* and *Abcg2* knockout alleles (Schinkel et al., 1994 and data not shown), we used RT-PCR probes positioned within the deleted exons of both genes. Forward 5'-CCCGGCTC ACAGATGATGTT-3' (F1) and reverse 5'- TTCC AGCCACGGGTAAATCC-3' (R1) specific primers (Invitrogen Life Technologies) were used for the detection of *Abcb1a* in the wild-type alleles, which resulted in a 121-bp band. Forward 5'-CAGCAAGGAAAGATCCAAAGGG-3' (F4) and reverse 5'- CACAACGTCATCTTGAACCACA-3' (R4) specific primers (Invitrogen Life Technologies) were used for the detection of *Abcg2* in the wild-type alleles, which resulted in a 110-bp band.

Statistical analysis

Pharmacokinetic parameters were calculated by non-compartmental methods using the software package PK Solutions 2.0.2 (Summit Research Services, Ashland, OH). The area under the plasma concentration-time curve was calculated using the trapezoidal rule, without extrapolating to infinity. The maximum drug concentration in plasma (C_{max}) and the time to reach maximum drug concentration in plasma (T_{max}) were determined directly from mean concentration-time data. Data are presented as means ± SD. For parametric statistical analysis, all the data except for plasma concentrations and $AUC_{0\text{-}6hr}$ values were log-transformed to obtain equality in variances. One-way analysis of variance (ANOVA) was used to determine statistical significance of differences between groups, after which post-hoc tests with Bonferroni correction were performed for comparison between individual groups. Differences were considered statistically significant when $P < 0.05$.

RESULTS

Expression levels of *Abcb1a* and *Abcg2* in small intestine and brain of wild-type, *Abcb1a/1b*(+/-);*Abcg2*(+/-) and *Abcb1a/1b*(-/-);*Abcg2*(-/-) mice

Since *Abcb1b* is not substantially expressed in wild-type mouse brain and small intestine (data not shown), we tested only *Abcb1a*

and *Abcg2* expression in these tissues of wild-type, *Abcb1a/1b*(+/-);*Abcg2*(+/-) and *Abcb1a/1b*(-/-);*Abcg2*(-/-) mice using RT-PCR. To circumvent spurious detection of non-functional RNA which is still transcribed from the *Abcb1a* and *Abcg2* knockout alleles (Schinkel et al., 1994) (data not shown), we used RT-PCR probes positioned within the deleted exons of both genes. We expected that the expression levels of wild-type *Abcb1a* and *Abcg2* alleles in the small intestine and brain of heterozygous mice would be about half of the expression levels observed in wild-type mice. However, the small intestinal expression levels of *Abcb1a* and *Abcg2* were not significantly different from those in wild-type mice, although experimental variation was quite substantial (Figure 1A and B). As expected, there was no significant expression of *Abcb1a* and *Abcg2* in the small intestine of *Abcb1a/1b*(-/-);*Abcg2*(-/-) mice. The results suggest that, for small intestine, expression levels of *Abcb1a* and *Abcg2* were not halved upon halving the gene copy number of the genes, but instead remained similar to the wild-type expression levels.

In contrast, *Abcb1a* RNA was 3.4-fold, and *Abcg2* RNA 2.3-fold lower in the brain of male heterozygous mice as compared with wild-type mice, albeit with substantial variation in both wild-type and heterozygous values (Figure 1C and D). There was no significant expression of *Abcb1a* and *Abcg2* in the homozygous knockout mice. *In vivo* brain accumulation studies have also been performed using female mice (Durmus et al., 2012), and we now found that in female heterozygous mice, the brain expression levels of *Abcb1a* and *Abcg2* were also about half of the levels observed in wild-type mice (Figure 1E and F). Of note, relative expression levels of either *Abcb1a* or *Abcg2* in brain were not significantly different between heterozygous males and females, and pooled results for both genders indicated roughly half the wild-type expression levels of *Abcb1a* and *Abcg2* in brain of heterozygous mice (Figure 1G and H). This 2-fold reduction (or perhaps slightly more for *Abcb1a* in males) of transporter expression in brains of heterozygous compared to wild-type mice allowed the intended analysis of transporter activity effects on brain accumulation of the TKIs.

Plasma pharmacokinetics of dasatinib, sorafenib and sunitinib in heterozygous *Abcb1a/1b*(+/-);*Abcg2*(+/-) mice

To assess the impact of heterozygous Abcb1 and Abcg2 on oral bioavailability of dasatinib, sorafenib and sunitinib, we orally administered these TKIs at 10 mg/kg to wild-type, *Abcb1a/1b*(+/-);*Abcg2*(+/-) and *Abcb1a/1b*(-/-);*Abcg2*(-/-) mice, and measured plasma concentrations over 6 hrs by LC-MS/MS. Upon dasatinib oral administration, the plasma $AUC_{0\text{-}6hr}$ in heterozygous *Abcb1a/1b*(+/-); *Abcg2*(+/-) mice was 1.6-fold increased, but not significantly compared to wild-type mice. In contrast, a statistically significant 2.1-fold ($P < 0.01$) higher plasma $AUC_{0\text{-}6hr}$ of dasatinib was observed in homozygous *Abcb1a/1b*(-/-);*Abcg2*(-/-) compared to wild-type mice (Figure 2A, D and Table 1), in line with the results of Lagas et al. (2009).

Upon sorafenib oral administration, although there were a few significant differences at individual time points, there was no significant difference in the overall plasma $AUC_{0\text{-}6hr}$ among the 3 tested strains. This suggests that Abcb1 and Abcg2 did not play a role in the overall $AUC_{0\text{-}6hr}$ of sorafenib (Figure 2B, E and Table 2), consistent with the data of Lagas et al. (2010).

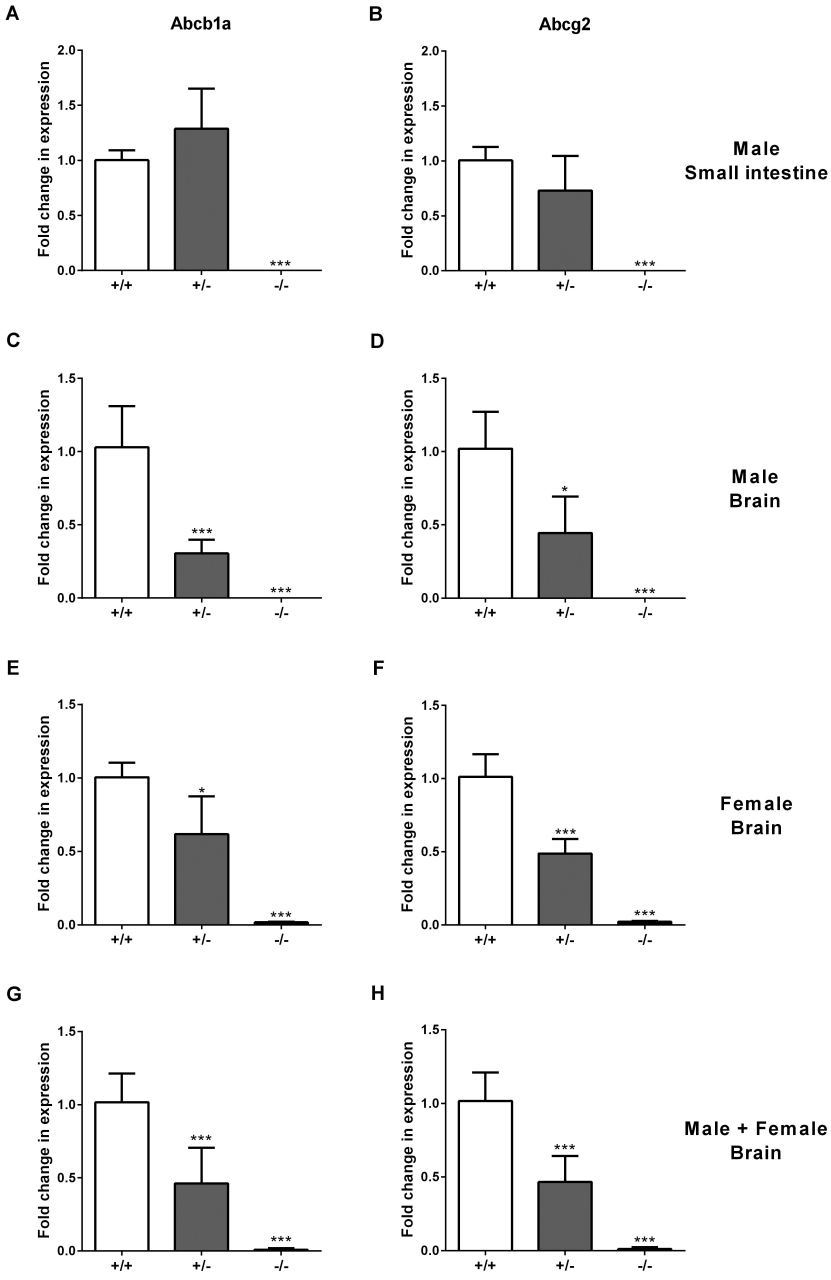

Figure 1. Small intestinal (A and B) and brain (C – H) RNA expression levels of *Abcb1a* (left panels) and *Abcg2* (right panels) in male (A – D), female (E and F) or pooled male and female (G and H) wild-type, *Abcb1a/1b*(+/-);*Abcg2*(+/-) and *Abcb1a/1b(-/-);Abcg2*(-/-) mice (+/+, +/- and -/-, respectively), as determined by real-time RT-PCR. Data are normalized to GAPDH expression. Values represent mean fold change ± SD, compared to wild-type mice (n = 4). *, ** and *** indicate $P < 0.05$, $P < 0.01$ and $P < 0.001$ compared with wild-type mice, respectively.

Table 1. Pharmacokinetic parameters, brain concentrations and relative brain accumulation of dasatinib in male wild-type, *Abcb1a/1b*(+/-);*Abcg2*(+/-) and *Abcb1a/1b*(-/-);*Abcg2*(-/-) mice receiving oral dasatinib at a dose of 10 mg/kg

	Strain		
Parameter	**Wild-type**	***Abcb1a/1b*(+/-);*Abcg2*(+/-)**	***Abcb1a/1b*(-/-);*Abcg2*(-/-)**
$AUC_{0\text{-}6hr}$, ng/ml.hr	1070.8 ± 595.7	1705.9 ± 224.6	2286.9 ± 344.6 **
Fold change $AUC_{0\text{-}6hr}$	1.0	1.6	2.1
C_{max}, ng/ml	265.7 ± 202.6	468.5 ± 360.6	690.5 ± 194.8
T_{max}, hr	4.00	0.25	0.50
C_{brain}, ng/g	2.4 ± 1.6	6.8 ± 1.4 **	138.2 ± 22.9 ***/†††
Fold increase C_{brain}	1.0	2.9	58.4
P_{brain}, ($*10^{-2}$ hr^{-1})	0.21 ± 0.08	0.40 ± 0.09 **	6.1 ± 0.8 ***/†††
Fold increase P_{brain}	1.0	1.9	29.2

Data represent mean ± SD (n = 5). ** and *** indicate $P < 0.01$ and $P < 0.001$ compared with wild-type mice, respectively; ††† indicates $P < 0.001$ compared with *Abcb1a/1b*(+/-);*Abcg2*(+/-) mice.
Abbreviations: $AUC_{0\text{-}6hr}$: area under the plasma concentration-time curve from 0 to 6 hr; C_{max}, maximum plasma concentration; T_{max}, time to reach maximum drug concentration in plasma; C_{brain}: brain concentration of drug at 6 hr after oral administration; P_{brain}: relative brain accumulation of drug at 6 hr after oral administration, calculated by determining the drug brain concentration relative to the $AUC_{0\text{-}6hr}$.

Heterozygous and homozygous knockout mice also showed oral sunitinib plasma $AUC_{0\text{-}6hr}$ values that were not significantly different from wild-type values (Figure 2C), although experimental variation was substantial. Probably related to that, the plasma $AUC_{0\text{-}6hr}$ of *Abcb1a/1b*(+/-);*Abcg2*(+/-) mice was 1.9-fold and significantly higher ($P < 0.01$) than that of *Abcb1a/1b*(-/-);*Abcg2*(-/-) mice (Figure 2C and F, Table 3). The homozygous data were in agreement with the results of Tang et al. (2012). Taken together, heterozygosity for Abcb1 and Abcg2 knockout alleles had no significant effect on the plasma $AUC_{0\text{-}6hr}$ of orally administered dasatinib, sorafenib and sunitinib.

Brain accumulation of dasatinib, sorafenib and sunitinib in *Abcb1a/1b*(+/-);*Abcg2*(+/-) and *Abcb1a/1b*(-/-);*Abcg2*(-/-) mice

In the same set of experiments, we also measured the brain concentrations at 6 hr after oral administration of dasatinib, sorafenib and sunitinib (10 mg/kg) in wild-type, *Abcb1a/1b*(+/-);*Abcg2*(+/-) and *Abcb1a/1b*(-/-);*Abcg2*(-/-) mice. Brain concentrations of all drugs were modestly increased (1.5- to 2.9-fold) in heterozygous *Abcb1a/1b*(+/-);*Abcg2*(+/-) compared to wild-type mice, albeit not significantly for sorafenib (Tables 1-3, Figure 3A-C). The homozygous *Abcb1a/1b*(-/-);*Abcg2*(-/-) mice had 58.4-, 27.8- and 19.7-fold higher brain concentrations of dasatinib, sorafenib and sunitinib than wild-type mice, respectively (Figure 3A-C; Tables 1-3). Brain accumulations of all drugs at 6 hr were also modestly increased (1.6- to 1.9-fold) in the heterozygous strain as compared to wild-type, albeit only statistically significant ($P < 0.01$) for dasatinib (Figure 3D-F; Tables 1-3). In contrast, *Abcb1a/1b*(-/-);*Abcg2*(-/-) mice had 29.2-, 35.9- and 23.7-fold increased brain accumulations ($P < 0.001$) of dasatinib,

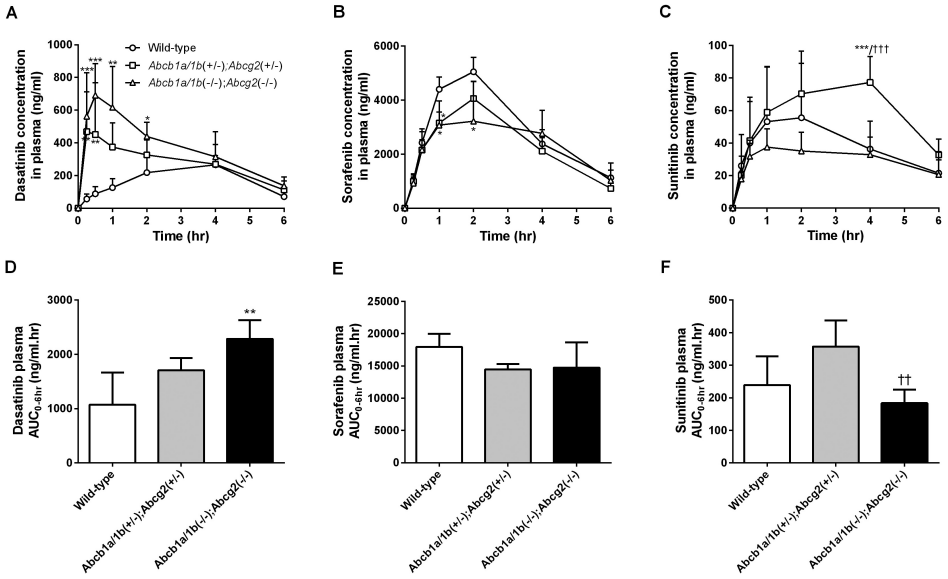

Figure 2. Plasma concentration-time curves (upper panels) and plasma $AUC_{0\text{-}6hr}$ (lower panels) of dasatinib (A and D), sorafenib (B and E) and sunitinib (C and F) in male wild-type, *Abcb1a/1b*(+/-);*Abcg2*(+/-) and *Abcb1a/1b*(-/-);*Abcg2*(-/-) mice receiving oral dasatinib, sorafenib or sunitinib at 10 mg/kg, respectively. Data represent mean ± SD (n = 5). *, ** and *** indicate $P < 0.05$, $P < 0.01$ and $P < 0.001$ compared with wild-type mice, respectively; †† and ††† indicates $P < 0.01$ and $P < 0.001$ compared with *Abcb1a/1b*(+/-);*Abcg2*(+/-) mice, respectively. Note the differences in Y-axis scales for the different drugs.

Table 2. Pharmacokinetic parameters, brain concentrations and relative brain accumulation of sorafenib in male wild-type, *Abcb1a/1b*(+/-);*Abcg2*(+/-) and *Abcb1a/1b*(-/-);*Abcg2*(-/-) mice receiving oral sorafenib at a dose of 10 mg/kg

	Strain		
Parameter	**Wild-type**	***Abcb1a/1b*(+/-);*Abcg2*(+/-)**	***Abcb1a/1b*(-/-);*Abcg2*(-/-)**
$AUC_{0\text{-}6hr}$, ng/ml.hr	17933.9 ± 2029.0	14464.7 ± 833.1	14746.4 ± 3879.8
Fold change $AUC_{0\text{-}6hr}$	1.0	0.8	0.8
C_{max}, ng/ml	5051.9 ± 532.4	4061.9 ± 626.8	3220.8 ± 1480.2
T_{max}, hr	2.00	2.00	2.00
C_{brain}, ng/g	25.7 ± 25.1	38.8 ± 23.8	714.0 ± 214.2 ***/†††
Fold increase C_{brain}	1.0	1.5	27.8
P_{brain}, ($*10^{-2}$ hr^{-1})	0.14 ± 0.15	0.27 ± 0.16	5.1 ± 2.0 ***/†††
Fold increase P_{brain}	1.0	1.8	35.9

Data represent mean ± SD (n = 5). *** indicates $P < 0.001$ compared with wild-type mice, respectively; ††† indicates $P < 0.001$ compared with *Abcb1a/1b*(+/-);*Abcg2*(+/-) mice.
Abbreviations: $AUC_{0\text{-}6hr}$: area under the plasma concentration-time curve from 0 to 6 hr; C_{max}, maximum plasma concentration; T_{max}, time to reach maximum drug concentration in plasma; C_{brain}: brain concentration of drug at 6 hr after oral administration; P_{brain}: relative brain accumulation of drug at 6 hr after oral administration, calculated by determining the drug brain concentration relative to the $AUC_{0\text{-}6hr}$.

Table 3. Pharmacokinetic parameters, brain concentrations and relative brain accumulation of sunitinib in male wild-type, *Abcb1a/1b*(+/-);*Abcg2*(+/-) and *Abcb1a/1b*(-/-);*Abcg2*(-/-) mice receiving oral sunitinib at a dose of 10 mg/kg

	Strain		
Parameter	**Wild-type**	***Abcb1a/1b*(+/-);*Abcg2*(+/-)**	***Abcb1a/1b*(-/-);*Abcg2*(-/-)**
$AUC_{0\text{-}6hr}$, ng/ml.hr	238.9 ± 88.7	357.4 ± 80.4	183.7 ± 41.2 ††
Fold change $AUC_{0\text{-}6hr}$	1.0	1.5	0.8
C_{max}, ng/ml	55.5 ± 33.4	77.2 ± 16.0	37.6 ± 11.2
T_{max}, hr	2.00	4.00	1.00
C_{brain}, ng/g	36.5 ± 17.5	88.4 ± 11.7 *	721.3 ± 337.8 ***/†††
Fold increase C_{brain}	1.0	2.4	19.7
P_{brain}, ($*10^{-2}$ hr^{-1})	16.4 ± 10.1	25.8 ± 6.6	389.1 ± 153.4 ***/†††
Fold increase P_{brain}	1.0	1.6	23.7

Data represent mean ± SD (n = 5). * and *** indicate $P < 0.05$ and $P < 0.001$ compared with wild-type mice, respectively; †† and ††† indicate $P < 0.01$ and $P < 0.001$ compared with *Abcb1a/1b*(+/-);*Abcg2*(+/-) mice, respectively. Abbreviations: $AUC_{0\text{-}6hr}$: area under the plasma concentration-time curve from 0 to 6 hr; C_{max}, maximum plasma concentration; T_{max}, time to reach maximum drug concentration in plasma; C_{brain}: brain concentration of drug at 6 hr after oral administration; P_{brain}: relative brain accumulation of drug at 6 hr after oral administration, calculated by determining the drug brain concentration relative to the $AUC_{0\text{-}6hr}$.

sorafenib and sunitinib, respectively, relative to wild-type mice (Figure 3D-F; Table 1-3). Taken together, these results show that halving the amount of active efflux by Abcb1 and Abcg2 at the BBB had only a small impact (<2-fold) on the brain accumulation of dasatinib, sorafenib and sunitinib. Even without knowing the exact contribution of each individual transporter, substitution in the equations developed by Kodaira et al. allows prediction of the effects of halving the total amount of active Abcb1- and Abcg2-mediated transport. In this case, based on the homozygous knockout values, brain accumulation values in the heterozygous mice were predicted to be 1.93-, 1.95-, and 1.92-fold increased relative to wild-type levels for dasatinib, sorafenib, and sunitinib, respectively. These values fall well within the range of the experimental values obtained for these drugs (1.6- to 1.9-fold increases, Figure 3D-F, Tables 1-3).

DISCUSSION

The present study shows that halving the amount of active drug efflux transport by Abcb1 and Abcg2 at the BBB results in less than 2-fold increases in brain accumulation of several TKIs, even when complete removal of these active drug transporters results in 24- to 36-fold increases in brain accumulation of these drugs. These observations are fully in line with predictions of the theoretical pharmacokinetic model of Kodaira et al. (2010), and thus provide further support for its validity. Moreover, the diversity in properties of the tested TKIs in terms of plasma levels obtained (i.e., oral availability), intrinsic capacity to accumulate into the brain, and extent to which brain accumulation is relatively affected by Abcb1 and Abcg2, suggests that many more drugs transported by ABCB1 and/or ABCG2 will be subject to the same behavior. It is worth noting that the

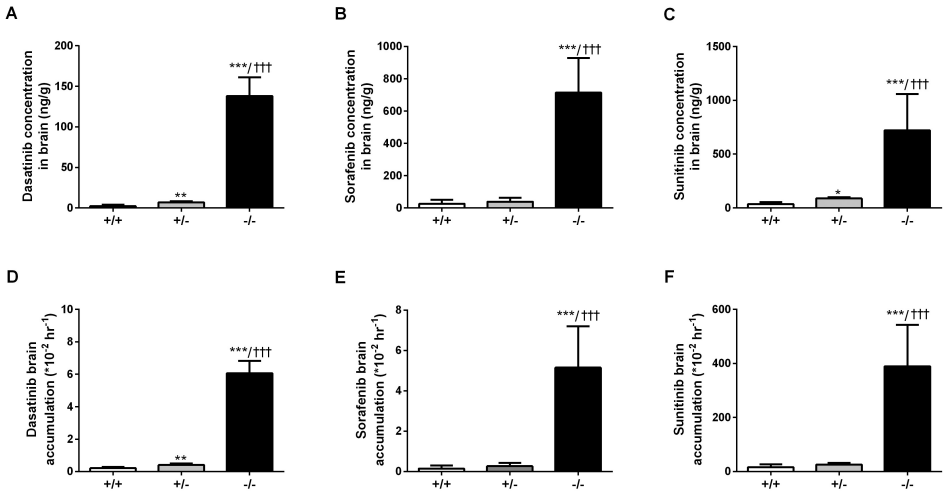

Figure 3. Brain concentration (upper panels) and relative brain accumulation (lower panels) of dasatinib (A and D), sorafenib (B and E) and sunitinib (C and F) at 6 hr in male wild-type, *Abcb1a/1b*(+/-);*Abcg2*(+/-) and *Abcb1a/1b*(-/-);*Abcg2*(-/-) mice (+/+, +/- and -/-, respectively) receiving oral dasatinib, sorafenib or sunitinib at 10 mg/kg, respectively. Data represent mean ± SD (n = 5). *, ** and *** indicate $P < 0.05$, $P < 0.01$ and $P < 0.001$ compared with wild-type mice, respectively; ††† indicates $P < 0.001$ compared with *Abcb1a/1b*(+/-);*Abcg2*(+/-) mice. Note the differences in Y-axis scales for the different drugs.

model will also apply to any other active drug efflux transporters present in the endothelial luminal membrane of the BBB, and can in principle, with some modification, be used for any number of these transporters.

The most important feature of the model is that it explains the counterintuitive disproportionate increase in drug accumulation into the brain seen when two active BBB drug efflux transporters of a drug are simultaneously knocked out (or inhibited), relative to the situation when only one is knocked out. This turns out to be simply a consequence of the fact that the active efflux transport by each of the transporters is considerably larger than the remaining (passive, or lowly active) efflux transport at the BBB in the absence of both the efflux transporters. Thus, the apparently "synergistic" effect of simultaneously removing the activity of both transporters on brain accumulation of a drug can be explained without postulating any direct or indirect interaction between the transporters that would somehow modulate the transport activity of each of the individual (remaining) transporters when the other is knocked out. As shown and summarized before (Agarwal et al., 2012; Durmus et al., 2012), single knockout of Abcb1 or Abcg2 in FVB mice also does not result in significant expression changes of the remaining transporter in the brain. Although conceptually somewhat different, the lack of change in brain expression per gene copy that we observed in the heterozygous *Abcb1a/1b*(+/-);*Abcg2*(+/-) is in line with this relative stability in brain expression of *Abcb1a* and *Abcg2*.

Unlike the brain expression of *Abcb1a* and *Abcg2*, in the intestine heterozygosity for the encoding genes does not result in halving of

the RNA levels, but rather in levels that are similar to those in the wild-type mice (compare Figure 1A-B vs. 1C-H). Possibly the intestine, as a primary flexible protective barrier directly exposed to numerous xenobiotics, is more adapted to upregulating detoxifying proteins depending on effective exposure than the endothelial cells of the BBB. It may well be that there are more and more highly active xenobiotic nuclear receptors present in intestinal epithelial cells than in brain capillary endothelial cells, and almost certainly the exposure to potentially regulating xenobiotic factors is far higher in the intestinal cells than in the BBB cells. Both factors can contribute to a more effective compensatory upregulation of *Abcb1a* and *Abcg2* in intestine than in brain upon halving of the gene dosage.

The three TKIs we tested at the same oral dosage (10 mg/kg) showed highly divergent oral availability and brain accumulation characteristics, in both wild-type and knockout mice (Tables 1-3). For instance, in wild-type mice the $AUC_{0\text{-}6hr}$ of sunitinib was nearly two orders of magnitude (75-fold) lower than that of sorafenib, whereas that of dasatinib was in between (16.7-fold lower than that of sorafenib). The relative $AUC_{0\text{-}6hr}$ results between the drugs in the knockout strain showed a similar profile. At the same time, the relative brain accumulation (K_p) of sunitinib in wild-type mice was 117- and 82-fold higher than that of sorafenib and dasatinib, respectively. Again, the profile of relative results for the K_ps in the knockout strain was similar, although at a ~70-fold higher absolute level. Thus, the drug with the lowest plasma levels, sunitinib, had the highest relative brain accumulation. Clearly there can be many factors that contribute to these differences between the drugs, including differential impact of drug uptake and drug efflux transporters in the various epithelial and endothelial barriers, drug-metabolizing enzymes, saturation phenomena, hydrophobicity of the drugs and other physicochemical properties that define e.g. binding to plasma and tissue proteins and lipids. Nonetheless, despite the profound differences in intrinsic properties between the three TKIs tested here, they all adhere similarly to the model of Kodaira et al. with respect to impact of Abcb1a and Abcg2 on brain accumulation. Moreover, a recent pilot analysis of the effect of Abcb1a/1b;Abcg2 heterozygosity on brain accumulation of oral vemurafenib, another TKI, yielded very similar results (Durmus et al., 2012). These observations make it very likely that the same principle will apply to many other drugs with a wide range of divergent intrinsic properties, as long as they are substantially transported by Abcb1 and/or Abcg2.

The model of Kodaira et al. (2010) was developed for describing the impact of drug efflux transporters on drug accumulation across the BBB and the testis-blood barrier. However, the model can also be applied to any other functionally similar blood-tissue barrier. In this respect it is interesting to retrospectively consider the results we obtained with transplacental accumulation of drugs into fetuses that were wild-type, heterozygous, or homozygous for *Abcb1a/1b* (Smit et al., 1999). As each mouse fetus forms its own placenta, and the placenta has the genotype of the fetus, the individual placental barriers are also either wild-type, heterozygous, or homozygous for *Abcb1a/1b*. By crossing a heterozygous mother with a heterozygous father, placental barriers of each genotype can be obtained within one

pregnant mother. As shown in Supplemental Figure 2, the transplacental fetal accumulation of the maternally administered drugs digoxin, saquinavir and paclitaxel was ~2.5-fold, ~7.5-fold, and ~16-fold increased in the homozygous knockout fetuses relative to wild-type, whereas accumulation in the heterozygous fetuses was 1.6-, 1.3-, and 1.3-fold increased, respectively. Also here we observed the pattern (for saquinavir and paclitaxel) that a profound accumulation in full knockouts is associated with a small (and even statistically insignificant) increase in the heterozygous situation. Considering the experimental variation, these results are consistent with the model of Kodaira et al.: assuming about half of the wild-type efflux activity in the heterozygous placenta, predicted values were 1.43-, 1.76-, and 1.88-fold increase relative to wild-type, respectively. The strong increase in homozygous fetuses indicates that the Abcb1a/1b transport activity in the placenta is considerably greater than any alternative remaining placental drug efflux activity. Also consistent with the model, the more modest impact of full knockout on digoxin fetal accumulation (~2.5-fold increase) was associated with a more or less intermediate (and statistically significant) ~1.6-fold increase in the heterozygous fetuses. We infer that the impact of efflux transporters on transplacental fetal accumulation of drugs can also be adequately described by the model of Kodaira et al., and that for saquinavir and paclitaxel Abcb1 is by far the most important drug efflux transporter limiting fetal drug accumulation.

Acknowledgement

This work was supported by an academic staff training scheme fellowship from the Malaysian Ministry of Higher Education to S.C.T. and in part by the Dutch Cancer Society [grant 2007-3764]. We thank Anita van Esch for assistance with RNA isolation and Dr. Hilde Rosing for supervision of bioanalytical analyses. We wish to thank Selvi Durmus and Dilek Iusuf for critical reading of the manuscript.

REFERENCES

1. Agarwal S, Sane R, Gallardo JL, Ohlfest JR and Elmquist WF (2010) Distribution of gefitinib to the brain is limited by P-glycoprotein (ABCB1) and breast cancer resistance protein (ABCG2)-mediated active efflux. *J Pharmacol Exp Ther* **334**:147-155.
2. Agarwal S, Uchida Y, Mittapalli RK, Sane R, Terasaki T and Elmquist WF (2012) Quantitative proteomics of transporter expression in brain capillary endothelial cells isolated from P-glycoprotein (P-gp), breast cancer resistance protein (Bcrp), and P-gp/Bcrp knockout mice. *Drug Metab Dispos* **40**:1164-1169.
3. Chen Y, Agarwal S, Shaik NM, Chen C, Yang Z and Elmquist WF (2009) P-glycoprotein and breast cancer resistance protein influence brain distribution of dasatinib. *J Pharmacol Exp Ther* **330**:956-963.
4. Durmus S, Sparidans RW, Wagenaar E, Beijnen JH and Schinkel AH (2012) Oral availability and brain penetration of the B-RAFV600E inhibitor vemurafenib can be enhanced by the P-GLYCOprotein (ABCB1) and breast cancer resistance protein (ABCG2) inhibitor elacridar. *Mol Pharm* **9**:3236-3245.
5. Escudier B, Eisen T, Stadler WM, Szczylik C, Oudard S, Siebels M, Negrier S, Chevreau C, Solska E, Desai AA, Rolland F, Demkow T, Hutson TE, Gore M, Freeman S, Schwartz B, Shan M, Simantov R and Bukowski RM (2007) Sorafenib in advanced clear-cell renal-cell carcinoma. *N Engl J Med* **356**:125-134.
6. Goodman VL, Rock EP, Dagher R, Ramchandani RP, Abraham S, Gobburu JV, Booth BP, Verbois SL, Morse DE, Liang CY, Chidambaram N, Jiang JX, Tang S, Mahjoob K, Justice R and Pazdur

R (2007) Approval summary: sunitinib for the treatment of imatinib refractory or intolerant gastrointestinal stromal tumors and advanced renal cell carcinoma. *Clin Cancer Res* **13**:1367-1373.

7. Jonker JW, Freeman J, Bolscher E, Musters S, Alvi AJ, Titley I, Schinkel AH and Dale TC (2005) Contribution of the ABC transporters Bcrp1 and Mdr1a/1b to the side population phenotype in mammary gland and bone marrow of mice. *Stem Cells* **23**:1059-1065.
8. Kantarjian H, Shah NP, Hochhaus A, Cortes J, Shah S, Ayala M, Moiraghi B, Shen Z, Mayer J, Pasquini R, Nakamae H, Huguet F, Boque C, Chuah C, Bleickardt E, Bradley-Garelik MB, Zhu C, Szatrowski T, Shapiro D and Baccarani M (2010) Dasatinib versus imatinib in newly diagnosed chronic-phase chronic myeloid leukemia. *N Engl J Med* **362**:2260-2270.
9. Kodaira H, Kusuhara H, Ushiki J, Fuse E and Sugiyama Y (2010) Kinetic analysis of the cooperation of P-glycoprotein (P-gp/Abcb1) and breast cancer resistance protein (Bcrp/Abcg2) in limiting the brain and testis penetration of erlotinib, flavopiridol, and mitoxantrone. *J Pharmacol Exp Ther* **333**:788-796.
10. Lagas JS, Damen CW, van Waterschoot RA, Iusuf D, Beijnen JH and Schinkel AH (2012) P-glycoprotein, multidrug-resistance associated protein 2, Cyp3a, and carboxylesterase affect the oral availability and metabolism of vinorelbine. *Mol Pharmacol* **82**:636-644.
11. Lagas JS, van Waterschoot RA, Sparidans RW, Wagenaar E, Beijnen JH and Schinkel AH (2010) Breast cancer resistance protein and P-glycoprotein limit sorafenib brain accumulation. *Mol Cancer Ther* **9**:319-326.
12. Lagas JS, van Waterschoot RA, van Tilburg VA, Hillebrand MJ, Lankheet N, Rosing H, Beijnen JH and Schinkel AH (2009) Brain accumulation of dasatinib is restricted by P-glycoprotein (ABCB1) and breast cancer resistance protein (ABCG2) and can be enhanced by elacridar treatment. *Clin Cancer Res* **15**:2344-2351.
13. Llovet JM, Ricci S, Mazzaferro V, Hilgard P, Gane E, Blanc JF, de Oliveira AC, Santoro A, Raoul JL, Forner A, Schwartz M, Porta C, Zeuzem S, Bolondi L, Greten TF, Galle PR, Seitz JF, Borbath I, Haussinger D, Giannaris T, Shan M, Moscovici M, Voliotis D and Bruix J (2008) Sorafenib in advanced hepatocellular carcinoma. *N Engl J Med* **359**:378-390.
14. Lombardo LJ, Lee FY, Chen P, Norris D, Barrish JC, Behnia K, Castaneda S, Cornelius LA, Das J, Doweyko AM, Fairchild C, Hunt JT, Inigo I, Johnston K, Kamath A, Kan D, Klei H, Marathe P, Pang S, Peterson R, Pitt S, Schieven GL, Schmidt RJ, Tokarski J, Wen ML, Wityak J and Borzilleri RM (2004) Discovery of N-(2-chloro-6-methyl-phenyl)-2-(6-(4-(2-hydroxyethyl)- piperazin-1-yl)-2-methylpyrimidin-4- ylamino)thiazole-5-carboxamide (BMS-354825), a dual Src/Abl kinase inhibitor with potent antitumor activity in preclinical assays. *J Med Chem* **47**:6658-6661.
15. Mittapalli RK, Vaidhyanathan S, Sane R and Elmquist WF (2012) Impact of P-glycoprotein (ABCB1) and breast cancer resistance protein (ABCG2) on the brain distribution of a novel BRAF inhibitor: vemurafenib (PLX4032). *J Pharmacol Exp Ther* **342**:33-40.
16. Polli JW, Olson KL, Chism JP, John-Williams LS, Yeager RL, Woodard SM, Otto V, Castellino S and Demby VE (2009) An unexpected synergist role of P-glycoprotein and breast cancer resistance protein on the central nervous system penetration of the tyrosine kinase inhibitor lapatinib (N-{3-chloro-4-[(3-fluorobenzyl)oxy]phenyl}-6-[5-({[2-(methylsulfonyl)ethyl]amino }methyl)-2-furyl]-4-quinazolinamine; GW572016). *Drug Metab Dispos* **37**:439-442.
17. Raymond E, Dahan L, Raoul JL, Bang YJ, Borbath I, Lombard-Bohas C, Valle J, Metrakos P, Smith D, Vinik A, Chen JS, Horsch D, Hammel P, Wiedenmann B, Van Cutsem E, Patyna S, Lu DR, Blanckmeister C, Chao R and Ruszniewski P (2011) Sunitinib malate for the treatment of pancreatic neuroendocrine tumors. *N Engl J Med* **364**:501-513.
18. Rock EP, Goodman V, Jiang JX, Mahjoob K, Verbois SL, Morse D, Dagher R, Justice R and Pazdur R (2007) Food and Drug Administration drug approval summary: Sunitinib malate for the treatment of gastrointestinal stromal tumor and advanced renal cell carcinoma. *Oncologist* **12**:107-113.
19. Schinkel AH, Smit JJ, van Tellingen O, Beijnen JH, Wagenaar E, van Deemter L, Mol CA, van der Valk MA, Robanus-Maandag EC, te Riele HP and . (1994) Disruption of the mouse mdr1a P-glycoprotein gene leads to a deficiency in the blood-brain barrier and to increased sensitivity to drugs. *Cell* **77**:491-502.
20. Smit JW, Huisman MT, van Tellingen O, Wiltshire HR and Schinkel AH (1999) Absence or pharmacological blocking of placental P-glycoprotein profoundly increases fetal drug exposure. *J Clin Invest* **104**:1441-1447.

21. Sparidans RW, Vlaming ML, Lagas JS, Schinkel AH, Schellens JH and Beijnen JH (2009) Liquid chromatography-tandem mass spectrometric assay for sorafenib and sorafenib-glucuronide in mouse plasma and liver homogenate and identification of the glucuronide metabolite. *J Chromatogr B Analyt Technol Biomed Life Sci* **877**:269-276.

22. Tang SC, Lagas JS, Lankheet NA, Poller B, Hillebrand MJ, Rosing H, Beijnen JH and Schinkel AH (2012) Brain accumulation of sunitinib is restricted by P-glycoprotein (ABCB1) and breast cancer resistance protein (ABCG2) and can be enhanced by oral elacridar and sunitinib coadministration. *Int J Cancer* **130**:223-233.

23. Zhou L, Schmidt K, Nelson FR, Zelesky V, Troutman MD and Feng B (2009) The effect of breast cancer resistance protein and P-glycoprotein on the brain penetration of flavopiridol, imatinib mesylate (Gleevec), prazosin, and 2-methoxy-3-(4-(2-(5-methyl-2-phenyloxazol-4-yl)ethoxy) phenyl)propanoic acid (PF-407288) in mice. *Drug Metab Dispos* **37**:946-955.

SUPPLEMENTAL DATA

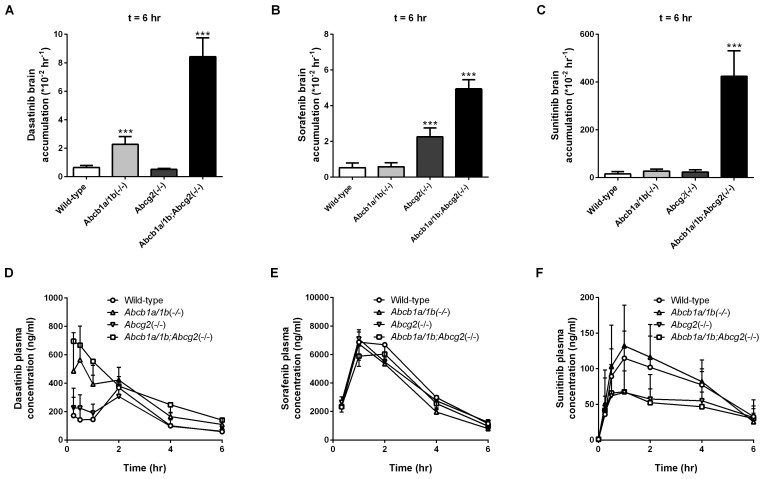

Supplemental Figure 1. Plasma concentration-time curves (upper panels) and relative brain accumulation (lower panels) of dasatinib (A and D), sorafenib (B and E) and sunitinib (C and F) at 6 hr in male wild-type, *Abcb1a/1b*(-/-), *Abcg2*(-/-) and *Abcb1a/1b*(-/-);*Abcg2*(-/-) mice receiving oral dasatinib, sorafenib or sunitinib at 10 mg/kg, respectively. Data represent mean ± SD (n = 5). *** indicates $P < 0.001$ compared with wild-type mice, respectively. Note the differences in Y-axis scales for the different drugs. Data are obtained from Lagas et al. (2009), Lagas et al. (2010) and Tang et al. (2012).

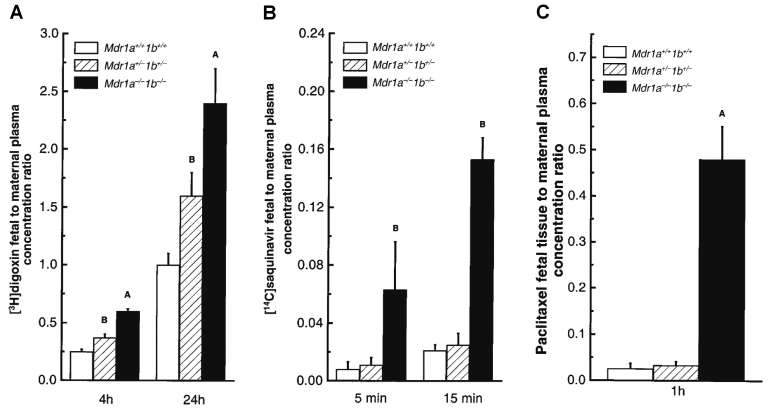

Supplemental Figure 2. Ratios of fetal concentration to maternal plasma concentration of [^{3}H]digoxin (A), [^{14}C]saquinavir (B) or paclitaxel (C) at indicated time-points in female *Mdr1a*$^{+/+}$*1b*$^{+/+}$, *Mdr1a*$^{+/-}$*1b*$^{+/-}$ and *Mdr1a*$^{-/-}$*1b*$^{-/-}$ fetuses in a *Mdr1a*$^{+/-}$*1b*$^{+/-}$ pregnant mother receiving intravenously 0.05 mg/kg [^{3}H]digoxin, 1 mg/kg [^{14}C] saquinavir or 10 mg/kg paclitaxel, respectively. *Mdr1a*$^{+/+}$*1b*$^{+/+}$ corresponds to *Abcb1a/1b*(+/+), *Mdr1a*$^{+/-}$*1b*$^{+/-}$ corresponds to *Abcb1a/1b*(+/-) and *Mdr1a*$^{-/-}$*1b*$^{-/-}$ corresponds to *Abcb1a/1b*(-/-). Data represent mean ± SD (n = 4 - 27). ^{A} and ^{B} indicate $P < 0.0001$ and $P < 0.005$ compared with *Mdr1a*$^{-/-}$*1b*$^{-/-}$ fetuses in pair-wise comparison. Note the differences in Y-axis scales for the different drugs. Data are obtained from Smit et al. (1999).

CHAPTER 3

PHARMACOKINETIC STUDIES ON EVEROLIMUS, A MAMMALIAN TARGET OF RAPAMYCIN INHIBITOR

3.1

IMPACT OF P-GLYCOPROTEIN, CYP3A AND PLASMA CARBOXYLESTERASE CES1C ON BLOOD PHARMACOKINETICS AND TISSUE DISPOSITION OF EVEROLIMUS (AFINITOR, ZORTRESS/CERTICAN) IN MICE

Seng Chuan Tang[1], Rolf W. Sparidans[2], Tatsuki Fukami[4], Els Wagenaar[1], Tsuyoshi Yokoi[4], Jos H. Beijnen[2,3], and Alfred H. Schinkel[1]

[1]Division of Molecular Oncology, the Netherlands Cancer Institute, Amsterdam, the Netherlands
[2]Division of Pharmacoepidemiology & Clinical Pharmacology, Department of Pharmaceutical Sciences, Utrecht, the Netherlands
[3]Department of Pharmacy & Pharmacology, Slotervaart Hospital, Amsterdam, the Netherlands
[4]Drug Metabolism and Toxicology, Faculty of Pharmaceutical Sciences, Kanazawa University, Kakuma-machi, Kanazawa, Japan

Submitted for publication

TRANSLATIONAL RELEVANCE

Everolimus is currently used to treat breast cancer patients, who have a high risk of developing brain metastases. We show here that brain accumulation of everolimus is primarily restricted by ABCB1 in mice, providing a rationale for combining everolimus with ABCB1 inhibitors to improve the therapeutic efficacy against primary and metastatic brain tumors. Unexpectedly, we found that several carboxylesterase (Ces) enzymes were upregulated in the Abcb1a/1b and Abcg2 knockout mice, and that this could strongly increase the blood exposure of everolimus, apparently by tight binding of everolimus to plasma Ces1c. As many groups and pharmaceutical companies use these knockout mouse strains for pharmacological and pharmacokinetic purposes, some of those studies could similarly be confounded by this Ces upregulation. Importantly, our results indicate that everolimus is a human CES2 inhibitor, which might be relevant in modulating the efficacy of (pro-)drugs that are hydrolyzed by human CES2.

ABSTRACT

Purpose: We aimed to clarify the role of ABCB1, ABCG2, and CYP3A in blood and brain exposure of everolimus using knockout mouse models.

Experimental Design: We used wild-type, *Abcb1a/1b*(-/-), *Abcg2*(-/-), *Abcb1a/1b;Abcg2*(-/-) and *Cyp3a*(-/-) mice to study everolimus oral bioavailability and brain accumulation.

Results: Following everolimus administration, brain concentrations and brain-to-liver ratios were substantially increased in *Abcb1a/1b*(-/-) and *Abcb1a/1b;Abcg2*(-/-) mice. A large fraction of everolimus was located in the plasma compartment of knockout mice after intravenous administration. *In vitro*, everolimus was less stable in wild-type plasma than in knockout plasma at 1000 ng/ml and 4000 ng/ml. Between 5- and 25-fold dilutions with wild-type plasma, the knockout plasmas showed similar degradation profiles as undiluted wild-type plasma. We found that Ces1c, a plasma carboxylesterase, was abundantly upregulated (70- to 80-fold) in the liver of knockout mice relative to wild-type mice, and likely protected everolimus by binding and stabilizing it. Binding of everolimus with Ces1c could be displaced by preincubation with the irreversible carboxylesterase inhibitor BNPP. In addition, everolimus markedly inhibited the hydrolysis of irinotecan and *p*-nitrophenyl acetate by mouse plasma Ces and recombinant human CES2, respectively.

Conclusions: Despite increased whole blood exposure in all knockout strains, brain accumulation of everolimus was clearly restricted by Abcb1. Ces1c is the most likely plasma carboxylesterase responsible for the tight binding and stabilization of everolimus, resulting in higher retention of everolimus in plasma of knockout mice. This tight binding confers protection to everolimus from being converted to a prominent metabolite.

INTRODUCTION

The mammalian target of rapamycin (mTOR) is a serine-threonine protein kinase of the phosphatidylinositol 3-kinase (PI3K)-protein kinase B signaling pathway (1, 2). This protein kinase is a downstream central effector of the PI3K pathway that controls cell growth, proliferation, survival and metabolism (3, 4). Deregulation of the PI3K-AKT-mTOR signaling pathway has been identified in many types of cancers (5-7). The macrocyclic lactone everolimus (Afinitor, Zortress/Certican, SDZ RAD or RAD001; Supplemental Data 1), a derivative of rapamycin (sirolimus), is an orally active inhibitor of mTOR and is used both in cancer therapy and as an immunosuppressant to prevent organ rejection in heart and kidney transplant recipients.

Everolimus is currently used either alone or in combination for treating multiple cancers such as advanced renal cell carcinoma (8), subependymal giant cell astrocytoma (9), advanced pancreatic neuroendocrine tumors (10) and advanced hormone receptor-positive, HER-2-negative breast cancer (11). Clinical trials to assess its efficacy in gastric cancer, hepatocellular carcinoma and lymphoma are ongoing, and it appears to be beneficial in refractory graft-versus-host disease after bone marrow transplantation. Given the sensitivity of human glioma cell lines to everolimus (12, 13), and the frequent alterations in the P13K-AKT-mTOR pathway in more than 80% of glioblastoma (14); Cancer Genome Atlas Research Network (2008), it might also be beneficial for the treatment of these primary brain tumors.

ATP-binding cassette (ABC) drug efflux transporters such as P-glycoprotein (P-gp; ABCB1) and breast cancer resistance protein (BCRP; ABCG2) are highly expressed in the intestinal epithelium and in the blood-brain barrier (BBB), as well as in a number of tumors. They can thus confer multidrug resistance, and have been shown to limit the oral absorption and brain penetration of many clinically used anticancer drugs *in vivo* (15-19), which may well limit the therapeutic efficacy of these drugs, especially against brain metastases. It is therefore important to know whether everolimus interacts with these transporters. Everolimus is transported by ABCB1 *in vitro*, as demonstrated in a Caco-2 cell line (20). Furthermore, everolimus was found to be an inhibitor for ABCB1 and ABCG2 *in vitro* (21). *In vivo*, the plasma $AUC_{0\text{-}24hr}$ of everolimus in *Abcb1a/1b*(-/-) mice was only 1.3-fold higher than that of wild-type mice upon oral administration of 0.25 mg/kg everolimus (22), suggesting little influence of Abcb1 on oral availability. However, everolimus coadministration could increase the brain accumulation of vandetanib, presumably by inhibiting Abcb1 and Abcg2 activity in wild-type mice (21). Although these studies suggest an interaction of everolimus with ABCB1 and ABCG2 *in vitro* and *in vivo*, the *in vivo* roles of Abcb1 and possibly Abcg2 in brain accumulation of everolimus remain unknown.

In vitro studies supported by clinical data have established that everolimus is metabolized by cytochrome P450 3A (CYP3A) (23), which is a concern for drug-drug interactions, as coadministered drugs or food components may drastically increase or decrease CYP3A activity, and therefore the systemic levels of orally administered everolimus. This could either result in undertreatment, or serious (life-threatening) side effects of this potentially highly toxic drug. The initial aim of this study was to clarify

the *in vivo* roles of ABCB1, ABCG2 and CYP3A in oral availability and brain accumulation of everolimus using knockout mouse models, as such insights may be useful to improve the therapeutic efficacy of everolimus, especially for brain tumors that are positioned behind an intact BBB.

MATERIAL AND METHODS

Chemicals and reagents

Everolimus and 7-ethyl-10-hydroxycamptothecin (SN-38) were purchased from Sequoia Research Products (Pangbourne, UK). Irinotecan HCl-trihydraat was from Hospira Benelux BVBA, (Brussel, Belgium). Bis(4-nitrophenyl) phosphate (BNPP) was from Sigma-Aldrich (Steinheim, Germany). EDTA disodium salt pH 8.0 was from Cambrex BioScience Inc. (Rockland, ME). Bovine serum albumin (BSA), fraction V, was purchased from Roche (Mannheim, Germany). Tetra-n-butylammonium bromide (TBABr) was purchased from Merck Schuchardt (Hohenbrunn, Germany). Acetonitrile (HPLC grade) was from Biosolve (Valkenswaard, the Netherlands). Heparin (5000 IE/ml) was purchased from Leo Pharma BV (Breda, the Netherlands). Isoflurane (Forane) was from Abbott Laboratories (Queenborough, Kent, UK). All other chemicals and reagents were obtained from Sigma-Aldrich (Steinheim, Germany).

Animals

Mice were housed and handled according to institutional guidelines complying with Dutch legislation. Male wild-type, *Abcb1a/1b*(-/-) (24), *Abcg2*(-/-) (25), *Abcb1a/1b;Abcg2*(-/-) (26), *Cyp3a*(-/-) and *Abcb1a/1b;Cyp3a*(-/-) (27) mice, all of a >99% FVB genetic background, were used between 8 and 14 weeks of age. Animals were kept in a temperature-controlled environment with a 12-hr light/12-hr dark cycle and received a standard diet (AM-II, Hope Farms B.V., Woerden, The Netherlands) and acidified water *ad libitum*. Mice that were fed with a semi-synthetic diet (20% casein, 4068.02; Hope Farms B.V., Woerden, The Netherlands) received this for 8 weeks prior to oral administration of everolimus.

Blood pharmacokinetics and tissue disposition of everolimus in mice

Everolimus was dissolved in ethanol:tween-80 (1:1) to obtain a concentration of 2 mg/ml and further diluted with saline to yield solutions of 0.3 mg/ml and 0.4 mg/ml for oral and intravenous administration, respectively.

To minimize variation in absorption on oral administration, mice were fasted for 3 hr before everolimus was administered by gavage into the stomach, using a blunt-ended needle. Three hours later, mice were anesthetized with isoflurane and blood was collected by cardiac puncture. Blood samples were collected in tubes containing Na_2EDTA as an anticoagulant. Immediately thereafter mice were sacrificed by cervical dislocation, and livers and brains were rapidly removed. Brains and livers were homogenized with 1 ml and 4 ml of 4% BSA, respectively and stored at -20°C until analysis.

For intravenous administration, mice were injected with a single bolus of everolimus (5 ml/kg) *via* the tail vein. One hour later, mice were anesthetized with isoflurane and blood was collected by cardiac puncture. Immediately thereafter mice were sacrificed by cervical dislocation, and livers and brains were processed as described above.

Blood cell distribution and tissue disposition of intravenous everolimus in mice

Everolimus was prepared as described above and administered intravenously to mice. At 5, 30 or 60 min after everolimus administration, mice were anesthetized and blood was collected by cardiac puncture. Immediately thereafter mice were sacrificed by cervical dislocation, and livers and brains were processed as described above. 50 µl of blood samples was transferred to new eppendorf tubes and stored at -20°C for further analysis. The remaining blood samples were immediately centrifuged at 2,100 x *g* for 6 min at 4°C, plasma and blood cell fractions were then collected and stored at -20°C for further analysis. The measured everolimus concentrations in plasma and blood cell fractions were adjusted to correspond to the ratio between plasma and red blood cells in total blood composition, which is 0.63 and 0.37, respectively.

Stability of everolimus in plasma of wild-type and knockout mice *in vitro*

Blood was freshly collected by cardiac puncture in anesthetized wild-type, *Abcb1a/1b*(-/-), *Abcg2*(-/-) and *Abcb1a/1b*;*Abcg2*(-/-) mice, followed by centrifugation at 2,100 x *g* for 6 min at 4°C for the separation of plasma from blood cells. The test was initiated by mixing 20 µl of everolimus solution with 980 µl of plasma pooled from mice of the same genotype to achieve final concentrations of 250, 1000 or 4000 ng/ml. The mixture was incubated at 37°C for 8 hr with gentle shaking. Samples (50 µl) were collected at different time points until 8 hr, and were stored frozen at -20°C until analysis.

Stability of everolimus in knockout plasma diluted with increasing amounts of wild-type plasma *in vitro*

Blood was freshly collected as described above. Pooled *Abcb1a/1b*(-/-), *Abcg2*(-/-) and *Abcb1a/1b*;*Abcg2*(-/-) plasma was diluted with increasing amounts of wild-type plasma, at dilution factors between 2 to 125-fold. Reaction was initiated by mixing 15 µl of everolimus with 735 µl of knockout plasma with or without increasing amounts of wild-type plasma. The final everolimus concentration was 4000 ng/ml and then the mixture was incubated at 37°C for 8 hr with gentle shaking. Samples (50 µl) were collected at different time points until 8 hr, and stored frozen at -20°C until analysis.

RNA isolation, cDNA synthesis and real-time RT-PCR

RNA isolation from mouse liver and subsequent cDNA synthesis and RT-PCR were performed as described (28). Specific primers (Qiagen, Hilden, Germany) were used to quantify the expression levels of the following mouse carboxylesterase genes: *Ces1b*, *Ces1c*, *Ces1d*, *Ces1e*, *Ces1f*, *Ces1g*, and *Ces2a*.

Stability of everolimus in mouse plasma preincubated with BNPP *in vitro*

Fresh plasma was obtained from wild-type, *Abcb1a/1b*(-/-), *Abcg2*(-/-) and *Abcb1a/1b;Abcg2*(-/-) mice. Experiments were carried out in 1.5 ml Eppendorf tubes at a total volume of 200 µl. For the inhibition experiment, 10 µl of BNPP stock (20 mM) was added to the reaction mixture and incubated for 15 min at 37°C with gentle shaking. After a 15-min preincubation at 37°C, the reaction was initiated by mixing 10 µl of everolimus with 190 µl of mouse plasma with or without BNPP. The final everolimus concentration was 4000 ng/ml and

the final BNPP concentration 1 mM, and then the mixture was incubated at 37°C for 8 hr with gentle shaking. Samples (30 µl) were collected at different time points until 8 hr, and stored frozen at -20°C until analysis.

Inhibitory effect of everolimus on irinotecan hydrolase activity by mouse plasma *in vitro*

The enzymatic activity of Ces1 in individual mouse plasma samples was measured using irinotecan as a substrate. Fresh plasma was obtained from wild-type, *Abcb1a/1b*(-/-), *Abcg2*(-/-) and *Abcb1a/1b;Abcg2*(-/-) mice. The hydrolysis of irinotecan was carried out in 1.5 ml Eppendorf tubes at a total volume of 150 µl. Before incubations, irinotecan at 20 mg/ml was dissolved in 20 mM Tris HCl (pH 7.8) to obtain a concentration of 50 µM. The solutions were incubated at 37°C for 30 min to achieve equilibrium between the carboxylate and lactone form of irinotecan. 15 µl of everolimus vehicle, everolimus or BNPP solution was added to the reaction mixture. The final concentrations of ethanol and tween-80 in the reaction mixture were 0.25% and 0.25%, respectively. After a 15-min preincubation at 37°C, the reaction was initiated by mixing 15 µl of irinotecan with 135 µl of mouse plasma with or without inhibitors. The final irinotecan concentration was 5 µM and then the mixture was incubated at 37°C for 30 min. The concentrations of irinotecan and SN-38 were quantified by high performance liquid chromatography.

Inhibitory effects of everolimus on *p*-nitrophenyl hydrolase activities by recombinant human CES1 and CES2 *in vitro*

For determination of the everolimus concentrations that caused 50% inhibition (IC_{50}), the *p*-nitrophenyl acetate hydrolase activities by recombinant human CES1 and CES2 were examined according to the method described previously (29).

Everolimus and metabolite analysis

Everolimus concentrations in whole blood, plasma, blood cells, brain homogenates and liver homogenates were determined using liquid chromatography coupled to tandem mass spectrometry (LC-MS/MS) in the selected reaction monitoring mode. Metabolite A was quantified semi-quantitatively. The analytical methods for everolimus and its metabolite A are described in detail in the Supplemental material

Irinotecan and SN-38 analysis

The concentrations of irinotecan and its metabolite SN-38 in plasma were analyzed by high performance liquid chromatography as described previously (30).

Statistical analysis

Data are presented as means ± SD. One-way analysis of variance (ANOVA) was used to determine the significance between groups, after which post-hoc tests with Bonferroni correction were performed for comparison between individual groups. Differences were considered statistically significant when $P < 0.05$.

RESULTS

Everolimus pharmacokinetics and tissue disposition *in vivo*

To assess the impact of Abcb1 and Abcg2 on oral bioavailability and tissue disposition of everolimus, we administered everolimus (2 mg/kg) orally or intravenously to wild-type, *Abcb1a/1b*(-/-), *Abcg2*(-/-) and *Abcb1a/1b;Abcg2*(-/-) mice, and measured blood concentrations by LC-MS/MS. 3 hr after

oral everolimus administration, 7 out of 10 wild-type mice had low whole blood levels of everolimus, while the remaining 3 wild-type mice had ~50-fold higher whole blood levels of everolimus (Figure 1A). As there were no wild-type mice that had intermediate blood everolimus levels, they fell into two clearly distinct groups. Also in later experiments we often observed that a variable, but usually minor fraction of wild-type mice displayed much higher everolimus blood levels. As explained later, we therefore separately present data for the "low" and "high" everolimus wild-type mice, in cases where the latter were present. Coincidentally, no "high" everolimus wild-type mice were present in the parallel experiment, where blood and tissue levels were assessed 1 hr after intravenous everolimus administration at 2 mg/kg (Figure 1B). Everolimus blood levels in all the knockout strains were ~80-fold higher than those in the "low" wild-type mice upon oral administration, and ~16-fold higher upon i.v. administration.

Surprisingly, in spite of the large differences in blood everolimus levels, the liver concentrations in wild-type (low and high) and knockout strains were quite similar, regardless of the route of administration (Figure 1C and D). These findings suggested that some factors affecting the blood-tissue distribution behavior of everolimus had drastically changed in the knockout strains, and likely also in the "high" wild-type mice, relative to the "low" wild-type mice.

To correct for a possibly altered blood-tissue distribution behavior of everolimus, when assessing brain accumulation of everolimus in the different strains, we plotted both the direct brain concentrations (Figure 1E and F), and the brain-to-liver concentration ratios (Figure 1G and H), rather than the more commonly used brain-to-blood concentration ratios. The brain-to-liver concentration ratios suggested that *Abcb1a/1b*(-/-) and *Abcb1a/1b;Abcg2*(-/-) mice had 10-14-fold increased brain accumulation of everolimus relative to wild-type mice (both "low" and "high", $P < 0.001$), whereas *Abcg2*(-/-) mice had ~3-fold increased brain accumulation ($P < 0.05$) upon oral administration (Figure 1G). Interestingly, despite the 50-fold higher blood concentration of everolimus in the "high" versus "low" wild-type mice, brain concentrations and brain-to-liver ratios between these groups were not significantly different (Figure 1E and G). Upon i.v. administration, brain-to-liver ratios were ~8-fold increased in both Abcb1-deficient strains ($P < 0.001$), and not altered in the *Abcg2*(-/-) strain (Figure 1H). Collectively, the data suggest that Abcb1 strongly restricts the brain accumulation of everolimus, whereas Abcg2 has little, if any, impact on brain accumulation of everolimus (the latter in view of the absence of an additional effect of the combination knockout versus the single Abcb1a/1b knockout). The first observation would be in line with the previous demonstration that everolimus is transported *in vitro* by ABCB1 (20).

Semi-synthetic diet does not prevent altered everolimus pharmacokinetics

We previously found in *Cyp3a*(-/-) mice that altered pharmacokinetics of some drugs was due to upregulation of some detoxifying proteins relative to wild-type mice by inducing compounds present in the diet, and that this upregulation could be reversed by feeding with a semi-synthetic diet (31). To test whether

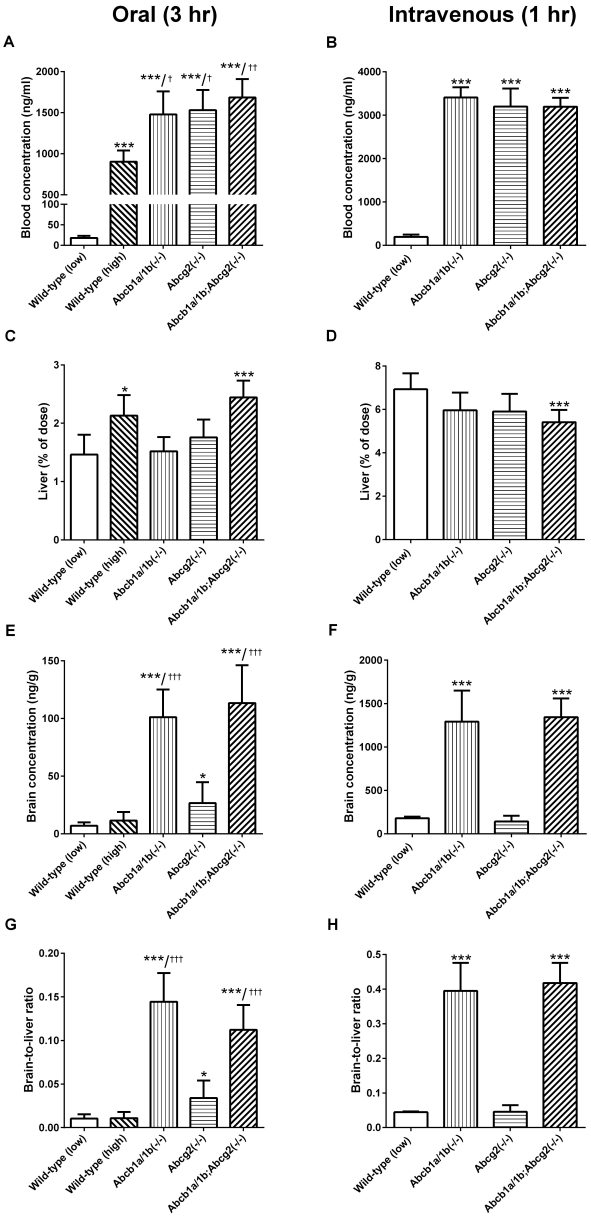

Figure 1. Blood pharmacokinetics and tissue disposition of everolimus. Blood concentration (ng/ml; A and B), liver accumulation (% of dose; C and D), brain concentration (ng/g; E and F) and brain-to-liver concentration ratio (G and H) of everolimus in male wild-type, *Abcb1a/1b*(-/-), *Abcg2*(-/-) and *Abcb1a/1b;Abcg2*(-/-) mice 3 hr after oral (left panels) or 1 hr after intravenous (right panels) administration of 2 mg/kg everolimus. All data are presented as mean ± SD (n = 3-7; *, $P < 0.05$; ***, $P < 0.001$ when compared with wild-type mice with low everolimus blood levels; †, $P < 0.05$; ††, $P < 0.01$; †††, $P < 0.001$ when compared with wild-type mice with high everolimus blood levels). 1% of doses for liver are 452 ng/g and 562 ng/g for oral and intravenous administration, respectively.

a similar process might be responsible for the altered everolimus pharmacokinetics in wild-type, *Abcb1a/1b*(-/-), *Abcg2*(-/-) and *Abcb1a/1b*;*Abcg2*(-/-) mice, we fed a cohort of these mice a semi-synthetic diet for 8 weeks, and assessed oral everolimus blood pharmacokinetics. However, data for the standard- and semi-synthetic-diet fed mice were virtually superimposable, except for a few "high" wild-type mice that were present in the semi-synthetic diet group (Supplementary Data 2A and B). This suggested that diet is not a determining factor of the altered everolimus pharmacokinetics in these knockout strains.

Blood cell distribution and tissue disposition of everolimus *in vivo*

The incongruous blood concentration and liver (plus brain) accumulation data of everolimus suggested that there might be some strong everolimus retention factors present in the blood of the knockout strains, and presumably also the "high" wild-type mice. Since everolimus in blood can sometimes distribute very extensively to red blood cells (e.g., ~80% in humans) (32), we assessed the *in vivo* plasma to blood-cells distribution of everolimus in the different strains, as well as the liver and brain accumulation, at 5, 30, and 60 min after i.v. administration of everolimus at 2 mg/kg (Figure 2). We again observed "low" and "high" wild-type mice in the 5 min and 60 min (but not the 30 min) groups (Figure 2A and B), and while there was an obvious (and significant) everolimus clearance observed in blood and plasma of the "low" wild-type mice between 5 and 60 min (3- to 4-fold decrease), this was not seen in any of the other strains. As observed before, blood levels of everolimus were greatly and similarly increased in all the knockout strains. Importantly, there was only little distribution of everolimus to the blood cells relative to whole blood and plasma, ranging from about 6% in the "low" wild-type mice to well below 2% in all the knockout strains (Figure 2C and D). Altered retention in blood cells could therefore not explain the observed marked alterations in total blood levels of everolimus. Liver and brain accumulation in this experiment (Figure 2E-H) were in line with the patterns observed in the experiments of Figure 1. It is noteworthy that in all strains a substantial fraction (~30% of the dose) of everolimus had accumulated in the liver within 5 min after administration, which was subsequently gradually cleared at similar rates (Figure 1F).

The higher blood cell-to-blood ratios in the "low" wild-type mice versus all the knockout strains and the "high" wild-type mice (Figure 2D) suggested that there might be more retention of everolimus in the plasma of the latter strains. Strong plasma retention of everolimus might also explain why there was very little if any clearance of everolimus from plasma in the knockout strains between 5 and 60 min after i.v. administration (Figure 2A and B). Of note, at 4000 ng/ml, a substantial fraction (~10%) of the administered everolimus dose was retained in the plasma.

Stability of everolimus in plasma of wild-type and knockout mice *in vitro*

Attempts to assess *in vitro* whether knockout and wild-type plasma had different levels of free and (protein-)bound amounts of everolimus were compromised by the rapid disappearance of everolimus from wild-type plasma (data not shown). Indeed,

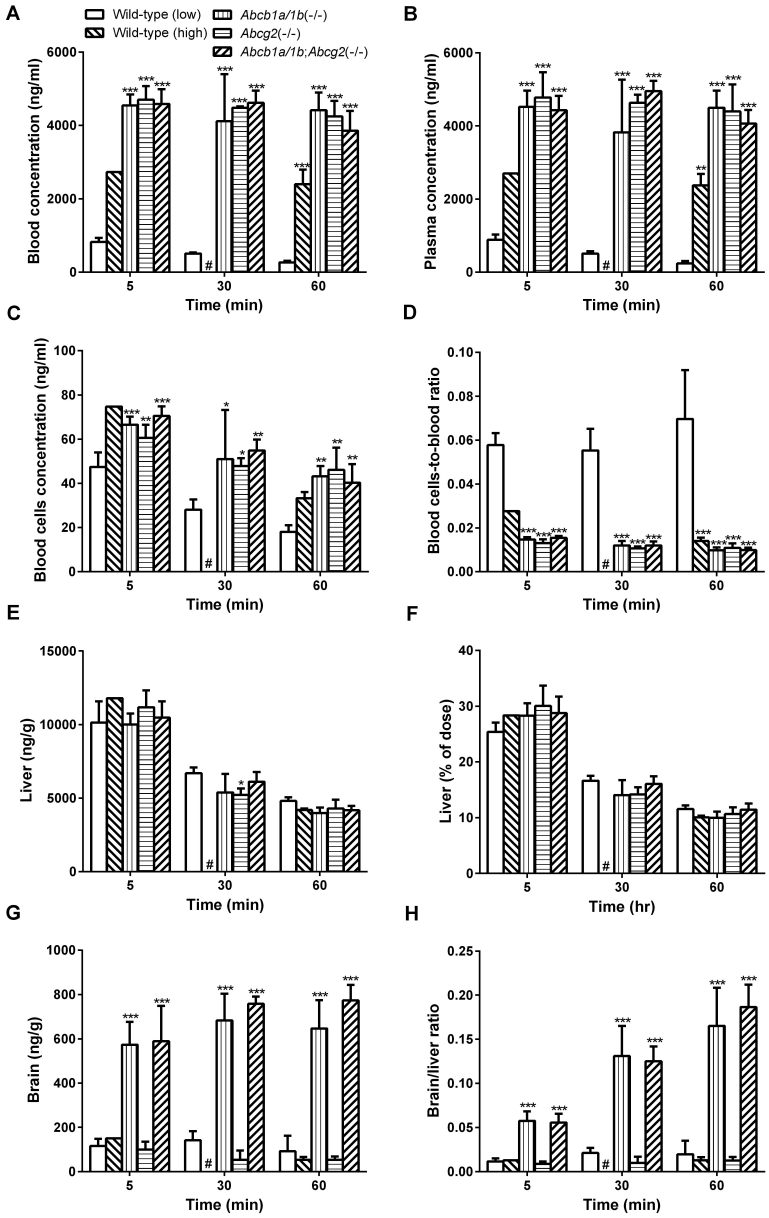

Figure 2. Blood, blood cell, and plasma distribution and tissue disposition of everolimus *in vivo*. Blood concentrations (ng/ml; A), plasma concentrations (ng/ml; B), blood cells concentrations (ng/ml; C), blood cells-to-blood ratio (D), liver concentration (ng/g; E), liver accumulation (% of dose; F), brain concentration (ng/g; G) and brain-to-liver ratio (H) of everolimus in male wild-type, *Abcb1a/1b*(-/-), *Abcg2*(-/-) and *Abcb1a/1b;Abcg2*(-/-) mice at 5, 30 or 60 min after intravenous administration of 2 mg/kg everolimus. All data are presented as mean ± SD (n = 1-5; *, $P < 0.05$; **, $P < 0.01$; ***, $P < 0.001$ when compared with wild-type mice with low everolimus blood levels; ††, $P < 0.01$; †††, $P < 0.001$ when compared with wild-type mice with high everolimus blood levels).

a possible cause of the very different blood and plasma levels of everolimus might be greater stability of everolimus in the plasma of the knockout strains relative to the ("low") wild-type mice. To assess this further, we incubated various concentrations of everolimus spiked into plasma of the different strains *in vitro*, roughly covering the range of concentrations observed in Figure 2B, at 37°C, and measured presence of everolimus over time. A parallel incubation in saline demonstrated that everolimus itself was quite stable at all concentrations (not shown). Interestingly, whereas there was very limited loss of everolimus at 250 ng/ml in plasma of all strains, at 4000 ng/ml there was marked loss in the wild-type plasma but not in the knockout plasmas. At 1000 ng/ml an intermediate pattern was observed (Figure 3A-C).

The stability of everolimus in wild-type plasma at low concentrations and its relative instability at high concentrations made it likely that there was a stabilizing protein present in the plasma that fully protected low amounts of everolimus. Upon saturation of this stabilizing protein with higher concentrations, more free everolimus existed, that was degraded in wild-type plasma, most likely by an as yet unidentified plasma enzyme. The results of figure 3A-C would best be explained by a much higher level of the stabilizing protein in the knockout plasmas than in the wild-type plasma, whereas the level of the everolimus-degrading enzyme might be similar between the strains. However, it was theoretically also possible that wild-type plasma had much higher levels of the everolimus-degrading plasma enzyme, whereas all the strains had similar (low) levels of everolimus-stabilizing protein. To discriminate between these two possibilities, we repeated the everolimus stability experiment at 4000 ng/ml with mixtures at various ratios of wild-type and knockout plasmas. In case of much higher concentrations of an everolimus-degrading enzyme in wild-type plasma, the prediction is that a 1 to 1 (i.e., 2-fold) dilution of wild-type plasma with knockout plasma should result in a degradation (loss) rate of everolimus that is about half the loss rate in wild-type plasma (half the amount of degrading enzyme, therefore half the rate of everolimus loss). The results of Figure 3D-F show that everolimus loss was somewhat increased in the 2-fold dilution mixtures compared to undiluted knockout plasma, but still clearly lower than half the everolimus loss rate seen in undiluted wild-type plasma. Only when knockout plasma was between 5- and 25-fold diluted with wild-type plasma did the everolimus loss rates approach that seen in undiluted wild-type plasma. These results are therefore more compatible with strong upregulation of an everolimus-stabilizing protein in the knockout plasmas, than with strong downregulation of an everolimus-degrading protein in the knockout plasmas relative to wild-type plasma.

Indirect information on the presumed everolimus-degrading activity in plasma came from the detection in the *in vitro* plasma incubations of Figure 3D-F of a prominent everolimus metabolite, metabolite A, especially in wild-type plasma (Figure 3G-I). Based on LC-MS/MS detection properties, metabolite A had the same mass over charge ratio as everolimus itself, but an apparently opened ring structure (data not shown). The absolute amount of metabolite A could not be determined in the absence of knowledge

of its exact structure and a suitable internal standard, but assuming that the LC-MS/MS signal strength is similar to that of everolimus itself, a substantial fraction (~50%) of everolimus was converted to metabolite A in undiluted wild-type plasma (Figure 3D-I). As was seen with the disappearance rate of everolimus, the formation rate of metabolite A was much more than 2-fold decreased in the 2-fold diluted wild-type plasmas (Figure 3G-I). In fact, the metabolite A formation rate was already about 2-fold reduced in a mixture of 80% wild-type plasma and 20% of *Abcb1a/1b*(-/-) plasma (5-fold dilution, Figure 3G). This again testifies to the likelihood that upregulation of an everolimus-stabilizing

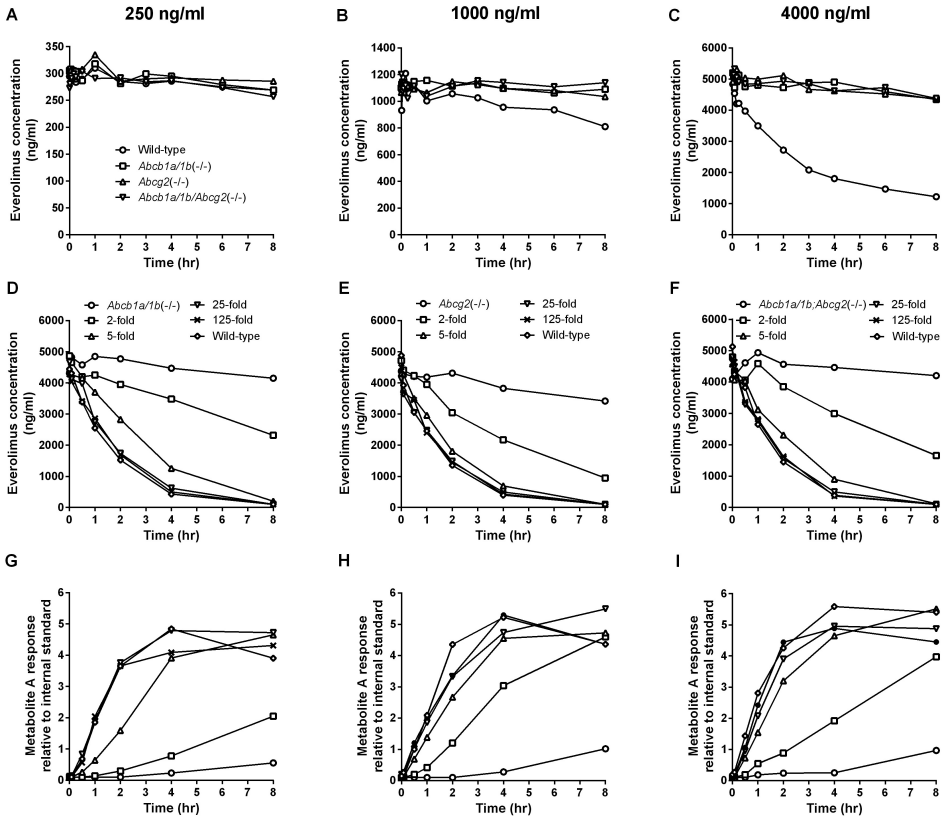

Figure 3. Stability of everolimus in plasma of wild-type and knockout mice *in vitro*. A-C, concentration-time curves of everolimus in wild-type, *Abcb1a/1b*(-/-), *Abcg2*(-/-) and *Abcb1a/1b;Abcg2*(-/-) plasma after incubation of 250 ng/ml (A), 1000 ng/ml (B) or 4000 ng/ml (C) spiked everolimus. D-I, stability of everolimus in knockout mouse plasmas diluted with increasing amounts of wild-type plasma *in vitro*. Concentration-time curves of everolimus (ng/ml, D-F) and metabolite A (response relative to internal standard, G-I) after incubation of 4000 ng/ml everolimus in *Abcb1a/1b*(-/-) (D and G), *Abcg2*(-/-) (E and H) and *Abcb1a/1b;Abcg2*(-/-) (F and I) pooled plasma diluted with increasing amounts of pooled wild-type plasma. Values below lower limit of quantifications were replaced with 100 ng/ml and 0.1 response relative to internal standard for everolimus and metabolite A, respectively. Each data point represents a single determination.

protein in the knockout plasmas was responsible for the observed changes, although it should be considered that metabolite A may be further metabolized, thus complicating interpretation of its appearance profile.

Increased levels of an everolimus-stabilizing (and thus presumably everolimus-binding) protein in the knockout plasmas would likely also cause increased plasma retention of everolimus, and much reduced levels of free everolimus relative to the total blood concentrations of everolimus. This would be compatible with the much reduced blood-to-tissue distribution of everolimus seen in the knockout strains in the pharmacokinetic experiments (Figure 1), and with the reduced blood cells-to-blood ratios in the knockout strains (Figure 2A-D) compared to ("low") wild-type mice. Collectively, our data suggest that everolimus in plasma of knockout strains is protected from degradation by an everolimus-binding protein.

Liver expression of *Ces1* genes is highly upregulated in *Abcb1a/1b*(-/-), *Abcg2*(-/-) and *Abcb1a/1b;Abcg2*(-/-) mice

While trying to identify the nature of the putative everolimus-stabilizing protein in plasma of the knockout strains, we discovered in an independent study that a range of carboxylesterase enzymes was highly upregulated in, amongst others, *Abcb1a/1b*(-/-) mice (28). As some carboxylesterases synthesized in the liver can be abundant in mouse plasma, we hypothesized that perhaps one or more of these plasma carboxylesterases could tightly bind everolimus, possibly by recognizing (but not hydrolyzing) the lactone ring-internal carboxylester bond present in everolimus (see Supplementary Figure 1), leading to a tight but non-processive protein-substrate complex. We therefore first tested the RNA expression levels of the main mouse *Ces* genes expressed in the liver, i.e. *Ces1b*-*Ces1g* and *Ces2a*, in wild-type, *Abcb1a/1b*(-/-), *Abcg2*(-/-) and *Abcb1a/1b;Abcg2*(-/-) mice using RT-PCR. Interestingly, *Ces1b* was about 8- to 10-fold upregulated, and *Ces1c* about 70-fold upregulated in all the knockout strains (Supplementary Data 3). The basal expression of *Ces1d* was virtually undetectable in male wild-type liver (in contrast to female wild-type liver) (28), leading to nominally ~40,000-fold upregulation in all the knockout strains (Supplementary Data 3), but the observed deltaCt values were in the same order as for the other upregulated *Ces1* genes, suggesting that the final expression levels were not extremely high (Supplementary Table 1). *Ces1e* was 3- to 6-fold upregulated, whereas *Ces1f*, *Ces1g* and *Ces2a* were not upregulated, and perhaps sometimes even downregulated (Supplementary Data 3). It was further striking that, parallel to the everolimus pharmacokinetic data, there was one "high" *Ces1* wild-type mouse, which consistently displayed clearly increased expression levels of *Ces1b*, *Ces1c*, *Ces1d* and *Ces1e* relative to the 2 "low" *Ces1* wild-type mice, albeit not completely up to the level of the knockout strains (Supplementary Data 3).

Of the upregulated Ces1 proteins, only Ces1b and Ces1c are lacking the ER retention signal that prevents secretion of the proteins from the liver into plasma, and are thus likely to occur in plasma. As Ces1b is hardly expressed in mouse liver (33, 34), the substantially expressed carboxylesterase

Ces1c is by far the most likely candidate everolimus-binding protein in plasma. Of note, a range of other esterases, including Ces2e, Ces3a, Aadac, and Pon1, 2, and 3, were previously shown not to be upregulated in *Abcb1a/1b*(-/-) mice (28), and thus unlikely to be involved in everolimus protection in the knockout strains studied here.

The carboxylesterase inhibitor BNPP reverses stabilization of everolimus in mouse plasma

To provide more direct evidence that plasma carboxylesterase is responsible for protecting everolimus from degradation in knockout plasma, we tested whether the stabilization of everolimus could be reversed using the carboxylesterase inhibitor BNPP. This organophosphate acts as an irreversible inhibitor of carboxylesterases through the generation of a stable phosphate ester covalently attached to the catalytic serine residue in the enzyme active site (35). If everolimus normally binds to the substrate binding site of carboxylesterase, one would expect it to be displaced by the presence of BNPP. We therefore preincubated BNPP (1 mM) for 15 min *in vitro* with individual plasmas freshly collected from wild-type, *Abcb1a/1b*(-/-), *Abcg2*(-/-) and *Abcb1a/1b*;*Abcg2*(-/-) mice, and measured disappearance of spiked everolimus (4000 ng/ml) over time. In the absence of BNPP, everolimus was rapidly decreased in 3 of 5 ("low") wild-type plasmas, whereas everolimus concentrations remained similar over time in 2 of 5 ("high") wild-type plasmas and all knockout plasmas (Figure 4A). After preincubation with BNPP, however, all knockout plasmas and the "high" wild-type plasmas displayed similar rapid degradation profiles as seen in the "low" wild-type plasma without or with BNPP preincubation (Figure 4B). These results strongly suggest that upregulated carboxylesterases in the knockout and 2 "high" wild-type plasmas are responsible for stabilizing everolimus. Moreover, the similarity in everolimus degradation rates between all the strains in the presence of BNPP indicates that there were no pronounced differences in the plasma everolimus-degrading activity between the strains. *Ces* expression analysis of livers of the individual mice tested in this experiment confirmed that the "high" wild-type mice had marked upregulation of *Ces1b-e* relative to the "low" wild-type mice, and that this upregulation approached the levels seen in the knockout strains (Figure 4C-F and Supplementary Table 2).

Everolimus inhibits the conversion of irinotecan to SN-38 by carboxylesterase 1c in knockout plasma

If everolimus binds tightly to the active site of plasma carboxylesterase, it might also inhibit the hydrolytic activity towards carboxylesterase substrates. The anticancer prodrug irinotecan is hydrolyzed to its active derivative SN-38 primarily by plasma Ces1c in mice (36). We therefore tested the conversion of spiked irinotecan (5 μM) to SN-38 in individual wild-type and knockout plasmas in a 30 min *in vitro* incubation, and the effect of preincubation of these plasmas with everolimus (100 μM). Without inhibitors, we observed very little disappearance of irinotecan in all wild-type plasmas, *versus* almost complete hydrolysis of irinotecan in all knockout plasmas (Figure 5A). This was confirmed by very low production of SN-38 in wild-type plasma, and very extensive formation of SN-38 in all the knockout

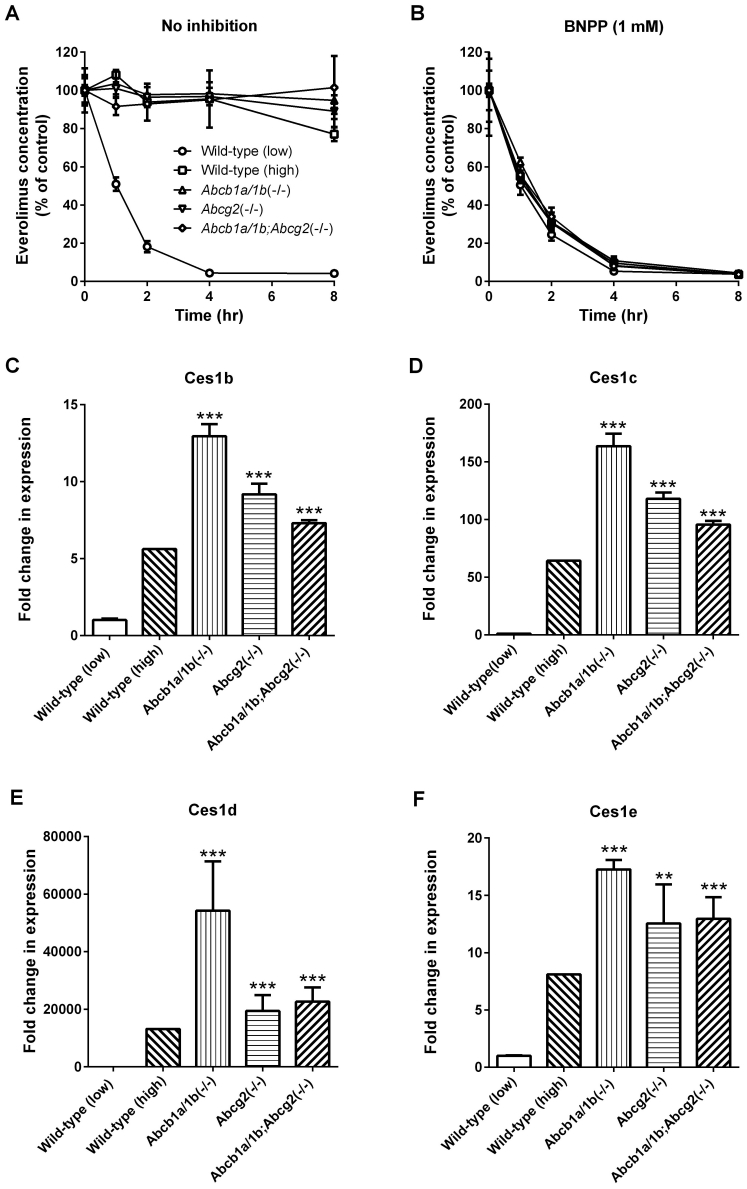

Figure 4. Stability of everolimus in mouse plasma after preincubation with the irreversible CES inhibitor BNPP *in vitro*. Concentration of everolimus (% of control) after incubation of 4000 ng/ml everolimus spiked into wild-type, *Abcb1a/1b*(-/-), *Abcg2*(-/-) and *Abcb1a/1b;Abcg2*(-/-) plasma either without (A), or with 1 mM BNPP pretreatment (B). All data are presented as mean ± SD (n = 2-3). Expression levels of Ces1b (C), Ces1c (D), Ces1d (E) or Ces1e (F) mRNA in livers of wild-type, *Abcb1a/1b*(-/-), *Abcg2*(-/-) and *Abcb1a/1b;Abcg2*(-/-) mice used in the stability experiment, as determined by real-time RT-PCR. Data are normalized to GAPDH expression. Values represent mean fold change ± SD, compared to wild-type mice with low Ces expression (n = 2-5; *, $P < 0.05$; **, $P < 0.01$; ***, $P < 0.001$ when compared with wild-type mice with low plasma everolimus levels).

plasmas (Figure 5B). The hydrolase activity towards irinotecan in knockout plasmas was at most weakly inhibited by the everolimus vehicle (0.25% ethanol and 0.25% polysorbate 80) (Figure 5A and B). Interestingly, the irinotecan hydrolase activity in all knockout plasmas was strongly inhibited by both everolimus and the positive control inhibitor BNPP (Figure 5A and B). These results indicate that there is highly increased hydrolysis of irinotecan in knockout plasmas, most likely due to the highly upregulated Ces1c, and that preincubation with everolimus could effectively inhibit this hydrolase activity. This strongly supports that everolimus binds to plasma carboxylesterase 1c, and most likely to its active site.

Everolimus inhibits hydrolysis by recombinant human CES1 and CES2 *in vitro*

Although there are no straightforward orthologues between the mouse Ces1 and Ces2 family members and the human CES1 and CES2 enzymes, and substrate and inhibitor specificity can differ quite widely between the species, we tested the inhibitory effect of everolimus at various concentrations on the *p*-nitrophenyl acetate hydrolase activity of recombinant human CES1 and CES2. The *p*-nitrophenyl acetate hydrolase activity was measured at a substrate concentration of 100 μM, similar to the K_m values of recombinant CES1 and CES2 (37). Everolimus inhibited both enzymes, albeit with relatively high IC_{50} values of 157.2 μM and 19.4 μM for CES1 and CES2, respectively (Figure 6). These results indicate that everolimus is a better inhibitor of human CES2 than CES1 *in vitro*.

Cyp3a, but not Abcb1, limits the oral availability of everolimus in mice

Having identified the complications caused by carboxylesterase upregulation and everolimus binding in the wild-type and knockout mouse strains, we could interpret an experiment aiming to assess the impact of Abcb1 and

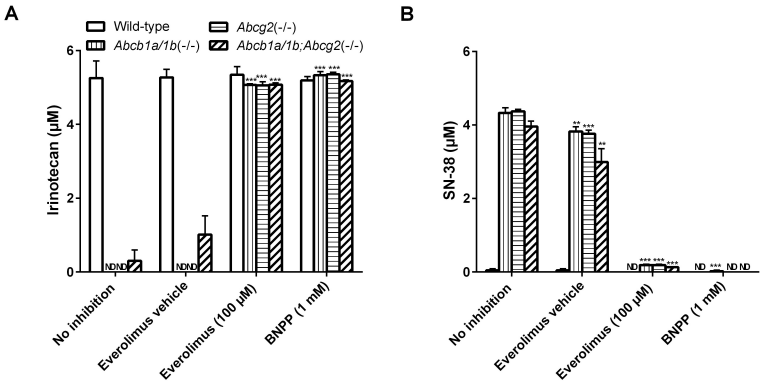

Figure 5. Inhibitory effect of everolimus on the conversion of irinotecan to SN-38 by Ces1c in wild-type and knockout mouse plasmas *in vitro*. Concentrations of irinotecan (A) and SN-38 (B) in wild-type, *Abcb1a/1b*(-/-), *Abcg2*(-/-) and *Abcb1a/1b;Abcg2*(-/-) individual plasmas 30 min after spiking with 5 μM irinotecan. All data are presented as mean ± SD (n = 3-5; *, $P < 0.05$; **, $P < 0.01$; ***, $P < 0.001$ when compared with plasmas of the same genotype without inhibitor). ND, not detectable; detection limits were 0.0148 μM and 0.0026 μM for irinotecan and SN-38, respectively.

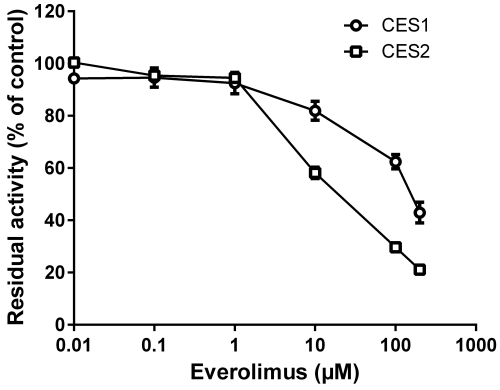

Figure 6. Inhibitory effect of everolimus on hydrolase activities by recombinant human CES1 and CES2 *in vitro*. The activities were determined at 100 μM *p*-nitrophenyl acetate substrate concentrations. Each data point represents the mean of triplicate determinations. The control activities by recombinant CES1 and CES2 were 542 and 300 nmol/min/mg, respectively.

CYP3A on the oral availability of everolimus in mice. Everolimus was orally administered at 2 mg/kg to wild-type and Abcb1a/1b, Cyp3a and combination Abcb1a/1b/Cyp3a knockout strains, and whole blood everolimus concentrations were assessed over a 24 hr period (Supplementary Data 4). Also in this experiment we observed a "low" (n = 3) and "high" (n = 2) wild-type group, most likely due to upregulation of plasma Ces in the "high" group, analogous to the observations in Figure 1A. Importantly, the Abcb1a/1b knockout did not result in a significant increase in oral AUC relative to the "high" wild-type group (Supplementary Data 4 and Supplementary Table 3). Considering the high upregulation of plasma Ces in both mouse groups, this indicates that Abcb1 has little impact on the oral availability of everolimus at this dosage. *Cyp3a*(-/-) mice, however, which have a similar level of hepatic *Ces1* upregulation as *Abcb1a/1b*(-/-) mice (28), did have a highly significant 7.8-fold higher everolimus blood AUC than the "high" wild-type group, indicating that Cyp3a markedly restricts the oral availability of everolimus (Supplementary Data 4, Supplementary Table 3). Additional knockout of *Abcb1a/1b* in *Abcb1a/1b;Cyp3a*(-/-) mice did not result in a further increase in blood AUC, consistent with the absence of a marked effect of Abcb1a/1b on everolimus oral availability.

The slow but gradual clearance of everolimus from blood in the *Abcb1a/1b*(-/-) mice indicates that everolimus is still gradually released from plasma Ces1c (Supplementary Data 4). The fact that everolimus blood clearance in *Cyp3a*(-/-) mice, with similar levels of Ces1c upregulation, was even slower suggests that Cyp3a contributes significantly to the overall everolimus clearance process from the body.

DISCUSSION

This study showed that Abcb1a/1b markedly reduces the brain accumulation, but not the oral availability of everolimus. Abcg2 does not seem to affect either oral availability or brain

accumulation of this drug. Cyp3a, however, markedly reduced the oral availability of everolimus. Most remarkable was the pronounced effect that upregulation of plasma Ces1c had on the plasma pharmacokinetics of everolimus in knockout and "high" wild-type strains. All data indicate that everolimus binds tightly to plasma Ces1c, and that this binding largely prevents degradation of everolimus by another plasma protein, and strongly reduces overall blood clearance of everolimus. Everolimus was also found to be an inhibitor of human CES1 and especially CES2.

Although we have described before that plasma Ces enzymes can be upregulated in some knockout strains, with obvious consequences for drugs hydrolyzed by these enzymes (28), we had not anticipated that strong binding of otherwise unhydrolyzed drugs to these enzymes might have such pronounced effects on blood pharmacokinetics. Since there may be many other drugs that can be bound but not hydrolyzed by these multispecific enzymes, this is a potential source of complications that should be considered in future studies with these knockout strains. Note that not all knockout strains for detoxifying proteins display hepatic *Ces1* upregulation: based on RT-PCR data, similar levels of *Ces1b-e* upregulation have been observed in *Abcb1a/1b*, *Abcg2*, and *Cyp3a* knockout strains and various combinations thereof (28 and the present study). However, *Abcc2* and *Abcc3* knockout strains do not show altered everolimus blood pharmacokinetics (data not shown), and are thus unlikely to have upregulated Ces1c.

The mechanism behind the upregulation of the *Ces1b-e* genes is currently unknown. The similarity in the upregulation profiles of these genes between the different knockout mouse strains suggests that there is some shared induction mechanism between the genes. Our observation that a semi-synthetic diet does not affect the Ces1 upregulation (as judged by everolimus blood pharmacokinetics) in the various transporter knockout strains (Supplementary Data 2) makes it less likely that altered exposure to some dietary xenobiotic is directly responsible. It might therefore be that some endogenous inducers are responsible, or possibly signaling pathways activated by xenotoxins derived from the intestinal microflora, but their nature remains speculative.

The observation that some wild-type mice display very similar, albeit slightly lower, upregulation of the same group of Ces1 genes is also puzzling (genotypes of "high" wild-type mice were double-checked). There were no obvious external clues to which wild-type mice displayed a "high" or "low" everolimus or Ces1 phenotype, and it varied also among siblings from one litter. We do not currently understand the mechanistic cause of Ces1 upregulation in wild-type mice. There were no intermediate Ces1c expression levels observed in wild-type mice, suggesting either that Ces1 upregulation is a fixed situation in individual wild-type mice, or that a switch from "low" to "high" Ces1 expression (or *vice versa*) occurs abruptly.

Whatever the mechanistic cause, it is clear that the endogenous variation in Ces1 expression in wild-type mice will complicate pharmacokinetic analyses for any drug that is hydrolyzed or bound by the upregulated Ces enzymes. For instance, oral everolimus pharmacokinetics in nude female BALB/c mice (32) show everolimus blood levels that are compatible with the levels in our wild-type FVB "high" mice, but not the "low"

mice. This suggests that the tested strain had constitutively "high" plasma Ces1 levels. This could also explain the extremely high plasma protein binding (99.9%) of everolimus reported for this mouse strain, as opposed to 92% in rats and 75% in humans. To test whether the "nude" mutation might be responsible for this presumed Ces1 upregulation, we tested FVB nude "wild-type" and *Abcb1a/1b*(-/-) and *Abcb1a/1b;Abcg2*(-/-) mice, but found similar low wild-type and high knockout *Ces1* expression in liver as in the normal FVB background (data not shown).

The prolonged retention of everolimus in blood and plasma of mice with high Ces1 plasma levels suggests a much reduced blood-to-tissue distribution of everolimus. However, our data indicate that, apart from the fraction of everolimus that is tightly bound to plasma Ces (~5% of the dose after oral, and ~10% of the dose after i.v. administration in Ces upregulated mice), there is also a "free" fraction of the drug in blood. The concentration of this free fraction does not seem to differ much between all the mouse strains, judging from the similar levels of liver accumulation between the knockout strains and the "low" and "high" wild-type mice, at least during the first few hours (Figure 1). Thus, although a significant fraction of everolimus is rapidly and tightly bound to plasma Ces1, the remainder (90-95% of the dose) seems to be more or less normally available for distribution. The overall impact of plasma binding of everolimus on tissue distribution of the drug is therefore limited, at least during the first few hours, and at the dosage tested.

The nature of the plasma enzyme that converts everolimus to its main metabolite A is unknown. Previous studies have established that human liver microsomes in both the absence and presence of NADPH convert everolimus to a lactone ring-opened product that is subsequently dehydrated to its seco acid (38). The responsible enzyme is thus not a P450. A plasma-localized mouse pendant of this enzyme might be responsible for the disappearance of free everolimus in mouse plasma. Its potential activity towards everolimus when Ces1c was blocked by BNPP appeared not to differ between all the wild-type and knockout mouse strains tested (Figure 4B). Of note, also in human plasma ring-opened everolimus metabolites predominate, suggesting that similar enzymes occur in human plasma (FDA application 21-560s000).

Everolimus showed higher inhibitory effect towards human CES2 than towards human CES1. A possible explanation of this difference could be size-limited access of the bulky everolimus, as the active site of CES1 is smaller than that of CES2 (39). The inhibitory effects of everolimus were also different between human CES1 and mouse Ces1c, possibly reflecting a similar size-access difference, although little is known about Ces1c structure. Species differences in inhibitor sensitivity between human and rat liver Ces have been demonstrated by Takahashi *et al*. (2009) (40).

The profound plasma carboxylesterase binding of everolimus we observed in mice is unlikely to play a role in humans as, unlike mouse Ces1c, human CES1 or CES2 are not normally substantially present in plasma (41). Also the inhibitory activity of everolimus towards human CES1 and CES2 is not very high, suggesting that it may bind less tightly to these proteins than to mouse Ces1c. However, inhibition of the hepatic

CES1 and especially CES2, which is primarily found in the intestine, by everolimus might play a role in drug-drug interactions with coadministered drugs. CES1 and CES2 hydrolyze many drugs and prodrugs (35). Upon oral everolimus administration local concentrations of everolimus might be high especially in the intestine, and possibly surpass the Ki of ~20 μM towards CES2. CES2 is for instance thought to be a main enzyme responsible for the conversion of irinotecan to SN-38 in humans (42), and for hydrolysis of a prodrug of gemcitabine (43). Coadministration of everolimus with ester (pro-)drugs affected by carboxylesterases, including the 5-FU anticancer prodrug capecitabine (44), should thus be assessed very carefully.

The limited brain accumulation of everolimus due to the activity of ABCB1 may restrict the therapeutic efficacy of everolimus towards brain tumor parts or (micro-)metastases that are effectively situated behind a functional blood-brain barrier. As we and others have shown before for many other drugs, it is very likely that this limited accumulation could be improved by coadministration of an effective ABCB1 inhibitor such as elacridar (16). Abcg2, in contrast, appeared to have little impact on brain accumulation of everolimus. ABCB1 itself also did not appear to have much impact on the oral availability of everolimus, when taking plasma Ces upregulation into account. This is a common observation for many ABCB1 substrates, which often display strong effects on brain accumulation, but little effect on oral availability. Given the complications of plasma carboxylesterase upregulation, we think that the small (1.3-fold) reported effect of ABCB1 on low-dose everolimus oral availability assessed with *Abcb1a/1b*(-/-) mice (22) should be interpreted with caution.

Keeping the complications of plasma Ces1 upregulation in mind, it seems clear that mouse Cyp3a can considerably reduce the oral availability of everolimus (Supplementary Data 4 and Supplementary Table 3). This is consistent with the demonstrated metabolism of everolimus by recombinant human CYP3A4, CYP3A5 and CYP2C8 *in vitro*, with CYP3A4 being the major enzyme involved in everolimus metabolism (45). Moreover, drug-drug interaction studies with various CYP3A inhibiting drugs further support that CYP3A is a major factor in the *in vivo* clearance of everolimus (FDA application 21-560s000). Accordingly, great caution is advised in the clinical co-application of everolimus with drugs that affect CYP3A activity.

Conflicts of Interest

The group of A.H.S. receives revenue from the commercial distribution of some of the mouse strains used in the study. The authors declare no other potential conflicts of interest.

Acknowledgements

An academic staff training scheme fellowship from the Malaysian Ministry of Higher Education to S.C.T. This work was supported in part by Dutch Cancer Society grant 2007-3764. We thank Dilek Iusuf, Fan Lin and Olaf van Tellingen for their assistance with high performance liquid chromatography analysis of irinotecan and SN-38. We thank Selvi Durmus and Dilek Iusuf for critical reading of the manuscript.

REFERENCES

1. Abraham RT, Eng CH. Mammalian target of rapamycin as a therapeutic target in oncology. Expert Opin Ther Targets 2008;12:209-22.
2. Manning BD, Tee AR, Logsdon MN, Blenis J, Cantley LC. Identification of the tuberous sclerosis complex-2 tumor suppressor gene product tuberin as a target of the phosphoinositide 3-kinase/akt pathway. Mol Cell 2002;10:151-62.
3. Engelman JA, Luo J, Cantley LC. The evolution of phosphatidylinositol 3-kinases as regulators of growth and metabolism. Nat Rev Genet 2006;7:606-19.
4. Wullschleger S, Loewith R, Hall MN. TOR signaling in growth and metabolism. Cell 2006;124:471-84.
5. Carracedo A, Pandolfi PP. The PTEN-PI3K pathway: of feedbacks and cross-talks. Oncogene 2008;27:5527-41.
6. Inoki K, Corradetti MN, Guan KL. Dysregulation of the TSC-mTOR pathway in human disease. Nat Genet 2005;37:19-24.
7. Yuan TL, Cantley LC. PI3K pathway alterations in cancer: variations on a theme. Oncogene 2008;27:5497-510.
8. Yuan R, Kay A, Berg WJ, Lebwohl D. Targeting tumorigenesis: development and use of mTOR inhibitors in cancer therapy. J Hematol Oncol 2009;2:45.
9. Krueger DA, Care MM, Holland K, Agricola K, Tudor C, Mangeshkar P et al. Everolimus for subependymal giant-cell astrocytomas in tuberous sclerosis. N Engl J Med 2010;363:1801-11.
10. Yao JC, Shah MH, Ito T, Bohas CL, Wolin EM, Van Cutsem E et al. Everolimus for advanced pancreatic neuroendocrine tumors. N Engl J Med 2011;364:514-23.
11. Baselga J, Campone M, Piccart M, Burris HA, III, Rugo HS, Sahmoud T et al. Everolimus in postmenopausal hormone-receptor-positive advanced breast cancer. N Engl J Med 2012;366:520-9.
12. Goudar RK, Shi Q, Hjelmeland MD, Keir ST, McLendon RE, Wikstrand CJ et al. Combination therapy of inhibitors of epidermal growth factor receptor/vascular endothelial growth factor receptor 2 (AEE788) and the mammalian target of rapamycin (RAD001) offers improved glioblastoma tumor growth inhibition. Mol Cancer Ther 2005;4:101-12.
13. Hjelmeland AB, Lattimore KP, Fee BE, Shi Q, Wickman S, Keir ST et al. The combination of novel low molecular weight inhibitors of RAF (LBT613) and target of rapamycin (RAD001) decreases glioma proliferation and invasion. Mol Cancer Ther 2007;6:2449-57.
14. Akhavan D, Pourzia AL, Nourian AA, Williams KJ, Nathanson D, Babic I et al. De-repression of PDGFRbeta transcription promotes acquired resistance to EGFR tyrosine kinase inhibitors in glioblastoma patients. Cancer Discov 2013.
15. de Vries NA, Zhao J, Kroon E, Buckle T, Beijnen JH, van Tellingen O. P-glycoprotein and breast cancer resistance protein: two dominant transporters working together in limiting the brain penetration of topotecan. Clin Cancer Res 2007;13:6440-9.
16. Lagas JS, van Waterschoot RA, van Tilburg VA, Hillebrand MJ, Lankheet N, Rosing H et al. Brain accumulation of dasatinib is restricted by P-glycoprotein (ABCB1) and breast cancer resistance protein (ABCG2) and can be enhanced by elacridar treatment. Clin Cancer Res 2009;15:2344-51.
17. Polli JW, Olson KL, Chism JP, John-Williams LS, Yeager RL, Woodard SM et al. An unexpected synergist role of P-glycoprotein and breast cancer resistance protein on the central nervous system penetration of the tyrosine kinase inhibitor lapatinib (N-{3-chloro-4-[(3-fluorobenzyl)oxy]phenyl}-6-[5-({[2-(methylsulfonyl)ethyl]amino }methyl)-2-furyl]-4-quinazolinamine; GW572016). Drug Metab Dispos 2009;37:439-42.
18. Tang SC, Lagas JS, Lankheet NA, Poller B, Hillebrand MJ, Rosing H et al. Brain accumulation of sunitinib is restricted by P-glycoprotein (ABCB1) and breast cancer resistance protein (ABCG2) and can be enhanced by oral elacridar and sunitinib coadministration. Int J Cancer 2012;130:223-33.
19. Zhou L, Schmidt K, Nelson FR, Zelesky V, Troutman MD, Feng B. The effect of breast cancer resistance protein and P-glycoprotein on the brain penetration of flavopiridol, imatinib mesylate (Gleevec), prazosin, and 2-methoxy-3-(4-(2-(5-methyl-2-phenyloxazol-4-yl) ethoxy)phenyl)propanoic acid (PF-407288) in mice. Drug Metab Dispos 2009;37:946-55.
20. Crowe A, Lemaire M. In vitro and in situ absorption of SDZ-RAD using a human intestinal cell line (Caco-2) and a single pass perfusion model in rats: comparison with rapamycin. Pharm Res 1998;15:1666-72.

21. Minocha M, Khurana V, Qin B, Pal D, Mitra AK. Co-administration strategy to enhance brain accumulation of vandetanib by modulating P-glycoprotein (P-gp/Abcb1) and breast cancer resistance protein (Bcrp1/Abcg2) mediated efflux with m-TOR inhibitors. Int J Pharm 2012;434:306-14.
22. Chu C, Abbara C, Noel-Hudson MS, Thomas-Bourgneuf L, Gonin P, Farinotti R et al. Disposition of everolimus in mdr1a-/1b- mice and after a pre-treatment of lapatinib in Swiss mice. Biochem Pharmacol 2009;77:1629-34.
23. Jacobsen W, Serkova N, Hausen B, Morris RE, Benet LZ, Christians U. Comparison of the in vitro metabolism of the macrolide immunosuppressants sirolimus and RAD. Transplant Proc 2001;33:514-5.
24. Schinkel AH, Mayer U, Wagenaar E, Mol CA, van Deemter L, Smit JJ et al. Normal viability and altered pharmacokinetics in mice lacking mdr1-type (drug-transporting) P-glycoproteins. Proc Natl Acad Sci U S A 1997;94:4028-33.
25. Jonker JW, Buitelaar M, Wagenaar E, van der Valk MA, Scheffer GL, Scheper RJ et al. The breast cancer resistance protein protects against a major chlorophyll-derived dietary phototoxin and protoporphyria. Proc Natl Acad Sci U S A 2002;99:15649-54.
26. Jonker JW, Freeman J, Bolscher E, Musters S, Alvi AJ, Titley I et al. Contribution of the ABC transporters Bcrp1 and Mdr1a/1b to the side population phenotype in mammary gland and bone marrow of mice. Stem Cells 2005;23:1059-65.
27. van Waterschoot RA, Lagas JS, Wagenaar E, van der Kruijssen CM, van Herwaarden AE, Song JY et al. Absence of both cytochrome P450 3A and P-glycoprotein dramatically increases docetaxel oral bioavailability and risk of intestinal toxicity. Cancer Res 2009;69:8996-9002.
28. Lagas JS, Damen CW, van Waterschoot RA, Iusuf D, Beijnen JH, Schinkel AH. P-glycoprotein, multidrug-resistance associated protein 2, Cyp3a, and carboxylesterase affect the oral availability and metabolism of vinorelbine. Mol Pharmacol 2012;82:636-44.
29. Maruichi T, Fukami T, Nakajima M, Yokoi T. Transcriptional regulation of human carboxylesterase 1A1 by nuclear factor-erythroid 2 related factor 2 (Nrf2). Biochem Pharmacol 2010;79:288-95.
30. Schoemaker NE, Rosing H, Jansen S, Schellens JH, Beijnen JH. High-performance liquid chromatographic analysis of the anticancer drug irinotecan (CPT-11) and its active metabolite SN-38 in human plasma. Ther Drug Monit 2003;25:120-4.
31. van Waterschoot RA, Rooswinkel RW, Wagenaar E, van der Kruijssen CM, van Herwaarden AE, Schinkel AH. Intestinal cytochrome P450 3A plays an important role in the regulation of detoxifying systems in the liver. FASEB J 2009;23:224-31.
32. O'Reilly T, McSheehy PM, Kawai R, Kretz O, McMahon L, Brueggen J et al. Comparative pharmacokinetics of RAD001 (everolimus) in normal and tumor-bearing rodents. Cancer Chemother Pharmacol 2010;65:625-39.
33. Jones RD, Taylor AM, Tong EY, Repa JJ. Carboxylesterases are uniquely expressed among tissues and regulated by nuclear hormone receptors in the mouse. Drug Metab Dispos 2013;41:40-9.
34. Zhang Y, Cheng X, Aleksunes L, Klaassen CD. Transcription factor-mediated regulation of carboxylesterase enzymes in livers of mice. Drug Metab Dispos 2012;40:1191-7.
35. Hatfield MJ, Potter PM. Carboxylesterase inhibitors. Expert Opin Ther Pat 2011;21:1159-71.
36. Morton CL, Iacono L, Hyatt JL, Taylor KR, Cheshire PJ, Houghton PJ et al. Activation and antitumor activity of CPT-11 in plasma esterase-deficient mice. Cancer Chemother Pharmacol 2005;56:629-36.
37. Fukami T, Takahashi S, Nakagawa N, Maruichi T, Nakajima M, Yokoi T. In vitro evaluation of inhibitory effects of antidiabetic and antihyperlipidemic drugs on human carboxylesterase activities. Drug Metab Dispos 2010;38:2173-8.
38. Dannecker R, Vickers AE, Ubeaud G, Hauck C. In vitro biotransformation of SDZ RAD: a new immunosuppressive macrolide in human liver microsomal preparations. Transplant Proc 1998;30:2206.
39. Wadkins RM, Morton CL, Weeks JK, Oliver L, Wierdl M, Danks MK et al. Structural constraints affect the metabolism of 7-ethyl-10-[4-(1-piperidino)-1-piperidino]carbonyloxycamptothecin (CPT-11) by carboxylesterases. Mol Pharmacol 2001;60:355-62.
40. Takahashi S, Katoh M, Saitoh T, Nakajima M, Yokoi T. Different inhibitory effects in rat and human carboxylesterases. Drug Metab Dispos 2009;37:956-61.
41. Li B, Sedlacek M, Manoharan I, Boopathy R, Duysen EG, Masson P et al.

Butyrylcholinesterase, paraoxonase, and albumin esterase, but not carboxylesterase, are present in human plasma. Biochem Pharmacol 2005;70:1673-84.

42. Hatfield MJ, Tsurkan L, Garrett M, Shaver TM, Hyatt JL, Edwards CC et al. Organ-specific carboxylesterase profiling identifies the small intestine and kidney as major contributors of activation of the anticancer prodrug CPT-11. Biochem Pharmacol 2011;81:24-31.
43. Pratt SE, Durland-Busbice S, Shepard RL, Heinz-Taheny K, Iversen PW, Dantzig AH. Human Carboxylesterase-2 Hydrolyzes the Prodrug of Gemcitabine (LY2334737) and Confers Prodrug Sensitivity to Cancer Cells. Clin Cancer Res 2013;19:1159-68.
44. Quinney SK, Sanghani SP, Davis WI, Hurley TD, Sun Z, Murry DJ et al. Hydrolysis of capecitabine to 5'-deoxy-5-fluorocytidine by human carboxylesterases and inhibition by loperamide. J Pharmacol Exp Ther 2005;313:1011-6.
45. Picard N, Rouguieg-Malki K, Kamar N, Rostaing L, Marquet P. CYP3A5 genotype does not influence everolimus in vitro metabolism and clinical pharmacokinetics in renal transplant recipients. Transplantation 2011;91:652-6.
46. Boernsen KO, Egge-Jacobsen W, Inverardi B, Strom T, Streit F, Schiebel HM et al. Assessment and validation of the MS/MS fragmentation patterns of the macrolide immunosuppressant everolimus. J Mass Spectrom 2007;42:793-802.
47. Vidal C, Kirchner GI, Sewing KF. Structural elucidation by electrospray mass spectrometry: an approach to the in vitro metabolism of the macrolide immunosuppressant SDZ RAD. J Am Soc Mass Spectrom 1998;9:1267-74.

SUPPLEMENTARY MATERIAL

Everolimus and metabolite analysis

The equipment consisted of an Accela pump and autosampler and a TSQ Quantum Ultra quadrupole mass spectrometer with heated electrospray ionization (Thermo Fisher Scientific, San Jose, CA, USA). Chromatographic separations of the analytes were carried out on an Aquity UPLC® BEH C18 300 column (50x2.1mm, d_p = 1.7 µm, Waters, Milford, USA) with an Aquity UPLC® BEH C18 VanGuard pre-column (Waters, 5x2.1mm, d_p = 1.7 µm). The column temperature was maintained at 60˚C and the autosampler was maintained at 4˚C. A mobile phase consisting of eluent A (1% (v/v) formic acid in water) and eluent B (methanol) was pumped through the column with a flow rate of 0.75 ml/min. Linear gradient elution was used from 50% to 80 % eluent B during 4 min, followed by a linear increase to 100% B during 0.5 min. Between 4.5 and 5 min, the elution was maintained at 100% eluent B. The percentage of eluent B was reduced to the initial composition (50% B) and from 5.01 to 6 min the column was reconditioned until the start of the next injection. The eluate was totally led into the electrospray probe from 2 to 4.96 min after injection. Ion spray tuning with sirolimus resulted in a 3900 V spray voltage, a 400°C capillary temperature, a 250°C vaporizer temperature and a 2.0 mTorr argon collision pressure, tuning with everolimus did not increase MS response. The dwell times were 0.05 s, skimmer off set was -8 V and the mass resolution was set at 0.7 full with at half height (unit resolution) for both separating quadrupoles. Mass transitions were m/z 980.6>389.2 for everolimus and metabolites and m/z 984.6>393.2 for the internal standard (IS; everolimus-d_4). The tube lens off set was 180 V and the collision energy -52 V for all compounds. The retention times were 3.7 min for everolimus and IS and 3.8 min for metabolite A.

Metabolite A was expected to be the dehydrated ring-opened derivative of everolimus because the product spectrum of this metabolite did not contain the m/z 686.4 and m/z 518.3 peaks (46, 47). In addition, in SRM mode both these product ions were only found for everolimus and not for metabolite A.

Mouse blood, plasma or tissue homogenate samples (50 µl) were pipetted into a well of a 96-well plate (0.5 ml), 50 µl of 500 ng/ml IS in 50% (v/v) methanol was added. After vortex mixing shortly, adding 150 µl of acetonitrile and vortex mixing again, the precipitate was separated by centrifuging at 2,643 *g* for 5 min. The clear supernatant was transferred into a second plate (1 ml wells) and 300 µl of 25% methanol (v/v) was added. After closing the wells and shaking manually 2 µl of the samples was injected.

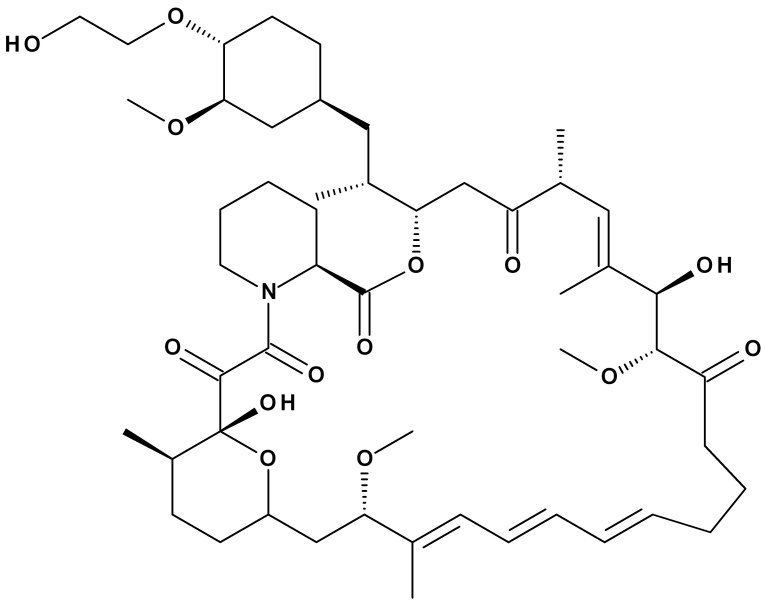

Supplementary Data 1. Molecular structure of everolimus.

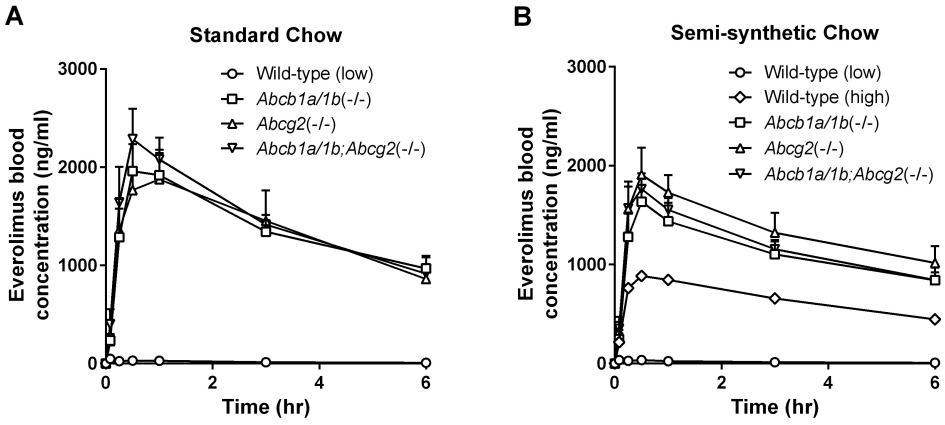

Supplementary Data 2. Blood concentration-time curves of everolimus in male wild-type, *Abcb1a/1b*(-/-), *Abcg2*(-/-) and *Abcb1a/1b;Abcg2*(-/-) mice that were given either a control (AM-II) (A) or semi-synthetic diet (B) for 8 weeks prior to oral administration of everolimus (2 mg/kg). All data are presented as mean ± SD (n = 2-5).

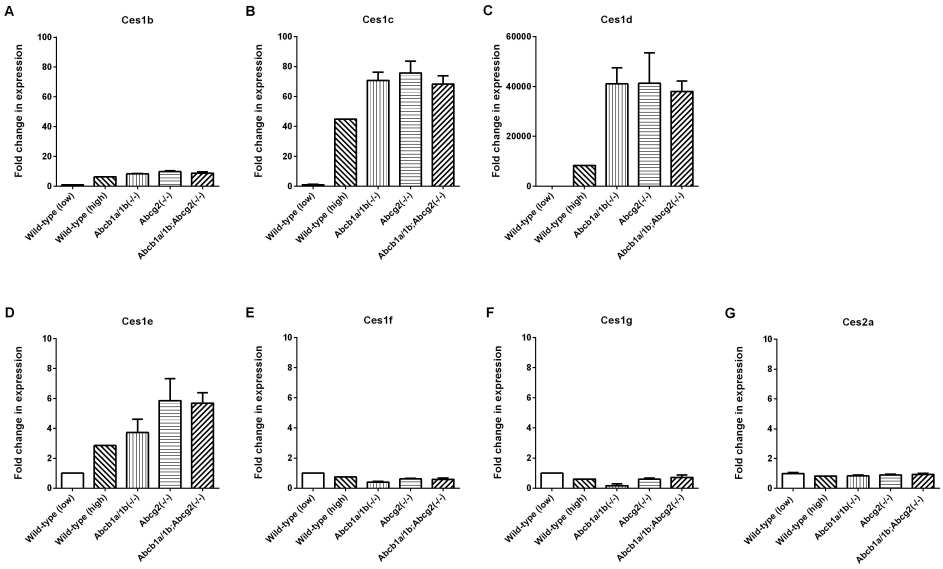

Supplementary Data 3. Liver expression of Ces1 and Ces2 genes in male wild-type, *Abcb1a/1b*(-/-), *Abcg2*(-/-) and *Abcb1a/1b;Abcg2*(-/-) mice. Expression levels of Ces1b (A), Ces1c (B), Ces1d (C), Ces1e (D), Ces1f (E), Ces1g (F) and Ces2a (G) mRNA in livers of wild-type, *Abcb1a/1b*(-/-), *Abcg2*(-/-) and *Abcb1a/1b;Abcg2*(-/-) mice, as determined by real-time RT-PCR. Data are normalized to GAPDH expression. Values represent mean fold change ± SD (n = 3), compared to wild-type mice with low Ces expression.

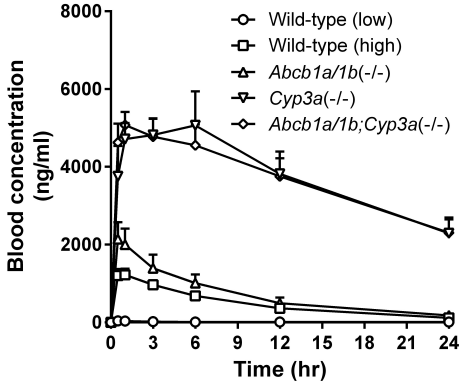

Supplementary Data 4. Blood concentration-time curves of everolimus in male wild-type, *Abcb1a/1b*(-/-), *Cyp3a*(-/-) and *Abcb1a/1b;Cyp3a*(-/-) mice receiving oral everolimus (2 mg/kg). All data are presented as mean ± SD (n = 3-5). Blood concentrations of "low" wild-type mice at 12 hr and 24 hr were below LLQ and therefore for calculation purposes replaced with the LLQ value (10 ng/ml).

Supplementary Table 1. Overview of the corresponding ΔC_t values belonging to the RT-PCR results as shown in Supplementary Figure 1. Analysis of the results was done by the comparative C_t method. Quantification of the target cDNAs in all samples was normalized against the endogenous control GAPDH ($C_{tCes1X} - C_{tGAPDH} = \Delta C_t$). Accordingly, the lower the values, the higher the expression levels. Three mice were used for each strain, except for "low" wild-type with two mice and "high" wild-type with only one mouse in this strain.

	Strain				
Gene	**"low" wild-type**	**"high" wild-type**	***Abcb1a/1b*(-/-)**	***Abcg2*(-/-)**	***Abcb1a/1b;Abcg2*(-/-)**
Ces1b	2.67	-0.02	-0.40 ± 0.03	-0.63 ± 0.07	-0.47 ± 0.13
Ces1c	4.75	-0.74	-1.39 ± 0.11	-1.49 ± 0.15	-1.34 ± 0.12
Ces1d	18.07	5.04	2.76 ± 0.23	2.78 ± 0.41	2.86 ± 0.15
Ces1e	5.23	3.72	3.37± 0.38	2.72 ± 0.40	2.73 ± 0.19
Ces1f	1.93	2.35	3.27 ± 0.22	2.64 ± 0.11	2.71 ± 0.21
Ces1g	1.88	2.59	5.03 ± 1.86	2.64 ± 0.17	2.38 ± 0.31
Ces2a	2.44	2.73	2.71 ± 0.09	2.60 ± 0.08	2.53 ± 0.11

Supplementary Table 2. Overview of the corresponding ΔC_t values belonging to the RT-PCR results as shown in Figure 4. Analysis of the results was done by the comparative C_t method. Quantification of the target cDNAs in all samples was normalized against the endogenous control GAPDH ($C_{tCes1X} - C_{tGAPDH} = \Delta C_t$). Accordingly, the lower the values, the higher the expression levels. Three mice were used for each strain, except for "high" wild-type with only 2 mice in this strain.

	Strain				
Gene	**"low" wild-type**	**"high" wild-type**	***Abcb1a/1b*(-/-)**	***Abcg2*(-/-)**	***Abcb1a/1b;Abcg2*(-/-)**
Ces1b	3.49 ± 0.13	1.00	-0.21 ± 0.09	0.29 ± 0.11	0.62 ± 0.04
Ces1c	6.07 ± 0.06	0.07	-1.28 ± 0.10	-0.81 ± 0.07	-0.51 ± 0.05
Ces1d	17.36 ± 0.38	3.68	1.69 ± 0.48	3.15 ± 0.40	2.92 ± 0.33
Ces1e	6.10 ± 0.05	3.12	1.99 ± 0.07	2.48 ± 0.39	2.41 ± 0.21

Supplementary Table 3. Pharmacokinetic parameters of everolimus in blood of wild-type, *Abcb1a/1b*(-/-), *Cyp3a*(-/-) and *Abcb1a/1b;Cyp3a*(-/-) mice receiving oral everolimus (2 mg/kg)

	Strain				
	"low" wild-type	**"high" wild-type**	***Abcb1a/1b*(-/-)**	***Cyp3a*(-/-)**	***Abcb1a/1b;Cyp3a*(-/-)**
$AUC_{0\text{-}24hr}$, ng/ml.hr	321.6 ± 43.5	11625 ± 1581***	17147 ± 4103***	90745 ± 11316***	88709 ± 9994***
Fold increase $AUC_{0\text{-}24hr}$	1.0	36.2	53.3	282.2	275.9
C_{max}, ng/ml	40.3 ± 14.5	1225.5 ± 159.7	2141.4 ± 438.1	5064.1 ± 873.4	5072.9 ± 340.5
T_{max}, hr	0.5	1.0	0.5	6.0	1.0

All data are presented as mean ± SD (n = 3-5). *** indicates $P < 0.001$ compared with "low" wild-type mice. Abbreviations: $AUC_{0\text{-}24hr}$: area under plasma concentration time curve from 0 to 24 hr; C_{max}, maximum blood concentration; T_{max}: time to reach maximum drug concentration in blood.

4

CHAPTER

CONCLUSION AND FUTURE PERSPECTIVES

CONCLUSION AND FUTURE PERSPECTIVES

In this work we have demonstrated the usefulness of single and combination transporter knockout mouse models to study the impact of ABCB1 and ABCG2 on oral availability and brain accumulation of drugs, including several TKIs and everolimus *in vivo*. Although increasing evidence, including from our own efforts, has shown that concomitant use of ABCB1 and ABCG2 dual inhibitors such as elacridar can effectively increase brain penetration of many targeted agents in mouse models, its use in patients with brain metastases or glioblastoma remains to be investigated.

We found that halving the transporter efflux activities at the BBB using heterozygous mice had only little, or even no significant impact on the brain accumulation of dual ABCB1 and ABCG2 substrate drugs such as dasatinib, sorafenib and sunitinib. These results have provided additional experimental support for the theoretical pharmacokinetic model of Kodaira *et al*. (2010) and imply that when either transporter shows strongly reduced transport activity caused by genetic polymorphisms or chemical inhibition, the remaining transporter activity could still effectively limit the brain penetration of shared ABCB1 and ABCG2 substrates.

It is important to note that upregulation of carboxylesterases in some of the knockout strains that we have developed may cause complications with a drug that can bind to, or be hydrolyzed by, these enzymes. Therefore, great caution is needed when interpreting results obtained for such drugs in these mouse strains. In addition, we have identified everolimus as an inhibitor of human CES1 and CES2, albeit slightly less potent for CES1. This would mean that inhibition of hepatic CES1 and especially intestinal CES2 by everolimus might play a role in drug-drug interactions with coadministered drugs. An implication of our work is therefore that coadministration of everolimus with potentially highly toxic ester prodrugs activated by carboxylesterases, including irinotecan, gemcitabine or LY2334737, should be assessed very carefully.

CHAPTER 5

SUMMARY

SUMMARY

ABCB1 and ABCG2 are two major ATP-binding cassette (ABC) efflux transporters that mediate the active efflux from the cell of many clinically used drugs. These transporters are amongst others expressed in the luminal or apical membrane of brain capillary endothelial cells and intestinal epithelial cells. They show overlapping substrate specificities and can transport a wide variety of anticancer drugs. In view of this, it is hypothesized that ABCB1 and ABCG2 play an important role in limiting oral availability and brain accumulation of many drugs. The studies described in this thesis utilize mouse models deficient of ABCB1 and/or ABCG2 to study the pharmacological functions of ABCB1 and ABCG2 *in vivo*. Tyrosine kinase inhibitors (TKIs) are small molecule inhibitors that selectively interfere with the intrinsic tyrosine kinase activity and thereby block receptor autophosphorylation and activation of downstream signal transducers (Levitzki, 1999). TKIs are increasingly used in anticancer pharmacotherapy, often resulting in substantial improvements in overall survival and quality of life of patients. However, their usually limited accumulation in brain tissue may limit their efficacy towards malignancies in the brain. In this thesis, we used several approaches to increase the brain accumulation of TKIs in mice, including coadministration of elacridar, a dual inhibitor of Abcb1 and Abcg2, or saturation of ABCB1 and ABCG2 with high initial plasma concentrations of drug.

Sunitinib is a broad-spectrum, orally available multitargeted TKI of the vascular endothelial growth factor receptor, the platelet-derived growth factor receptor, the stem cell factor receptor c-KIT, and FMS-like TK-3 kinase activity (Mendel *et al*., 2000). After administration, sunitinib is metabolized primarily by cytochrome P450 3A4 to a major and still pharmacologically active metabolite, *N*-desethyl sunitinib (Houk *et al*., 2009). In Chapters 2.1 and 2.2, we show that sunitinib and *N*-desethyl sunitinib are transported equally by both Abcb1 and Abcg2. Co-administration of oral elacridar can markedly increase brain accumulation of these agents in wild-type mice, albeit to a lower extent for *N*-desethyl sunitinib than for sunitinib. This suggested that elacridar had a much greater effect on the brain concentration of sunitinib than on that of *N*-desethyl sunitinib. These data were in line with other *in vivo* studies, suggesting that coadministration of elacridar could effectively increase brain accumulation of many TKIs in wild-type mice to levels similar to those in knockout mice (Bihorel *et al*., 2007; Breedveld *et al*., 2005; Durmus *et al*., 2012; Lagas *et al*., 2009). Although studies using mice have shown the potential of combining elacridar with TKIs to increase brain penetration of these agents, thus far, the effects of elacridar on brain penetration in patients with metastatic or primary brain tumors have not been investigated. However, the use of elacridar in patients for other purposes has been previously demonstrated by Kruijtzer *et al*. (2002), who showed that there was no elacridar-associated toxicity in patients receiving a single oral dose of 1000 mg elacridar. More importantly, the dose of elacridar used in our study is achievable in humans, as shown by Kemper *et al*. (2001), who found that a patient receiving 1000 mg of elacridar orally had almost the same elacridar plasma concentration as mice treated with 100 mg/kg elacridar orally. Extrapolating

from our results and those of other groups, it may prompt an interest to utilize elacridar in patients with brain metastases or primary brain tumors. The aim would be to inhibit efflux activities mediated by ABCB1 and ABCG2, thereby causing increased brain and brain tumor accumulation of dual ABCB1 and ABCG2 substrate TKIs, and thus ultimately improving the therapeutic efficacy of TKIs.

Even though elacridar has been shown to be an effective inhibitor for ABCB1 and ABCG2 *in vitro* and *in vivo*, its inhibitory effect on ABCB1 may be greater (Allen *et al.*, 2002; Matsson *et al.*, 2009). In our study, we only observed a partial inhibition of Abcb1 and Abcg2 in wild-type mice treated with elacridar, consistent with our *in vitro* data indicating that elacridar is not an efficient inhibitor of mouse Abcg2-mediated transport of *N*-desethyl sunitinib. However, elacridar almost completely inhibited human ABCG2-mediated *N*-desethyl sunitinib transport in *vitro*, suggesting that elacridar might have different efficacies towards mouse Abcg2 and human ABCG2. It could thus be that elacridar would be more effective in humans than in mice.

Another approach to increase brain accumulation of a drug is to saturate the efflux transporters with a high initial plasma concentration of the drug, which can be achieved shortly after intravenous administration. In Chapter 2.1 we demonstrate that a high initial plasma concentration of sunitinib can lead to partial and complete saturation of Abcb1 and Abcg2 transport activities, respectively, in the BBB of wild-type mice. Consequently, this approach resulted in highly increased brain concentrations of sunitinib in wild-type mice. However, this saturation approach probably has limited clinical potential, as it required a near lethal-dose of sunitinib that presumably would also lead to severe toxicity in patients.

In Chapter 2.3 crizotinib, an oral inhibitor for treatment of NSCLC patients with ALK rearrangements, was found to be a transported substrate of ABCB1, but not of ABCG2. *In vivo*, Abcb1 had a modest effect on oral availability of crizotinib during both the intestinal absorption and systemic clearance phases in mice. Importantly, the brain accumulation of crizotinib was markedly increased in mice lacking Abcb1. At a high oral dose of 50 mg/kg, the absence of Abcb1a/1b in knockout mice no longer affected the oral availability of crizotinib, but crizotinib brain accumulation was still profoundly increased. These data illustrate that the relative impact of drug transporters on pharmacokinetics can be quite dose-dependent, as seen before with for instance vemurafenib (Durmus *et al.*, 2012). In addition, these results strongly suggest that the intestinal Abcb1a/1b is more readily saturated than brain Abcb1 upon high oral dose of crizotinib. This is in itself not surprising, given the far higher crizotinib concentrations in the intestinal lumen than in the blood circulation. Nonetheless, together with the high-dose sunitinib data, we have shown that it is possible to saturate efflux transporters using high doses of drugs in mice.

An interesting finding from many *in vivo* brain accumulation studies was that single disruption of either Abcb1 or Abcg2 in mice often has little or even no significant effect on brain accumulation, whereas simultaneous genetic deletion of these two transporters often results in a disproportionate increase on brain accumulation of many TKIs that are dual substrates of Abcb1 and Abcg2. The pharmacokinetic model developed

by Kodaira *et al*. (2010) provides a straightforward theoretical explanation for this seemingly disproportionate effect of combined disruption of these transporters compared with the single disruptions, without postulating any direct or indirect interaction between the transporters. In view of this theoretical explanation, we hypothesized that halving the amount of active transporter-mediated drug efflux activity at the BBB should also result in only a minor increase of drug accumulation into the brain, even if complete removal of the active transporter-mediated efflux results in a very large increase in brain accumulation. In Chapter 2.4, we aimed to experimentally test this model and its wider relevance for TKIs and other drugs using dasatinib, sorafenib, and sunitinib. These TKIs have widely divergent behavior with respect to impact of the individual transporters on brain accumulation, different intrinsic capacity to accumulate into the brain, and different plasma levels upon oral administration at the same oral dosage (10 mg/kg). As predicted by the model, halving the amount of ABCB1 and ABCG2 at the BBB in heterozygous knockout mice only resulted in very small (<2-fold) or no significant increases in brain accumulation of these TKIs in heterozygous knockout mice. These results were in line with the model proposed by Kodaira *et al*. (2010) and imply that when either transporter shows strongly reduced transport activity caused by genetic polymorphisms or chemical inhibition, the remaining transporter activity could still effectively limit the brain penetration of shared ABCB1 and ABCG2 substrates.

In Chapter 3.1, we analyzed the roles of ABCB1, ABCG2 and CYP3A in blood and brain exposure of everolimus. The macrocyclic lactone everolimus (Afinitor, Zortress/Certican), a derivative of sirolimus (rapamycin), is an orally active mTOR inhibitor that is currently used both in cancer therapy and as an immunosuppressant to prevent organ rejection in heart and kidney transplant recipients. A striking finding in this chapter was the upregulation of a few liver mRNA carboxylesterases, including *Ces1b-e*, in several transporter knockout mouse strains and also in some of the wild-type mice. This upregulation correlated with drastically increased retention of everolimus in the plasma of these knockout strains. Of the upregulated Ces1 proteins, only Ces1c is predicted to be abundant in the plasma of these mice. Collectively, the results indicate that everolimus binds tightly to plasma Ces1c, and that this binding largely prevents degradation of everolimus by another plasma protein, and strongly reduces overall blood clearance of everolimus. These data imply that strong binding of otherwise unhydrolyzed drugs to plasma carboxylesterases may have pronounced effects on plasma and blood pharmacokinetics of such drugs. Since there may be many other drugs that are either bound but not hydrolyzed, or directly metabolized by these mouse plasma enzymes, results obtained with these knockout mouse models may be confounded by the Ces upregulation. However, such results are unlikely to be recapitulated in the human situation, as human CES1 or CES2 are not normally substantially present in plasma. Thus, plasma Ces upregulation is a potential source of complications that should be considered in future studies with these knockout strains.

Although human plasma contains no carboxylesterase (Li *et al*., 2005), CES1 and CES2 are predominantly expressed in

the liver and small intestine, respectively. Importantly, we have identified everolimus as an inhibitor of human CES1 and CES2, albeit slightly less potent for CES1. This would mean that inhibition of hepatic CES1 and especially intestinal CES2 by everolimus might play a role in drug-drug interactions with coadministered drugs. Upon oral everolimus administration, the intestinal mucosa is exposed to usually high concentrations of everolimus and this could inhibit the catalytic activity of CES2 in clinical practice. Therefore, coadministration of everolimus with ester prodrugs activated by carboxylesterases, including irinotecan, gemcitabine or LY2334737, should be assessed carefully.

In summary, we have demonstrated in this thesis that single and combination transporter knockout mice are indispensable tools to study the impact of ABCB1 and ABCG2 on oral availability and brain accumulation of drugs, such as TKIs and everolimus. In addition, by using mice heterozygous for Abcb1 and Abcg2 gene disruptions, we have provided new experimental support for the theoretical pharmacokinetic model developed by Kodaira *et al*. (2010). Unexpectedly, we found upregulation of liver carboxylesterases in some of the knockout strains used in this thesis. This phenomenon may cause complications with a drug such as everolimus and many other drugs that are potentially affected by these enzymes. Therefore, great caution is needed when interpreting results obtained for such drugs in these mouse strains.

REFERENCES

1. Allen JD, van Loevezijn A, Lakhai JM, van der Valk M, van Tellingen O, Reid G, Schellens JH, Koomen GJ and Schinkel AH (2002) Potent and specific inhibition of the breast cancer resistance protein multidrug transporter in vitro and in mouse intestine by a novel analogue of fumitremorgin C. *Mol Cancer Ther* **1**:417-425.
2. Bihorel S, Camenisch G, Lemaire M and Scherrmann JM (2007) Influence of breast cancer resistance protein (Abcg2) and p-glycoprotein (Abcb1a) on the transport of imatinib mesylate (Gleevec) across the mouse blood-brain barrier. *J Neurochem* **102**:1749-1757.
3. Breedveld P, Pluim D, Cipriani G, Wielinga P, van Tellingen O, Schinkel AH and Schellens JH (2005) The effect of Bcrp1 (Abcg2) on the in vivo pharmacokinetics and brain penetration of imatinib mesylate (Gleevec): implications for the use of breast cancer resistance protein and P-glycoprotein inhibitors to enable the brain penetration of imatinib in patients. *Cancer Res* **65**:2577-2582.
4. Durmus S, Sparidans RW, Wagenaar E, Beijnen JH and Schinkel AH (2012) Oral availability and brain penetration of the B-RAFV600E inhibitor vemurafenib can be enhanced by the P-GLYCOprotein (ABCB1) and breast cancer resistance protein (ABCG2) inhibitor elacridar. *Mol Pharm* **9**:3236-3245.
5. Houk BE, Bello CL, Kang D and Amantea M (2009) A population pharmacokinetic meta-analysis of sunitinib malate (SU11248) and its primary metabolite (SU12662) in healthy volunteers and oncology patients. *Clin Cancer Res* **15**:2497-2506.
6. Kemper EM, Jansen B, Brouwer KR, Schellens JH, Beijnen JH and van Tellingen O (2001) Bioanalysis and preliminary pharmacokinetics of the acridonecarboxamide derivative GF120918 in plasma of mice and humans by ion-pairing reversed-phase high-performance liquid chromatography with fluorescence detection. *J Chromatogr B Biomed Sci Appl* **759**:135-143.
7. Kodaira H, Kusuhara H, Ushiki J, Fuse E and Sugiyama Y (2010) Kinetic analysis of the cooperation of P-glycoprotein (P-gp/Abcb1) and breast cancer resistance protein (Bcrp/Abcg2) in limiting the brain and testis penetration of erlotinib, flavopiridol, and mitoxantrone. *J Pharmacol Exp Ther* **333**:788-796.
8. Kruijtzer CM, Beijnen JH, Rosing H, Bokkel Huinink WW, Schot M, Jewell RC, Paul EM

and Schellens JH (2002) Increased oral bioavailability of topotecan in combination with the breast cancer resistance protein and P-glycoprotein inhibitor GF120918. *J Clin Oncol* **20**:2943-2950.

9. Lagas JS, van Waterschoot RA, van Tilburg VA, Hillebrand MJ, Lankheet N, Rosing H, Beijnen JH and Schinkel AH (2009) Brain accumulation of dasatinib is restricted by P-glycoprotein (ABCB1) and breast cancer resistance protein (ABCG2) and can be enhanced by elacridar treatment. *Clin Cancer Res* **15**:2344-2351.
10. Levitzki A (1999) Protein tyrosine kinase inhibitors as novel therapeutic agents. *Pharmacol Ther* **82**:231-239.
11. Li B, Sedlacek M, Manoharan I, Boopathy R, Duysen EG, Masson P and Lockridge O (2005) Butyrylcholinesterase, paraoxonase, and albumin esterase, but not carboxylesterase, are present in human plasma. *Biochem Pharmacol* **70**:1673-1684.
12. Matsson P, Pedersen JM, Norinder U, Bergstrom CA and Artursson P (2009) Identification of novel specific and general inhibitors of the three major human ATP-binding cassette transporters P-gp, BCRP and MRP2 among registered drugs. *Pharm Res* **26**:1816-1831.
13. Mendel DB, Laird AD, Smolich BD, Blake RA, Liang C, Hannah AL, Shaheen RM, Ellis LM, Weitman S, Shawver LK and Cherrington JM (2000) Development of SU5416, a selective small molecule inhibitor of VEGF receptor tyrosine kinase activity, as an anti-angiogenesis agent. *Anticancer Drug Des* **15**:29-41.

&

APPENDICES

NEDERLANDSTALIGE SAMENVATTING

ABCB1 en ABCG2 zijn twee belangrijke ATP-bindingscassette (ABC) efflux pompen die de actieve efflux uit de cel bewerkstelligen van een groot aantal klinisch toegepaste geneesmiddelen. Deze pompen komen onder andere tot expressie in de luminale of apicale membraan van de endotheelcellen in capillaire bloedvaatjes in de hersenen en in de epitheelcellen van de darm. Ze vertonen een aanzienlijke overlap in substraatspecificiteit en transporteren een ruime variëteit aan kankergeneesmiddelen. Er wordt derhalve verondersteld dat ABCB1 en ABCG2 een belangrijke rol spelen in het beperken van de orale beschikbaarheid en de hersenaccumulatie van veel geneesmiddelen. De studies beschreven in dit proefschrift gebruiken muismodellen die deficiënt zijn voor ABCB1 en/of ABCG2, teneinde de *in vivo* farmacologische functies van deze twee eiwitten te bestuderen. Tyrosine kinase remmers (TKIs in Engelse afkorting) zijn klein-moleculaire remmers die selectief de intrinsieke tyrosine kinase activiteit verstoren, en daarmee de receptor autofosforylering en/of activatie van benedenstrooms signaaltransductoren in kinase-afhankelijke signaaltransductie paden (Levitzki, 1999). TKIs worden in toenemende mate gebruikt in kanker chemotherapie, vaak met aanzienlijke verbeteringen in totale overleving en kwaliteit van leven voor de patiënt tot gevolg. Echter, de gewoonlijk beperkte accumulatie van deze middelen in hersenweefsel zou hun werkzaamheid tegen maligniteiten in de hersenen kunnen beperken. In dit proefschrift hebben we verschillende benaderingen gebruikt teneinde de hersenaccumulatie van TKIs in muizen te verbeteren, waaronder gelijktijdige toediening van elacridar, een gecombineerde remmer van Abcb1 en Abcg2, of verzadiging van ABCB1 en ABCG2 met hoge initiële plasmaconcentraties van het geneesmiddel.

Sunitinib is een breed-spectrum, oraal beschikbare TKI die zowel de activiteit van de "vascular endothelial growth factor receptor", de "platelet-derived growth factor receptor", de stamcel factor c-KIT, als die van het "FMS-like TK-3 kinase" remt (Mendel et al., 2000). Na toediening wordt sunitinib gemetaboliseerd, primair door cytochroom P450 3A, tot een belangrijke en nog steeds farmacologisch actieve metaboliet, *N*-desethyl sunitinib (Houk et al., 2009). In Hoofdstukken 2.1 en 2.2 laten we zien dat sunitinib en *N*-desethyl sunitinib in ongeveer gelijke mate worden getransporteerd door Abcb1 en Abcg2. Gelijktijdige orale toediening van elacridar kan de hersenaccumulatie van deze twee stoffen in wild-type muizen aanzienlijk doen toenemen, hoewel minder voor *N*-desethyl sunitinib dan voor sunitinib. Deze gegevens waren in overeenstemming met andere *in vivo* studies, die aangaven dat gelijktijdige toediening van elacridar de hersenaccumulatie van veel TKIs in wild-type muizen effectief kon verhogen, tot niveaus vergelijkbaar met die in knockout muizen (Bihorel et al., 2007; Breedveld et al., 2005; Durmus et al., 2012; Lagas et al., 2009). Hoewel studies in knockout muizen het potentieel hebben aangetoond van het combineren van elacridar met TKIs teneinde de hersenaccumulatie van deze stoffen te verhogen, is het effect van een dergelijke behandeling in patiënten met gemetastaseerde of primaire hersentumoren

nog niet onderzocht. Echter, het gebruik van elacridar in patiënten voor andere doeleinden is voorheen aangetoond door Kruijtzer *et al*. (2002), die lieten zien dat er geen elacridar-geassocieerde toxiciteit was in patiënten die een enkelvoudige orale dosis van 1000 mg elacridar ontvingen. Belangrijker nog, de effectieve dosis elacridar die wij gebruikten in muizen is ook haalbaar in patiënten, zoals aangetoond door Kemper *et al*. (2001), die vonden dat een patiënt die 1000 mg elacridar oraal ontving, bijna dezelfde elacridar plasmaspiegel behaalde als muizen behandeld met 100 mg/kg oraal elacridar. Extrapolerend vanuit deze resultaten en die van andere groepen, zou dit aanleiding kunnen geven tot een poging om elacridar te gebruiken in patiënten met primaire of gemetastaseerde hersentumoren. Doel zou zijn om de efflux activiteit van ABCB1 en ABCG2 te remmen, en aldus verhoogde hersen- en hersentumor-accumulatie te verkrijgen van TKIs die gedeelde substraten zijn van beide transporteurs. Zo zou uiteindelijk de therapeutische werkzaamheid van TKIs verbeterd kunnen worden.

Alhoewel is aangetoond dat elacridar een effectieve remmer kan zijn van zowel ABCB1 als ABCG2 *in vivo* en *in vitro*, zou het remmend effect op ABCB1 groter kunnen zijn (Allen et al., 2002; Matsson et al., 2009). In onze studie werd slechts een gedeeltelijke remming van Abcb1 en Abcg2 waargenomen in wild-type muizen behandeld met elacridar, in overeenstemming met *in vitro* resultaten die aangaven dat elacridar geen efficiënte remmer is van muis Abcg2-gemedieerd transport van *N*-desethyl sunitinib. Echter, elacridar remde wel het humane ABCG2-gemedieerd *in vitro* transport van *N*-desethyl sunitinib volledig, wat suggereert dat elacridar uiteenlopende effectiviteit zou kunnen hebben voor muis Abcg2 en humaan ABCG2. Mogelijk is elacridar dus effectiever in mensen dan in muizen.

Een andere benadering om de hersenaccumulatie van een geneesmiddel te verhogen is het verzadigen van de efflux transporteurs met een hoge initiële plasmaconcentratie van het geneesmiddel, die bereikt kan worden kort na een intraveneuze toediening. In Hoofdstuk 2.1 laten we zien dat een hoge initiële plasmaconcentratie van sunitinib kan leiden tot gedeeltelijke of volledige verzadiging van de transportactiviteit van Abcb1 en Abcg2, respectievelijk, in de bloed-hersen barrière van wild-type muizen. Dientengevolge resulteerde deze benadering in sterk toegenomen hersenconcentraties van sunitinib in wild-type muizen. Echter, deze verzadigingsbenadering heeft waarschijnlijk maar beperkt klinisch potentieel, aangezien het nodig was om een bijna-lethale dosis van sunitinib te gebruiken die vermoedelijk ook in patiënten tot zeer ernstige toxiciteit zou leiden.

In Hoofdstuk 2.3 werd gevonden dat crizotinib, een orale remmer voor de behandeling van NSCLC patiënten met herrangschikkingen van het ALK gen, een getransporteerd substraat was van ABCB1, maar niet van ABCG2. *In vivo* had Abcb1 een matig effect op de orale beschikbaarheid van crizotinib in muizen gedurende zowel de absorptiefase vanuit de darm als de systemische klaringsfase. Belangrijk was dat de hersenaccumulatie van crizotinib sterk was toegenomen in Abcb1-deficiënte muizen. Bij een hoge orale dosis van 50 mg/kg had de afwezigheid van Abcb1 niet langer een effect op de orale beschikbaarheid van crizotinib, maar de hersenaccumulatie was nog steeds sterk verhoogd. Deze gegevens illustreren dat de relatieve impact van

geneesmiddel transporteurs behoorlijk dosis-afhankelijk kan zijn, zoals eerder ook was gevonden bij de TKI vemurafenib (Durmus et al., 2012). Bovendien suggereren deze resultaten dat darm Abcb1a/1b makkelijker verzadigd wordt dan Abcb1 in de hersenen bij een hoge oral dosis sunitinib. Dit is op zichzelf niet onverwacht, gezien de veel hogere concentraties van crizotinib in het darmlumen dan in de bloedsomloop. Desalniettemin, tezamen met de gegevens bij hoge-dosis sunitinib, hebben we laten zien dat het mogelijk is om deze efflux transporteurs te verzadigen met hoge doses geneesmiddelen in muizen.

Een interessante bevinding in vele *in vivo* hersenaccumulatie studies was dat enkelvoudige disruptie van hetzij Abcb1 of Abcg2 in muizen vaak weinig of zelfs geen significant effect had op de hersenaccumulatie, terwijl gelijktijdige genetische inactivatie van deze twee transporteurs vaak resulteerde in een disproportioneel hoge toename in hersenaccumulatie van TKIs die gedeelde substraten zijn van Abcb1 en Abcg2. Een farmacokinetische model dat is ontwikkeld door Kodaira *et al*. (2010) leverde een rechttoe-rechtaan verklaring voor dit schijnbaar disproportionele effect, zonder dat er een directe of indirecte interactie tussen beide transporteurs gepostuleerd hoefde te worden. In het licht van deze theoretische verklaring hypothetiseerden we dat halvering van de actieve transporteur-gemedieerde geneesmiddel efflux activiteit in de bloed-hersen barrière ook zou moeten resulteren in slechts een geringe toename van geneesmiddel accumulatie in de hersenen, zelfs als de volledige verwijdering van transporteur activiteit resulteert in een zeer grote toename in hersenaccumulatie. In Hoofdstuk 2.4 was ons doel om dit model experimenteel te testen, evenals zijn bredere relevantie voor TKIs en andere geneesmiddelen. We maakten gebruik van dasatinib, sorafenib, en sunitinib. Deze TKIs vertonen sterk uiteenlopende eigenschappen wat betreft impact van de individuele transporteurs op hersenaccumulatie, verschillende intrinsieke capaciteit om in de hersenen te accumuleren, en verschillende plasmaspiegels die bereikt worden na dezelfde orale dosis (10 mg/kg). Zoals voorspeld door het model resulteerde de halvering van de hoeveelheid ABCB1 en ABCG2 in de bloed-hersen barrière van heterozygote knockout muizen in slechts een geringe (<2-voudige), of zelfs niet-significante toename in hersenaccumulatie van deze TKIs. Deze resultaten waren geheel in lijn met het model van Kodaira *et al*. (2010) en geven aan dat, wanneer één van beide transporteurs sterk verminderde transportactiviteit vertoont als gevolg van genetische polymorfismen of chemische remming, de overblijvende transporteur nog steeds effectief de hersenaccumulatie kan beperken van gedeelde ABCB1 en ABCG2 substraten.

In Hoofdstuk 3.1 hebben we de bijdrage onderzocht van ABCB1, ABCG2 en CYP3A aan de bloed- en hersenblootstelling van everolimus. Het macrocyclische lacton everolimus (Afinitor, Zortress/Certican), een derivaat van sirolimus (rapamycine), is een oraal actieve mTOR remmer, die momenteel wordt gebruikt in kanker chemotherapie en als immunosuppressief geneesmiddel om orgaanafstoting te onderdrukken bij ontvangers van hart- en niertransplantaten. Een opvallende bevinding in dit hoofdstuk

was de opregulatie van het mRNA van enkele carboxylesterase genen in de lever, waaronder *Ces1b-e*, in diverse muis knockout stammen, maar ook in enkele wild-type muizen. Deze opregulatie hing samen met een sterk verhoogde retentie van everolimus in het plasma van de knockout stammen. Van de opgereguleerde Ces1 eiwitten wordt alleen Ces1c geacht in aanzienlijke hoeveelheden in het plasma van deze knockout muizen voor te komen. De resultaten laten zien dat everolimus sterk bindt aan plasma Ces1c, en deze binding voorkomt grotendeels de afbraak van everolimus door een ander plasma eiwit, en vermindert derhalve sterk de bloedklaring van everolimus. Deze gegevens impliceren dat sterke binding van niet-gehydrolyseerde geneesmiddelen aan plasma carboxylesterasen uitgesproken effecten kan hebben op de plasma en bloed farmacokinetiek van deze geneesmiddelen. Aangezien er vele andere geneesmiddelen kunnen zijn die hetzij gebonden, maar niet gehydrolyseerd, dan wel direct gemetaboliseerd kunnen worden door deze muis plasma enzymen, kunnen resultaten verkregen in deze knockout muizenstammen verstoord worden door de Ces opregulatie. Zulke resultaten worden echter vermoedelijk niet gereproduceerd in de humane situatie, aangezien humaan CES1 of CES2 normaal gesproken niet in plasma voorkomen. Ces opregulatie in plasma is derhalve een mogelijke bron van complicaties, die in aanmerking genomen dient te worden in toekomstige studies met deze knockout stammen.

Alhoewel humaan plasma geen carboxylesterasen bevat (Li *et al*., 2005), komen humaan CES1 en CES2 wel sterk tot expressie in respectievelijk de lever en dunne darm. Het is daarom van belang dat we hebben vastgesteld dat everolimus een remmer is van humaan CES1 en CES2, ofschoon wat minder voor CES1. Dit kan betekenen dat remming van lever CES1 en vooral darm CES2 door everolimus een rol speelt in geneesmiddel-geneesmiddel interacties met tegelijk toegediende geneesmiddelen. Na orale toediening van everolimus wordt de mucosa van de dunne darm blootgesteld aan hoge concentraties van everolimus, en dit zou de katalytische activiteit van CES2 ook in de klinische praktijk kunnen remmen. Gelijktijdige toediening van everolimus met ester-type "prodrugs" die geactiveerd worden door carboxylesterasen, zoals irinotecan, gemcitabine en LY2334737, zou dus met de nodige voorzichtigheid geëvalueerd moeten worden.

Samenvattend, in dit proefschrift hebben we laten zien dat enkelvoudige en gecombineerde transporteur "knockout" muizen onmisbare hulpmiddelen zijn om de invloed van ABCB1 en ABCG2 op de orale beschikbaarheid en hersenaccumulatie van geneesmiddelen zoals de TKIs en everolimus te bestuderen. Bovendien, gebruikmakend van muizen heterozygoot voor de Abcb1 en Abcg2 gen-disrupties, hebben we nieuw experimenteel bewijs aangedragen voor het theoretische farmacokinetische model van Kodaira *et al*. (2010). Geheel onverwacht hebben we gevonden dat er sterke opregulatie is van lever carboxylesterasen in een aantal knockout muisstammen die zijn toegepast in dit proefschrift. Dit verschijnsel kan complicaties veroorzaken bij een geneesmiddel zoals everolimus, en bij andere geneesmiddelen die potentieel beïnvloed worden door deze enzymen. Grote voorzichtigheid is dus geboden bij het interpreteren van resultaten verkregen voor dit soort geneesmiddelen in deze muizenstammen.

REFERENCES

1. Allen JD, van Loevezijn A, Lakhai JM, van der Valk M, van Tellingen O, Reid G, Schellens JH, Koomen GJ and Schinkel AH (2002) Potent and specific inhibition of the breast cancer resistance protein multidrug transporter in vitro and in mouse intestine by a novel analogue of fumitremorgin C. *Mol Cancer Ther* **1**:417-425.
2. Bihorel S, Camenisch G, Lemaire M and Scherrmann JM (2007) Influence of breast cancer resistance protein (Abcg2) and p-glycoprotein (Abcb1a) on the transport of imatinib mesylate (Gleevec) across the mouse blood-brain barrier. *J Neurochem* **102**:1749-1757.
3. Breedveld P, Pluim D, Cipriani G, Wielinga P, van Tellingen O, Schinkel AH and Schellens JH (2005) The effect of Bcrp1 (Abcg2) on the in vivo pharmacokinetics and brain penetration of imatinib mesylate (Gleevec): implications for the use of breast cancer resistance protein and P-glycoprotein inhibitors to enable the brain penetration of imatinib in patients. *Cancer Res* **65**:2577-2582.
4. Durmus S, Sparidans RW, Wagenaar E, Beijnen JH and Schinkel AH (2012) Oral availability and brain penetration of the B-RAFV600E inhibitor vemurafenib can be enhanced by the P-GLYCOprotein (ABCB1) and breast cancer resistance protein (ABCG2) inhibitor elacridar. *Mol Pharm* **9**:3236-3245.
5. Houk BE, Bello CL, Kang D and Amantea M (2009) A population pharmacokinetic meta-analysis of sunitinib malate (SU11248) and its primary metabolite (SU12662) in healthy volunteers and oncology patients. *Clin Cancer Res* **15**:2497-2506.
6. Kemper EM, Jansen B, Brouwer KR, Schellens JH, Beijnen JH and van Tellingen O (2001) Bioanalysis and preliminary pharmacokinetics of the acridonecarboxamide derivative GF120918 in plasma of mice and humans by ion-pairing reversed-phase high-performance liquid chromatography with fluorescence detection. *J Chromatogr B Biomed Sci Appl* **759**:135-143.
7. Kodaira H, Kusuhara H, Ushiki J, Fuse E and Sugiyama Y (2010) Kinetic analysis of the cooperation of P-glycoprotein (P-gp/Abcb1) and breast cancer resistance protein (Bcrp/Abcg2) in limiting the brain and testis penetration of erlotinib, flavopiridol, and mitoxantrone. *J Pharmacol Exp Ther* **333**:788-796.
8. Kruijtzer CM, Beijnen JH, Rosing H, Bokkel Huinink WW, Schot M, Jewell RC, Paul EM and Schellens JH (2002) Increased oral bioavailability of topotecan in combination with the breast cancer resistance protein and P-glycoprotein inhibitor GF120918. *J Clin Oncol* **20**:2943-2950.
9. Lagas JS, van Waterschoot RA, van Tilburg VA, Hillebrand MJ, Lankheet N, Rosing H, Beijnen JH and Schinkel AH (2009) Brain accumulation of dasatinib is restricted by P-glycoprotein (ABCB1) and breast cancer resistance protein (ABCG2) and can be enhanced by elacridar treatment. *Clin Cancer Res* **15**:2344-2351.
10. Levitzki A (1999) Protein tyrosine kinase inhibitors as novel therapeutic agents. *Pharmacol Ther* **82**:231-239.
11. Li B, Sedlacek M, Manoharan I, Boopathy R, Duysen EG, Masson P and Lockridge O (2005) Butyrylcholinesterase, paraoxonase, and albumin esterase, but not carboxylesterase, are present in human plasma. *Biochem Pharmacol* **70**:1673-1684.
12. Matsson P, Pedersen JM, Norinder U, Bergstrom CA and Artursson P (2009) Identification of novel specific and general inhibitors of the three major human ATP-binding cassette transporters P-gp, BCRP and MRP2 among registered drugs. *Pharm Res* **26**:1816-1831.
13. Mendel DB, Laird AD, Smolich BD, Blake RA, Liang C, Hannah AL, Shaheen RM, Ellis LM, Weitman S, Shawver LK and Cherrington JM (2000) Development of SU5416, a selective small molecule inhibitor of VEGF receptor tyrosine kinase activity, as an anti-angiogenesis agent. *Anticancer Drug Des* **15**:29-41.

LIST OF ABBREVIATIONS

ABC	ATP-binding cassette
Akt	protein kinase B
ALK	anaplastic lymphoma kinase
ANOVA	analysis of variance
AUC	area under the plasma concentration-time curve
BBB	blood-brain barrier
BCRP	breast cancer resistance protein
BM	brain metastases
BNPP	bis(4-nitrophenyl) phosphate
BSA	bovine serum albumin
CAR	constitutive androstane receptor
C_{brain}	brain concentration
cDNA	complementary DNA
CES	carboxylesterase
C_{max}	maximum drug concentration in plasma
CYP3A	cytochrome P450 3A
DMSO	dimethyl sulfoxide
EML4	echinoderm microtubule associated protein-like 4
Ent	equilibrative nucleoside transporter
HPLC	high performance liquid chromatography
hu (as prefix)	human
IC_{50}	drug concentration that causes 50% inhibition of enzyme activity
IS	internal standard
i.v.	intravenous
LC-MS/MS	liquid chromatography coupled with tandem mass spectrometry
LLQ	lower limit of quantification
MDCK-II	Madine-Darby canine kidney-II
mRNA	messenger RNA
MRP	multidrug resistance-associated protein
mTOR	mammalian target of rapamycin
mu (as prefix)	murine
NSCLC	non-small cell lung cancer
OATP	organic anion-transporting polypeptide
Oct	Organic cation transporter
P_{app}	apparent permeability coefficient
P_{brain}	relative brain accumulation
PCN	pregnenolone 16α-carbonitrile
PDGFRA	platelet derived growth factor receptor α
P-gp	P-glycoprotein
PI3K	phosphatidylinositol 3-kinase

PXR	pregnane X receptor
RCC	renal cell carcinoma
RTK	receptor tyrosine kinase
RT-PCR	reverse transcriptase polymerase chain reaction
S.D.	standard deviation
SLC	solute carrier
SN-38	7-ethyl-10-hydroxycamptothecin
TCGA	The Cancer Genome Atlas
TCPOBOP	1,4-bis[2-(3,5-dichloropyridyloxy)] benzene
TKI	tyrosine kinase inhibitor
T_{max}	time to reach maximum drug concentration in plasma

LIST OF PUBLICATIONS

Tang SC, Hendrikx JJ, Beijnen JH, Schinkel AH (2013) Mouse models for oral drug absorption and disposition.
To be submitted in modified form to Curr Opin Pharmacol.

Tang SC, Nguyen LN, Sparidans RW, Wagenaar E, Beijnen JH, Schinkel AH (2013) Increased oral availability and brain accumulation of the ALK inhibitor crizotinib by coadministration of the P-glycoprotein (ABCB1) inhibitor elacridar.
Submitted for publication

Tang SC, de Vries N, Sparidans RW, Wagenaar E, Beijnen JH, Schinkel AH (2013) Impact of P-glycoprotein (ABCB1) and breast cancer resistance protein (ABCG2) gene dosage on plasma pharmacokinetics and brain accumulation of dasatinib, sorafenib and sunitinib.
Submitted for publication

Tang SC, Sparidans RW, Fukami T, Wagenaar E, Yokoi T, Beijnen JH, Schinkel AH (2013) Impact of P-glycoprotein, CYP3A and plasma carboxylesterase Ces1c on blood pharmacokinetics and tissue disposition of everolimus (Afinitor, Zortress/Certican) in mice.
Submitted for publication

Sparidans RW, **Tang SC**, Nguyen LN, Schinkel AH, Schellens JH, Beijnen JH (2012) Liquid chromatography-tandem mass spectrometric assay for the ALK inhibitor crizotinib in mouse plasma.
J Chromatogr B Analyt Technol Biomed Life Sci. 905:150-4.

Tang SC, Lankheet NA, Poller B, Wagenaar E, Beijnen JH, Schinkel AH (2012) P-glycoprotein (ABCB1) and breast cancer resistance protein (ABCG2) restrict brain accumulation of the active sunitinib metabolite *N*-desethyl sunitinib.
J Pharmacol Exp Ther. 341(1):164-73.

Tang SC, Lagas JS, Lankheet NA, Poller B, Hillebrand MJ, Rosing H, Beijnen JH, Schinkel AH (2012) Brain accumulation of sunitinib is restricted by P-glycoprotein (ABCB1) and breast cancer resistance protein (ABCG2) and can be enhanced by oral elacridar and sunitinib coadministration.
Int J Cancer. 130(1):223-33.

Poller B, Wagenaar E, **Tang SC**, Schinkel AH (2011) Double-transduced MDCKII cells to study human P-glycoprotein (ABCB1) and breast cancer resistance protein (ABCG2) interplay in drug transport across the blood-brain barrier.
Mol Pharm. 8(2):571-82.

CURRICULUM VITAE

Seng Chuan Tang was born on April 16th, 1981 in Ipoh, Malaysia. In May 2004 he received his bachelor's degree in the field of Biomedical Sciences from the Universiti Putra Malaysia. After completing his bachelor's degree, he worked as a research assistant in the laboratory of Dr. Johnson Stanslas for a year, where he conducted three studies for a local pharmaceutical company. He screened several local plant extracts for anticancer effects *in vitro* and *in vivo*, and he also evaluated a local plant extract for its hepatoprotective effect on paracetamol-induced liver damage in rats. In May 2005 he started his Master's program under supervision of Dr. Johnson Stanslas, Dr. Hairuszah Ithnin and Dr. Nashiru Billa in the Department of Biomedical Sciences at the Universiti Putra Malaysia. During the course of his study, he identified several potential compounds that could inhibit tumor angiogenesis. These were further evaluated for their pharmacokinetic and toxicological profiles. In February 2009 he obtained his master's degree in Pharmacology and Toxicology. At the end of his master's program, he received a government fellowship to pursue a PhD in the field of Pharmacogenomics. In April 2009, he started his PhD study in the Division of Molecular Biology at the Netherlands Cancer Institute under supervision of Prof. Dr. Jos H. Beijnen and Dr. Alfred H. Schinkel. His PhD project concerned investigation of the impact of ABC transporters on pharmacokinetics of targeted anticancer drugs. The results of the research are described in this thesis.

ACKNOWLEDGEMENT

My book is finally out! Despite all the hard work and stressful times, I have had some good times and unforgettable memories throughout my study in Amsterdam that I will definitely treasure in the future. When I look back at what has happened over the past four years, I realize that my decision to pursue a PhD in Amsterdam was a wise choice. In such a multicultural city, I have learned not only about science, but also many different cultures. The only thing that would have made my life here more complete would have been the Dutch team winning the world cup in 2010. I sincerely hope that they will do well in the coming world cup in Brazil. But enough about football...

There are many individuals who have contributed in one way or another to the success of this thesis and made it an unforgettable experience. The journey to the west (the Netherlands) would not have been possible without the help of these people. First and foremost, I would like to express my utmost gratitude to you, **Dr. Alfred Schinkel**, for allowing me to perform my doctoral studies under your supervision. Dear **Alfred**, during the course of my study, I have learned immensely from you, especially on data interpretation and manuscript writing. Your patience, dedication, hard work and attention to detail have been a great inspiration to me. You always have helpful suggestions when I have problems in my experiments. In addition to helping me succeed in the lab, I remember us watching one of the world cup matches in front of my computer on a Friday evening. What a great way to spend a Friday!

I would also like to express heartfelt thanks to my promotor **Prof. dr. Jos Beijnen**. Dear **Jos**, despite your busy schedule, you could always find the time to help me, for example with the pharmacogenomic internship in Slotervaart Hospital. Although I have only met you on a few occasions, your support and enthusiasm for the studies that Alfred and I proposed to you was always appreciated. I sincerely wish you and your family good health, happiness and success in your future endeavors.

My special thanks to **Assoc. Prof. dr. Abas Hussin** and **Prof. dr. Syed Azhar Syed Sulaiman** for giving me an opportunity to study in Amsterdam under the academic staff training scheme fellowship from the Malaysian Ministry of Higher Education, Malaysia.

I am also grateful to the members of my PhD committee including **Prof. dr. Jacques Neefjes**, **Prof. dr. Hein te Riele** and **Dr. Olaf van Tellingen** for your time and valuable comments.

I would also like to specially thank **Prof. dr. Piet Borst** for your valuable comments and suggestions during my presentations. It is amazing to see you still actively engage in club seminars, work discussions and meetings. I wish you good health and happiness in life.

The results described in this thesis would not have been obtained without a close collaboration with a few individuals. Dear **Dr. Hilde Rosing**, I am very thankful for your supervision and support in bioanalytical analyses. Dear **Dr. Rolf Sparidans**, you have contributed a lot to my studies (almost three chapters in my thesis). To be frank, I think you are very efficient in measuring my samples, and I am sorry if I have sent you sometimes too many. Dear **Dr. Fukami** and **Prof. dr. Yokoi**, thank you for your interest in collaborating with us on the everolimus study. I thank **Nienke Lankheet** for your help in measuring those sunitinib and *N*-desethyl sunitinib samples. Good luck with your training in hospitals. Dear **Anita Kort**, many thanks for measuring the cabazitaxel samples. Although we still need to sort out some complications, I am confident that we will manage to get

&

the results published in the future. Dear **Niels**, many thanks for helping me to measure the sunitinib and dasatinib samples. Dear **Michel**, I am much grateful for your assistance and supervision in the bionalytical analyses. Dear **Bas Teunissen**, it would have been a lot nicer if we had managed to get a publication from the tamoxifen study. Unfortunately, we raised more questions than answers, but I think we both learned a lot from this study. I wish you the best in the future. Dear Rudi, many thanks for your efforts in measuring bilirubin concentrations in mouse plasma.

Dear **Selvi** and **Janneke**, thank you so much for being my paranymphs. Dear **Selvi**, you are such a good and close friend of mine. You are always there for me when I most need help. Despite the difficulties in your study, I am confident that you will finish your PhD with flying colors. Apart from work, we had some great time in Texel and also in Turkey. It was an eye-opening experience for me when I attended your wedding in Turkey. I wish you and **Fatih** a wonderful life together. Dear **Janneke**, you are one of the most confident and hardworking people I have ever met at the NKI. We had some great encounters in and outside of the NKI. I remember one occasion where we went together for the world cup celebration in Museumplein. It was nice to see that we were both wearing orange and cheering for the Dutch team. I have full confidence that you will do well in finishing your study. Thanks for helping out with my promotion. I hope you and **Tom** have a happy life together.

I can't forget all my colleagues whom I shared countless moments of laughter and frustration over the years. Dear **Els** and **Dilek**, on the first day I arrived in the Netherlands, you were the ones that I met. Thanks for picking me up in the airport. Dear **Els**, many thanks for your relentless effort in lab and mouse administration works. Dear **Dilek**, I very much appreciate your constant support and advices throughout my study, especially during work discussions. You are such a sociable person and I am glad that we have had some great times in the course of my study. Good luck in finishing your thesis. Dear **Anita van Esch**, you are very efficient in your work; I am so amazed that you can cope with your work and also take care of your four children at the same time. Dear **Jeroen**, you are undoubtedly very efficient in your works, keep up the efforts and I wish you lots of success for the future.

Thanks to the past members of Schinkel lab that have given me some ideas and suggestions when I first started in the group. When I first came, most of the PhD students at that time were almost finished with their studies. Although I did not have much time interacting with you all, I am glad to have met you during my studies. Dear **Marijn**, it was nice to meet you in the first month of my study. I can still remember helping you to carry your stuff to your car on the day you left NKI. I wish you all the best in both your personal and professional life. Dear **Jurjen**, my first experiment in mice was done together with you, you are vey helpful in giving suggestions and ideas, it was nice to have you around. I still remember one of your jokes about me wearing a tie on my first day to the lab. Dear **Robert**, one thing that I recall was that you showed me how to isolate small intestine tissue for RNA isolation. I also very much enjoyed the boat trip that we had in the canals of Amsterdam. Dear **Evita**, thanks for showing me how to perform gall bladder cannulation in mice. I wish you the best of luck in your working life at TNO. Dear **Birk**, thanks for teaching me how to perform a transwell experiment. Not forgetting also the wonderful time that we spent together in Amsterdam, Basel and Grindelwald, it was my first time sledging

and having cheese fondue. Keep in touch and definitely we will visit you again in Basel. Dear **Kazuya**, you have impressed me a lot with your work attitude. Furthermore, I would like to thank my student, **Luan Nguyen** for working together with me on the crizotinib studies. Dear **Luan**, I think you are very efficient and also enthusiastic about your studies. I have benefited a lot from you when you were around. I wish you all the best in the future. Dear **Ahmed**, I enjoyed having discussions with you about works. Besides works, we seem to talk a lot about football, and we had some fun together in playing snooker almost every week during your internship in our group. Dear **Marion**, it was nice to spend time together for dinner and drinks, Ich wünsche Dir alles Gute für dein Studium! Dear **Jyoti**, I have an impression that you are very positive about your work. I wish you all the best in your studies. Dear **Ning**, it was nice to have you around in the lab for a year. You are very humble, kind and helpful, I particularly appreciated your effort in making dumplings for us during Chinese New Year.

Dear **Henri**, I think you are such a kind and charming person. It was nice to talk with you over beers in Glasgow and during lab outings. You have been very supportive when I wanted to join the Dutch lessons and also to reimburse my thesis printing costs. Dear **Tom**, you are such an important person to have both in P2 and H5. You have always tried to help whenever I wanted to send some documents or tissue samples to Utrecht or Malaysia.

Since most of the works that I have done are associated with mice, I am very grateful for the continued support from the animal caretakers in G3, including **Marissa**, **Yvonne**, **Adrie**, **Klaas**, **Jeroen**, **Sido**, **Jurriaan** and **Ton**. In addition, I would like to extend my special thanks to **Marco**, **Roel**, **Filip**, **Maaike** and **Carla** with respect to the animal welfares and DEC protocols.

Many more people from NKI have helped me overcome experimental and personal issues. Dear **Olaf**, I enjoy discussing projects with you and many thanks for allowing me to use the HPLC and some chemicals in your lab. Dear **Lin**, I really appreciate all the help and time that you have given to me. Thanks for the great moments we have shared together, I wish you a lot of success in your postdoc and stay in Singapore. Dear **Levi** and **Stephan**, many thanks for your continued support while I was using the HPLC in your lab. Thanks **Melinda** and **Romy** for your help in handling my residence permit application. I would like to thank **Soenita** for your kind support in arranging a room for me upon my arrival to Amsterdam. Thanks **Patty** and **Caroline Kapper** for the excellent preparation and organization of the annual graduate student retreats and OOA courses.

I have had the pleasure to meet many people that are working or have worked at the NKI. Some of them, I would particularly like to thank. Dear **Jelle**, many thanks for your help and support throughout all these years, we have some great time watching football and having dinner together. You are the only friend I know that has been to Ipoh (the place where I grew up)! We will definitely take a photo in the city center when you visit me in Ipoh next time. Dear **Sanne**, I could not believe that you invited me to experience Dutch culture by staying in your parent's house in Groningen. Thanks for showing me the place where you grew up, I really enjoyed every moment at your parent's house, it was the most amazing experience in my life. Dear **Harmke**, you showed me some basic salsa dance moves, and it motivated me to learn salsa dancing. Dear **Jorma**, it was nice to talk with you and try food from a variety of countries in several restaurants. Dear **Charlotte**, it was a pleasant experience to share the office with you in P2 and also hang out.

&

Dear **Wendy**, thanks for being the model for my photography course. Dear **Ariena**, we had some great times at parties and thanks for introducing Bianca to me for the studio shoot. Dear **Robert**, I tried to speak some Dutch with you, and you are always very patient to speak back with me in Dutch. Dear **Koen**, thanks for showing me how to perform vesicle transport assay. Dear **Petra**, thanks so much for playing squash with me. Dear **Min Chul**, I enjoyed our encounters in and outside of NKI, all the best to you and your family. Dear **Viknesvaran**, thanks for your effort and time in getting articles that I could not get in my institute.

I am very much thankful to **David Alexander** for improving my English writing and presenting skills. Not forgetting all the students that I met during this course, including **Abinaya**, **Caroline**, **Ellen**, **Flora**, **Martijn**, **Naomi**, **Nynke**, **Rogier** and **Wilma**.

There are many people that I want to thank for the pleasant talks at the coffee corner, during Christmas dinners, during lab outings or in the borrels. These people are from the Jos Beijnen group: **Coen van Hasselt** and **Huixin**; the Karin de Visser group: **Metamia**, **Kelly**, **Tisee**, and **Chris Doornebal**; the Hein te Riele group: **Erika Canteli**, **Marleen**, and **Anja**; the Lodewyk Wessels group: **Lodewyk**, **Andreas**, **Sidney**, **Ewald**, **Christine** and **Theo**; the Michael Hauptmann group: **Michael**, **Marta** and **José**; the Piet Borst group: **Serge**, **Sunny**, **Asli**, **Guotai**; the Daniel Peeper group: **Nils**, **Sedef Iskit**, **Patricia**, **Judith**, **Sirith**, **Joanna** and **Barbara**, the Jacqueline Jacobs group: **Jaco**, **Marieke**, **Vera**, **Inge** and **Tessa**; the Rene Bernards group: **Sid**, **Liqin**, **Klaas**, **Jackie**, **Loredana**, **Valentina** and **Donna**; the Maarten van Lohuizen group: **Gaetano, Denise** and **Nienke de Vries**; the Jan-Hermen Dannenberg group: **Roel Wilting** and **Cesare**, and the Anton Berns group: **Jitendra**. I wish you all the best in your studies and every success in your future, and look forward to seeing you again. Besides, I have also met many people outside of the NKI such as **Hui Ting**, **Lee Cheng**, **Tae Yeong**, **Jin Yoo**, **Lian Yee**, **Kee Wee**, **Yanru**, **Vivian Dong**, **Mark Pieterse**, **Sedef Ayhan**, **Annelie Vink**, **Cigdem Ercan**, **Seçil Hulya Danakol**, **Chris Wever**, **Marzia Cosenza**, **Jezrael** and **Alex Wu**. Thanks for the many nice and interesting conversations.

There are a lot of other wonderful people that have been there for me through hard times, in particular **Hui Khee**, **Yoon Lai**, **Chung Tuck**, **Chang Khaw**, **Yeat Harn, Tian Kooi, Tian Fu**, **Joong Harnn** and **Mun Li**. Many thanks for all the moral support and camaraderie. Certainly this is not a complete list of people that I want to thank. For those whose names are not included in this acknowledgement, I would like to express my sincere gratitude to all of you who have contributed in one way or another to the success of this thesis and my stay in Amsterdam. I wish you all the best in your future endeavors.

My deepest gratitude goes to **Zheng** for all your support, faith and understanding that you have given to me during my difficult moments. Dear **Zheng**, I am very fortunate to have met you in Amsterdam. I am so glad that you came into my life, and I look forward to our future life together.

Last but not least, I am very much grateful to my sister, **Chia Ling** for my book cover design. Thanks to my brother, **Seng Hong** for taking care of my parents when I was not in Malaysia. Finally, I am forever indebted to my parents for their understanding, endless patience and encouragement when I was not with them over the years. Therefore, I dedicate this thesis to my parents.

Seng Chuan Tang